KNOWLEDGE-BASED MODELLING AND SIMULATION OF OPERATIONAL PROBLEMS OF MICROBIOLOGICAL ORIGIN IN WASTEWATER TREATMENT PLANTS

Jordi DALMAU SOLÉ

Dipòsit legal: GI-1060-2011
http://hdl.handle.net/10803/33690

Universitat de Girona

lequia
UdG
Laboratori d'Enginyeria Química i Ambiental

Knowledge-based modelling and simulation of operational problems of microbiological origin in wastewater treatment plants

Jordi Dalmau Solé

Thesis submitted in fulfilment of the requirements for the degree of Doctor (PhD) in Environmental Sciences (Physics and Environmental Technology)

This thesis was financially supported by Spanish Ministry of Education and Science projects (MYCT-DPI2006-15707-C02-01) and NOVEDAR_Consolider-CSD2007-00055 and a mobility grant from the University of Girona under the Catalan DRAC program.

IGNASI RODRÍGUEZ-RODA i JOAQUIM COMAS MATAS

Professors del Departament d'Enginyeria Química, Agrària i Tecnologia Agroalimentària de la Universitat de Girona.

Certifiquen

Que el llicenciat en Química Jordi Dalmau Solé ha realitzat, sota la seva direcció, el treball que amb el títol "**Knowledge-based modelling and simulation of operational problems of microbiological origin in wastewater treatment plants**", es presenta en aquesta memòria la qual constitueix la seva Tesi per optar al Grau de Doctor en Medi Ambient per la Universitat de Girona.

I perquè en prengueu coneixement i tingui els efectes que corresponguin, presentem davant la Facultat de Ciències de la Universitat de Girona l'esmentada Tesi, signant aquesta certificació a

Girona, 9 de Setembre de 2009

Ignasi Rodríguez-Roda

Joaquim Comas Matas

AGRAÏMENTS

Voldria expressar la meva més sincera gratitud a tothom en general pel vostre suport durant aquests anys.

En primer lloc vull agrair molt sincerament als meus directors, Quim i Ignasi, tot el suport i el recolzament que m'heu donat durant tots aquests anys. Per les hores que m'heu dedicat, pels consells, per les correccions, per les idees, per la paciència, per tot. I també per tot allò que no apareix en aquest document.

Secondly, I want to express my gratitude to the people that have collaborated directly or indirectly in the development of this thesis and the related work, they have supported me both professionally and personally, so, many thanks to Jean-Philippe, Eric, Gurkan, Kris, Ivan, Krishna, to the *benchmarkers* in general and to the people from LBE.

També vull agrair el suport de tot el LEQUIA durant aquests anys, altra vegada professional i personalment. He de donar les gràcies al munt de lequians amb qui hem compartit incomptables bones estones, tant dins com fora de la feina, de les que guardaré un record molt especial.

De la mateixa manera, vull donar les gràcies a la colla de Cassà i a la gent de Granollers dels que tant se'm sent parlar doncs ells també m'han ajudat a passar les males estones i a gaudir més de les bones.

Finalment, donar les gràcies, pel recolzament que m'han donat durant tots aquests anys, a la meva mare, al meu pare i a l'Eduard. També vull agrair especialment a la Miriam el seu suport i la paciència que ha tingut durant aquest temps, especialment en el tram final de la tesis.

ABSTRACT

The activated sludge (AS) and anaerobic digestion (AD) systems are the most frequently used systems included in wastewater treatment plants (WWTPs) either separately or together. In any case, the biological nature of the wastewater treatment entails a microbiological complexity which is sometimes difficult to handle. This microbiological complexity is potentially the main cause of operational problems in world-wide WWTPs. When the balance among microbiological populations within these biological systems becomes perturbed by operational conditions or by the changing influent characteristics, severe problems may appear with their related economical and environmental consequences.

The main biological degradation processes (AS and AD) have been successfully modelled in a mechanistic way resulting in widely spread models. Nevertheless, these models still have some limitations when describing operational problems of microbiological origin (for example, filamentous bacteria proliferation). These limitations become especially important when evaluating simulation results since conditions that would promote the growth of undesirable species have no effect in the model. Simulation results performing well from an economical and environmental point of view could, when confronted with reality, result in suitable conditions for severe operational problems of microbiological origin.

Artificial intelligence techniques have shown to be useful when dealing with complex environmental problems. Therefore, this sort of techniques represents a suitable complement to the mechanistic modelling of operational problems of microbiological origin.

The main objective of this thesis is to develop a knowledge-based model, which integrates mathematical modelling and qualitative aspects, to simulate risk of plant-wide operational problems of microbiological origin. The main operational problems of microbiological origin have to be included. The most relevant variables for each operational problem of microbiological origin have to be identified. The risk model has to provide new criteria for simulation performance evaluation and has to be platform independent to be applied to a wide variety of simulation platforms.

Firstly, the development of the risk model is presented divided basically between the AS and the AD risk model. For each one, a different development procedure has been performed taking into account the availability of real data. In the case of the AS risk model, heuristic knowledge from experts and literature has been translated into decision trees. These trees have been afterwards implemented in a fuzzy logic rule-based system to infer a risk index for the main operational problems of microbiological origin (i.e. filamentous bulking, biological foaming and rising sludge). Next, the system has been extended with the risk of deflocculation and the effect of temperature on *Microthrix parvicella*. With regard to the AD risk model, real data from a pilot plant provided the basis for the development of the model. A data mining technique based on artificial neural networks is applied to select the most relevant variables. This method is first applied to the acidogenic states, a well-known operational problem of the AD. Then, the same method is applied to biological foaming of the AD. This finally shows the relevant variables related to biological foaming which, combined with some knowledge from the literature, results in the input variables for the AD risk model. Latterly, the extracted

knowledge is implemented in a fuzzy logic rule-based system to be integrated with the AS risk model.

The final risk model is applied and evaluated in the Benchmark Simulation Models (BSMs). BSM1 provides an example of how the AS risk model responds to changes in operational parameters and a first example of control strategies comparison in different weather influent scenarios. In terms of BSM1_LT the AS risk model filter and temperature effect is evaluated. The analysis of four different time constants shows that the 3-day provided a more feasible interpretation of the risk model results. The profiles of the risks show that the filter is valuable when taking into account the slow dynamics related to some of the operational problems of microbiological origin. The inclusion of temperature to represent the seasonal dynamics in BSM1_LT allows to test the extension of the AS risk model with temperature applied to *Microthrix parvicella* related risks. The results show that the AS risks related to *Microthrix parvicella* were increased during winter periods and decreased during summer showing a behaviour according to what is stated in the literature. BSM2 allows to test the whole risk model focusing in the AD part. Firstly, general results are presented in an open-loop case study showing the profile for the risk of foaming in AD. Secondly, variation of the main operational parameters show the influence of both external recycle and waste sludge flow rates in the FAD risk. Next, two control strategies affecting the AD organic loading rates are tested. The results illustrate that a control strategy with a control of the TSS in the biological reactors causes a higher variation in the AD loading rates increasing the risk of foaming in the AD. Following, the results in a plant-wide basis are presented comparing the open-loop case with four different control strategies showing the influence of the external carbon sources on the risk of foaming in the AD.

Discussion is also provided about the risk model advantages, limitations and considerations related to its validation and future research. The final conclusions drawn from this thesis are stated at the end immediately followed by the references. Finally, the MATLAB® files to apply the risk model to the different BSM layouts are provided.

RESUM

Els sistemes de fangs activats i de digestió anaeròbia són els més freqüentment utilitzats inclosos a les EDAR, ja sigui conjuntament o per separat. En qualsevol cas, la naturalesa biològica del tractament d'aigües residuals implica una complexitat microbiològica difícil de gestionar. Aquesta complexitat microbiològica és la principal causa dels problemes operacionals a les EDAR de tot el món. Quan l'equilibri entre les poblacions de microorganismes dins d'aquests sistemes resulta pertorbat per les condicions d'operació o per les canviants característiques de l'afluent, greus problemes operacionals poden aparèixer amb les seves respectives conseqüències econòmiques i ambientals.

Els principals processos de degradació biològica (fangs activats i digestió anaeròbia) han estat modelats mecanísticament amb èxit en uns models àmpliament acceptats. No obstant, el modelat mecanístic del tractament biològic de les aigües residuals encara té algunes limitacions quan es modelen problemes operacionals d'origen microbiològic (p. ex. proliferació de bacteris filamentosos). Aquesta limitació esdevé especialment important quan s'avaluen resultats de simulació donat que les condicions que promouen el creixement d'espècies no desitjades no tenen un efecte en el model. Uns bons resultats de simulació des d'un punt de vista econòmic i ambiental en ser confrontats amb la realitat podrien resultar en unes condicions adequades pel desenvolupament de problemes operacionals greus d'origen microbiològic.

Les tècniques de la intel·ligència artificial han demostrat ser útils quan es tracta amb problemes ambientals complexes. Per tant, aquest tipus de tècniques representen una alternativa fiable al modelat mecanístic dels problemes operacionals d'origen microbiològic.

El principal objectiu de la present tesis és desenvolupar un model basat en el coneixement que integri aspectes numèrics i qualitatius per simular el risc de problemes operacionals d'origen microbiològic en planta completa. Els principals problemes operacionals d'origen microbiològic han de ser inclosos. Les variables més importants per a cadascun dels problemes operacionals d'origen microbiològic han de ser identificades. El model de risc ha de proporcionar nous criteris per a l'avaluació dels resultats de simulació i ha de ser independent de la plataforma utilitzada per poder ser aplicat a diferents plataformes de simulació.

Primerament, es presenta el desenvolupament del model de risc dividit bàsicament entre els models de risc dels fangs actius i de la digestió anaeròbia. Cadascun d'ells s'ha desenvolupat de diferent manera tenint en compte la disponibilitat de dades reals. En el cas del model de risc per als fangs activats només coneixement empíric d'experts i de la bibliografia ha estat transformat en arbres de decisió. Després, ha estat implementat en un sistema en lògica difusa basat en regles per inferir un índex de risc per als principals problemes operacionals d'origen microbiològic, és a dir, esponjament del fang filamentós, escumes biològiques i desnitrificació incontrolada. A continuació, el sistema s'ha ampliat amb el risc de desfloculació i l'efecte de la temperatura sobre la *Microthrix parvicella*. Pel que fa al model de risc de la digestió anaeròbia, dades reals obtingudes d'una planta pilot han estat la base per al desenvolupament del model. Una tècnica de mineria de dades basada en xarxes neuronals va ser aplicada per seleccionar les variables més importants. Aquest mètode va ser primerament aplicat al problema

dels estats acidogènics, un problema operacional ben conegut de la digestió anaeròbia. Aleshores, el mateix mètode és aplicat a les escumes biològiques de la digestió anaeròbia. Finalment, això proporciona unes variables importants relacionades amb les escumes biològiques que, més tard combinades amb coneixement de la bibliografia resulta en les variables d'entrada per al model de risc de la digestió anaeròbia. Més tard, aquest coneixement extret és implementat en un sistema expert basat en lògica difusa per a ser integrat amb el model de risc dels fangs activats.

El model de risc final és aplicat i avaluat amb els Benchmark Simulation Models (BSMs). El BSM1 proporciona un exemple de com el model de risc de fangs activats respon als canvis en els paràmetres operacionals i un primer exemple de comparació d'estratègies de control amb diferents escenaris. Pel que fa al BSM1_LT s'avaluen el filtre del model de risc dels fangs actius i l'efecte de la temperatura. L'anàlisi de quatre constants mostra que la constant de 3 dies proporciona una adequada interpretació dels resultats del model de risc. Els perfils dels riscos mostren que el filtre és indicat per tenir en compte les lentes dinàmiques relacionades amb els problemes operacionals d'origen microbiològic. La inclusió de la temperatura per representar les dinàmiques estacionals en el BSM1_LT permet comprovar l'extensió del model de risc dels fangs actius amb la temperatura aplicada als riscos relacionats amb la *Microthrix parvicella.* Els resultats mostren que els riscos dels fangs actius relacionats amb la *Microthrix parvicella* s'incrementen durant els períodes d'hivern i disminueixen durant l'estiu mostrant un comportament d'acord amb els que apareix a la bibliografia. El BSM2 permet comprovar tot el model de risc centrant-se en la part de la digestió anaeròbia. Primerament, es presenten els resultats generals en un cas d'estudi amb llaç obert mostrant el perfil del risc d'escumes biològiques en digestió anaeròbia. En segon lloc, la variació dels principals paràmetres operacionals mostra la influència del cabal de recirculació externa i del cabal de purga en el risc d'escumes biològiques en el digestor. A continuació, es mostren els resultats de dues estratègies de control que afecten la càrrega orgànica en el digestor anaerobi. Els resultats mostren com demostren que una estratègia de control dels sòlids en els reactors biològics causa una variació més alta de les càrregues orgàniques incrementant el risc d'escumes biològiques en el digestor. Després, els resultats des d'un punt de vista de planta completa es presenten comparant el cas de llaç obert amb quatre estratègies de control diferents mostrant la influència de la font externa de carboni en el risc d'escumes biològiques en el digestor.

També es presenta una discussió sobre els avantatges, validació, treball futur, limitacions i consideracions relacionades amb l'implementació en d'altres configuracions del Model de Risc. Les conclusions finals extretes de la present tesis s'exposen al final, seguides per les referències i finalment es proporciona el codi per implementar el model de risc en MATLAB®.

CONTENTS

CHAPTER 1

INTRODUCTION

1. Introduction

1.1 Problem statement

Mathematical modelling of biological systems has become a powerful tool for design, optimization and control of wastewater treatment plants (WWTPs). Indeed, both the activated sludge (AS) and the anaerobic digestion (AD) systems have been already described in widely accepted mechanistic models (ASM family – Henze *et al.*, 2000- and ADM1 –Batstone *et al.*, 2002-) and even integrated in plant-wide models. Models have a wide range of applications, from the objective evaluation of control strategies to statistical analysis, such as uncertainty analysis (Ma *et al.*, 2006; Flores-Alsina *et al.*, 2009a).

Although AS and AD systems can be modelled, the biological nature of the wastewater treatment entails a microbiological complexity which is sometimes difficult to handle. This microbiological complexity can be the origin of operational problems in many real WWTPs. When the balance among microbiological populations within these biological systems becomes perturbed by operational conditions or by the changing influent characteristics, severe operational problems may appear with their related economical and environmental consequences. Despite this microbiological complexity, the systems must be controlled in order to achieve efficient pollution removal in order to fulfil the legal discharge requirements with minimum costs and minimal sludge production (Copp, 2002).

In any case, effluent violations and economical loss due to the appearance of operational problems of microbiological origin may occur. These may produce a biased evaluation of simulated WWTP performances, since operational problems of microbiological origin cannot be taken into account in the current mechanistic models. There have been some attempts to mechanistically model the mechanisms for the development of filamentous microorganisms, but there is not a general and validated model yet and none of the proposed models are able to predict sludge settling characteristics (Martins *et al.*, 2004). Despite the lack of knowledge on the specific mechanisms of the filamentous bacteria that causes operational problems of microbiological origin, there are a lot of experiences and sometimes even real data related to this sort of imbalances.

1.2 Hypothesis

Although there is a lack of knowledge on the specific dynamics and kinetics to model the development of operational problems of microbiological origin (filamentous bulking, AS and AD foaming, deflocculation and rising sludge), a lot of experiences and case studies exist in real WWTPs. Therefore, there is enough empiric knowledge to define the different conditions that can cause these operational problems of microbiological origin and their effects on the WWTP performance.

Some of the conditions that can lead to operational problems of microbiological origin are related to variables that can be modelled or estimated in the standard AS and AD models.

The qualitative cause-effect relationships for the development of operational problems of microbiological origin are not enough to build a general deterministic model.

However, these relationships and heuristic knowledge can be used to build a qualitative model, based on AI techniques, to assess the favourable conditions leading to microbiology-related operational problems. The performance of such a knowledge-based model can be evaluated within a simulation platform.

Besides when real data are available, some AI (soft computing) techniques can be of high interest to find relevant information about the relationship between a given operational problem of microbiological origin and its related variables.

Finally, we state that operational units of the WWTPs do not act as independent units, i.e. AS systems interact with AD systems. Therefore they form integrated systems implying that (control) actions taken in one part may have an impact in others. A plant-wide control perspective should be taken into account. Likewise, simulation of operational problems of microbiological origin should also be considered at a plant-wide scale i.e. some problems appearing in one system may affect others.

1.3 Contributions

The main contribution of this thesis is a simulation complement to the still limited mechanistic modelling of filamentous bacteria. This alternative consists of a knowledge-based risk model developed to alert of operational problems of microbiological origin that cause imbalances during the simulation results evaluation within the current AS and AD models. Such a system, based on heuristic knowledge, provides a risk index that includes the four main operational problems of microbiological origin in the AS systems: (i) filamentous bulking, (ii) foaming, (iii) rising sludge and (iv) deflocculation. A risk model is also presented for the AD which considers the main operational problem of microbiological origin within the AD system, biological foaming.

The knowledge related to the main operational problems of microbiological origin embodied in the AS risk model is provided. The fuzzy logic features to build the AS risk model are also provided; meaning membership function (MF) ranges and rules to be applied to assess each risk. For the development of the AD risk model, a methodology to select the most related variables for AD biological foaming is presented, which has shown to be of interest for the study of microbiology related imbalances. The information extracted from data is afterwards combined with the existing knowledge in the literature to finally integrate both approaches.

The full implementation and application (including the fuzzy implementation of MFs and rules) of the risk model to the BSM (Copp, 2002) is presented for use in any of the BSM simulation platforms (i.e. MATLAB™ & Simulink™, FORTRAN, WEST®, GPS-X™). The risk model is afterwards implemented and applied to the different BSM layouts (i.e. BSM1, BSM1_LT and BSM2).

When evaluating simulation results within the BSM, the risk model offers a third dimension to be added to the environmental and economical performance.

My contribution on the whole work starts on the extension of the AS risk model and continues with the whole development of the AD risk model, knowledge acquisition, selection of relevant variables for foaming in AD, implementation in fuzzy logic. The implementation ofin the Benchmark Simulation Model and the different applications for

evaluation of the different risk models through simulations presented in this thesis were also part of my work. Last, I performed the first approach for validation of the AD risk model with real data. The whole work presented in this thesis has been published in seven journal papers and in four international conferences. Among these publications, the contributions pointed above appear in Dalmau *et al.* (2009a), Dalmau *et al.* (2009b), Dalmau *et al.* (2009c) Dalmau *et al.* (2008), Dalmau *et al.* (2007).

1.4 Outline

The structure of the present thesis is divided as follows:

In **Chapter 2**, a literature review is provided with a description of the main biological systems (AS and AD) in WWTPs. Following that, there is a section devoted to the main operational problems of microbiological origin in both AS and AD systems. They are all described with their causes, development and effects on the WWTP. Afterwards, a brief review of mathematical modelling is presented from AS and AD to plant-wide models. Last but not least, the attempts to mechanistically model filamentous bacteria are presented with its related limitations to finally present possible alternatives to the mathematical modelling of operational problems of microbiological origin. In **Chapter 3** the objectives of this thesis are presented.

Chapter 4 describes the different methods used in this thesis. This includes the ASM1, ADM1 and the BSM family (BSM1, BSM1_LT and BSM2). This chapter also introduces a full description to implement a fuzzy logic rule-based system and description of the artificial neural networks (ANNs) used.

The results of this thesis are comprised by **Chapters 5** and **6**. In **Chapter 5,** the development of the AS risk model is presented with its implementation in fuzzy logic and the outcomes the model provides. The AS risk model extensions are explained to include the deflocculation and the effect of temperature. The AD risk model development is explained together with its implementation and outcomes. In **Chapter 6**, the implementation showing the model variables used to calculate the inputs of the risk model in the different BSMs layouts is presented. Then, the performance of the risk model is evaluated in open-loop scenarios, changing operational parameters and finally, in closed-loop scenarios. At the end, in **Chapter 7** a general discussion presenting implications, possibilities and future work on the risk model is provided.

Chapter 8 presents the conclusions drawn from the results of the thesis. **Chapter 9** provides the references and finally an **Annex** is provided with the MATLAB^{TM} scripts for direct implementation of the risk model in the BSM.

CHAPTER 2

STATE-OF-THE-ART

2. State-of-the-art

2.1 Wastewater Treatment Plants

WWTPs became important questions at the beginning of the 20th century and are nowadays a key factor in issues to deal with water quality. In an early stage the wastewater treatment was centred in the secondary treatment by means of the AS system. Over time, the variety of pollutants and the different requirements in water quality caused the system to evolve through different technologies and configurations. Besides, the need to treat the sludge produced in WWTPs caused the inclusion of AD systems in new or sometimes existing facilities creating the concept of plant-wide WWTP. As complex biological systems, AS and AD systems are subject to specific problems related to the microbiological community. These operational problems of microbiological origin have large economical and environmental consequences for the WWTP.

The increasing complexity inherent to the evolution of the WWTP presented new challenges to the research community and soon, the need of mathematical models to design, assess, predict and control the different systems arose. Thus, just as WWTPs did, mathematical modelling evolved to represent the AS processes first and, AD processes recently. As a last step on the mathematical modelling of wastewater treatment, mathematical models have been integrated to represent the plant-wide WWTP and nowadays the evolution is moving towards complete catchments models. The mathematical modelling research has also paid attention to the operational problems of microbiological origin and some attempts to model these matters were performed. Still, there is a long way to go in which AI can provide tools to overcome the obstacles.

In this chapter, the main wastewater and sludge treatment systems are explained together with the related operational problems of microbiological origin. Following that there is a brief description of the evolution of the respective mathematical models for both the systems and the above mentioned problems. At the end, a description of useful tools to tackle the modelling of this sort of problems is given.

2.1.1 Activated Sludge system

The combined efforts of engineers, chemists and biologists to improve existing wastewater treatment bore fruit in 1914, at a time that coincided with the end of the industrial revolution, when Ardern and Lockett developed the first AS system. Nowadays, among all the available wastewater treatment systems, the AS system is the most common and represents the most important system in a WWTP.

2.1.1.1 System description

An AS system is a complex biological system in which organic matter and nutrients (nitrogen - N - and phosphorous - P -) are removed from the wastewater. The basic system for organic matter removal consists of a biological reactor where O_2 is selectively supplied and used by the microbial consortia (i.e. biomass, solids, mixed liquor suspended solids - MLSS - and/or sludge) to enable it to grow and reproduce by consuming the substrate (i.e. pollutants) present in the wastewater. The treated water is subsequently separated from the biomass in the secondary settler. The secondary settler

has another significant function, consisting of compacting the sludge at the bottom so that it can be efficiently returned to the biological reactor and maintaining the biomass in the reactor at a constant level (return activated sludge - RAS -; **Figure 2.1**). A fraction from the RAS is removed from the system to avoid the excess production of biomass; this is the waste activated sludge (WAS).

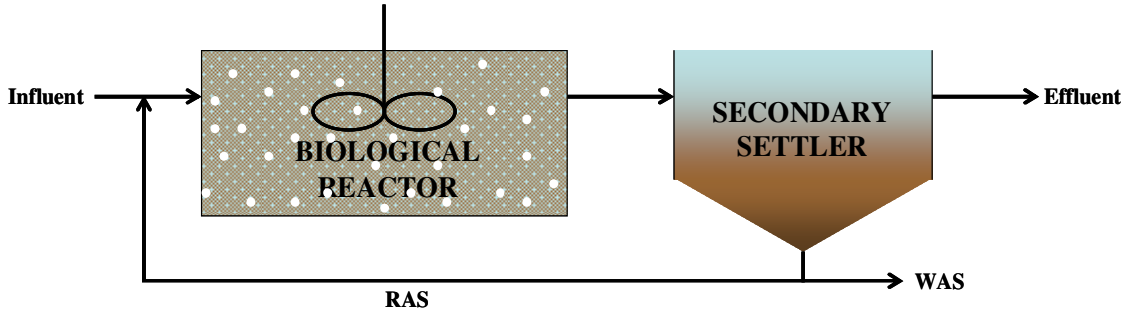

Figure 2.1. An aerobic AS layout.

In an aerobic system, influent wastewater is mixed in the biological reactor through stirring (mechanically or with O_2 that is supplied). In this way, the biomass uses the supplied O_2 to oxidise organic matter and remove it from the wastewater. From this organic matter oxidation, microorganisms obtain the necessary energy to develop their vital functions, including reproduction (WEF, 1996). Moreover, they can extract energy by means of endogenous respiration. The essential process can be summarised in terms of three reactions (Metcalf and Eddy, 2003).

Oxidation:

$$\text{CHONS (organic matter)} + O_2 + \text{bacteria} \rightarrow CO_2 + H_2O + NH_3 + \begin{matrix}\text{other}\\ \text{end}\\ \text{products}\end{matrix} + \text{energy}$$

Synthesis:

$$\text{CHONS (organic matter)} + O_2 + \text{bacteria} + \text{energy} \rightarrow C_5H_7NO_2\ \text{(new cells)}$$

Endogenous respiration:

$$C_5H_7NO_2\ \text{(cells)} + 5O_2 \rightarrow 5CO_2 + NH_3 + 2H_2O$$

Nitrogen removal in AS facilities is performed in a two-phase biological process: nitrification and denitrification. In nitrification, ammonium is converted aerobically to nitrate in two steps: first to nitrite, then to nitrate. In denitrification, nitrate produced in the previous phase, together with the nitrate contained in the wastewater, are converted in an anoxic process to N_2.

Nitrification:

$$NH_4^+ + \frac{3}{2}O_2 \rightarrow NO_2^- + H_2O + 2H^+$$

$$NO_2^- + \frac{1}{2}O_2 \rightarrow NO_3^-$$

Denitrification:

$$C_{10}H_{19}O_3N + 10\,NO_3^- \rightarrow 5N_2 + 10CO_2 + 3H_2O + NH_3 + 10OH^-$$

Phosphorous removal is achieved in WWTPs in two stages by phosphate accumulating organisms (PAOs). In the first, anaerobic stage, the PAOs assimilate organic matter by accumulating storage products, and phosphate is released. In the second, aerobic/anoxic stage, storage products are consumed for cell growth using the energy from the storage products' oxidation to form polyphosphates, which take phosphate from the media. The final result is that more P is taken up than released and thus it ends up inside the PAOs. When the sludge is removed from the system through the WAS, P is as well.

2.1.1.2 Operational parameters

Because optimal nutrient removal in the AS system depends on living microorganisms, it is influenced by the environmental changes affecting such microorganisms. A successful operation can be achieved only if operators are able to recognise system changes and trends and make the proper decisions to successfully counteract potentially harmful changes.

AS system control consists of reviewing present and historical operating data and laboratory test results so that the proper operational parameters that provide the best performance at the lowest cost can be selected. For secondary treatment, the most important of these include DO, RAS, WAS and sludge retention time (SRT; WEF, 1996).

Dissolved oxygen (DO): DO is particularly important in the aerobic treatment of wastewater. It must be dissolved in sufficient quantities to keep the organisms active and, when required, the mixture in the biological reactor must be stirred enough for the solids in it to be suspended. Typically, if there is sufficient O_2 to oxidise the organic matter, the mixing requirements will be met too. Depending on the process, more or less DO will be required, but a typical reference value is 2 mg $O_2 \cdot L^{-1}$. For anaerobic and anoxic processes it has to be as close to 0 mg $O_2 \cdot L^{-1}$ as possible.

When the DO is limited, undesired microorganisms (see **Section 2.2.1. Activated sludge**) may predominate, thereby affecting the sludge quality and the settling process. On the other hand, over-aeration, apart from being a pointless waste of energy, can result in the break up of the flocs that are formed and consequently bad settling properties.

Food to Microorganisms ratio (F/M): This is an operational parameter commonly used to characterise process design and operating conditions. It expresses the ratio between incoming BOD and the amount of biomass (**Equation 2.1**). It is expressed in g substrate (BOD) · g biomass^{-1} · d^{-1}. Typical F/M values range from 0.04 to 1.0 g · g^{-1} · d^{-1}. A good F/M ratio will ensure that the microorganisms use most of the substrate supply in the wastewater.

$$F/M = \frac{BOD_{in}}{V \cdot MLVSS} \qquad \textbf{(Eq. 2.1)}$$

where

BOD_{in} = Biochemical oxygen demand in the inflow ($g \cdot d^{-1}$);
V = Volume of the reactor (m^3);
MLVSS = Mixed liquor volatile suspended solids in the reactor ($g \cdot m^{-3}$).

Return Activated Sludge (RAS): In a properly operated AS system the settling is an essential part since RAS control aims to maintain the optimal concentration of MLSS in the reactor. The settling solids form a sludge blanket on the bottom of the secondary settler and allow the return of a more concentrated flow, thus reducing pumping costs. The blanket depth increases as the biomass entering is higher than the biomass removed through the WAS. There are three ways of working with RAS according to WEF (1996):

- At a constant rate. This results in varying MLSS concentration in the reactor. During peaks of inflow rates (Q_{in}) the sludge can accumulate in the secondary settler and act as an MLSS reservoir. On the other hand, when the Q_{in} is low, MLSS will accumulate in the biological reactor. This is not a good option for WWTPs with high Q_{in} variability.

- At a constant percentage of the Q_{in}. This tends to provide more or less constant sludge blanket and MLSS concentration levels in the biological reactor. RAS can be kept directly proportional to the Q_{in} to maintain the MLSS concentration level constant in the reactor. This means that when the Q_{in} peaks there is a risk of losing MLSS through the effluent. Otherwise, the RAS can be kept inversely proportional to the Q_{in}, with the aim of keeping the hydraulic load on the secondary settler constant.

- At a varying rate to optimise the secondary settler conditions. Two options are available here. The objective of the first is to keep the sludge blanket level as low as possible so as to have a high MLSS concentration in the reactor. The second option is suitable for optimising the concentration and retention time in the secondary settler. In order to set the proper Q_r value, there are different alternatives depending on sludge blanket level, sludge quality, mass balance in the secondary settler, mass balance in the reactor, etc.

It is worth highlighting that RAS will influence another important parameter, F/M, since it allows the MLVSS in the reactor to increase or decrease.

Waste activated sludge (WAS): WAS is used to control the solids inventory in the system. According to WEF (1996) WAS mainly affects effluent quality, the growth rate and the type of the microorganisms, O_2 consumption and settleability. As is made clear, there is a close relationship between the WAS and F/M ratio given that the microorganisms consume the biochemical oxygen demand (BOD) and chemical oxygen demand (COD). The amount of biomass increase in one day is the net growth rate. The WAS is the manipulated variable when the objective is to control solids retention time (SRT, see below) and/or F/M. However, this steady-state is only approximative given the variable nature of the influent wastewater BOD and of the microorganism population.

Solids retention time (SRT): This represents the average period of time that the biomass remains in the system before it is wasted either intentionally or unintentionally (**Equation 2.2**). SRT affects treatment performance, biological reactor volume, SP and O_2 requirements. SRT is calculated as the relationship between the biomass present in

the reactor and the amount of biomass which is wasted and/or lost through the effluent. SRT is defined by Metcalf and Eddy (2003) as follows:

$$SRT = \frac{V \cdot MLVSS}{Q_{eff} \cdot MLVSS_{eff} + Q_w \cdot MLVSS_w} \quad \textbf{(Eq. 2.2)}$$

where
V = reactor volume (m^3);
MLVSS = concentration of biomass in the reactor (g MLVSS· m^{-3});
Q_{eff} = effluent flow rate ($m^3 \cdot d^{-1}$);
$MLVSS_{eff}$ = concentration of biomass in the effluent (g VSS· m^{-3});
Q_w = WAS flow rate ($m^3 \cdot d^{-1}$);
$MLVSS_w$ = concentration of WAS (g VSS· m^{-3}).

From the SRT equation it is easy to see how WAS influences SRT and, as stated above, its influence on the type and growth rate of microorganisms. Only those microorganisms with growth rates lower than that of the SRT are selected. Increasing WAS will lower the SRT (i.e. microorganisms will spend less time in the system), and vice versa. It is important to note that the SRT also decreases as a result of less MLVSS (MLVSS in **Equation 2.2**) being present in the system. For instance, increasing WAS is also a way to increase the F/M ratio when the incoming BOD load is low.

Internal recycle flow rate (Q_{intr}): Depending on the system configuration, internal recycle streams are needed to provide required nutrients at certain stages of the system. For instance, in nutrient removal processes organic matter and nitrate are required for denitrification. Thus, when designing an AS system for nitrogen removal the anoxic part is usually placed first, before the aerobic one, since otherwise there might not be enough organic matter available for denitrification because most of it would have been consumed beforehand. This way, nitrate is removed after getting the benefit of the incoming organic matter, while the ammonium remains unchanged. Later, in the aerobic phase, the ammonium is nitrified to nitrate while the nitrate remains unchanged. The Q_{intr} stream serves as the mean to bring the nitrate back to the anoxic zone to be denitrified.

2.1.1.3 Configurations

Simultaneously with the nutrient removal requirements, new configurations of AS systems were developed. Depending on the nutrient to be removed, various different configurations can be chosen for optimal wastewater treatment. As will be seen, aerobic treatment is suitable for carbon removal whereas for N and/or P removal anoxic and/or anaerobic conditions are required. Several examples of typical configurations for N and/or P removal follow below.

Oxidation ditches: These have to be large enough for there to be anoxic and aerobic zones in the same reactor. There are different ditches (carrousel of alternate phases), that work in anaerobic or anoxic conditions depending on the requirements, in which feeding is changed from one ditch to another after certain periods of time. The most common design is the Biodenitro, which operates with four alternate phases, where the feeding is variable and there are anoxic and aerobic conditions in each ditch.

Whurmann: This consists of a single step with an aerobic zone followed by an anoxic zone, so that nitrification takes place before denitrification. Nevertheless, it is necessary to bypass some of the feeding to the anoxic biological reactor and/or add an external carbon source (EC) to be able to denitrify in the anoxic biological reactor.

Ludzack-Ettinger: This inverts the order of the biological reactor to avoid the use of an EC: first the anoxic zone and then the aerobic. Since nitrate is produced in the aerobic zone, it is necessary to return nitrates to the anoxic zone so that they can be denitrified; this flow rate is the internal recycle of a modified Ludzack-Ettinger.

Bardenpho: This consists of four biological reactors in a single step. The first two reactors (anoxic-aerobic + internal recycle) are equivalent to a modified Ludzack-Ettinger. With the aim of completely removing all the nitrate, the third biological reactor (anoxic) removes nitrate that has not been recycled to the first biological reactor, using endogenous respiration to get the organic matter to complete the denitrification. Finally the last biological reactor can remove any remaining organic matter as well as help the P accumulation that takes place in aerobic conditions. No P is removed with the classic Bardenpho configuration but the five-stage Bardenpho includes an anaerobic biological reactor ahead of the first anoxic reactor.

A/O: The main feature of this is the use of multiple-stage anaerobic and aerobic reactors. In this system there is no nitrification, and the anaerobic retention time needed to provide the selective conditions for biological phosphorus removal is 30 minutes to one hour.

A^2/O: This is a modification of the A/O system and provides an anoxic zone for denitrification with an internal recycle from the aerobic to the anoxic stage.

UCT (University of Cape Town): The UCT system is similar to the A^2/O system with two exceptions. The RAS is recycled to the anoxic stage instead of the aeration stage, and the internal recycle is from the anoxic stage to the anaerobic stage, in order to avoid any negative effects on the initial phosphorus removal efficiency from the nitrate present in the RAS.

SBR (Sequencing Batch Reactor): This is a fill-and-draw AS system. Whereas in conventional AS systems the process is carried out in a spatial dimension, in an SBR it is carried out in a time dimension (i.e. all the steps take place in the same biological reactor). As currently designed, all SBR systems have several steps in common: fill, react, settle and draw. During settle and draw sludge wasting takes place. This system is versatile, so that depending on the conditions provided for the biological reactor in the react phase, one or more nutrients will be treated. In other words, for C removal or nitrification, the reaction step has to include an aerobic phase, for denitrification an anoxic phase, and for P removal an anaerobic phase.

Membrane bio-reactors: The relevant feature of this technology is that it uses membranes with small pores. These allow ultra-filtration obtaining effluents with a high quality regarding the solids discharge limits. Its main advantage is that they are very compact systems. On the other hand, they have high operational costs. One of the consequences of this technology is the membrane fouling which requires periodical backwashes and additional maintenance.

SHARON: This is a continuous process in which a partial oxidation of ammonium takes place in a continuous stirred tank reactor (CSTR). Its operation requires high temperatures (35-37ºC) and a relatively low hydraulic retention times (HRT). These operational conditions promote the growth of ammonium-oxidizing bacteria, while the lower growth rate of the nitrite-oxidizing bacteria leads to its wash-out.

Microbial fuel cell (MFC): This technology also known as biological fuel cell, converts chemical energy, available in a bio-convertible substrate such as wastewater pollutants, directly. As the bacteria consume the pollutants, they shed electrons, which flow through a circuit and generate electricity. In the process, pollutants are broken down, resulting in clean water.

2.1.2 Anaerobic Digestion system

AD involves the breakdown of organic matter by the concerted action of a wide range of microorganisms in the absence of O_2. AD is a set of natural processes that take place in a variety of anaerobic environments, such as the intestinal tract of animals, marine and fresh water sediment, sewage sludge, paddy fields, water logged soils and in the region of volcanic hot springs and deep sea hydrothermal vents. To date, the biogas process has been widely applied in the field of waste and wastewater treatment, often coupled with energy recovery. Currently, AD also represents one of the most common alternatives for sludge treatment.

The system consists of a complex series of reactions, the sum of these being a fermentation which converts a wide array of substrate materials with carbon atoms at various oxidation/reduction states to one-carbon molecules in the most oxidised (CO_2) and the most reduced (CH_4) states. Minor quantities of (N_2), hydrogen (H_2), ammonia (NH_3) and hydrogen sulphide (H_2S; usually less than 1% of the total gas volume) are also generated.

The interest in the process is mainly due to the following reasons:

- The production of biogas can be used to generate different forms of energy (heat and electricity).
- Compared to aerobic systems less energy is required since aeration is not needed.
- Higher volumetric loadings are accepted in AD systems; therefore, smaller reactor volumes and less space may be required for treatment.

However, there are a number of disadvantages linked to AD systems:

- Longer start-up time (months) to obtain the necessary biomass inventory compared with the AS system (days).
- Biological N and P removal is not possible. Hence, further treatment processes are required in these cases.
- Reaction rates are more sensitive to low temperatures.
- AD may require alkalinity addition, thereby decreasing the net energy benefit.

- It is more susceptible to upsets due to toxic substances.

2.1.2.1 Process description

The general model for the degradation of organic material (polymeric substances like carbohydrates, protein, and fats) under anaerobic conditions operates principally with three main groups of bacteria which together convert the organic material to methane (CH_4), CO_2 and water. The AD process involves three main steps (**Figure 2.2**): (i) hydrolysis; (ii) fermentation; (iii) methanogenesis (Stafford *et al.*, 1980).

Hydrolysis: The most important components in sludge/manure are polymeric compounds such as carbohydrates, protein and fats. Hydrolysis of these compounds into smaller units is the first step of the AD process. Different groups of fermentative bacteria (Group I) can degrade complex polymeric compounds in the waste into oligomers and monomers by excreting extracellular enzymes. Proteolytic bacteria produce proteases that catalyse the hydrolysis of proteins into amino acids, the cellulytic and xylanolytic bacteria degrade cellulose and xylan (both carbohydrates) to glucose and xylose, and finally the lipolytic bacteria degrade lipids to glycerol and long-chain fatty acids.

Fermentation (acidogenesis): Next, the hydrolysis products are absorbed by the fermentative bacteria (Group I). The fermentation products are smaller compounds such as acetate and other fatty acids, alcohols and H_2.

Short-chain fatty acids longer than acetate and alcohols are oxidised by the hydrogen-producing acetogenic bacteria (Group II), resulting in the formation of H_2, acetate, formate and CO_2.

In an AD system that is functioning well, most of the organic material will be transformed directly by the fermentative bacteria into methanogenic substrates (H_2, CO_2 and acetate). However, a significant part (approximately 30%) will be transformed into other lower fatty acids and alcohols. This part will be larger if the system is out of balance, i.e. if the H_2 formed is not consumed fast enough.

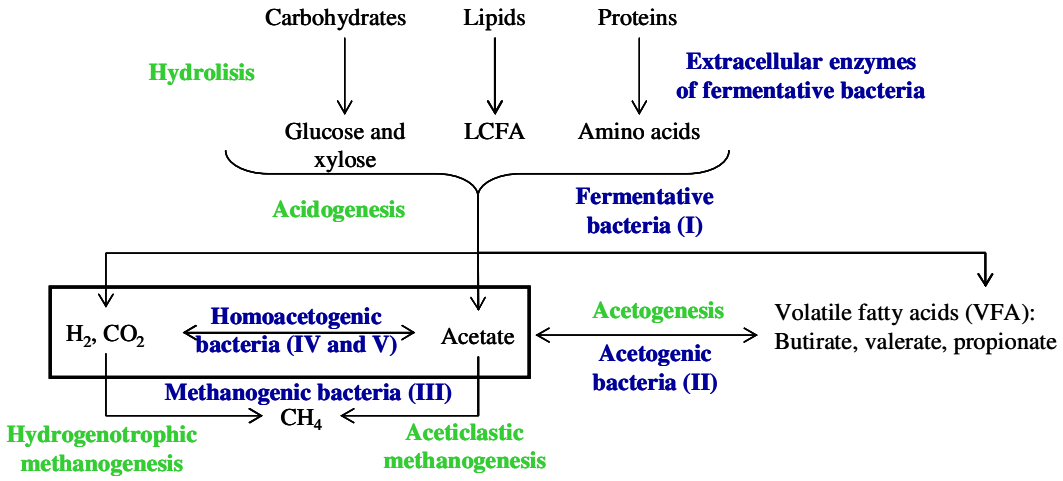

Figure 2.2. AD process diagram.

Methanogenesis: The end products of the metabolism of the fermentative and acetogenic bacteria – acetate, formate and H_2 – are transformed into CH_4 by the methanogenic bacteria (Group III). The most important CH_4 precursor is acetate (70%), while the remaining 30% is formed from H_2/CO_2 or formate. The methanogenic bacteria are divided into two main groups: aceticlastic methane bacteria, degrading acetate, belonging to the genera *Methanosarcina* and *Methanosaeta* (formerly *Methanothrix*), and the hydrogen-consuming methanogens of which an array of genera exists. A number of *Methanosarcina* species can transform H_2 as well as acetate. Substrates of less quantitative importance for methanogens are methanol, methylsulfides, methylamines and some higher alcohols.

This three-step model showing the anaerobic transformation of organic material can be used to provide an overall view, but it does simplify things. A more complete model must take into account the other groups of bacteria which can play a major role under certain conditions.

Homoacetogenic bacteria (Group IV) degrade a large spectrum of substances, e.g. glucose and H_2/CO_2, and produce acetate as the only fermentation end-product.

A special subgroup of homoacetogenic organisms is Group V. These perform the opposite reaction by oxidising acetate to H_2 and CO_2.

2.1.2.2 Operational parameters

Temperature: Choice of temperature and its control are of crucial significance for AD. Temperature is one of the main environmental factors affecting bacterial growth. Anaerobic and aerobic bacteria are affected in the same way. Growth rates increase to a certain limit with temperature, and from this point (the limit for bacteria survival) they start to decrease. But in addition, temperature affects other physical parameters such as viscosity, mass transfer properties, etc. (Whitmore *et al.*, 1985). Most experiments with AD have been performed in the mesophilic (30-40ºC) and in the thermophilic (50-60ºC) temperature ranges (**Figure 2.3**).

Operating in thermophilic as opposed to mesophilic conditions provides a number of advantages:

- Faster digestion rates, reduction of retention time in the plant.
- Smaller volumes required for the same amount of waste.
- Good destruction of pathogenic organisms.
- Greater possibility of separation of solid matter from the liquid phase.
- Better degradation of long-chain fatty acids.
- Less biomass formation compared with the product formation.
- Improved solubility and availability of substrates.

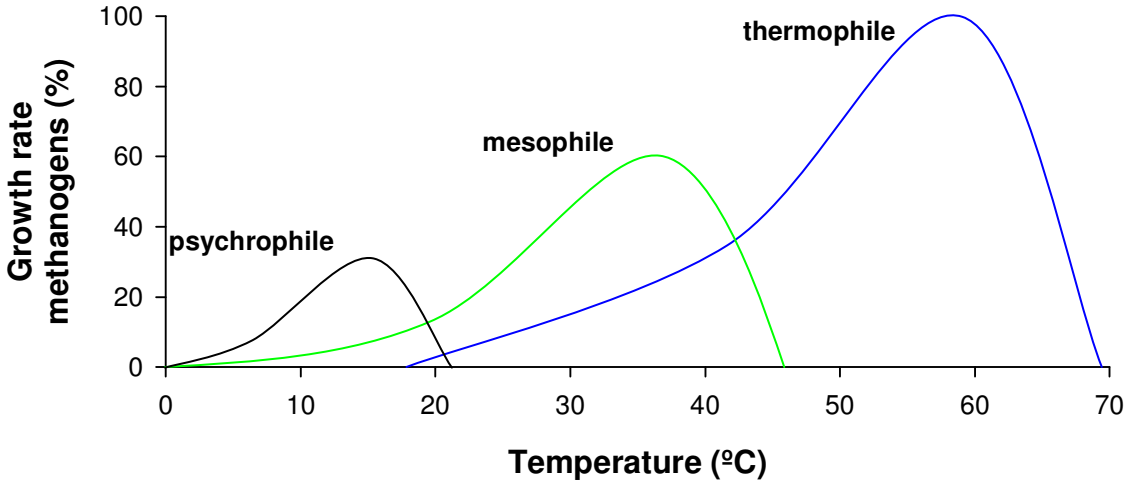

Figure 2.3. Relative growth rate of methanogenic bacteria versus temperature.

Essential disadvantages are:

- Larger degree of instability.
- Demand for larger amount of system energy.
- Greater risk of ammonia inhibition.

The effect of temperature on growth rates can only be seen when the loadings rates are high or retention times are reduced. De La Rubia *et al.* (2006) show how in thermophilic conditions good performances are achieved in spite of reduced SRT.

pH: CH_4 formation is limited to a relatively narrow pH interval, from 5.5 to 8.5 approximately. Most methanogens have an optimum pH of between 7 and 8 while acid-forming bacteria often have a lower optimum level. Apart from the influence of the pH on the growth of the microorganisms, pH can affect other factors such as dissociation of important compounds (ammonia, sulphide, organic acids) of importance for the AD process.

The optimal pH for mesophilic biogas reactors is between 6.5 and 8, and the process is severely inhibited if pH is below 6 or above 8.3. The actual pH value in thermophilic biogas reactors is generally higher than in mesophilic plants, as dissolved CO_2 forms carbonic acid by reaction with water. No specific investigations of the significance of this phenomenon exist. The pH in anaerobic reactors is mainly controlled by the bicarbonate buffer system. Therefore, pH in biogas plants depends on the partial pressure of CO_2 and the concentration of alkaline and acid components in the liquid phase. Ammonia produced during degradation of proteins, or ammonia in the feed stream, for example, can result in an increase in pH.

Organic loading rate (OLR): The OLR can be varied by changing the influent concentration and the flow rate (**Equation 2.3**). Changing the flow rate entails changing the HRT.

$$OLR = \frac{Q_{in,a} \cdot COD}{V} = \frac{COD}{HRT} \quad \textbf{(Eq. 2.3)}$$

where
OLR = organic loading rate (kg COD·m^{-3} ·d^{-1});
COD = chemical oxygen demand (kg COD·m^{-3});
$Q_{in,a}$ = AD inflow rate (m^3·d^{-1});
V = reactor volume (m^3);
HRT = hydraulic retention time (d).

When the anaerobic digester feed is sludge, VS concentration can be used instead of COD concentration to express OLR. Typical loading rates can be from 1.6 to 4.8 kg VS · m^{-3}·d^{-1}. OLR does not usually control the process but organic overloads can occur if feeding exceeds the consumption rate.

2.1.2.3 Configurations

There are several different configurations for anaerobic treatment (Metcalf and Eddy, 2003).

Continuous stirred tank reactor (CSTR): The CSTR is a continuously or frequently mixed reactor, where the fresh substrate is totally mixed with the active reactor content. In- and out-flow of the substrate is on a continuous or semi-continuous basis. One important limitation of these reactors is their retention time. Since the SRT is equal to the HRT, if the HRT exceeds the growth rate of the slowest-growing bacteria the stability of the system can be lost. To solve the problem of biomass retention, other anaerobic systems were developed.

Anaerobic contact process: This consists of a CSTR reactor with a separation recycling stage. The separation unit can be a settler, a filter or a centrifuge. It is essential to keep the particulate matter of the effluent in the reactor. The SRT is kept high to achieve a good degree of degradation while helping to ensure adequate populations of slow-growing bacteria. The problem with this system is the practical separation and concentration of the sludge. It is solved with chemical flocculation, vacuum filter design and system modifications such as degasification, centrifugation, etc.

Fixed bed reactors: Active biomass is immobilised as a film on inert support material (e.g. porous ceramic materials, plastic packings, etc.). The extra-cellular polymers that the micro-organisms produce are the binding that holds the micro-organisms together. The support material affects the growth of bacteria and, therefore, system performance.

Fluidised and expanded bed systems: These are a modified version of the previous configuration. Here, carrier particles are included to retain the biomass. Sand was previously used as a common carrier but it has now been substituted for plastic and other low density particles. The particles, together with the attached biofilm, are fluidised by high influent and recirculation flow rates.

Upflow anaerobic sludge blanket (UASB): Influent is distributed at the bottom of the UASB reactor and travels in an upflow mode through the sludge blanket without any inert carrier. The biomass forms dense aggregates which are retained in the reactor due to their relatively high density. Some UASB reactors have a secondary settler after the anaerobic treatment. The main advantage of UASB reactors is the high volumetric COD loadings compared with other anaerobic systems that they are able to treat, thanks to the development of a dense granular sludge. This immobilisation can be achieved by means

of partial control of the inflow and gas production rates. A UASB consists of a sludge bed, a sludge blanket, a gas-solids separation trap and a settling compartment. The sludge bed is a layer of granulated biomass settled on the bottom. The sludge blanket is a suspension of sludge particles mixed with the gas produced in the process. In the gas-solids separation trap, the gas that is produced is separated from the liquid by the gas-solids separator. A gas-free secondary settling zone is created in the top compartment, where most of the sludge particles that have entered this zone (carried from the bed by gas convection) settle back in the reactor, while the rest, i.e. the smallest, are washed out with the effluent. The UASB system is able to retain a high concentration of biomass with high specific activity and handle high organic loading rates (OLRs) with good COD removal.

Expanded granular sludge bed reactors (EGSB): This type of reactor is characterised by an expanded form of granular sludge, obtained as a result of ultra high flows through the reactor. These reactors are relatively insensitive to suspended solids given the low settling velocity of these solids compared to the superficial liquid velocity of the reactor. The suspended solids do not become hydrolysed to any significant degree due to their short retention time in the reactor. These reactors are efficient at removing soluble organic matter because of the good contact between the influent organic matter and the granular biomass, and they also seem to be effective for low strength wastewaters and at low temperatures.

2.2 Operational problems of microbiological origin

Operational problems of microbiological origin is the general term or classification given to a group of problems occurring within a WWTP. These problems represent one of the most complex issues for efficient operation of a WWTP. Since biological processes involve a wide variety of microorganisms, the inherent complexity of these populations hampers the control of their dynamics. When the equilibrium between populations is broken operational problems can appear. The physical and microbiological causes of each of these problems have been described in several studies and publications (Jenkins *et al.*, 2003; Casey *et al.,* 1995; Wanner, 1994). In a WWTP, operational problems of microbiological origin appear mainly in the biological systems of the facility (i.e. AS and AD).

2.2.1 Activated Sludge

In AS systems, operational problems of microbiological origin are linked to the secondary settling process and result in a drastic decrease in the efficiency of the process, especially regarding TSS. To fully understand some of the AS operational problems of microbiological origin, it is important first to comment on floc formation.

Floc formation: In order to achieve good separation between the biomass and the treated water, the biomass must form compact and dense flocs. Floc-forming bacteria are able to compact to some extent but in order to be dense enough to settle properly they need filamentous microorganisms which can link several flocs together to provide enough weight to ease the gravity settling.

There are two main components in the AS sludge flocs: (i) a mixture of biological components (i.e. bacteria, protozoa, fungi and metazoa) and (ii) a non-biological component, comprising of particles and extracellular polymeric substances which are

the key to floc formation. Flocs are composed of a combination of bacteria belonging to different genera: *Pseudomonas, Achromobacter, Flavobacterium, Alcaligenes, Arthrobacter, Citromonas and Zoogloea* (Jenkins *et al.*, 2003). These and other bacteria can create extracellular polymeric substances. As long as it is an organic polymer, water viscosity increases and the individual cells stick to each other or to solid surfaces, thereby creating large aggregates that can settle easier due to their increased weight.

The structure of an AS floc can be explained by the filamentous backbone theory, which assumes two levels:

- Microstructure: a result of microbial adhesion. This is the basis for a floc to form thanks to extracellular polymeric substances (EPS). The flocs are usually small, spherical and compact but mechanically rather weak.

- Macrostructure: this is provided by filamentous microorganisms. When an AS culture contains filamentous organisms, large floc sizes are possible because the filamentous microorganisms form a backbone within the floc, to which the floc-formers are firmly attached by their EPS. This backbone provides the floc with enough strength not to be break up in the turbulent environment of the biological reactor.

Operational problems of microbiological origin in the AS can be divided into four categories: (i) filamentous bulking, (ii) biological foaming, (iii) deflocculation and (iv) viscous bulking. A fifth category – rising sludge – is not included among them because it is not caused by an imbalance in population dynamics and/or poor floc formation. Nevertheless, it shares the same effects (loss of TSS) as the others and will therefore be presented here as well.

2.2.1.1 Bulking

Filamentous bulking (**Figure 2.4**) is probably the most frequent operational problem of microbiological origin around the world. The sludge's density tends to decrease as a consequence of the overabundance of filamentous microorganisms. Whenever the settling velocities of the sludge are within a range sufficient for efficient separation in secondary settlers, the effluent will not be affected, since all the microflocs can be enmeshed and trapped in the filamentous network, resulting in a clear effluent. However, when the filamentous bulking is severe, and the sedimentation zone of the secondary settler is full of poorly compacted sludge, an overflow of the sludge blanket may occur (Wanner, 1994).

This bulking sludge is due to the proliferation of filamentous microorganisms. Depending on the environmental conditions, these have growth kinetics that are higher than those of floc-forming bacteria. According to Martínez (2006) different operational parameters and wastewater features have an effect on the growth of filamentous microorganisms.

SRT: The correlation between SRT and filamentous microorganisms is based on the backbone theory, since generally a high sludge age is associated with the growth of filaments more than a low sludge age. Nevertheless some species can grow in low SRT as well.

Figure 2.4. Filamentous bulking.

F/M: This is usually inversely related to SRT. At low F/M (i.e. low substrate concentrations) the non-filamentous, floc-forming microorganisms have a high μ_{max} but a low affinity for the substrate (high K_S), whereas the filamentous forms are slow-growing organisms that have a low μ_{max} but a high affinity for the substrate (low K_S - see **Figure 2.5-**). Morphologically, filamentous microorganisms have a bigger surface area than floc-forming microorganisms, which makes the substrate more available to them at low substrate concentrations.

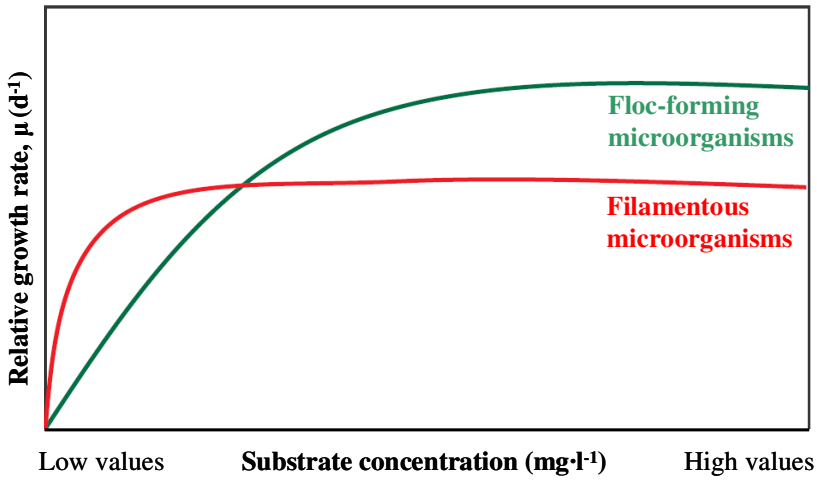

Figure 2.5. Relative growth rates of floc-forming and filamentous bacteria in relation to substrate concentration. (Martínez, 2006)

DO: The growth of some filamentous microorganisms is favoured at low DO levels in the biological reactor. Taking into account that the higher the F/M, the higher the DO that is required, a safe DO concentration, i.e. one high enough to prevent filamentous bulking, will be dependant on the F/M ratio (Palm *et al.*, 1980). Although the correct DO set-point may seem enough to avoid bulking, dead zones in the biological reactors, failures in probes and similar problems can cause filamentous microorganisms to proliferate.

Biological reactor configuration: Despite many filamentous microorganisms being favoured in uniformly aerated, completely mixed, continuously fed biological reactors, the growth of others is favoured in different configurations. For instance, low F/M microorganisms find a suitable environment to proliferate in configurations which alternate anoxic-aerobic conditions (Musvoto *et al.*, 1999). Moreover, in biological reactors with a "selector" effect, i.e. an initial high F/M feed zone (especially if it is anoxic or aerobic), the growth of filamentous microorganisms can be suppressed. The same effect is seen in an SBR with a non-aerated feed with an initial reaction period (Jenkins *et al.*, 2003).

Nutrient deficiency: Among the macronutrients required by the microorganisms (i.e. C, H, N, O, S and P), N and P are usually the growth limiting ones. In general, a C/N/P ratio of 100/5/1 is required for complete BOD removal (Grau, 1991). The growth of certain filamentous microorganisms is related to the low F/M theory. As explained above, in a low nutrient concentration, filamentous microorganisms have a higher affinity for these nutrients than floc-forming microorganisms due to their low half-velocity constant (K_S).

Nature of organic substrate: Rapidly biodegradable organic matter can favour the growth of some filamentous microorganisms (e.g. *S. Natans*, *Thiothrix spp.*, *H hydrossis*, etc.). On the other hand, slowly biodegradable substrates favour other filamentous microorganisms, such as *M. parvicella* and *Type 0041* (Jenkins *et al.*, 2003).

Temperature: Generally speaking, filamentous microorganisms grow faster as temperature increases in the range between 8º and 25 ºC. However, *M. parvicella* is an exception showing growth in temperatures below 12-15 ºC (Knoop and Kunst, 1998; Rossetti *et al.,* 2005). The explanation for this phenomenon could be the low level of solubility of lipids and fats at low temperatures, which makes them more available for *M. parvicella* than for the floc-forming microorganisms (Eikelboom *et al.,* 1998; Rossetti *et al.,* 2005).

The consequence of bulking sludge is the loss of solids through the effluent. This has many implications for the receiving media: the ecosystem is polluted with high COD content, creating problems of oxygen depletion or future contamination due to the long term release of N, P and organic matter due to degradation; bacterial contamination; process efficiency is affected given that part of the sludge that should have been used in the treatment process is removed; and finally, RAS and WAS concentrations get very low, hampering, for example, the control of SRT.

2.2.1.2 Biological foaming

Biological foaming (**Figure 2.6**) represents one of the most common problems in AS systems. It is a variant of filamentous bulking in which the excessive growth of certain

species causes foam to appear in the biological reactor and on secondary settler surfaces. Although other types of foaming can appear, both biological and non-biological, only biological foaming will be considered here. Compared to filamentous bulking, the number of microorganisms that cause biological foaming is limited. The most common are nocardioforms (the name given to those actinomycetes similar to Nocardia sp.), *M. parvicella* and Type 1863 (Jenkins *et al.*, 2003; Richard, 1989). The main feature of foam-causing microorganisms is their hydrophobicity, which causes the floc to float when they are in contact with air bubbles. Foam-forming filamentous microorganisms also produce hydrophobic extracellular substances (e.g. lipids, lipopeptides, proteins, etc.) which act as surface-active agents (Wanner, 1994). The final result is a stable, viscous foam layer that covers the secondary settler; in the worst cases even the biological reactor can end up covered by foam. As pointed out by Eikelboom (1994), when foaming caused by *M. parvicella* or nocardioforms appears, there will probably also be bulking caused by these same species.

Figure 2.6. Biological foaming in a biological reactor.

In general, the growth of bacteria responsible for foaming is associated to: temperature, lipids or oils present in the treated water, high SRT and high readily biological organic matter concentration (HRBOM). Specifically, the causes for foaming are linked to each foam-forming species.

Nocardioforms: Their growth is associated with high temperatures, grease, oil and fat present in wastewater. It takes more than 9 days for nocardioforms to grow in the system, but once present they can develop in 2 days. Nocardioforms tend to consume easily degradable substrates but they can grow in a wide range of F/M ratios (Jenkins *et al.*, 2003).

M. parvicella: This filamentous bacterium can cause both foaming and bulking. However, its growth is favoured in low F/M conditions or long SRT and it is also capable of growing below 12ºC. The temperature influence is linked to the higher availability of lipids and fats at low temperatures due to their low solubility. The substrate storage capacity of *M. parvicella* allows it to survive under stress conditions imposed by long anaerobic periods; what is more, it has a strong competitive advantage over floc-forming microorganisms which are not able to take up and store substrates anaerobically. Their storage compounds make it possible for *M. parvicella* to survive starvation periods inherent in domestic WWTPs (Rossetti *et al.*, 2005).

Type 1863: This bacterium is not common in AS systems and as a result it has not been thoroughly studied. It can be found under low DO conditions (Scruggs and Randall, 1998) and in high F/M ratios when the SRT is low.

According to Martínez (2006), the main consequences of foaming are:

- Foam lost through the effluent, thereby increasing discharges of TSS and BOD/COD and violating the permitted limits.
- If the foam layer is deep it can overflow onto walkways and surrounding areas, creating hazardous slippery areas.
- Electricity consumption can increase since foam can cause problems for surface aeration equipment.
- Solids trapped in the foam layer make it very difficult to keep track of MLSS for control purposes and are not taken into account in calculations of SRT, see for example Richard (1989). If the trapped solids are not taken into account, and if WAS is maintained, the biomass retention time can be greatly reduced.
- During cold periods foam can even freeze, thus hampering its removal. On the other hand, during hot periods foaming can start to decompose and cause odour.
- Some of the organisms in the foam can be pathogenic. The aerosols derived from foam-producing organisms are considered a potential health hazard (Blackall *et al.*, 1988).
- Foaming sludge fed to an anaerobic digester can also cause the digester to foam (see below).

2.2.1.3 Rising sludge

Although this operational problem is not caused by a population imbalance, its consequences are similar to those previously presented. Rising sludge is an uncontrolled denitrification; nitrite and nitrate present in the wastewater are converted to N_2 in the secondary settler instead in the reactor.

Conditions in the secondary settler which make it possible for this phenomenon to occur include:

Nitrate present: Usually more than 5 mg/L.

Organic matter: Usually more than 10 mg/L.

Low DO conditions: Less than 0.5 mg/L within the secondary settler. This can be a result of slow removal of the sludge.

Denitrifying bacteria: Without their presence denitrification is impossible.

Regarding the causes of rising sludge, it has to be taken into account that in plants that usually remove N, rising sludge can be a result of incomplete denitrification within the reactors due to problems with setting the appropriate anoxic conditions (for example low denitrification time, insufficient organic matter, etc.). In plants that have no nitrification/denitrification processes, there are a number of possible causes for rising sludge whenever nitrification is carried out intentionally or unintentionally, and denitrification is not complete in the reactor:

Long SRT in secondary settler: Too long time with the same sludge at the bottom of the secondary settler can have two consequences: (i) denitrifying bacteria have enough time to grow and (ii) the sludge becomes anoxic due to the activity of the microorganisms which consume the remaining DO.

High temperatures: High temperatures cause the process to nitrify at a higher F/M ratio due to an increase in the activity of microorganisms. The same phenomenon will cause the DO to be consumed faster in the bottom of the secondary settler.

Denitrifying bacteria consumes the BOD, nitrite and nitrate to produce N_2. As the N_2 bubbles start to form they end up trapped in the sludge blanket. After a short period of accumulation the sludge blanket becomes buoyant and floats towards the surface. There, the solids are lost through the effluent with consequences similar to those described for other operational problems of microbiological origin.

2.2.1.4 Deflocculation

Deflocculation refers to an operational problem of microbiological origin characterised by the formation of a very small sludge floc, or the absence of floc formation. Two types of deflocculation problems can be distinguished: pin-point flocs and dispersed growth, but no distinction will be made here. According to Martínez (2006), the phenomenon has several causes:

Extreme values of SRT: Either very low or very high SRT can cause deflocculation. Very high values imply an over-oxidation of sludge and the exposure of flocs to low concentrations of exogenous substrates (low F/M). In these conditions the only available substrates are extracellular polymeric substances (endogenous metabolism) which lead to the destruction of the polymeric matrices of AS flocs (Wanner, 1994). On the other hand, low SRT can lead to deflocculation because filaments do not have enough time to develop and form the macrostructure of the sludge. This cause is typical during start-up conditions.

Extreme values of DO: Excessive aeration can result in excessive shearing in the biological reactor, which can break the macrostructure of the floc. In the case of limited DO, under anaerobic conditions the growth of aerobic floc-forming microorganisms and the production of EPS can be inhibited (Eikelboom and van Buijsen, 1983; Starkey and

Karr, 1984). However, the opposite effect is sometimes seen during low DO conditions, so further research is required here.

The improper formation of AS flocs causes poor separation between the microorganisms and the treated water, which results in effluent turbidity and, consequently, lower clarifier efficiency (Comas *et al.*, 2003).

2.2.1.5 Viscous bulking

Apart from filamentous bulking, there is another microbiological problem in AS systems that can transform suspended solids into a bulky solution and hinder their ability to settle well in clarifiers. This problem is known as viscous bulking and it is caused by the excessive production of extracellular polymers that may or may not be associated with the growth of a group of floc-forming bacteria: *Zooglea* spp. (Jenkins *et al.*, 2003). This excessive growth can cause an increase in slime production that may affect the compaction and settleability of the sludge in several ways. The slime produced is insoluble in and less dense than water. The microbial cells become surrounded by large amounts of water-retentive polymers which produce a viscous sludge that settles and becomes compact only with difficulty. The slime can also entrap air bubbles and become more buoyant, thereby generating foam on the surface due to aeration and mixing (Gerardi, 2002).

The main causes of viscous bulking are:

Nutrient deficiency: Specially related to N and P. Bacteria inside the floc particles cannot degrade some of the soluble COD and this is stored within the floc.

High F/M or HRBOM: High concentrations of easily degradable carbohydrates, volatile fatty acids (VFAs) or readily biodegradable COD in wastewater can cause viscous bulking. It is common to find viscous bulking in those AS systems designed to improve settling properties by using a concentration gradient (e.g. systems with selectors or plug-flow) due to the high F/M in the first compartments.

The effects of viscous bulking are similar to those of filamentous bulking: low effluent quality due to an increase in suspended solids and BOD in the effluent, and the dilution of RAS and WAS.

2.2.2 Anaerobic Digestion

A couple of operational problems of microbiological origin are distinguished here: (i) acidogenic states that can be caused by different conditions (i.e. hydraulic and organic overloads, toxicity and underloads) and, (ii) biological foaming.

2.2.2.1 Acidogenic states

Many AD disturbances can end up in acidogenic states that entail high VFA concentrations associated with a decrease in pH and methanogenic inhibition (Guiot, 1991) with a related decrease in methane production (MP). For example, toxicants can cause VFAs to accumulate via methanogenic bacteria inhibition (Hickey *et al.*, 1987) as well as inhibition due to accumulation of long chain fatty acids (LCFA), which also leads to acids accumulating (Lalman and Bagley, 2001). However, acidogenic states are

not only related to the build-up of VFAs and are sometimes difficult to detect (Dupla *et al.,* 2004).

Some of the operational problems that can cause acidogenic states are listed below.

Underload: The incoming COD is totally degraded but the steady state reached has a low biomass concentration. Due to low biomass concentration, the anaerobic digester can become sensitive to a loading peak causing an organic overload. During underload, the organic loading rate is low and there is a decrease in biogas production (Lardon, 2004).

Organic overload: Incoming COD is higher than the digester's treatment capacity. There is an accumulation of organic matter inside the digester and a risk of system washout. The point at which the overload happens will depend on the digester. When it does, the increasing COD causes the increased growth of bacteria until the slowest processes act as bottle necks and substrates (soluble COD, TOC and VFA) are accumulated (Dupla *et al.*, 2004).

Consequences of organic overloads are multiple (Marchaim and Krause, 1993; Dupla *et al.*, 2004; Müller *et al.*, 1997; Lardon, 2004):

- Risk of biomass wash out, decreasing biomass concentration.
- Decreasing MP and increased CO_2 and H_2 contents in the biogas.
- Increased gas flow rate.
- Acidogenic states.

Hydraulic overload: The loading applied corresponds to the digester's treatment capacity but the dilution is high and causes digester washout. In practice, any efficient volume reduction can cause a hydraulic overload, due to bad stirring or a sudden increase in the volume of substrate pumped to the digester (combined hydraulic and organic overload). The most relevant bacteria do not have enough time to grow properly and can be easily washed out of the digester. This affects especially acetate and propionate degraders which have low growth rates.

The hydraulic overload effects includes (Lardon, 2004; Carrasco *et al.*, 2004):

- Accumulation of VFA in the digester that leads to acidogenic states.
- Biogas production medium or weak.
- Accumulation of substrate and intermediate products.

Toxicity: An inhibitory source other than VFA diminishes the microorganisms' growth rate. As in the organic overload case, it is followed by fatty acids accumulation, pH and alkalinity ratio decrease. For instance, the heavy metals in wastewater can accumulate in sludge as a result of physical, chemical or biological treatment and have a negative effect when the sludge is digested anaerobically (Lin, 1992). Two examples of AD inhibition sources are:

- Ammonia: Inhibition of anaerobic fermentation with ammonia (NH_3 / NH_4^+) is a well-known phenomenon. Methanogenic bacteria are especially sensitive to ammonia inhibition. This inhibition is higher under thermophilic than under mesophilic conditions. The reason for this is that the active component responsible for ammonia inhibition is the unionised form of ammonia. Free ammonia, NH_3, is thought to be the fraction of ammonia which actually causes this phenomenon (Hansen *et al.*, 1998).

- Substrate inhibition: Apart from specific toxic compounds in the waste, certain relatively easily degradable compounds can also inhibit the anaerobic digestion process. Especially lipids and protein in the feed stream to biogas plants must be especially carefully controlled. A sudden addition of lipids to a biogas plant can cause inhibition of anaerobic degradation, since hydrolytic, acidogenic and methanogenic bacteria can be inhibited by accumulation of LCFA produced during hydrolysis of the lipids. The toxicity of lipids therefore depends on how fast hydrolysis proceeds in relation to further fermentation. When a biogas plant is adapted to degrade high concentrations of lipids, a higher gas yield can be obtained. Lipids have high energy content and can be nearly completely degraded to biogas in suitably adapted biogas plants (Cirne *et al.*, 2007). The degradation of proteins will result in the formation of ammonia, which in turn can inhibit anaerobic fermentation. A long adaptation period may be required when a large quantity of proteins is added to a biogas reactor not adapted to ammonia.

2.2.2.2 Biological foaming

Among the various operating problems of microbiological origin that affect AD in WWTPs, foaming is one of the most extensive and consequential (**Figure 2.7**). Digester foam is formed by fine gas bubbles trapped in a semi-liquid matrix. Further gas bubbles generated below are trapped in the sludge layer as they form.

Figure 2.7. Biological foaming in an anaerobic digester (Massart *et al.*, 2006).

There is not yet complete agreement on the causes of biological foaming in AD. Many are put forward, but there are some that are commonly stated in the literature.

WAS: Biological foaming in AD is reported to be caused by the presence of filamentous microorganisms in the WAS, mainly Nocardioforms (Pagilla *et al.*, 1997; Lemmer and Baumann, 1988) and *M. parvicella* (Barjenbruch and Kopplow, 2003; Westlund *et al.*, 1998). Thus, any cause of biological foaming in the AS system can cause foaming in the anaerobic digester.

Loading rates: There are many examples that show a relationship between loading rates and foaming. Most of them show that inconsistent or high rates cause foaming in anaerobic digesters. For instance, in Massart *et al.* (2006) examples are given of foaming in WWTPs as a result of inconsistent loading rates. In Murto *et al.* (2004) foaming appears when the loading rate is increased beyond a certain value. Barber (2005) shows that overloading can cause a sudden increase in biogas production which can exacerbate foaming.

Mixing: Pagilla *et al.* (1997) showed that gas-mixed anaerobic digesters can promote more foaming than mechanically-mixed digesters. Massart *et al.* (2006) state that if the sludge in the digester is not properly mixed, a scum layer may accumulate on its surface and adhere to the gas bubbles, forming a foam layer. The biogas generated will not be completely stripped off the digesting solids. Consequently, the gas bubbles can adhere to the solids, reducing their density and propelling them to the surface. Mixing can also have an adverse effect by increasing the entrapment of gas bubbles in the liquid, thereby generating foam. It is clear, that inefficient mixing in the anaerobic digester can have a negative effect on the digester's performance. The reasons may be related to the presence of hydrophobic substances in the wastewater which, as noted before, act as surface-active agents that create the foam layer.

According to Pagilla *et al.* (1997), the consequences of foaming are numerous:

- Blockage of gas mixing devices.
- Inversion of digester solids profiles.
- Foam binding of recirculation pumps.
- Fouling of gas collection pipes (due to entrapped foam solids).
- Foam penetration between floating covers and digester walls.
- Decrease in digestion efficiency.

2.3 Modelling

A model is a description of the processes occurring in a system, and is used to understand and predict certain aspects of reality (Meijer, 2004). As in many other systems in nature, the biological treatment of wastewater can be modelled, i.e. simplified and expressed in equations.

2.3.1 Activated sludge

It was the need to understand and predict the biological treatment of wastewater that led to the development of activated sludge models. In 1982, the International Association on Water Pollution Research and Control established a Task Group on Mathematical

Modelling for Design and Operation of Activated Sludge Processes. At that time models were little used due to several different factors including lack of confidence in them, computational limitations, and the fact they were usually written in a complicated way. In 1987, the Activated Sludge Model No1 (ASM1; see **Section 4.1 Activated Sludge Model No1**) was presented. It aimed to review and reach a consensus among already existing models (Henze *et al.*, 1987). ASM1 has acted as a common platform for modelling biological wastewater treatment. Currently, ASM1 is widely used but seldom alone. It has almost always acted as a basis for other models. After ASM1, which includes COD, N removal and still remains the core model, extensions and improvements aimed at overcoming some of its limitations were developed. These extensions include: (i) ASM2, which includes biological P removal; (ii) ASM2d, which includes the denitrification capacity of the PAOs and (iii) ASM3, which recognises the importance of storage polymers and changing the growth-decay-growth concept for the decay-endogenous respiration model (Henze *et al.*, 2000). Detailed information on modelling of activated sludge systems can be found in Gernaey *et al.* (2004). Many examples of models based on the ASM family exist. For example, in Van Veldhuizen *et al.* (1999) and Brdjanovic *et al.* (2000) a modified version of ASM2 is used to model the COD, N and P removal of a full scale plant. Other modifications are the inclusion of pH calculation in ASM1 (Magrí *et al.*, 2005) and in ASM2d (Serralta *et al.*, 2004).

2.3.2 Anaerobic digestion

An increasing interest in the use of models applied to another important process of many WWTPs -AD- also appeared. At first, a lack of specific knowledge about AD mechanisms caused the models to be developed with very specific purposes. This was the case with the model demonstrated in Vavilin *et al.* (1995) in which changes in H_2 pressure as a result of bacteria competition were modelled. The lack of a general model for the whole AD system was the motivation behind the Anaerobic Digestion Model No1 (ADM1; see **Section 4.2 Anaerobic Digestion Model No1**), whose focus was a more complete and versatile model, based on the first AD models (Batstone *et al.*, 2002). ADM1 is now widely used in AD research (Batstone *et al.*, 2005). Some examples of this research include an adaptation of ADM1 to model a two-stage pilot plant (Blumensaat and Keller, 2005) and a full-scale industrial application based on an ADM1 modification to simulate the dynamic behaviour of an anaerobic digester treating corn processing wastewaters (Ersahin *et al.*, 2007). Bernard *et al.* (2001) proposed a two-step model that can be easily used for closed loop control and optimisation of AD systems. Other studies have focused on sulphate reduction in AD (Knobel and Lewis, 2002).

2.3.3 Plant-wide modelling

The release of ADM1 as a more standardised model of AD, along with different AS models, has led to the development of plant-wide models. These have provided researchers with greater knowledge of systems as they can consider the interactions between the different units that constitute the system. This has meant that the consequences of changes in one part of the system can be studied in other parts.

According to the paper by Grau *et al.* (2009) there are two main approaches to plant-wide modelling. The first one, the *Interfaces* approach, relies on interfaces to integrate established models making possible to communicate each model with the others despite their different units. One example of this methodology is the IWA Simulation

Benchmark No 2 (Jeppsson *et al.*, 2007; see **Section 4.3.3 Benchmark Simulation Model No2**) which will be referred to later since it is the model used in the case studies of the present thesis. In this case, the ASM1 is integrated with the ADM1 by a series of interfaces (Nopens *et al.*, 2009) which transform the variables of one model into the variables of the other, and vice-versa.

The second approach is to model the whole plant based on a common components vector. This makes all the transformations active in all the units and streams. Despite they may be zero; they are still taken into account. Components and transformations are in common in every unit of the model so the problem of designing appropriate interfaces is avoided. However, it is difficult to incorporate new processes in this approach, and the size of the model increases as it is adapted to new processes. This second approach is divided in the *Standard Supermodel* and the *Tailored Supermodel.*

The S*tandard Supermodel* approach is based on the use of a set of standard supermodels that describe the most relevant processes within the whole WWTP. This way, the model state variables are consistent eliminating the need for interfaces. On the other hand, new processes would require the development of new supermodels. The *Tailored Supermodel* is based on the construction of a specific model for a given plant including only the most relevant processes. From a list of the compatible transformation the user would select the transformations that take place in the plant under study. The flexibility of this approach can be a limitation if there is not a procedure to select the most suitable transformations in each case. To cope with this, Grau (2007) presented a methodology to construct *Tailored Supermodels*.

2.3.4 Modelling of operational problems of microbiological origin

There are several models that aim to describe filamentous bacteria mechanistically. According to Martins *et al.* (2004) two general types of models dealing with the development of filamentous bacteria exist: (i) those based on kinetic selection theory and (ii) those which consider both kinetic selection theory and the micromorphology of filamentous bacteria.

Within the first group there is the Kappeler and Gujer model for bulking due to low DO (Kappeler and Gujer, 1994a) which they afterwards validated in pilot and full-scale plants (Kappeler and Gujer, 1994b). This model assumed two kinds of substrates: readily biodegradable and slowly biodegradable chemical oxygen demand (RBCOD and SBCOD, respectively). The final result of both works is a model able to predict the behaviour of AS in the case of aerobic bulking. More recently, Hug *et al.* (2006) modelled the seasonal dynamics of *M. parvicella* but concluded that the model would have to be applied to new data to find the significant mechanisms in the competition between *M. parvicella* and floc formers in AS. Makinia *et al.* (2006) developed a model to explain the rapid substrate removal in selectors and finally concluded that the relationship between the kinetics of absorption and storage may be a potential factor affecting the growth of different heterotrophic bacteria, such as filamentous bacteria.

The most recent studies on the mechanistic modelling of operational problems of microbiological origin are centred on *M. parvicella*. The promising work by Spering *et al.* (2009) is based on the previous studies by Andreasen and Nielsen (2000) and the above mentioned Hug *et al.* (2006). In their study, Spering *et al.* developed a conceptual model of the growth of *M. parvicella*. This conceptual model allowed to build a

mechanistic model to complement the ASM3 with the dynamics of *M. parvicella*. Apart from the general mechanistic model for *M. parvicella*, they also proposed a calibration approach; however, they concluded that the method was not suitable or maybe there was an incomplete model structure.

In the second category of models, Lau *et al.* (1984) developed a diffusion and consumption model of DO and soluble organic substrate of a floc with *S.Natans* and a floc-forming microorganism before experimental determination of the kinetic parameters (i.e. half saturation constant and maximum growth rate). They studied the influence of parameters like floc shapes and sizes to predict the growth rate of filamentous and floc-forming bacteria. This model is able to predict resistance to substrate diffusion related to the floc structure. However, results cannot represent other kinds of filamentous bacteria because the kinetic parameters are limited to *S.Natans*. There is also the model by Takács and Fleit (1995) which focuses on the diffusivity of the substrate through the flocs, and thus also considers whether its micromorphology is able to simulate the directional growth of filamentous microorganisms. The model was tested in low substrate scenarios: normal, low DO and low F/M, and showed promising results since it can provide a better understanding of the relationship between different parameters of the process, such as influent conditions, plant operation and settling characteristics of the AS. Later, in a study by Cenens *et al.* (2000a) it was stated that the generic coexistence of the two species cannot be predicted with a simple model describing a biological reactor modelled according to kinetic selection. In a second part of this paper, Cenens *et al.* (2000b) develop a model based on both the kinetic selection theory and the backbone theory, but it was not validated.

As a general conclusion, further research is required to mechanistically model filamentous microorganism dynamics. Although the models mentioned above take into account the micromorphology of filamentous microorganisms, they are not able to predict sludge settling characteristics. Despite all the attempts to explain the development of filamentous microorganisms by means of mathematical modelling, none has led to a general and experimentally validated model (Martins *et al.*, 2004).

In terms of AD, none of the models are able to overcome the limitations of modelling to properly describe the dynamics of feed characteristics responsible for operational imbalances (i.e. the presence of foam caused by filamentous microorganisms), which is highly practical when evaluating simulation results. However, there are a few promising studies on modelling of microbial diversity. Previous to the ADM1, the model by Merkel *et al.* (1999) addressed the role of substrate composition and SRT in population dynamics. Later, ADM1 assigned one kind of biomass to each process. Still later, the work by Ramirez and Steyer (2008) addressed the significance of the role of microbial diversity regarding modelling and control of AD systems. Their study showed how microbial diversity dampens the effect of a toxic. Nevertheless, these studies neither deal with the modelling of filamentous species nor provide a comprehensive model of the mechanisms involved in biological foaming development. Other approaches, therefore, have to be studied.

2.3.5 Alternatives to mechanistic modelling of operational problems of microbiological origin

As shown, although there are a few models for certain operational problems of microbiological origin, depending on the AS or AD model used, some variables

required for the mechanistic modelling of filamentous microorganisms may not be available. For instance, biological foaming caused by *M. parvicella* cannot be mechanistically modelled using, a related feature as the polymer storage capacity, in ASM1 since this model does not take it into account (whereas ASM3 does).

The impossibility of modelling some of the mechanisms of filamentous microorganisms confirms the need for other approaches to consider filamentous bacteria related problems, specifically, those approaches that do not need a comprehensive understanding of the mechanisms but are more based on either heuristic knowledge (e.g. KBSs) or on input-output relationships (black box models).

2.3.5.1 Black box models

Black box models try to estimate both the functional form of relationships between variables and the numerical parameters in a given function in order to adapt it to the behaviour of the data. Using a priori information a black box model can end up, for example, with a set of functions that can describe the system adequately. An often-used approach for black box models is neural networks (see **Section 4.4 Artificial neural networks**), which usually do not make assumptions about incoming data. The problem with using a large set of functions to describe a system is that estimating the parameters becomes increasingly difficult when the number of parameters (and different types of functions) increases.

Black box models have provided good results in applications in which there is only a little knowledge but a lot of data. In WWTP modelling there are some examples of black box model applications (e.g. Ráduly *et al.*, 2007) in which artificial neural networks are used to decrease the simulation time. For instance, in Moral *et al.* (2008) an artificial neural network is used to model a hypothetical and a real WWTP with good results. However, the main limitation of such models is that their performance is closely related to the amount and range of available data. More specifically, when focusing on operational problems of microbiological origin, it is difficult to find a reliable variable which allows us to directly quantify the problem (i.e. bulking, foaming, etc.). This explains why only a few examples of these applications can be found, such as the work by Belanche *et al.* (2000) in which the occurrence of bulking is modelled through ANNs. Often, other relationships have to be proposed to quantify the extent of a given operational problem of microbiological origin, as in the study by Smets *et al.* (2006) which focused on relating sludge volume index (SVI) tests to organic matter and the image detection of filaments and flocs. Results were promising, but validation failed and the authors concluded that further experimentation was required.

2.3.5.2 Knowledge-Based Systems

Knowledge-based systems (KBSs) use heuristic knowledge and human experience to apply reasoning to the problems that can affect a system. As an alternative to mechanistic and black box models, the complexity involved in the description of operational problems of microbiological origin can be tackled by KBSs. Examples can be found in the literature of the application of knowledge-based tools (e.g. expert systems and case-based systems) to AS. For example, in Yong *et al.* (2006), a fuzzy (see **Section 4.5 Fuzzy logic rule-based systems** for more detail) controller is used to optimise aeration and external carbon flow rate (Q_{carb}), thereby improving effluent quality. Likewise, Fiter *et al.* (2005) demonstrate that an energy saving of more than

10% is possible by using fuzzy logic controllers. In Poch *et al.* (2004), two successful examples of KBS applications are given, one for WWTP supervision and another for WWTP building planning.

In the specific case of operational problems of microbiological origin, the work by Rodríguez-Roda *et al.* (2002) presents a hybrid support system based on expert and case-based systems that is developed and implemented successfully in a real plant. The system also includes a classical mathematical model to simulate off-line possible scenarios with different conditions. Already in this paper, the authors think of using the model by Belanche *et al.* (2000) to be able to simulate bulking effects in their mathematical model. After its implementation, the results showed good performance demonstrating that the system is able to recognize the 80% of the process situation.

In addition, in Comas *et al.* (2003) the deflocculation problem is tackled by a KBS for diagnosis and solution. It also establishes a methodology to be applied to any microbiology related problem. The rule-based system developed was validated resulting in more than 89% accuracy when detecting deflocculation situations. The work also highlights the relevance of the experts' opinion in the development of the system.

Martínez *et al.* (2006) is another example of how to face many operational problems of microbiological origin in the AS system by means of a case-based system. The paper points out the relevance of the day-to-day experience of plant operators which is often the unique knowledge on which to base their decisions when facing operational problems of microbiological origin. Anchored in case-based reasoning the system retrieves past experiences to help operators to make decisions.

There are applications to the AD system as well. For example, Lardon *et al.* (2005) applied a modular fuzzy inference system based on rules to diagnose the state of the system (i.e. normal, hydraulic overload, organic overload…). The system is especially useful when resolving conflicting situations since the evidence theory embodied in the system can reliably deal with the uncertainties of the system.

In Puñal *et al.* (2003), a KBS is applied to the monitoring and diagnosis of an AD plant. The system is able to identify the current state of the process; it can also predict its trend, failures in the instrumentation and propose actuations. The validation shows that the system can present valuable solutions that end up in recovering the normal operation of the process.

To sum up, these techniques can be useful to represent the knowledge to detect, via simulation, that the process is moving towards a situation of risk of operational problems of microbiological origin.

CHAPTER 3

OBJECTIVES

3. Objectives

The main objective of this thesis is to develop a knowledge-based risk model that integrates numerical modelling and qualitative aspects to simulate risk of plant-wide operational problems of microbiological origin. The achievement of this main objective requires defining the following sub-objectives:

- The risk model has to be developed to include the assessment of the most common operational problems of microbiological origin for both AS and AD (i.e. filamentous bulking, activated sludge foaming, rising sludge and anaerobic sludge foaming).

- The most relevant variables to each operational problem of microbiological origin have to be identified using either heuristic knowledge and/or data mining techniques.

- The risk model has to provide a suitable output to allow the evaluation of simulated results using criteria related to the risk of microbiological operational problems, in addition to any other performance criteria related to environmental and economical aspects.

- The risk model has to be standardized enough to complement any of the existing wastewater treatment models during plant-wide simulations. This also implies that the implementation of the risk assessment model has to be software and platform independent.

- The performance and usefulness of the risk model will be evaluated using a benchmark simulation platform for objective comparison of control strategies and with different case studies (with different influent conditions, different control strategies, different operational conditions, etc.).

CHAPTER 4

METHODS

4. Methods

This chapter is dedicated to the different models used along the thesis. The ASM1, which is the basis of the BSM, is explained first. Secondly, the ADM1 is detailed since it also features in the BSM2. Finally, descriptions of how to implement fuzzy logic and ANNs are given. The aim of the chapter is principally to prepare the reader for the implementation of the risk models that will be detailed later (in **Chapters 5 and 6**) with their own simulation platform.

The different models have already been explained in a general terms in the state-of-the-art. Here, their main features are described. For further details on stoichiometric parameters, suggested parameter values etc., see the references given in **Section 2.3 Modelling**.

4.1 Activated Sludge Model No1

The processes explained below are summarized in **Figure 4.1**. **Table 4.1** summarizes all the related components with their units. In **Table 4.2** all the processes and components of the Petersen matrix are summarised**.**

Table 4.1. State variables of the ASM1.

STATE VARIABLE	Symbol	Units
Soluble inert organic matter	S_I	g COD · m^{-3}
Readily biodegradable substrate	S_S	g COD · m^{-3}
Particulate inert organic matter	X_I	g COD · m^{-3}
Slowly biodegradable substrate	X_S	g COD · m^{-3}
Active heterotrophic biomass	$X_{B,H}$	g COD · m^{-3}
Active autotrophic biomass	$X_{B,A}$	g COD · m^{-3}
Particulate products arising from biomass decay	X_P	g COD · m^{-3}
Oxygen	S_O	g COD · m^{-3}
Nitrate and nitrite nitrogen	S_{NO}	g N · m^{-3}
$NH_4^+ + NH_3$ nitrogen	S_{NH}	g N · m^{-3}
Soluble biodegradable organic nitrogen	S_{ND}	g N · m^{-3}
Particulate biodegradable organic nitrogen	X_{ND}	g N · m^{-3}
Alkalinity	S_{ALK}	mol · L^{-1}

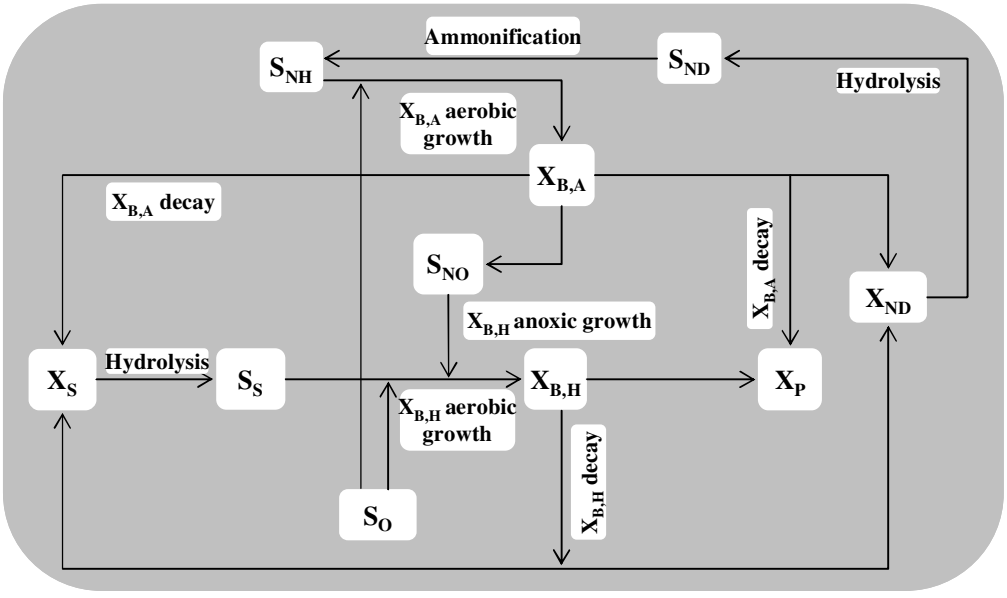

Figure 4.1. ASM1 processes and components diagram.

Non-biodegradable organic matter is biologically inert and passes through the system unchanged. Two fractions - inert soluble organic matter (S_I) and inert particulate organic matter (X_I) - have to be distinguished. S_I leaves the model in the same concentration while X_I is partially removed through the WAS. Biodegradable organic matter is divided into the readily and slowly biodegradable, which are treated as soluble (S_S) and particulate (X_S) material, respectively. Heterotrophic biomass ($X_{B,H}$) grows in either aerobic (S_O as DO) or anoxic conditions but is assumed to stop growing under anaerobic conditions. The decayed biomass is transformed into X_S and X_P, of which the latter is inert to biological degradation.

With regard to N, the non-biodegradable particulate N as part of X_I, X_P and S_I is not modelled, and the soluble portion is too small to be considered in the model. The biodegradable fraction is divided into:

S_{NH}: Free ammonia and its salts.

S_{ND}: Soluble organic N linked to S_S.

X_{ND}: Particulate organic N which can be hydrolysed to S_{ND} linked to X_S.

S_{ND} is converted to ammonia nitrogen by ($X_{B,H}$); S_{NH} serves as the N supply for the synthesis of heterotrophic biomass and for autotrophic nitrifying bacteria ($X_{B,A}$) growth. Conversion of ammonia nitrogen to nitrate (S_{NO}) is considered in a single step needing aerobic conditions. Conversion of S_{NO} to N_2 is performed by $X_{B,H}$ under anoxic conditions. The decay of both biomasses ($X_{B,H}$ and $X_{B,A}$) releases X_{ND} (as part of X_S).

S_{ALK} is included in the model but it is not essential. However, it can provide information on changes in pH which is constant and near neutrality. Some processes which would involve pH changes affect S_{ALK}.

Table 4.2. Matrix representation of the ASM1 from Henze *et al.* (2000).

Component V_{ij} i / j Process	S_I	S_s	X_I	X_s	$X_{B,H}$	$X_{B,A}$	X_p	S_O	S_{NO}	S_{NH}	S_{ND}	X_{ND}	S_{ALK}	Process rate, ρ_j
1.Aerobic heterotrophic growth		$-\frac{1}{Y_H}$			*1*			$-\frac{1-Y_H}{Y_H}$		$-i_{XB}$			$-\frac{i_{XB}}{14}$	$\mu_{mH}\left(\frac{S_S}{K_S+S_S}\frac{S_O}{K_{OH}+S_O}\right)X_H$
2.Anoxic heterotrophic growth		$-\frac{1}{Y_H}$							$\frac{1-Y_H}{2.86Y_H}$	$-i_{XB}$			$\frac{1-Y_H}{14\cdot 2.86Y_H}-\frac{i_{XB}}{14}$	$\mu_{mH}\left(\frac{S_S}{K_S+S_S}\frac{K_{OH}}{K_{OH}+S_O}\frac{S_{NO}}{K_{NO}+S_{NO}}\right)\eta_g X_H$
3.Aerobic autotrophic growth						*1*		$-\frac{4.57-Y_A}{Y_A}$	$\frac{1}{Y_A}$	$-i_{XB}-\frac{1}{Y_A}$			$\frac{i_{XB}}{14}-\frac{1}{7Y_A}$	$\mu_{mA}\left(\frac{S_{NH}}{K_{NH}+S_{NH}}\frac{S_O}{K_{OA}+S_O}\right)X_A$
4.Heterotrophic death				*1-f_p*	*-1*		*f_p*					*i_{XB}-f_p.i_{XP}*		$b_H X_H$
5.Autotrophic death				*1-f_p*		*-1*	*f_p*					*i_{XB}-f_p.iX_P*		$b_A X_A$
6.Ammonification										*1*	*-1*		$\frac{i_{XB}}{14}$	$k_a S_{ND} X_H$
7.Hydrolysis of organics		*1*		*-1*										$k_H \frac{X_S/X_H}{K_X+X_s/X_H}\left(\frac{S_O}{K_{OH}+S_O}+\eta_h\frac{K_{OH}}{K_{OH}+S_O}\frac{S_{NO}}{K_{NO}+S_{NO}}\right)X_H$
8.Hydrolysis of organic nitrogen											*1*	*-1*		$\rho_7(X_{ND}/X_s)$
Conversion rate	$r_j=\sum_j v_{ij}\rho_j$													

Stoichiometric parameters: Heterotrophic yield: Y_H Autotrophic yield: Y_A Fraction of biomass yielding particulate products: f_P	Mass N/Mass COD in biomass: i_{XB} Mass N/Mass COD: i_{XP}	Kinetic parameters: Heterotrophic growth and decay: μ_{mH}, K_S, K_{OH}, K_{NO}, b_H Autotrophic growth and decay: μ_{mA}, K_{NH}, K_{OA}, b_A Correction factor for anoxic growth of heterotrophs: η_g	Ammonification: k_A Hydrolysis: k_H, K_X Correction factor for anoxic hydrolysis: η_H

4.2 Anaerobic Digestion Model No1

Biochemical and physical-chemical transformations are considered in the ADM1. Certain transformations and components for specific applications of AD have been excluded from the model to avoid excessive complexity. The Petersen matrix for both the soluble and particulate components of the ADM1 is given in **Tables 4.4 and 4.5**. **Figure 4.2** depicts the state variables of the model except for cations and anions (S_{cat} and S_{an}, respectively) and soluble inorganic carbon and nitrogen (S_{IC} and S_{IN}, respectively).

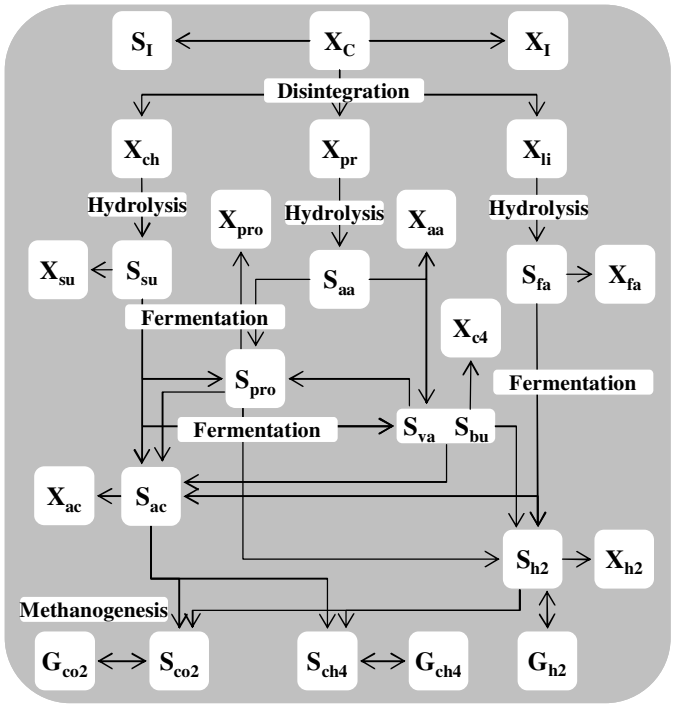

Figure 4.2. Schematic view of the ADM1 (Grau, 2007).

In **Table 4.3** the state variables of the ADM1 are listed with their respective units and description.

Processes are also included in **Figure 4.2** except for the decay of the different kinds of biomass (X_{su}, X_{fa}, X_{pro}, X_{ac}, X_{aa}, X_{c4}, X_{h2}), which all end up as complex composite particulate (X_c). X_c disintegrates into carbohydrate, protein and lipid particulate substrate (X_{ch}, X_{pr} and X_{li}) and soluble and inert particulate matter (S_I and X_I). X_{ch}, X_{pr} and X_{li} are then hydrolysed to soluble sugar, amino acids and fatty acid substrates (S_{su}, S_{aa} and S_{fa}, respectively). These are taken up by their specific biomass (X_{su}, X_{aa} and X_{fa}) to ferment: (i) S_{su} into acetate (S_{ac}), propionate (S_{pro}), butyrate (S_{bu}) and soluble hydrogen (S_{h2}); (ii) S_{aa} into S_{pro}, valerate (S_{va}), S_{bu} and S_{h2}; and (iii) S_{fa} into S_{ac} and S_{h2}. Propionate degraders (X_{pro}) convert S_{pro} into S_{ac} and S_{h2}. Valerate and butyrate degraders (X_{c4}) transform S_{va} into S_{pro}, S_{ac} and S_{h2}, whereas S_{bu} degrades to S_{ac} and S_{h2}. Finally, hydrogen and acetate degraders (X_{h2} and X_{ac}) produce soluble methane (S_{ch4}), soluble carbon dioxide (S_{co2}) and soluble S_{h2}, which are all in equilibrium with their gas components (G_{ch4}, G_{h2}, G_{co2}).

Table 4.4. Biochemical rate coefficients and kinetic rate equations for soluble components of the ADM1.

Component → i		1	2	3	4	5	6	7	8	9	10	11	12	Rate (ρ_j, kg COD·m^3·d^{-1})
j	**Process ↓**	S_{su}	S_{aa}	S_{fa}	S_{va}	S_{bu}	S_{pro}	S_{ac}	S_{h2}	S_{ch4}	S_{IC}	S_{IN}	S_I	
1	Disintegration												$f_{sI,xc}$	$k_{dis} \cdot X_c$
2	Hydrolysis Carbohydrates	1												$k_{hyd,ch} \cdot X_{ch}$
3	Hydrolysis of Proteins		1											$k_{hyd,pr} \cdot X_{pr}$
4	Hydrolysis of Lipids	1-$f_{fa,li}$		$f_{fa,li}$										$k_{hyd,li} \cdot X_{li}$
5	Uptake of Sugars	-1				$(1-Y_{su})\,f_{bu,su}$	$(1-Y_{su})\,f_{pro,su}$	$(1-Y_{su})\,f_{ac,su}$	$(1-Y_{su})\,f_{h2,su}$		$-\sum_{i=1-9,11-24} C_i \nu_{i,5}$	$-(Y_{su})\,N_{bac}$		$k_{m,su} \frac{S_{su}}{K_S + S_{su}} X_{su} I_1$
6	Uptake of Amino Acids		-1		$(1-Y_{aa})\,f_{va,aa}$	$(1-Y_{aa})\,f_{bu,su}$	$(1-Y_{aa})\,f_{pro,su}$	$(1-Y_{aa})\,f_{ac,su}$	$(1-Y_{aa})\,f_{h2,aa}$		$-\sum_{i=1-9,11-24} C_i \nu_{i,6}$	$N_{aa}-(Y_{aa})N_{bac}$		$k_{m,aa} \frac{S_{aa}}{K_S + S_{aa}} X_{aa} I_1$
7	Uptake of LCFA			-1				$(1-Y_{fa})$ 0.7	$(1-Y_{fa})$ 0.3			$-(Y_{fa})N_{bac}$		$k_{m,fa} \frac{S_{fa}}{K_S + S_{fa}} X_{fa} I_2$
8	Uptake of Valerate				-1		$(1-Y_{c4})$ 0.54	$(1-Y_{c4})$ 0.31	$(1-Y_{c4})$ 0.15			$-(Y_{c4})N_{bac}$		$k_{m,c4} \frac{S_{va}}{K_S + S_{va}} X_{c4} \frac{1}{1+S_{bu}/S_{va}} I_2$
9	Uptake of Butyrate					-1		$(1-Y_{c4})$ 0.8	$(1-Y_{c4})$ 0.2			$-(Y_{c4})N_{bac}$		$k_{m,c4} \frac{S_{bu}}{K_S + S_{bu}} X_{c4} \frac{1}{1+S_{va}/S_{bu}} I_2$
10	Uptake of Propionate						-1	$(1-Y_{pro})$ 0.57	$(1-Y_{pro})$ 0.43		$-\sum_{i=1-9,11-24} C_i \nu_{i,10}$	$-(Y_{pro})N_{bac}$		$k_{m,pr} \frac{S_{pro}}{K_S + S_{pro}} X_{pro} I_2$
11	Uptake of Acetate							-1		$(1-Y_{ac})$	$-\sum_{i=1-9,11-24} C_i \nu_{i,11}$	$-(Y_{ac})N_{bac}$		$k_{m,ac} \frac{S_{ac}}{K_S + S_{ac}} X_{ac} I_3$
12	Uptake of Hydrogen								-1	$(1-Y_{h2})$	$-\sum_{i=1-9,11-24} C_i \nu_{i,12}$	$-(Y_{h2})N_{bac}$		$k_{m,h2} \frac{S_{h2}}{K_S + S_{h2}} X_{h2} I_1$
13	Decay of X_{su}													$k_{dec,Xsu} \cdot X_{su}$
14	Decay of X_{aa}													$k_{dec,Xaa} \cdot X_{aa}$
15	Decay of X_{fa}													$k_{dec,Xfa} \cdot X_{fa}$
16	Decay of X_{C4}													$k_{dec,Xc4} \cdot X_{c4}$
17	Decay of X_{pro}													$k_{dec,Xpro} \cdot X_{pro}$
18	Decay of X_{ac}													$k_{dec,Xac} \cdot X_{ac}$
19	Decay of X_{h2}													$k_{dec,Xh2} \cdot X_{h2}$
		Monosaccharides (kgCOD m^{-3})	Amino acids (kgCOD m^{-3})	Long chain fatty acids (kgCOD m^{-3})	Total valerate (kgCOD m^{-3})	Total butyrate (kgCOD m^{-3})	Total propionate (kgCOD m^{-3})	Total acetate (kgCOD m^{-3})	Hydrogen gas (kgCOD m^{-3})	Methane gas (kgCOD m^{-3})	Inorganic carbon (kmoleC m^{-3})	Inorganic nitrogen (kmoleN m^{-3})	Soluble inerts (kgCOD m^{-3})	Inhibition factors: $I_1=I_{pH}\,I_{IN,lim}$ $I_2=I_{pH}\,I_{IN,lim}\,I_{h2}$ $I_3=I_{pH}\,I_{IN,lim}\,I_{NH3,Xac}$

Table 4.5. Biochemical rate coefficients and kinetic rate equations for particulate components of the ADM1.

Component → i		13	14	15	16	17	18	19	20	21	22	23	24	Rate (ρ_j, kg COD·m^{-3}·d^{-1})
j	**Process ↓**	X_c	X_{ch}	X_{pr}	X_{li}	X_{su}	X_{aa}	X_{fa}	X_{c4}	X_{pro}	X_{ac}	X_{h2}	X_I	
1	Disintegration	-1	$f_{ch,xc}$	$f_{pr,xc}$	$f_{li,xc}$								$f_{xI,xc}$	$k_{dis} \cdot X_c$
2	Hydrolysis Carbohydrates		-1											$k_{hyd,ch} \cdot X_{ch}$
3	Hydrolysis of Proteins			-1										$k_{hyd,pr} \cdot X_{pr}$
4	Hydrolysis of Lipids				-1									$k_{hyd,li} \cdot X_{li}$
5	Uptake of Sugars					Y_{su}								$k_{m,su} \frac{S_{su}}{K_S + S_{su}} X_{su} I_1$
6	Uptake of Amino Acids						Y_{aa}							$k_{m,aa} \frac{S_{aa}}{K_S + S_{aa}} X_{aa} I_1$
7	Uptake of LCFA							Y_{fa}						$k_{m,fa} \frac{S_{fa}}{K_S + S_{fa}} X_{fa} I_2$
8	Uptake of Valerate								Y_{c4}					$k_{m,c4} \frac{S_{va}}{K_S + S_{va}} X_{c4} \frac{1}{1 + S_{bu}/S_{va}} I_2$
9	Uptake of Butyrate								Y_{c4}					$k_{m,c4} \frac{S_{bu}}{K_S + S_{bu}} X_{c4} \frac{1}{1 + S_{va}/S_{bu}} I_2$
10	Uptake of Propionate									Y_{pro}				$k_{m,pr} \frac{S_{pro}}{K_S + S_{pro}} X_{pro} I_2$
11	Uptake of Acetate										Y_{ac}			$k_{m,ac} \frac{S_{ac}}{K_S + S_{ac}} X_{ac} I_3$
12	Uptake of Hydrogen											Y_{h2}		$k_{m,h2} \frac{S_{h2}}{K_S + S_{h2}} X_{h2} I_1$
13	Decay of X_{su}	1				-1								$k_{dec,Xsu} \cdot X_{su}$
14	Decay of X_{aa}	1					-1							$k_{dec,Xaa} \cdot X_{aa}$
15	Decay of X_{fa}	1						-1						$k_{dec,Xfa} \cdot X_{fa}$
16	Decay of X_{C4}	1							-1					$k_{dec,Xc4} \cdot X_{c4}$
17	Decay of X_{pro}	1								-1				$k_{dec,Xpro} \cdot X_{pro}$
18	Decay of X_{ac}	1									-1			$k_{dec,Xac} \cdot X_{ac}$
19	Decay of X_{h2}	1										-1		$k_{dec,Xh2} \cdot X_{h2}$
		Composites (kgCOD m^{-3})	Carbohydrates (kgCOD m^{-3})	Proteins (kgCOD m^{-3})	Lipids (kgCOD m^{-3})	Sugar degraders (kgCOD m^{-3})	Amino acid degraders (kgCOD m^{-3})	LCFA degraders (kgCOD m^{-3})	Valerate and butyrate degraders (kgCOD m^{-3})	Propionate degraders (kgCOD m^{-3})	Acetate degraders (kmoleC m^{-3})	Hydrogen degraders (kmoleN m^{-3})	Particulates inerts (kgCOD m^{-3})	Inhibition factors: $I_1 = I_{pH}\, I_{IN,lim}$ $I_2 = I_{pH}\, I_{IN,lim}\, I_{h2}$ $I_3 = I_{pH}\, I_{IN,lim}\, I_{NH3,Xac}$

Table 4.3. Dynamic state variables of ADM1 (Batstone *et al.,* 2002).

STATE VARIABLE	Symbol	Units
Composite	X_c	kg COD · m^{-3}
Carbohydrates	X_{ch}	kg COD · m^{-3}
Proteins	X_{pr}	kg COD · m^{-3}
Lipids	X_{li}	kg COD · m^{-3}
Particulate inerts	X_I	kg COD · m^{-3}
Soluble inerts	S_I	kg COD · m^{-3}
Monosaccharides	S_{su}	kg COD · m^{-3}
Amino acids	S_{aa}	kg COD · m^{-3}
Total long chain fatty acids	S_{fa}	kg COD · m^{-3}
Total valerate	S_{va}	kg COD · m^{-3}
Total butyrate	S_{bu}	kg COD · m^{-3}
Total propionate	S_{pro}	kg COD · m^{-3}
Total acetate	S_{ac}	kg COD · m^{-3}
Hydrogen	S_{h2}	kg COD · m^{-3}
Methane	S_{ch4}	kg COD · m^{-3}
Inorganic carbon	S_{IC}	M
Inorganic nitrogen	S_{IN}	M
Monosaccharides degraders	X_{su}	kg COD · m^{-3}
Amino acids degraders	X_{aa}	kg COD · m^{-3}
Long chain fatty acids degraders	X_{fa}	kg COD · m^{-3}
Butyrate and valerate degraders	X_{c4}	kg COD · m^{-3}
Propionate degraders	X_{pro}	kg COD · m^{-3}
Acetate degraders	X_{ac}	kg COD · m^{-3}
Hydrogen degraders	X_{h2}	kg COD · m^{-3}
Cations	S_{cat}	M
Anions	S_{an}	M

4.3 Benchmark Simulation Model

The main features of the IWA/COST simulation benchmark are described here as a reference; for further details on each BSM the reader should refer to Copp (2002), Rosen *et al.* (2004), Jeppsson *et al.* (2007) and Nopens *et al.* (2008). The main aim of Benchmark Simulation Models (BSMs) is to provide a protocol to objectively compare different CSs. However, the protocol used in the evaluation is critical and must be defined in such a way as to ensure unbiased comparisons. To make unbiased comparisons, each CS must be evaluated under the same conditions. Furthermore, the effect of the CS must be compared to a fully defined and suitable reference output. Only then is it possible to accurately evaluate a CS and compare it with another strategy. The simulation benchmark defines such a protocol and provides a suitable reference output.

4.3.1 Benchmark Simulation Model No1

The description of the BSM1 is structured as follows: first the plant layout is presented, then comes process models, a description of influent files, a simulation protocol, performance indices and finally default controllers.

4.3.1.1 Plant layout

The simulation benchmark plant design is comprised of five reactors in series with a secondary settler. **Figure 4.3** shows a schematic representation of the layout.

The layout is fully defined and has the following characteristic features:

- Five biological reactors in series with a secondary settler and a total biological volume of 6000 m^3 (biological reactors 1 & 2 are each 1000 m^3 and biological reactors 3, 4 & 5 are each 1333 m^3).

- Biological reactors 1 & 2 unaerated, but fully mixed.
- Aeration of biological reactors 3, 4 & 5 achieved using a maximum oxygen transfer coefficient (K_La) of 360 d^{-1}.
- Default K_La of 240 d^{-1} in biological reactors 3 & 4 and 84 d^{-1} in biological reactor 5.
- DO saturation of 8 $gO_2\,m^{-3}$ in biological reactors 3, 4 & 5.
- A non-reactive secondary settler with a volume of 6000 m^3 (area of 1500 m^2 and a depth of 4 m) subdivided into 10 layers.
- A feed point to the secondary settler at 2.2 m from the bottom (i.e. feed enters the secondary settler in the middle of the sixth layer).
- Two internal recycles:
  - A nitrate Q_{intr} from the 5th to the 1st biological reactor at 55338 $m^3 \cdot d^{-1}$.
  - A RAS from the underflow of the secondary settler to the front end of the plant at a default flow rate of 18446 $m^3 \cdot d^{-1}$ (as there is no biological reaction in the secondary settler, the O_2 concentration in the recycle is the same as in the fifth biological reactor).
- WAS is pumped continuously from the secondary settler underflow at a default rate of 385 $m^3 \cdot d^{-1}$.

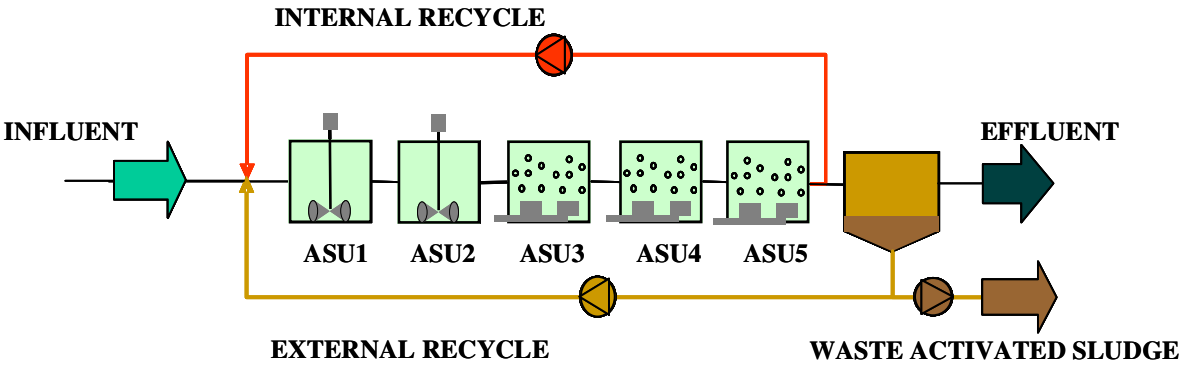

Figure 4.3. Schematic representation of the 'simulation benchmark' configuration.

The physical attributes of the biological reactors and the secondary settler are listed in **Table 4.6** and there is a selection of system variables listed in **Table 4.7**.

Table 4.6. Physical attributes of the biological reactors and the secondary settler for the IWA/COST simulation benchmark system configuration.

	Physical configuration	Units
Volume - Biological reactor 1	1000	m^3
Volume - Biological reactor 2	1000	m^3
Volume - Biological reactor 3	1333	m^3
Volume - Biological reactor 4	1333	m^3
Volume - Biological reactor 5	1333	m^3
Depth – Secondary settler	4	m
Area – Secondary settler	1500	m^2
Volume – Secondary settler	6000	m^3

Table 4.7. System variables.

	Default system flow rates	Units
Inflow rate	18446	$m^3 \cdot day^{-1}$
Recycle flow rate	18446	$m^3 \cdot day^{-1}$
Internal recycle flow rate	55338	$m^3 \cdot day^{-1}$
Waste sludge flow rate	385	$m^3 \cdot day^{-1}$
K_La – Biological reactor 1	n/a	-
K_La – Biological reactor 2	n/a	-
K_La – Biological reactor 3	10	hr^{-1}
K_La – Biological reactor 4	10	hr^{-1}
K_La – Biological reactor 5	3.5	hr^{-1}

4.3.1.2 Process models

As explained above, the biological processes are modelled using the ASM1. **Table 4.8** shows the stoichiometric and kinetic parameters, at approximately 15ºC, used in the BSM1 adaptation of the ASM1.

The secondary settler is modelled as a 10-layer non-reactive unit (i.e. with no biological reaction). The 6th layer (counting from bottom to top) is the feed layer. The secondary settler has an area (A) of 1500 m^2. The height of each layer *m* (z_m) is 0.4 m, making a total height of 4 m. The secondary settler's volume, therefore, is 6,000 m^3. The parameter values for the settling velocity function are given in **Table 4.9**.

Table 4.8. Stoichiometric and kinetic parameter values for the ASM1 in the BSM1.

PARAMETER DESCRIPTION	Parameter symbol	Value	Units
Autotrophic yield	Y_A	0.24	g $X_{B,A}$ COD formed (g N utilised)$^{-1}$
Heterotrophic yield	Y_H	0.67	g $X_{B,H}$ COD formed (g COD utilised)$^{-1}$
Fraction of biomass to particulate products	f_P	0.08	Dimensionless
Nitrogen fraction in biomass	i_{XB}	0.08	g N (g COD)$^{-1}$ in biomass ($X_{B,A}$ & $X_{B,H}$)
Nitrogen fraction in particulate products	i_{XP}	0.06	g N (g COD)$^{-1}$ in X_P
Maximum heterotrophic growth rate	μ_{mH}	4.0	day^{-1}
Half-saturation (hetero, growth)	K_S	10.0	g COD · m^{-3}
Half-saturation (hetero, oxygen)	K_{OH}	0.2	g O_2 · m^{-3}
Half-saturation (nitrate)	K_{NO}	0.5	g NO_3 · m^{-3}
Heterotrophic decay rate	b_H	0.3	day^{-1}
Anoxic growth rate correction factor	η_g	0.8	dimensionless
Anoxic hydrolysis rate correction factor	η_h	0.8	dimensionless
Maximum specific hydrolysis rate	K_h	3.0	g X_S (g $X_{B,H}$ COD · day)$^{-1}$
Half-saturation (hydrolysis)	K_X	0.1	g X_S (g $X_{B,H}$ COD)$^{-1}$
Maximum autotrophic growth rate	μ_{mA}	0.5	day^{-1}
Half-saturation (auto. growth)	K_{NH}	1.0	g NH_3-N · m^{-3}
Autotrophic decay rate	b_A	0.05	day^{-1}
Half-saturation (auto. oxygen)	K_{OA}	0.4	g O_2 · m^{-3}
Ammonification rate	K_a	0.05	m^3 (g COD · day)$^{-1}$

The solid flux due to gravity is $J_s=v_s(X)\cdot X$ where X is the total sludge concentration. A double-exponential settling velocity function (Takács *et al.,* 1991) has been selected (**Equations 4.1**):

$$v_s(X) = \max\left(0, \min\left(v'_0, v_0\left(e^{-r_h(X-X_{min})} - e^{-r_p(X-X_{min})}\right)\right)\right) \quad \textbf{(Eq. 4.1)}$$

where

$$X_{min}=f_{ns}\cdot X_f \quad \textbf{(Eq. 4.2)}$$

Table 4.9. Secondary settler model parameters and default values.

	Parameter	Units	Value
Maximum settling velocity	v_0'	$m \cdot day^{-1}$	250
Maximum Vesilind settling velocity	v_o	$m \cdot day^{-1}$	474
Hindered zone settling parameter	r_h	$m^3 \cdot (g\ SS)^{-1}$	0.000576
Flocculant zone settling parameter	r_p	$m^3 \cdot (g\ SS)^{-1}$	0.00286
Non-settleable fraction	f_{ns}	dimensionless	0.00228

4.3.1.3 Influent file design

To achieve a complete and unbiased evaluation, it is important that each CS be subjected to a series of defined disturbances. To this end, several dynamic influent files have been defined in the simulation benchmark description (Copp, 1999; Vanhooren and Nguyen, 1996). In total, there are three influent descriptions and each is meant to be representative of a different weather condition. Each file contains 14 days of influent data at 15-minute intervals. The data included in the files are listed in the following order: time, S_I, S_S, X_I, X_S, $X_{B,H}$, $X_{B,A}$, X_P, S_O, S_{NO}, S_{NH}, S_{ND}, X_{ND}, S_{ALK}, Q_0, assuming S_O, $X_{B,A}$, X_P and S_{NO} to be 0, and S_{ALK} = 7 mol·m^{-3}. In general, these files depict expected daily variations in Q_{in}, COD and N. In addition, expected trends in weekly data have been incorporated, which means that much lower peak flows are depicted in the "weekend" data, which is consistent with normal load behaviour at a municipal treatment facility.

The files are representative of three disturbances: dry weather, a storm event and a rain event. The first file depicts what is considered to be normal daily variations in flow rates and COD and N loads. The second file is a variation on the first with the incorporation of two storm events. The first storm event in this file is of high intensity and short duration and is expected to flush the sewer of particulate material. The resuspension of these particles is reflected in the data through a significant increase in inert and biodegradable suspended solids. The second storm event assumes the sewers were cleared of particulate matter during the first storm event; hence, only a modest increase in COD load is noted during the second storm. This result occurs even though the peak flow for both storms is the same and the peak flow of the second storm is maintained over a longer period of time. The third file is meant to represent a long rain event. The influent flow during this event does not reach the level attained during the storm events, but the increased flow is sustained for a much longer period of time. Unlike the storm events, there is no increase in COD load to the plant. The flow-weighted average concentrations of the influent components for the three files are shown in **Table 4.10**.

Table 4.10. Flow weighted average influent composition in the influent files.

COMPONENT	Dry weather	Storm event	Rain event	Units
S_S	69.50	64.93	60.13	g COD·m^{-3}
$X_{B,H}$	28.17	27.25	24.37	g COD·m^{-3}
X_S	202.32	193.32	175.05	g COD·m^{-3}
X_I	51.20	51.92	44.30	g COD·m^{-3}
S_{NH}	31.56	29.48	27.30	g N·m^{-3}
S_I	30.00	28.03	25.96	g COD·m^{-3}
S_{ND}	6.95	6.49	6.01	g N·m^{-3}
X_{ND}	10.59	10.24	9.16	g N·m^{-3}
Q	18446	19745	21320	m^3·day^{-1}

4.3.1.4 Simulation procedure

The simulation procedure involves two steps: steady state and dynamic simulation. In the first, the system is simulated with a constant influent flow rate and composition. One hundred days of simulation using the flow-weighted average dry weather influent is used to ensure a consistent starting point and eliminate the influence of the starting conditions.

The dynamic simulation starts by simulating the system for 14 days with the dynamic dry weather influent. After this, the state variables are saved and used as the starting

conditions for the last 14 days of simulation in the desired weather conditions (i.e. dry weather, storm event or rain event).

Only the last 7 days of simulation are used for performance evaluation purposes (i.e. from day 22 to day 28). In total, data for all variables are stored every 15 min during the 7 days of evaluation.

4.3.1.5 Performance indices

The flow-weighted average values of the effluent concentrations over the three evaluation periods (dry, rain and storm weather: 7 days for each) should obey the limits given in **Table 4.11**. Total N (N_{tot}) is calculated as the sum of $S_{NO,e}$ and $S_{NKj,e}$, where S_{NKj} is the Kjeldahl N concentration.

Table 4.11. Concentration limits for pollutants in the effluent.

VARIABLE	VALUE
N_{tot}	< 18 g N·m^{-3}
COD_t	< 100 g COD·m^{-3}
S_{NH}	< 4 g N·m^{-3}
TSS	< 30 g SS·m^{-3}
BOD_5	< 10 g BOD·m^{-3}

As performance indices the percentage of time in violation (%TIV) of the limits in **Table 4.11** is given. The performance assessment also includes the effluent quality (EQI; **Equation 4.3**). The EQI (kg pollution unit.d^{-1}) is averaged over the period of observation T (d) (i.e. the second week or last 7 days of each weather file), based on a weighting of the effluent loads of compounds that have a major influence on the quality of the receiving water and that are usually included in regional legislation.

EQI is defined as:

$$EQI = \frac{1}{T \cdot 1000} \int_{t=7days}^{t=14days} \left(\begin{matrix} B_{SS} \cdot SS_e(t) + B_{COD} \cdot COD_e(t) + B_{Nkj} \cdot S_{Nkj,e}(t) + \\ B_{NO} \cdot S_{NO,e}(t) + B_{BOD5} \cdot BOD_e(t) \end{matrix} \right) \cdot Q(t) \cdot dt \quad \textbf{(Eq. 4.3)}$$

where

$$S_{Nkj,e} = S_{NH,e} + S_{ND,e} + X_{ND,e} + i_{XB}\left(X_{B,H,e} + X_{B,A,e}\right) + i_{XP} \quad \textbf{(Eq. 4.4)}$$

$$SS_e = 0.75 \cdot \left(X_{S,e} + X_{I,e} + X_{B,H,e} + X_{B,A,e} + X_{P,e}\right) \quad \textbf{(Eq. 4.5)}$$

$$BOD_{5,e} = 0.25 \cdot \left(S_{S,e} + X_{S,e} + \left(1 - f_P\right) \cdot \left(X_{B,H,e} + X_{B,A,e}\right)\right) \quad \textbf{(Eq. 4.6)}$$

$$COD_e = \left(S_{S,e} + S_{I,e} + X_{S,e} + X_{I,e} + X_{B,H,e} + X_{B,A,e} + X_{P,e}\right) \quad \textbf{(Eq. 4.7)}$$

and the B_i are weighting factors that convert the different types of pollution (**Equation 4.8**) into pollution units (**Table 4.12**). The concentrations will be expressed in g.m^{-3}. The values for B_i have been deduced from Vanrolleghem *et al.* (1996).

Likewise, an influent quality index (IQI) can be calculated:

$$IQI = \frac{1}{T \cdot 1000} \int_{t=7days}^{t=14days} \left(\begin{matrix} B_{SS} \cdot SS_0(t) + B_{COD} \cdot COD_0(t) + B_{Nkj} \cdot S_{Nkj,0}(t) + \\ + B_{NO} \cdot S_{NO,0}(t) + B_{BOD5} \cdot BOD_0(t) \end{matrix} \right) \cdot Q_0(t) \quad \textbf{(Eq. 4.8)}$$

where

$$S_{Nkj,0} = S_{NH,0} + S_{ND,0} + X_{ND,0} + i_{XB}\left(X_{B,H,0} + X_{B,A,0}\right) + i_{XP}\left(X_{P,0} + X_{i,0}\right) \quad \textbf{(Eq. 4.9)}$$

$$SS_0 = 0.75 \cdot \left(X_{S,0} + X_{I,0} + X_{B,H,0} + X_{B,A,0} + X_{P,0}\right) \quad \textbf{(Eq. 4.10)}$$

$$BOD_{5,0} = 0.65 \cdot \left(S_{S,0} + X_{S,0} + \left(1 - f_P\right)\left(X_{B,H,0} + X_{B,A,0}\right)\right) \quad \textbf{(Eq. 4.11)}$$

$$COD_0 = \left(S_{S,0} + S_{I,0} + X_{S,0} + X_{I,0} + X_{B,H,0} + X_{B,A,0} + X_{P,0}\right) \quad \textbf{(Eq. 4.12)}$$

Table 4.12. *Bi* values

FACTOR	B_{SS}	B_{COD}	B_{Nkj}	B_{NO}	B_{BOD5}
Value (g pollutions units·g^{-1})	2	1	30	10	2

Ninety-fifth percentiles of the effluent ammonia ($S_{NH,95}$), effluent total N ($N_{tot,95}$) and total suspended solids (TSS_{95}) have to be shown as well. These percentiles represent the S_{NH}, $N_{tot,95}$ and *TSS* effluent concentrations that are exceeded 5% of the time.

Performance assessment also includes operational costs. Operational costs include several elements:

- Sludge production (SP; kg·d^{-1}) to be disposed of. This is the sum of the WAS and the solids that have accumulated in the system. The amount of TSS in the biological reactor at time t can be expressed as follows (**Equation 4.13**):

$$\mathrm{TSS}(t) = \mathrm{TSS}_a(t) + \mathrm{TSS}_s(t) \quad \textbf{(Eq. 4.13)}$$

where TSS_a is the total suspended solids in the biological reactor,

$$\mathrm{TSS}_a(t) = 0.75 \cdot \sum_{i=1}^{i=n} (X_{S,i} + X_{I,i} + X_{B,H,i} + X_{B,A,i} + X_{P,i}) \cdot V_i \quad \textbf{(Eq. 4.14)}$$

with $n = 5$

TSS_S is the total suspended solids in the secondary settler,

$$\mathrm{TSS}_S(t) = 0.75 \cdot \sum_{j=1}^{j=m} (X_{S,j} + X_{I,j} + X_{B,H,j} + X_{B,A,j} + X_{P,j}) \cdot z_j \cdot A \quad \textbf{(Eq. 4.15)}$$

with $m = 10$

- Total SP, which takes into account the sludge to be disposed of and the sludge lost at the weir (**Equation 4.16**):

$$\mathrm{SP}_{total} = \mathrm{SP} + \frac{0.75}{T} \cdot \sum_{t=7days}^{t=14days} (X_{S,e} + X_{I,e} + X_{B,H,e} + X_{B,A,e} + X_{P,e}) \cdot Q_e(t) \cdot dt \quad \textbf{(Eq. 4.16)}$$

where

$$\mathrm{SP} = \frac{1}{T}\left(\begin{array}{l} \mathrm{TSS}(14\ \mathrm{days}) - \mathrm{TSS}(7\ \mathrm{days}) + 0.75 \cdot \\ \cdot \sum_{t=7days}^{t=14days} (X_{S,w} + X_{I,w} + X_{B,H,w} + X_{B,A,w} + X_{P,w}) \cdot Q_w(t) \cdot dt \end{array} \right) \quad \textbf{(Eq. 4.17)}$$

- Pumping energy (PE; kWh·d^{-1}) and aeration energy (AE; kWh·d^{-1}) are also included in the operational costs (**Equations 4.18** and **4.19,** respectively).

$$PE = \frac{1}{T} \int_{t=7\,days}^{t=14\,days} \left(0.004 \cdot Q_a(t) + 0.008 \cdot Q_r(t) + 0.05 \cdot Q_w(t)\right) \cdot dt \quad \textbf{(Eq. 4.18)}$$

where
flow rates are in $m^3 \cdot d^{-1}$

AE should take into account the type of diffuser, bubble size, etc., and is calculated from the K_La according to **Equation 4.19**, valid for Degrémont DP230 porous disks at an immersion depth of 4 m.

$$AE = \frac{S_O^{sat}}{T \cdot 1.8 \cdot 1000} \int_{t=7\,days}^{t=14\,days} \sum_{i=1}^{5} V_i \cdot K_L a_i(t) \cdot dt \quad \textbf{(Eq. 4.19)}$$

where K_La is in d^{-1} and *i* refers to the compartment.

- Consumption of external carbon source (EC; kg COD·d^{-1}). This can be added to improve denitrification (**Equation 4.20**).

$$EC = \frac{COD_{EC}}{T \cdot 1000} \int_{t=7\,days}^{t=14\,days} \left(\sum_{i=1}^{i=n} Q_{carb,i} \right) \cdot dt \quad \textbf{(Eq. 4.20)}$$

where

COD_{EC} = 400000 gCOD·m^{-3}

- Mixing energy (ME; kWh·d^{-1}) as a function of the compartment's volume (**Equation 4.21**).

$$ME = \frac{24}{T} \int_{t=7\,days}^{t=14\,days} \sum_{i=1}^{i=5} \begin{bmatrix} 0.005 \cdot V_i \text{ if } K_L a_i(t) < 20\,d^{-1} \\ 0 \text{ otherwise} \end{bmatrix} \cdot dt \quad \textbf{(Eq. 4.21)}$$

The weighted sum of **Equations 4.17, 4.18, 4.19, 4.20, 4.21** represents the operational cost index (OCI; **Equation 4.22**).

$$OCI = AE + PE + 5 \cdot SP + 3 \cdot EC + ME \quad \textbf{(Eq. 4.22)}$$

4.3.1.6 Default controllers

A number of default controllers were developed and implemented in the BSM1 to test the evaluation criteria in closed-loop scenarios. Two proportional integral (PI) controllers were implemented, the first to maintain the nitrate concentration in the second biological reactor at 1 g·m^{-3} by manipulating the internal recycle from the fifth to the first biological reactor, and the second to maintain the DO at 2 g (-COD) · m^{-3} manipulating K_La in the fifth biological reactor. In addition, specific evaluation criteria for the control handles is available by maximal deviation from set points and by error variance.

The default controllers have the following features:

- The DO: DO sensor ranges from 0 to 10 g(-COD)·m^{-3} with a noise of 0.25 g(-COD)·m^{-3}. K_La in the fifth biological reactor is constrained between 0 and 360 d^{-1}.

- The Q_{intr} ranges from 0 to 5 times the $Q_{in,0}$ (18446 $m^3 \cdot d^{-1}$). The nitrate sensor has a 10 minutes delay, a measurement noise of 0.5 $gN \cdot m^{-3}$ and the measurement range is between 0 to 20 $gN \cdot m^{-3}$.

4.3.2 Long-term Benchmark Simulation Model No1

The BSM1_LT is a natural evolution development of the BSM1. The BSM1_LT was developed to address certain BSM1 limitations. The main changes (Rosen *et al.*, 2004) are: evaluation time period, addition of temperature changes, temperature dependency, toxicity, inhibition for kinetic reactions and the influent file design. Within the BSM1_LT, new control handles that made no sense in the BSM1 are possible mainly for monitoring. For instance, the consequences of WAS flow rate manipulation might not be seen in a seven-day evaluation period, but they will in a 365-day period.

4.3.2.1 Evaluation time period

It is well known that seasonal effects have a significant influence on WWTP performance, and that some probe failures only occur a few times a year. Therefore, a seven-day evaluation period of the BSM1 would not be sufficient to evaluate the long-term influence of seasonal effects on CSs. For this reason, the simulation period was extended to 609 days, with performance being evaluated over the last 365 days. The first 63 days are simulated with dynamic influent to reach a 'pseudo' steady state, and are followed by 18 months' simulation. From this period the first 6 months can be used for the training of monitoring strategies and control algorithms, while the last 12 months (starting the 1st July) are used for evaluation purposes. In general terms, the extended evaluation period makes the BSM1_LT more realistic.

4.3.2.2 Temperature changes

The temperature has been modelled as a sinusoidal function (**Equation 4.23**):

$$T\ (^{\circ}C) = 15 + 5 \cdot \cos\left(\frac{2\pi}{365(t-28)}\right) \quad \textbf{(Eq. 4.23)}$$

The function represents the roughly sinusoidal behaviour of the temperature during the year, at its maximum at the beginning of autumn and its minimum in February. Also, the diurnal effect is included with a sine wave with a period of 1 day and amplitude of 0.5ºC.

4.3.2.3 Temperature dependency

As a consequence, the values of the temperature dependent kinetic parameters in the ASM1 model vary during the evaluation period. In Henze *et al.* (1987), kinetic parameter values are given for 10 and 20°C and intermediate values can be calculated according to an Arrhenius function. The BSM1 parameter values are defined at 15°C, but rounded to one or two decimal points. Since it is desirable that the BSM1 and BSM1_LT have exactly the same parameter values at 15°C, the Arrhenius function should be based on values at 10 and 15°C, using the BSM1 values for 15°C. At 20°C, this gives slightly different values to those of Henze *et al.* (1987).

It should be noted that the saturation concentration for DO is temperature dependent. This has an impact on the mass transfer rate of O_2, since it is modelled as $K_La\ (S_{O,sat}-S_O)$. K_La is also temperature dependent. In BSM1, and also in the proposed BSM1_LT, the O_2 mass

transfer rate is expressed as K_La. This means that no temperature compensation is required for K_La. However, as soon as K_La is to be expressed in terms of energy (an important evaluation criterion), the temperature dependency is crucial (Rosen *et al.*, 2004).

4.3.2.4 Influent file design

The design of the influent file is based on the BSM2 influent file (see **Section 4.3.3.2 Influent file design**). However, there is a difference: since the influent file of BSM2 is defined as the influent to the plant, whereas the influent file in BSM1 is defined as the influent to the biological treatment, there is a need to modify the BSM2 influent file for use in the BSM1_LT. This is done by simply letting the influent file of BSM2 be applied to the same type of primary clarifier used in BSM2 and the output of the clarifier becomes the influent file of BSM1_LT (IWA Task Group on Benchmarking of Control Strategies for WWTPs, 2009).

4.3.3 Benchmark Simulation Model No2

None of the BSMs provides a model suitable for simulation on a plant-wide basis. This is the limitation that the BSM2 overcomes, principally by including the sludge line with the ADM1. Only the main features of the BSM2 are commented on here; for further details the reader can refer to Jeppsson *et al.* (2006) and Nopens *et al.* (2008).

4.3.3.1 Plant layout

Specifically, the BSM2 contains seven components (**Figure 4.4**): (i) a primary clarifier based on the description of Otterpohl and Freund (1992) and Otterpohl *et al.* (1994); (ii) five-reactor (two anoxic plus three aerobic) N removal AS configuration based on the ASM1 (Henze *et al.*, 1987); (iii) a secondary clarifier based on the double exponential model of Takács *et al.* (1991); (iv) an ideal gravity thickening unit; (v) AD based on the ADM1 (Batstone *et al.*, 2002); (vi) an ideal dewatering unit and, (vii) a storage tank between the dewatering unit and the primary clarifier.

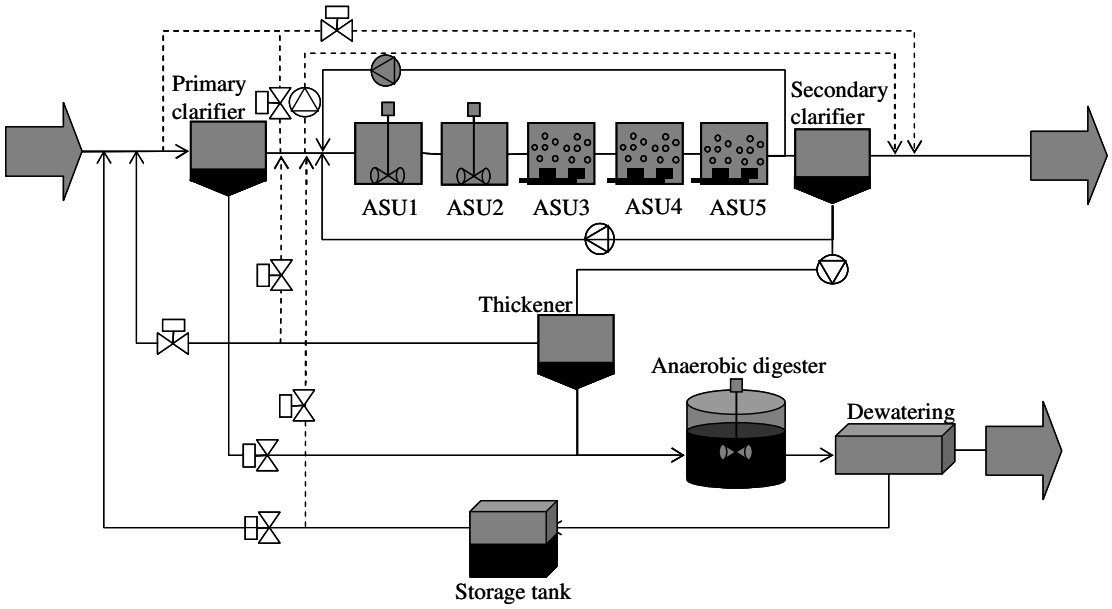

Figure 4.4. BSM2 layout used for AD risk model simulations.

Compared to BSM1 and BSM1_LT the volumes of the five biological reactor reactors were increased due to the high N-loads caused by the reject water (**Table 4.13**).

Table 4.13. New biological reactor volumes for BSM2.

	Physical configuration	Units
Volume - Biological reactor 1	1500	m^3
Volume - Biological reactor 2	1500	m^3
Volume - Biological reactor 3	3000	m^3
Volume - Biological reactor 4	3000	m^3
Volume - Biological reactor 5	3000	m^3

The changes in volumes also resulted in more changes in flow rates in order to maintain a reasonable HRT. **Table 4.14** summarises the changes in flow rates, HRTs, sludge loadings and digester SRT.

Table 4.14. BSM2 plant specifications.

	Default system values	Units
Inflow rate	20648	$m^3 \cdot day^{-1}$
Recycle flow rate	20648	$m^3 \cdot day^{-1}$
Internal recycle flow rate	61944	$m^3 \cdot day^{-1}$
Waste sludge flow rate	300	$m^3 \cdot day^{-1}$
K_La – Biological reactor 1	n/a	-
K_La – Biological reactor 2	n/a	-
K_La – Biological reactor 3	120	d^{-1}
K_La – Biological reactor 4	120	d^{-1}
K_La – Biological reactor 5	60	d^{-1}
HRT-Primary clarifier	1	h
HRT-Overall biological reactor	14	h
Sludge loading – Secondary settler	0.6	$m \cdot h^{-1}$
Anaerobic digester SRT	19	d

4.3.3.2 Influent file design

The influent file for BSM2 has been generated with the dynamic disturbance model presented in Gernaey *et al.* (2006). The influent model includes the diurnal flow rate and concentration variations, rain events, a holiday effect which lasts for several weeks with reduced wastewater flow rate and pollutants fluxes. The seasonal effect on the inflow rate is also present represented by a high infiltration rate during the winter period and low infiltration during summer. Variation of temperature is also included as explained in **Section 4.3.2.2 Temperature changes**.

4.3.3.3 Simulation procedure

The BSM2 simulation is run for a total of 809 days. The initial 200 days are used to reach a steady state with constant input data, while of the remaining 609 days, 245 are used to reach a quasi-steady state for dynamic input data and to provide adaptive controllers with enough time to estimate parameters. This means that only the last 364 days are to be used for evaluation purposes.

4.3.3.4 Performance indices

The main changes in the evaluation criteria that the BSM2 encompass are related to OCI (dimensionless). This includes the BSM1 costs (**Equation 4.10**) accrued from PE, aeration, ME, sludge disposal, EC and, in addition (**Equation 4.24**), the costs related to the AD system such as methane production (MP) and heating energy (HE):

$$OCI = AE + PE + 3 \cdot SP + 3 \cdot EC + ME - 6 \cdot MP + \max(0, HE^{net}) \quad \textbf{(Eq. 4.24)}$$

in which

HE^{net} is the net needed energy to heat the anaerobic digester (**Eq. 4.25**).

$$HE^{net} = HE - 7 \cdot MP \quad \textbf{(Eq. 4.25)}$$

4.3.3.5 Anaerobic Digestion Model No1 implementation in the Benchmark Simulation Model No2

The models included in the BSM2 have already been presented; however, some changes had to be made in order to integrate the ADM1 and ASM1 in the BSM2. A list of the main features adapted appears in more detail in Rosen *et al.* (2006). They describe how the problem of the wide range of the time constants (the stiffness problem) is solved. There is also an explanation of the adaptations made to the interfaces created by Copp *et al.* (2003) for implementation in the BSM2, as well as a discussion about algebraic solvers for pH and other troublesome variables. Recently, Nopens *et al.* (2009) identified the drawbacks and modified the interface by Copp *et al.* (2003) resulting in a more general and applicable interface.

4.4 Artificial Neural Networks

ANNs have the capacity to find the solution to a problem from a set of examples. A feed-forward ANN is a mathematical function that transforms a set of input variables into a set of output variables. The exact form in which this is done is regulated by a set of parameters called *weights,* which act as coefficients of the mathematical function. The values of these parameters are determined during a process called *training*. During this process, a set of real input and output data is presented to the ANN. Different weight values are generated to obtain a function which should represent the output variables presented to the ANN. An error is calculated for each set of weights. The weights that generate the function with the lowest error at the end are selected (Bishop, 1994). The exact architecture of the ANN is determined by the number of neurons and layers they have: the more neurons and layers, the more complex the ANN structure will be. Therefore, it is better to have simpler structures given that the more complex ones entail higher training and computation times. **Figure 4.5** presents a general view of an ANN. The white circles represent the nodes (i.e. neurons) of the hidden layers while the grey circles represent the input and output layers (i.e. y_i and x_i, respectively). The lines represent the interconnections between the nodes (i.e. the *weights*).

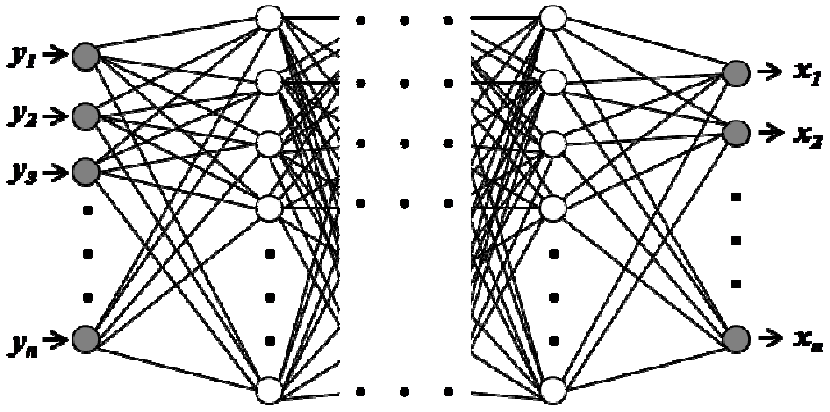

Figure 4.5. A general ANN.

The main advantage of ANNs is their high processing speed and to avoid the need to develop a first-principles model of the process, sometimes difficult or even impossible. On the other hand, the principal disadvantage of an ANN is that a sufficient amount of reliable data is required to provide enough information with which to both train and validate it, with the guarantee that sensor failures and/or data loss will not affect the training process. On top of this, severe problems may arise when extrapolating an ANN to new data outside the range of the data used during the training process.

A feed-forward neural network toolbox for static models for use in MATLAB 5.3 or higher was used in this thesis. Three layers were chosen in all the ANN architectures: an input layer, a hidden layer of neurones with sigmoid transfer functions, and an output layer with linear transfer functions for outputs. Initialisation was performed using the Nguyen-Widrow algorithm, which initialises the weights with random values, later selecting their probability distributions to make all neurones active for the expected data ranges (Nguyen and Widrow, 1990). It also provides automatic data scaling and weights conversion. Bayesian regularisation is used to prevent over-fitting.

4.5 Fuzzy rule-based systems

Fuzzy rules are linguistic IF-THEN constructions that have the general form "IF A THEN B" where A and B are (collections of) propositions containing linguistic variables. A is called the *premise* and B is the *consequence* of the rule. In effect, the use of linguistic variables and fuzzy IF-THEN rules exploits the tolerance for imprecision and uncertainty. In this respect, fuzzy logic mimics the crucial ability of the human mind to summarize data and focus on decision-relevant information.

Rule-based systems have two main parts:

- *Knowledge base*: The knowledge base includes a set of decision trees (see, for example, **Figure 5.1**) or decision matrices (see, for example, **Table 5.2**) which contain the overall knowledge of the process.

- *The inference engine*: The inference engine is the software that controls the reasoning operation by scanning the knowledge in the knowledge base.

In this work, the description of heuristic and empirical knowledge is tackled using the principles of fuzzy decision theory (Bellmann and Zadeh, 1970; Pedrycz, 1995). It was L.A. Zadeh who expanded Boolean logic to real numbers. In Boolean logic 1 represents “true” and 0 “false”. In fuzzy logic, all the values between 0 and 1 are included, in order that a partial truth can also be represented.

The use of fuzzy logic has increased due to the need to quantify rule-based systems. Basically, it allows us to assign degrees of truth, between 0 and 1, by quantifying numeric variables with linguistic tags such as *often, never, approximately, some, very, a few, high, very high*, etc. This allows fuzzy logic to provide data interpretations which, in the case of existing well-defined limits, would not be possible. For instance, SVI values higher than 150 $mg \cdot L^{-1}$ are typically considered high. With fuzzy logic, values higher than 150 $mg \cdot L^{-1}$ could be considered 100% high, whereas a value of 145 $mg \cdot L^{-1}$ could be considered 90% high and 10% medium. With Boolean logic, a value of 145 $mg \cdot L^{-1}$ would be considered as normal despite being very close to the value defined as high.

4.5.1 Fuzzification

For each input and output variable selected, at least two membership functions (MFs) has to be defined - normally three and sometimes more. A qualitative category is defined for each of them: for example, 'low', 'normal' or 'high'. The shapes of these functions are diverse but the usual is to work with triangles and trapezoids (in fact, usually pseudo-trapezoids) (see **Figure 4.6**). For this reason at least three (for triangles) or four (for trapezoids) points are required to define one MF of one variable.

Example: If **x** is taken as a variable and 'low', 'normal' and 'high' as trapezoidal, triangle and trapezoidal MFs, respectively (**Figure 4.6**),

- the **'low'** MF will in fact be defined by three points: (x_1, x_2, x_3) since x_1 will always be 0. However, in order to define a real trapezoid a fourth point to the left of x_1 (any negative one, e.g. x_0) has to be defined.
- the **'high'** MF, following the same reasoning, has to be defined by four points: (x_3, x_4, x_5, x_6) (x_6 any positive > x_5). Despite this, any x value higher than x_5 will have a degree of membership to the 'high' MF of 1, even though the degree of membership decreases beyond x_5.
- the **'normal'** MF (like any other triangular MF) will be defined by three points: (x_2, x_3, x_4).

If the MFs are trapezoids (or pseudo-trapezoids, i.e. 'low' and 'high'), they can be defined as (**Equations 4.26** and **4.27**):

$$y^{low}_{(trap)}(x;x_0,x_1,x_2,x_3)=\begin{cases}\max\left(\min\left(\frac{x-x_0}{x_1-x_0},1,\frac{x_3-x}{x_3-x_2}\right),0\right) & \text{for } x_3\geq x\geq x_1\\ 1 & \text{for } x<x_1\end{cases} \qquad \textbf{(Eq. 4.26)}$$

$$y^{high}_{(trap)}(x;x_3,x_4,x_5,x_6)=\begin{cases}\max\left(\min\left(\frac{x-x_3}{x_4-x_3},1,\frac{x_6-x}{x_6-x_5}\right),0\right) & \text{for } x_5\geq x\geq x_3\\ 1 & \text{for } x>x_5\end{cases} \qquad \textbf{(Eq. 4.27)}$$

If the MFs are triangles (in this case 'normal'), they can be defined as (**Equation 4.28**):

$$y^{normal}_{(tri)}(x;x_2,x_3,x_4)=\max\left(\min\left(\frac{x-x_2}{x_3-x_2},\frac{x_4-x}{x_4-x_3}\right),0\right) \qquad \textbf{(Eq. 4.28)}$$

It is important to emphasise that the computation of all the functions/equations for all the MFs of all variables has to be done every time the shape and interval of the MFs is changed (conversely, once computed the first time, the computations do not have to be done again if the MFs are not changed).

4.5.1.1 How the fuzzification step works

The next question to be solved is how to fuzzify all the real values of the variable x. First, for a given value of x, for example x_n, which can belong to one or more MFs, the y value is calculated for each of the MFs which x_n belongs to. This y value has to be between 0 and 1. Consider, for example, three MFs: 'low', 'normal' and 'high' and a given value of x_n. The degrees of membership to each MF (y values) for x_n could be, for example: 0.6 for the 'low' MF and 0.4 for the 'normal' MF (see **Figure 4.6**). Likewise, all the values of any variable can be fuzzyfied. Any of the values will belong to at least one MF with a certain degree of membership.

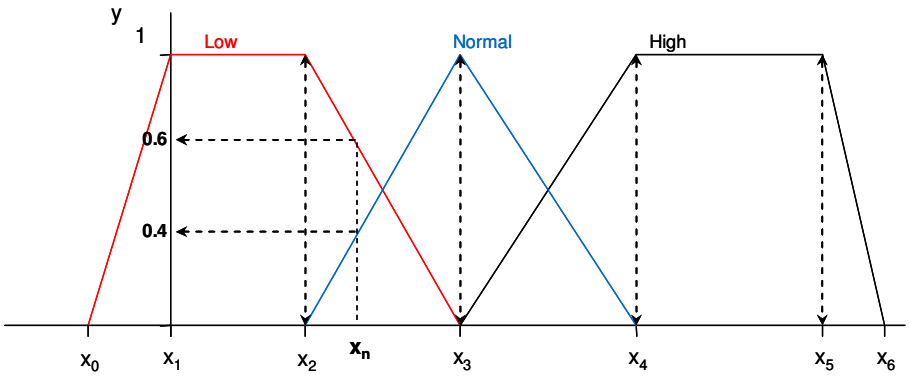

Figure 4.6. Example of the three MF for a given input.

4.5.2 Rule base (decision matrix) definition

Once the input and output variables and the MF are defined, the next step is to design the rule base (or decision matrix of the fuzzy knowledge base) composed of expert IF <antecedents> THEN <conclusions> rules. These rules transform the input variables into an output that will tell us the risk of operational problems (this output variable, the risk of a problem, also has to be defined with the MF, which will usually be 'low', 'normal' or 'high' risk). Depending on the number of MFs for the input and output variables, a greater or lesser number of potential rules can be defined. The easiest case will be a rule base with only one input and one output variable.

Example: For a given variable x involved in the development of a problem, the following "theoretical" rule can be stated:

IF x is 'normal' THEN risk of problem is 'medium'.

The more variables there are present, the more rules can be defined in order to make the inference reliable.

Once realistic rules based on expert knowledge have been defined, they will become the knowledge base of each of the problems considered in the risk model. It needs to be pointed out that not all the knowledge necessarily has to be translated into rules; sometimes some of the rules will be redundant. Let us demonstrate by a decision matrix (**Table 4.15**) that contains the expert knowledge to detect the risk of a problem from inputs X and Y:

Table 4.15. Example of MFs for each variable considered.

		Input Y			
		LOW	**NORMAL**	**HIGH**	**VERY HIGH**
Input X	**LOW**	low	high	high	high
	NORMAL	low	low	medium	medium
	HIGH	low	low	low	low
	VERY HIGH	low	low	low	low

4.5.2.1 How the rule base works

The next issue is to compute the degree of membership to the MF ('low', 'normal' or 'high') of the output (the risk of the problem). As explained in the fuzzification section, once a variable is fuzzified it takes a value between 0 and 1 indicating degree of membership to a given MF of that specific variable. The degrees of membership of the input variables have to be combined to get the degree of membership of the output variable.

Example 4: For a given variable x involved in the cause of a problem (the risk-output has its own MF, 'low', 'normal' or 'high' risk), a rule base can be described by "saying", for example, that:

IF x is 'low' THEN risk of problem is 'low'.

IF x is 'normal' THEN risk of problem is 'medium'.

IF x is 'high' THEN risk of problem is 'high'.

According to these rules, if the degree of membership for x is supposed to be 0.6 to the 'low' MF, then the risk of the problem will be 'low' 0.6, too.

In a case where more than one input variable is present (which in fact is the usual case), the degree of membership for the output value will be the minimum value of the degree of membership for the different inputs.

Example 5: Looking at Figure 3, let us suppose that for a set of 9 rules resulting from the decision matrix (see **Table 4.15** above) Input X = 0.55 has a membership degree of 0.8 to the 'normal' MF (rules 4, 6 and 7), and a membership degree of 0.2 to the 'high' MF (rule 8). On the other hand, Input Y = 6.5 has a membership degree of 0.2 to the 'high' MF (rules 1 and 7) and a membership degree of 0.9 to the 'normal' MF (rules 3 and 4). When a rule is totally satisfied (the antecedent is satisfied, those with (1) in **Figure 4.7**, rules: 4, 7 and 8), it will have an output with a certain membership degree to an output MF. These rules are satisfied in this example:

IF Input X is 'normal' (degree of 0.8) and Input Y is 'normal' (degree of 0.9) THEN Risk of problem is 'low' (degree of 0.8) (Rule 4)

IF Input X is 'normal' (degree of 0.8) and Input Y is 'high' (degree of 0.2) THEN Risk of problem is 'medium' (degree of 0.2) (Rule 7)

IF Input X is 'high' (degree of 0.2) THEN Risk of problem is 'low' (degree of 0.2) (Rule 8)

The MF of the output will have a degree of membership equal to the lowest of the inputs.

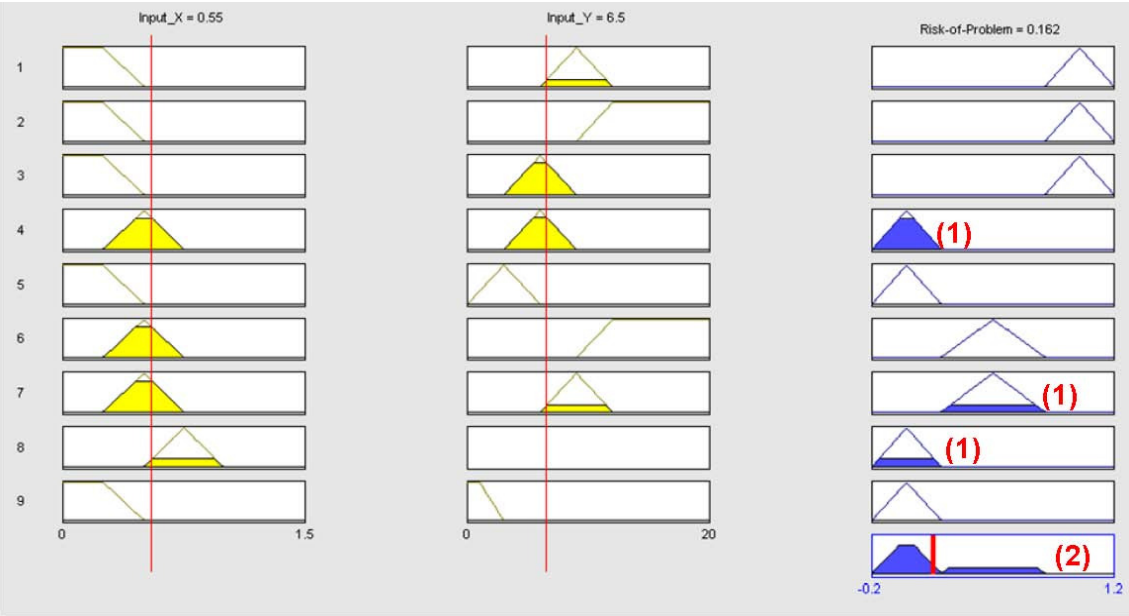

Figure 4.7. Example of the rules for the determination of a hypothetic risk of problem (detected by the rules in **Table 1**).

From here, only the satisfied rules (4, 7 and 8) are taken into account. The resulting figure for output (2) has a 'low' MF due to rules 4 and 8 and a 'normal' MF due to rule 7. To sum up, the final output figure (2) is the integration (sum) of the MF from the satisfied rules (1). Among the satisfied rules, the membership degree of each output MF will be the highest from among the rules that have as a result that MF. This means that the degree of membership of the 'normal' MF (0.2) (in (2)) is due to rule 7 and that the degree of membership of the 'low' MF (0.8) (in (2)) is due to the higher of rules 4 and 8 (those that have as a conclusion that the MF is 'low').

4.5.3 Defuzzification

In this thesis the MFs of the output always have the same shape and configuration and the risk of any problem has the same rank: 'low', 'normal' or 'high'. There is never any overlapping and the range of the output is from -0.2 to 1.2. **Figure 4.8** shows the shape of each MF of the output variable.

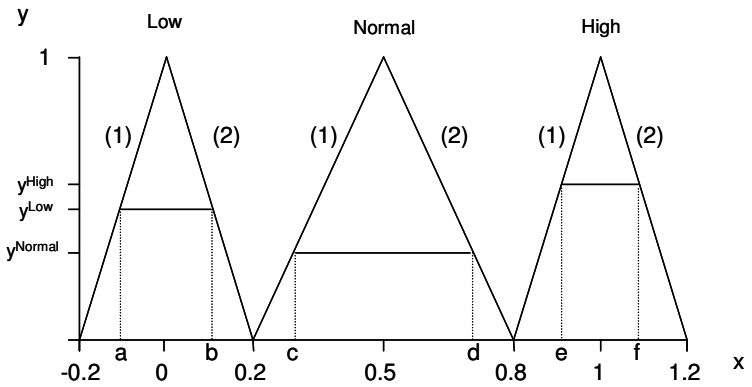

Figure 4.8. Output MFs.

The equations of the straight lines of each output MF have to be calculated. The calculations for each of the MFs are presented next:

For 'low' MF:

$$\begin{aligned} y_1^{low} &= m_1 \cdot x_1 + n_1 \\ y_2^{low} &= m_2 \cdot x_2 + n_2 \\ m_1 &= (1-0)/(0.2-0) = 5 \\ m_2 &= (1-0)/(0-0.2) = -5 \end{aligned} \qquad \text{(Eq. 4.29 and 4.30)}$$

To find n, the point (0, 1) is substituted on both straight lines to obtain the two equations:

$$\begin{aligned} y_1^{low} &= 5 \cdot x + 1 \\ y_2^{low} &= -5 \cdot x + 1 \end{aligned}$$

A similar calculation is performed for 'medium' (or 'normal'; **Equations 4.31** and **4.32**) and 'high' MFs (**Equations 4.33** and **4.34**), to finally obtain:

$$\begin{aligned} y_1^{medium} &= \frac{1}{0.3} \cdot x - 0.665 \\ y_2^{medium} &= -\frac{1}{0.3} \cdot x + 2.665 \end{aligned} \qquad \text{(Eq. 4.31 and 4.32)}$$

$$\begin{aligned} y_1^{high} &= 5 \cdot x - 4 \\ y_2^{high} &= -5 \cdot x + 6 \end{aligned} \qquad \text{(Eq. 4.33 and 4.34)}$$

The value of each MF between each letter (i.e. between a and b, c and d, and e and f) corresponds to the value of the degree of membership for that function.

To calculate a, b, c, d, e and f, the degree of membership has to be substituted in the y of the corresponding function, while x will be the corresponding letter (i.e. a, b, c, d, e or f).

Example 6: From Example 5 two output MFs were obtained, 'low' and 'medium', with a degree of membership of 0.8 and 0.2, respectively. Thus, to find points a and b, 0.8 has to be substituted in **Equations 4.29** and **4.30**:

$$\begin{cases} y_1^{low} = 5 \cdot a + 1 \\ y_2^{low} = -5 \cdot b + 1 \end{cases}$$

where the degree of membership is 0.8 as in:

$$\begin{cases} 0.8 = 5 \cdot a + 1 \\ 0.8 = -5 \cdot b + 1 \end{cases}$$

And finally,

$$\begin{cases} a = -0.04 \\ b = 0.04 \end{cases}$$

The same is true for the 'medium' MF (**Equations 4.31** and **4.32**),

$$\begin{cases} y_1^{medium} = \frac{1}{0.3} \cdot c - 0.665 \\ y_2^{medium} = -\frac{1}{0.3} \cdot d + 2.665 \\ 0.2 = \frac{1}{0.3} \cdot c - 0.665 \\ 0.2 = -\frac{1}{0.3} \cdot d + 2.665 \end{cases}$$

$$\begin{cases} c = 0.2595 \\ d = 0.7395 \end{cases}$$

4.5.3.1 How the defuzzification step works

The next step involves calculating the area of the resulting figures for each MF, taking into account that these areas will not be triangles in all cases (most of the time they will be triangles or trapezoids).

The basic idea is to evaluate each output activated MF at intervals of 0.014. Those output MFs that have not been activated by the rules in Step 1.2 of the rule base take the full range of 0 as their value (see Example 7).

It will be necessary to store each pair (x, y) for later calculation of the centroid.

So, 'low' MF should be as shown in **Table 4.16**.

Table 4.16. Intervals to be evaluated in steps of 0.014 for low output MF. Letters refer to **Figure 4.8**.

From -0.2 to a	$y_1^{low} = 5 \cdot x + 1$
From a to b	The value in this interval is the degree of membership of the resulting MF of **Section 4.5.2 – Rule base**
From b to 0.192	$y_1^{low} = -5 \cdot x + 1$

The same is true for the remaining MFs with their respective functions (**Tables 4.17** and **4.18**).

Table 4.17. Intervals to be evaluated in steps of 0.014 for medium output MF. Letters refer to **Figure 4.8**.

From 0.206 to c	$y_1^{medium} = 1/0.3 \cdot x - 0.665$
From c to d	The value in this interval is the degree of membership of the resulting MF of **Section 4.5.2 – Rule base**
From d to 0.794	$y_2^{medium} = -1/0.3 \cdot x + 2.665$

Table 4.18. Intervals to be evaluated in steps of 0.014 for high output MF. Letters refer to **Figure 4.8**.

From 0.808 to e	$y_1^{high} = 5 \cdot x - 4$
From e to f	The value in this interval is the degree of membership of the resulting MF of **Section 4.5.2 – Rule base**
From f to 1.2	$y_2^{high} = -5 \cdot x + 6$

As stated above, if any of these three MFs have not been activated by the rules, they will take the evaluation range 0 as their value.

The final result of all these calculations will be 101 (x, y) pairs, with x ranging from -0.2 to 1.2 in steps of 0.014. To calculate the final output of the risk model, the centroid has to be calculated as follows (**Equation 4.35**):

$$x_c = \frac{\sum_{i=1}^{i=101} x_i \cdot y_i}{\sum_{i=1}^{i=101} y_i} \qquad \textbf{(Eq. 4.35)}$$

Example 7: From Example 6 a, b, c and d are known. By evaluating the MF as stated above, **Table 4.19** is obtained.

Table 4.19. Example of centroid calculation.

I	x	y
1	-0.2 (-0.2 ➔a)	0 ($y_1^{low} = 5 \cdot x + 1$)
…	…	…
17	0.024 (a➔b)	0.8 (degree of membership 'low')
…	…	…
28	0.178 (b➔0.192)	0.11 ($y_1^{low} = -5 \cdot x + 1$)
…	…	…
31	0.22 (0.206➔c)	0.068 ($y_1^{medium} = 1/0.3 \cdot x - 0.665$)
…	…	…
44	0.402 (c➔d)	0.2 (degree of membership 'medium')
…	…	…
71	0.78 (d➔0.794)	0.065 ($y_2^{medium} = -1/0.3 \cdot x + 2.665$)
…	…	…
73➔101	(0.808➔1.2)	0 (The 'high' MF is not active for this example)
	$\sum_{i=1}^{i=101} y_i$	21.47
	$\sum_{i=1}^{i=101} x_i \cdot y_i$	3.87

By applying the centroid equation to the 101 (x, y) pairs the centroid can be calculated as follows:

$$x_c = \frac{\sum_{i=1}^{i=101} x_i \cdot y_i}{\sum_{i=1}^{i=101} y_i}$$

$$x_c = \frac{3.87}{21.47}$$

$$x_c = 0.18$$

4.6 Concluding remarks

This chapter has firstly presented the two standardized models for AS and AD: ASM1 which is the basis for the BSMs, and ADM1, which together with ASM1 allows the evaluation of BSM2 plant-wide control strategies. Next, BSM1 for short term has been detailed presenting the layout and the different specifications, simulation procedure and evaluation criteria. Afterwards the modifications (i.e. temperature changes and effects, influent files, etc.) to BSM1 for long-term simulation (BSM1_LT) are described to finally detail BSM2 main features.

The ANNs section presents the description of the ANN used in this thesis in the risk model development. The detailed description for a fuzzy logic system implementation using standard modelling description and equations was presented. The aim is to help

the benchmark developers to implement the risk model on their BSMs regardless of the simulation platform with the details that will appear in the following chapters.

CHAPTER 5

RISK MODEL DEVELOPMENT

Part of the work in this chapter has appeared in:

Dalmau J., Comas J., Rodríguez-Roda I., Latrille E. and Steyer J.P. (2009a). Selecting the most relevant variables for anaerobic digestion imbalances: two case studies. Water Environment Research (accepted).

Dalmau J., Comas J., Rodríguez-Roda I., Pagilla K. and Steyer J.P. (2009b). Risk model development and simulation for foaming in anaerobic digestion. Bioresource Technology, ***101****(12), 4306-4314.*

Dalmau J., Comas J. and Rodríguez-Roda I. (2009c). Extension of a risk model to include deflocculation and temperature. Water Science and Technology (submitted).

Dalmau J., Comas J., Rodriguez-Roda I., Latrille E. and Steyer J.P. (2008). A neural network approach for selecting the most relevant variables for foaming in anaerobic digestion. Proceedings of the International Congress on Environmental Modelling and Software. 4th Biennial Meeting (iEMSs 2008), 7-10 March, Barcelona, Spain.

Dalmau J., Comas J., Rodríguez-Roda I., Latrille E. and Steyer J.P. (2007). Using artificial neural networks for selecting relevant information in anaerobic digestion. Proceedings of the 11th IWA Specialist Conference on Anaerobic Digestion. 23-27 September, Brisbane, Australia.

5. Risk Model development

As discussed in **Section 2.3.5 Alternatives to mechanistic modelling of operational problems of microbiological origin,** two alternative approaches can be used when mechanistic modelling cannot be applied: a knowledge-based approach linked to the heuristic knowledge and a black-box approach. The approach selected will depend on the sort of information available.

The following section (**5.1 AS risk model**) is devoted to the development of the risk model for operational problems of microbiological origin which uses only information available in the simulation outputs, either directly or after simple data processing. For the AS risk model plenty of heuristic and bibliographic information was available. Hence, the risk model makes use of a KBS based on decision trees and fuzzy logic. This section details the following: the knowledge included in each operational problem of microbiological origin, its implementation in fuzzy logic, the range and shape of each MF, the outcomes of the model with the response surfaces for each operational problem of microbiological origin, and finally two extensions to the original AS risk model: (i) the inclusion of the deflocculation risk, and (ii) the effect of temperature on the risks associated with bulking and foaming caused by *M. parvicella.*

The second section (**5.2 AD risk model**) is devoted to the AD risk model. The inclusion of the ADM1 in the BSM2 was the main motivation behind the development of the AD risk model. **Section 2.2.2 Anaerobic Digestion** presented a possible classification of different operational problems of microbiological origin. Among them, the AD risk model needs to consider biological foaming since the other problems can be modelled in the ADM1. For example, organic overloads cause VFA accumulation and pH inhibition, which have already been taken into account of in the ADM1. Acidogenic states have been considered as well, since they are characterised by the above-mentioned VFA accumulation and pH inhibition. Only biological foaming cannot be modelled mechanistically, and therefore this was the operational problem of microbiological origin considered in ADM1. The fact that real data from a pilot plant was available enabled the use a different approach in the development of the AD risk model.

Section 5.2 AD risk model is divided in three main parts: (i) development, divided in a black-box approach and a knowledge-based approach; (ii) implementation of the developed AD risk model and finally, (iii) model outcomes, showing the response of the AD risk model. The first step to develop the AD risk model was a black box approach (**Section 5.2.1.1 Black box approach**); given that real data from a pilot plant was available it was decided to use a wrapper approach (Kohavi and John, 1997). It was implemented using ANN in order to objectively select the most important variables related to biological foaming. Afterwards, a literature research (**Section 5.2.1.2 Knowledge-based approach**) about biological FAD was performed. In **Section 5.2.1.3** conclusions are drawn on both approaches. Next the implementation of the AD risk model is presented.

5.1 Activated sludge risk model

The operational problems considered in this approach are those system situations caused by imbalances of microorganisms (filamentous bulking and activated sludge foaming) and undesirable operating conditions (rising sludge in clarifiers). The core of the risk

assessment approach is a knowledge base composed of heuristic and empirical knowledge acquired from the literature and domain experts (i.e. information that can not be adequately represented by mechanistic models). Interestingly though, a significant part of this knowledge can be captured by means of equations, graphs, relationships, etc. that are based on numerical data which are directly related to state variables or parameters of the mechanistic models. The central idea is to select and interpret those process variables that could be available in real-time in a simulation (e.g. readily biodegradable substrate concentration (S_S), ammonium nitrogen (NH_4^+-N), nitrate nitrogen (NO_3^--N), etc.) and which, albeit following human expert-like processing, would allow meaningful patterns relating to operational risks to be obtained. Note that due to a lack of affordable and reliable sensors only a minority of the simulated state variables used as inputs to the AS risk model presented here are monitored on-line in full-scale WWTPs. Instead, most variables are only available sporadically and after some delay following sampling and off-line analysis. This section is divided in three main subsections: development, knowledge formalisation and model outcomes.

5.1.1 Development

A review of the state-of-the-art understanding of filamentous bulking, foaming and rising sludge has led to the identification of symptoms, relationships and inference methods. This knowledge, founded on data used by experts in their reasoning strategies, has been organized and formalised by means of three decision trees or knowledge-based flow diagrams (Comas *et al.*, 2003). It was not possible to create a data-driven risk assessment model in this case because large input-output data sets were required. Such experimental data sets relating to the risk of settling process disturbances are not usually available, while expert knowledge is. In a simulation the decision trees explore a set of process state variables relating to water and sludge quality at different sampling points (e.g. S_S, heterotrophic biomass concentration ($X_{B,H}$), BOD or TSS) together with the operational parameters in the AS system (e.g. the Q_w or the Q_r) and a set of calculated parameters like the food-to-microorganism ratio (F/M) or the SRT. These diagrams consist of hierarchical, top-down descriptions of the linkages and interactions between pieces of knowledge used for problem solving. Their representation in decision trees has allowed an easy interpretation and verification of the available knowledge by a panel of internationally recognised wastewater treatment experts. As a result of that evaluation and of the suggestions received during and after the 2nd IWA conference on Instrumentation, Control and Automation, where the decision trees were first introduced (Comas *et al.*, 2006 and Comas *et al.*, 2008), the original decision trees and the resulting knowledge base have been updated to the version presented here.

5.1.1.1 Filamentous bulking decision tree

The knowledge relating to risk of filamentous bulking proliferation was synthesised into a decision tree with three branches (**Figure 5.1**). Each branch of the tree evaluates one of the three main causes: low DO concentration (left), nutrient deficiency (middle) and low F/M ratio or substrate limiting conditions (right). The other common causes of filamentous bulking (septic conditions or low pH in the influent) were not considered within the current approach since standard mechanistic models include neither sulphur (S) nor pH modelling.

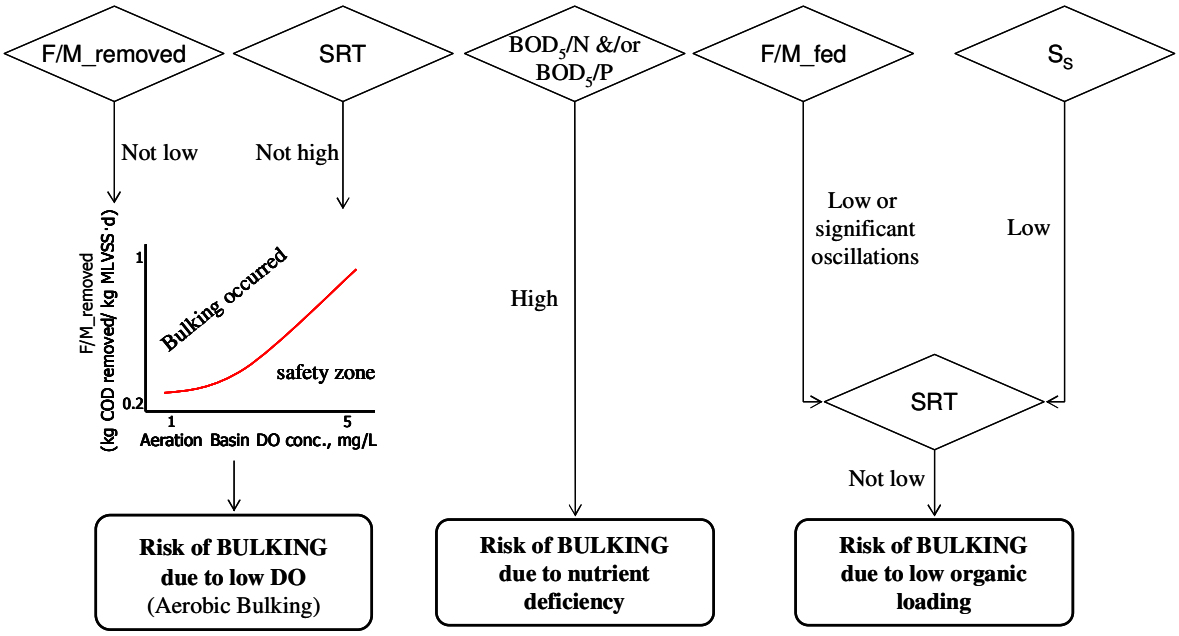

Figure 5.1. Decision tree developed to evaluate the risk of filamentous bulking.

According to the substrate-diffusion and the kinetic selection theories (Martins *et al.*, 2004) the growth of filaments is favoured during conditions of low DO concentration. The left branch of the tree illustrates that the level of occurrence of limiting DO conditions in the biological reactors is related to the current F/M ratio in a non-linear way (Grady *et al.*, 1999). So, although DO control is considered standard for most plants, favourable conditions for low DO caused bulking might arise if the DO set-point is not high enough when the WWTP experiences a high F/M ratio. The branch in the middle evaluates whether or not there are N and/or P limiting conditions. Finally, promoting conditions for the growth of low F/M filamentous microorganisms can be caused by both readily biodegradable substrate limiting conditions (S_S) in the bioreactor and by a low or oscillating influent OLR. Thus, up to seven variables can be used by the knowledge-based decision trees as indicators to assess risk of filamentous bulking: SRT (measured as biomass present in the system per biomass removed from the system per day), DO, F/M_removed (measured as kg of COD removed per kg of biomass per day), F/M_fed (measured as kg of BOD_5 supplied per kg of biomass per day), BOD_5/N, BOD_5/P and S_S.

5.1.1.2 Foaming decision tree

The set of indicators that were found to be the most useful in detecting favourable conditions for filamentous foaming included F/M_fed, SRT, DO and the ratio between S_S and slowly biodegradable substrate (X_S) (**Figure 5.2**). Two main branches allow for investigation of the operational conditions enhancing the growth of different filamentous microorganisms that would cause biological foaming problems.

Nocardioforms and *M. parvicella*, the most common filamentous organisms causing foaming (Wanner, 1994; Jenkins *et al.*, 2003; Rossetti *et al.*, 2005), experience better conditions for growth than floc-forming bacteria when the AS system experiences low F/M ratios or significant oscillations of F/M ratios combined with high SRT. In the case of *M. parvicella*, which also causes sludge bulking, foam formation is favoured by the two former conditions together with low DO concentrations in the aerobic reactors. The

development of biological foams due to growth of type 1863, although less frequent, is also probable if the F/M ratio fed to the bioreactor is very high (or the SRT is very low) and the influent contains a high fraction of HRBOM (a high S_S/X_S ratio).

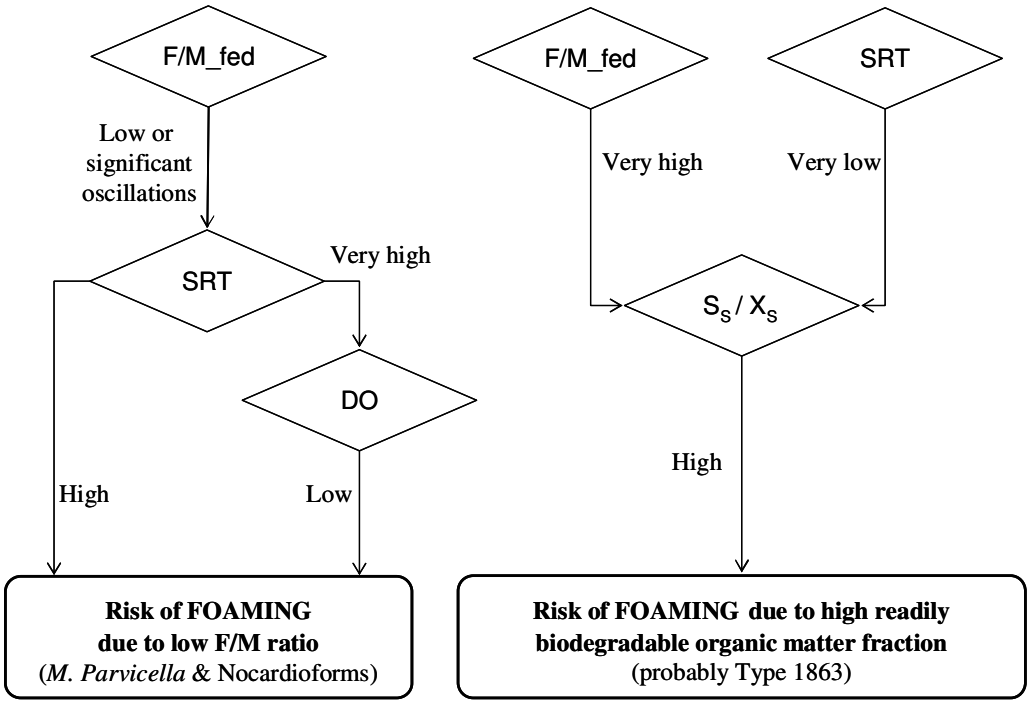

Figure 5.2. Decision tree developed to evaluate the risk of foaming.

5.1.1.3 Rising sludge decision tree

Figure 5.3 illustrates the decision tree developed to estimate the risk of rising sludge in AS systems.

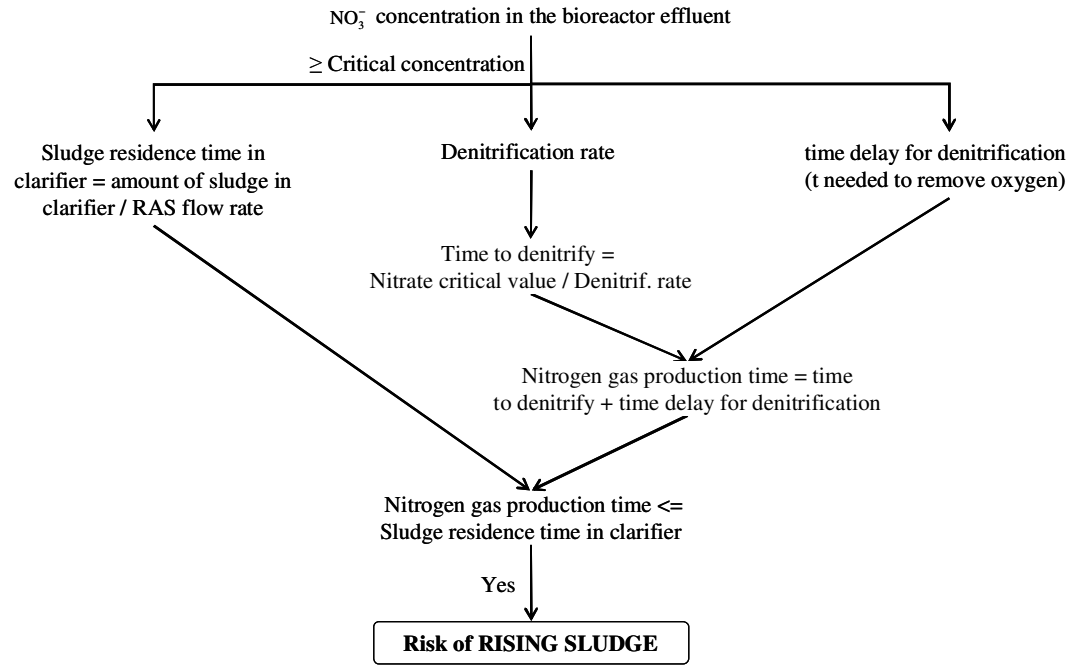

Figure 5.3. Decision tree developed to evaluate the risk of rising sludge.

According to Henze *et al.* (1993), rising sludge becomes a problem when the nitrate concentration in the secondary clarifier influent is higher than the critical nitrate concentration (8 mg NO_3^--N L^{-1} at 15ºC). In this situation, the time required for nitrogen gas production (NGPT) is calculated (based on the denitrification rate and the time delay caused by removal of the remaining O_2 at the bottom of the clarifier), and compared to the sludge retention time in the clarifier (estimated as the amount of sludge in the sludge blanket divided by the Q_r). The denitrification rate is calculated as for the ASM1, but using the active heterotrophic biomass concentration at the bottom of the clarifier. Whenever the nitrate concentration is higher than critical and the NGPT is lower than or equal to the sludge retention time in the secondary settler, then favourable conditions for denitrification are inferred, and consequently the risk of occurrence of solids separation problems due to rising sludge increases. Fast DO consumption is assumed in the secondary settler and therefore the denitrification rate is always computed assuming no O_2 inhibition (DO = 0 mg $O_2 \cdot L^{-1}$). Hence, the variables used as indicators for rising sludge are NO_3^--N, Q_r, sludge blanket depth and denitrification rate.

5.1.2 Knowledge formalisation

The model estimates the risk of occurrence of microbiology-related solids separation problems by processing the data used by the mechanistic model (not only simulation outputs but also influent data and operational parameters; see **Figure 5.4**).

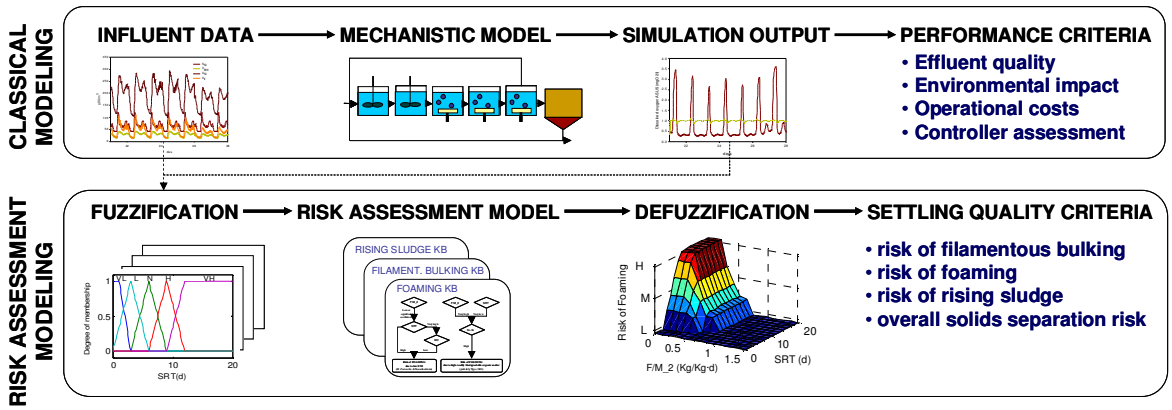

Figure 5.4. Relationship between the mechanistic model and the fuzzy knowledge base to estimate risk of microbiology-related solids separation problems.

Risk estimation involves three main steps:

5.1.2.1 Fuzzification

The crisp values of numerical data are converted into linguistic/qualitative descriptors or input fuzzy sets (i.e. low, high, etc.) by means of corresponding MFs. MFs are defined for each variable used as a risk assessment indicator or symptom in the decision trees: F/M_removed (F/M 1) ratio, F/M_fed (F/M 2) ratio, DO, SRT, BOD_5/N ratio, S_S, and S_S/X_S. Triangular or pseudo-trapezoidal functions are used to define the MFs. **Figure 5.5** illustrates an example of the MFs used in this approach.

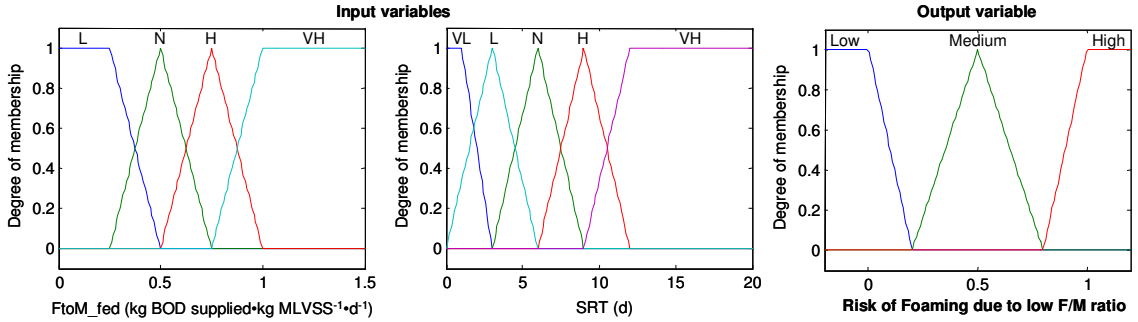

Figure 5.5. Example of MFs for the input and output variables for risk of foaming due to low F/M ratio.

Table 5.1 summarises the number of MFs and the ranks and shapes for each of the input and output fuzzy sets considered in the AS risk model. The limits of these MFs as well as their degree of overlapping, can be customised by the user according to the configuration and characteristics of the AS plant simulated.

Table 5.1. MFs for each variable considered in the AS risk model.

Variable\Modality		Very low	Low	Normal	High	Very high
F/M 1	**Shape**	-	Trapezoidal	Triangular	Triangular	Trapezoidal
	Range	-	[-0.1429 -0.1429 0.25 0.5]	[0.25 0.5 0.75]	[0.5 0.75 1]	[0.75 1 4.027 4.187]
F/M 2	**Shape**		Trapezoidal	Triangular	Triangular	Trapezoidal
	Range	-	[-0.0536 -0.0536 0.25 0.5]	[0.25 0.5 0.75]	[0.5 0.75 1]	[0.75 1 1.51 1.57]
DO	**Shape**	Trapezoidal	Triangular	Triangular	Triangular	Trapezoidal
	Range	[-0.4488 -0.1164 0 1]	[0 1 2]	[1 2 3]	[2 3.5 5]	[3.5 5 8.021 8.261]
SRT	**Shape**	Trapezoidal	Triangular	Triangular	Triangular	Trapezoidal
	Range	[-7.2 -0.8 1 3]	[0 3 6]	[3 6 9]	[6 9 12]	[9 12 20.29 23.4]
BOD5/N in the influent	**Shape**	-	Trapezoidal	Triangular	Trapezoidal	-
	Range	-	[-7.145 -7.145 10 20]	[10 20 33.33]	[20 33.3 201.3 209.3]	-
BOD5/P in the influent	**Shape**	-	Trapezoidal	Triangular	Trapezoidal	-
	Range	-	[-10 -1 0 10]	[10 50 100]	[50 100 200 210]	-
SS in biological reactor 1	**Shape**	-	Trapezoidal	Triangular	Trapezoidal	-
	Range	-	[-4.645 -4.645 4 14]	[9 20 34]	[29 40 131.6 143]	-
SS/XS in the influent	**Shape**	-	Trapezoidal	Triangular	Trapezoidal	-
	Range	-	[-0.08415 -0.02183 0.1 0.2]	[0.15 0.25 0.35]	[0.3 0.45 1.55 1.56]	-
SNO in biological reactor 5	**Shape**	-	Trapezoidal	Triangular	Trapezoidal	-
	Range	-	[-1.429 -1.429 2 5]	[2 5 8]	[5 8 40.27 41.87]	-
NGPT	**Shape**	-	Trapezoidal	Triangular	Trapezoidal	-
	Range	-	[-0.135 -0.0437 0.046 0.056]*	[0.046 0.056 0.066]*	[0.056 0.066 2.205 2.272]*	-
Risk of filamentous bulking	**Shape**	-	Triangular	Triangular	Triangular	-
	Range	-	[-0.2 0 0.2]	[0.2 0.5 0.8]	[0.8 1 1.2]	-
Risk of foaming	**Shape**	-	Triangular	Triangular	Triangular	-
	Range	-	[-0.2 0 0.2]	[0.2 0.5 0.8]	[0.8 1 1.2]	-
Risk of rising sludge	**Shape**	-	Triangular	Triangular	Triangular	-
	Range	-	[-0.2 0 0.2]	[0.2 0.5 0.8]	[0.8 1 1.2]	-

*These limits may vary in every simulation time step since they are a function of the amount of sludge in the clarifier and the sludge recycle flow rate (i.e. of the sludge residence time in clarifier; **Equations 5.1-5.3**).

5.1.2.2 Fuzzy inference

The inference of the risk is provided by the Mamdani approach, to generate a fuzzy output from the corresponding input fuzzy sets based on implications contained in the

fuzzy rule base. All the fuzzy rules in the model are derived from a review of the literature and based on the existing empirical knowledge of the cause-effect relationships of microbiology-related solids separation problems in the AS system. The decision trees shown in the previous section (**Figures 5.1, 5.2 and 5.3**) only represent those IF-THEN production rules leading to high risk of each particular microbiology-related separation problem, while the rule base of the AS risk model is shown in **Tables 5.2 to 5.7**. The Max-Min Mamdani fuzzy inference method (Mamdani and Assilan, 1975) was proposed as the mechanism with which to concatenate the set of IF-THEN rules.

$$\text{Limit1} = \frac{\text{Sludge Volume in Clarifier}}{Q_r + 1}$$

$$\text{Limit2} = \text{Limit1} + 0.01 \qquad \textbf{(Eq. 5.1-5.3)}$$

$$\text{Limit3} = \text{Limit1} + 0.02$$

where
sludge volume in clarifier calculation is shown in **Section 6.1.6 Rising sludge**.

Tables 5.2 to 5.7 present the rules extracted from each decision tree which combined with the MFs limits of **Table 5.1** produce the surfaces presented in **Figure 5.6 to Figure 5.14**. Whenever surfaces are presented the high risks are indicated by the red zone while the blue zones denote the low risks.

Figure 5.6 shows the profile of the risk of bulking due to nutrient deficiency caused by nitrogen. Likewise, **Figure 5.7** shows the profile of the risk of bulking caused by P deficiency. In the first case the profile shows that ratios higher than 20 increase the risk of bulking. For the second case, the P deficiency risk of bulking become high with a BOD5/P ratio from 90 to 100.

Table 5.2. Knowledge base of the risk of bulking due to nutrient deficiency (L: low, N: normal, H: high).

Bulking due to nutrient deficiency		
Input variables	**MFs**	**Risk**
BOD5/N or BOD5/P	L	Low
	N	Low
	H	High

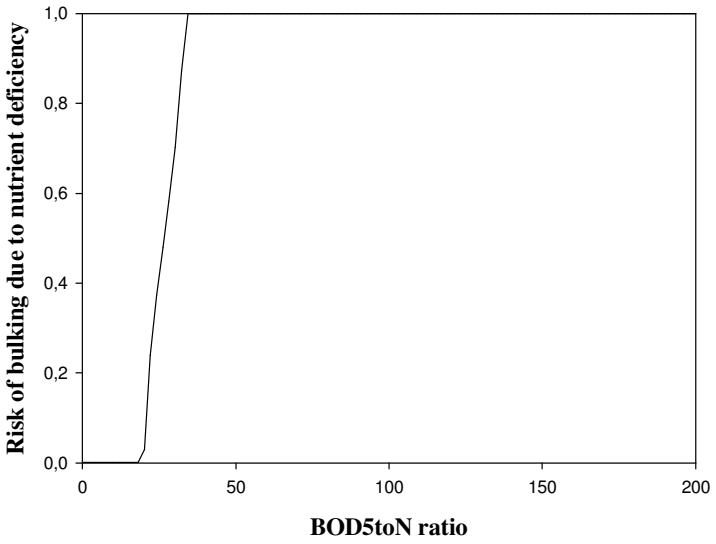

Figure 5.6. Risk of bulking due to N deficiency.

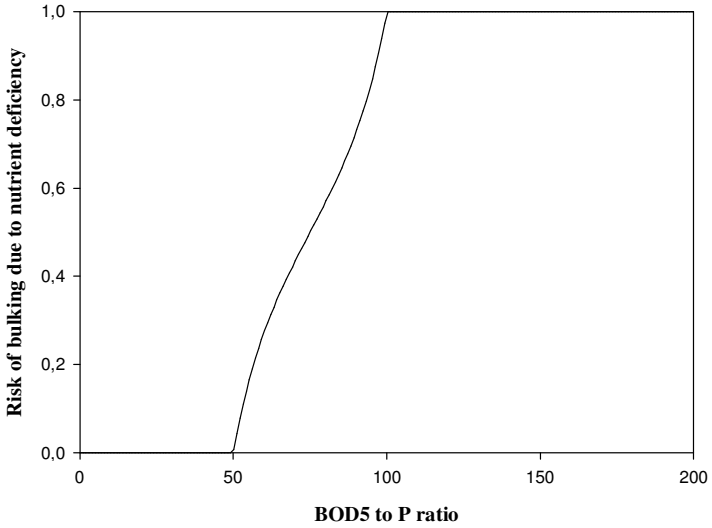

Figure 5.7. Risk of bulking due to P deficiency.

The surface in **Figure 5.8** shows the risk of bulking due to low DO. The red zone is roughly delimited by F/M 1 ratios above 0.5 and DO lower than 2 mg·l^{-1}.

Table 5.3. Knowledge base of the risk of bulking due to low DO (VL: Very low; L: low, N: normal, H: high; VH: Very high).

Bulking due to low DO						
		DO (mg/L^{-1})				
		VL	**L**	**N**	**H**	**VH**
F/M 1	**L**	Low	Low	Low	Low	Low
	N	High	Medium	Low	Low	Low
	H	High	High	Medium	Low	Low
	VH	High	High	High	Medium	Low

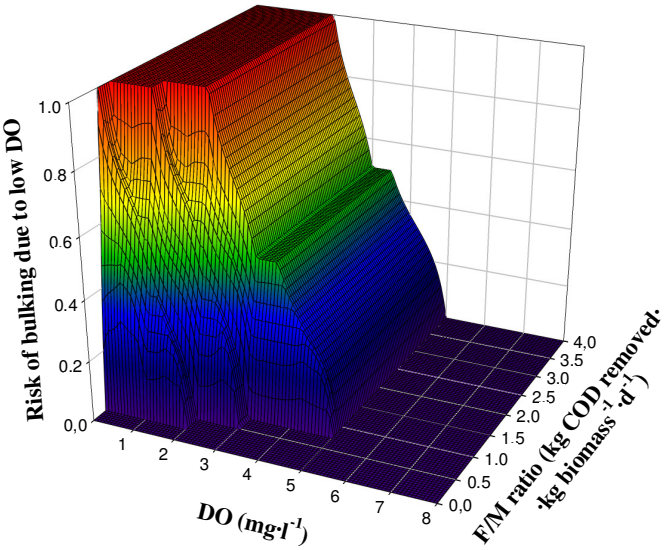

Figure 5.8. Risk of filamentous bulking due to low DO.
(F/M ratio –g COD removed·(g biomass)$^{-1}$·d^{-1}- vs. DO –g·m^{-3}-).

Figures 5.9 and **5.10** show the risk of bulking due to limited substrate. In the first case, the high risk zone is enclosed above approximately 0.3 F/M 1 and over 9 days for SRT. In the second case, the zone with the maximum risk is much narrower, in accordance

with the MFs defined. **Figure 5.11** has the same response surface as **Figure 5.9**, since both risks are related to *M. parvicella*.

Table 5.4. Knowledge base of the risk of bulking due to low organic loading (VL: Very low; L: low, N: normal, H: high; VH: Very high).

Bulking due to low organic loading						
		SRT				
		VL	**L**	**N**	**H**	**VH**
Ss	**L**	Low	Low	Medium	High	High
	N	Low	Low	Low	Low	Low
	H	Low	Low	Low	Low	Low
F/M 2	**L**	Low	Low	High	High	High
	N	Low	Low	Low	Medium	Medium
	H	Low	Low	Low	Low	Low
	VH	Low	Low	Low	Low	Low

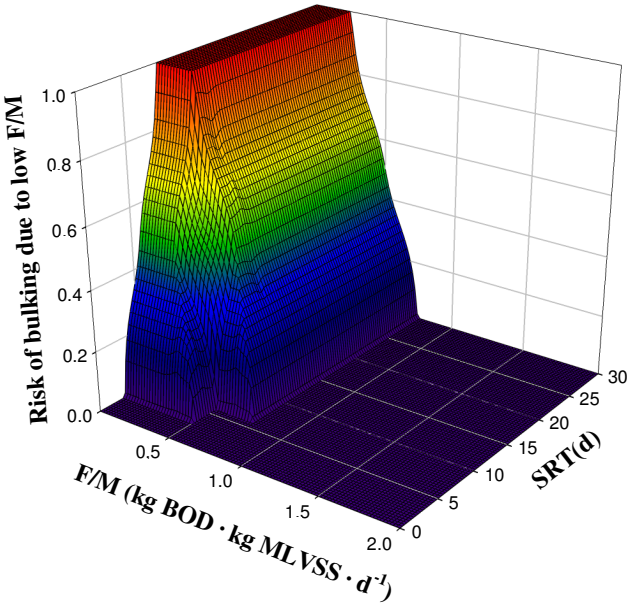

Figure 5.9. Risk of bulking due to low F/M 2.
(F/M ratio -g BOD_5 supplied·(g biomass)$^{-1}$·d^{-1}- vs. SRT –d-).

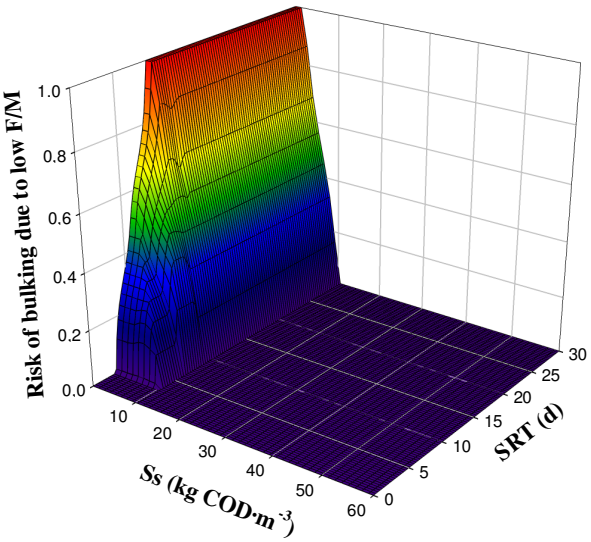

Figure 5.10. Risk of bulking due to low organic loading.
(readily biodegradable substrate, Ss –kg COD·m^{-3}- vs. SRT -d-).

Table 5.5. Knowledge base of the risk of foaming due to low organic loading (VL: Very low; L: low, N: normal, H: high; VH: Very high).

Foaming due to low F/M ratio					
		F/M 2			
		L	**N**	**H**	**VH**
SRT	**VL**	Low	Low	Low	Low
	L	Low	Low	Low	Low
	N	Moderate	Low	Low	Low
	H	High	Moderate	Low	Low
	VH	High	Moderate	Low	Low

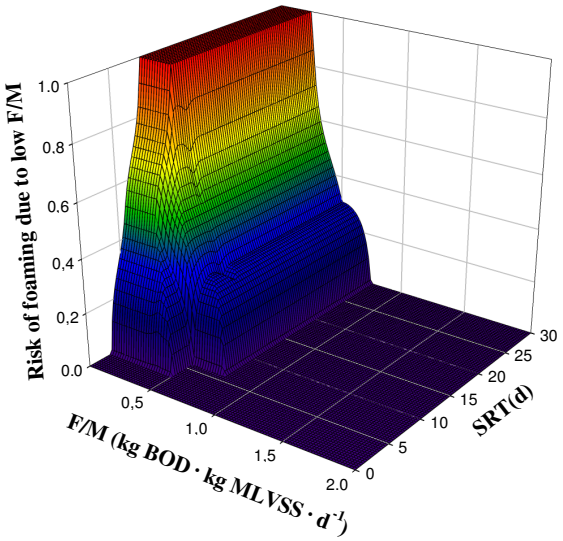

Figure 5.11. Risk of foaming due to low F/M 2.
(F/M ratio -g BOD_5 supplied·(g biomass)$^{-1}$·d^{-1}- vs. SRT -d-).

Figures 5.12 and **5.13** explain the risk of foaming due to HRBOM. The first surface shows an increasing risk of foaming from 0.5 F/M 2. On the other hand, when the HRBOM (Ss/Xs) ratio is considered the risk of foaming suddenly increases from 0.2 approximately. **Figure 5.13** presents the same behaviour from the Ss/Xs perspective, where the SRT has to be very low (less than 2-3 days approximately).

Table 5.6. Knowledge base of the risk of foaming due to HRBOM (VL: Very low; L: low, N: normal, H: high; VH: Very high).

Foaming due to HRBOM fraction				
		Ss/Xs		
		L	**N**	**H**
SRT	**VL**	Low	Medium	High
	L	Low	Low	Medium
	N	Low	Low	Low
	H	Low	Low	Low
	VH	Low	Low	Low
F/M 2	**L**	Low	Low	Low
	N	Low	Low	Low
	H	Low	Medium	Medium
	VH	Low	Medium	High

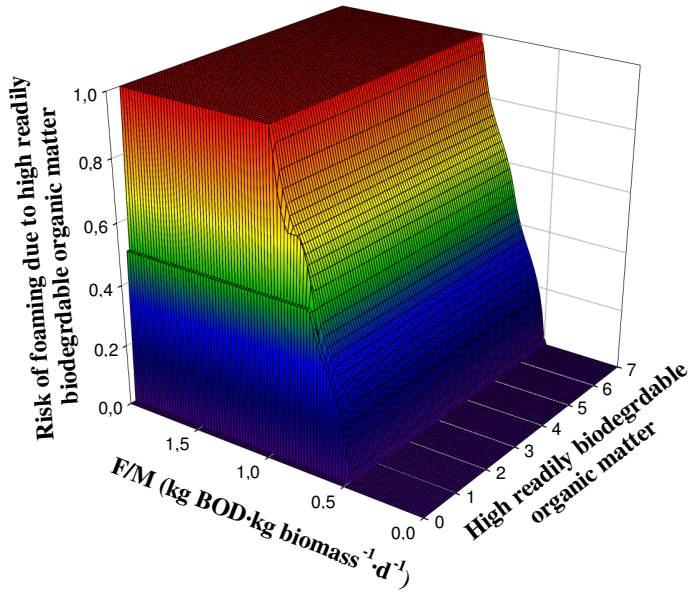

Figure 5.12. Risk of foaming due to HRBOM (S_S/X_S) fraction. (S_S/X_S vs. F/M ratio -g BOD_5 supplied·(g biomass)$^{-1}$·d^{-1}-)

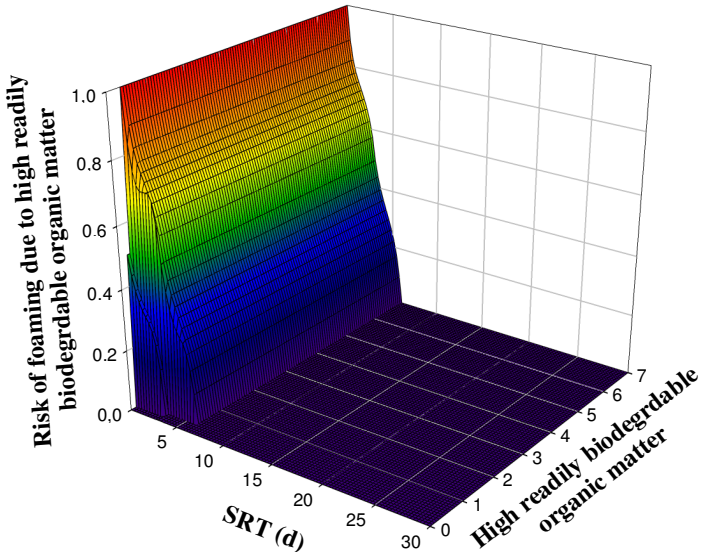

Figure 5.13. Risk of foaming due to HRBOM (S_S/X_S) fraction. (SRT –d- vs. S_S/X_S).

The response surface for the risk of rising sludge shows high risk progressively increasing from 2 g N·m^{-3} (**Figure 5.14**). NGPT below approximately 2 hours cause a high risk of rising sludge.

Table 5.7. Knowledge base of the risk of rising sludge (L: low, N: normal, H: high).

Rising sludge				
		NGPT		
		L	**N**	**H**
NO3	**L**	Low	Low	Low
	N	Medium	Low	Low
	H	High	Medium	Low

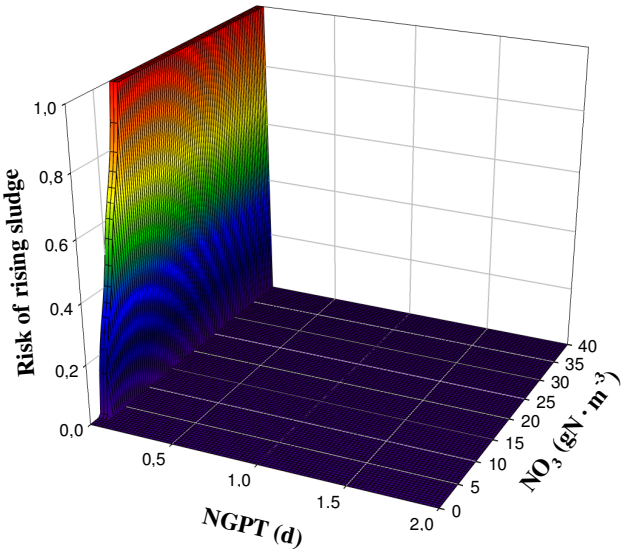

Figure 5.14. Risk of rising sludge.
(NGPT-d- vs. S_{NO} concentration –g N·m^{-3}-).

5.1.2.3 Defuzzification

The linguistic fuzzy output has to be translated into a numerical value as the outcome of the risk assessment (again, MFs were defined for the three output variables of the module: 'risk of filamentous bulking', 'risk of foaming' and 'risk of rising sludge') by means of the Centre of Gravity (COG) method (Fiter *et al.*, 2005).

The knowledge used to develop the fuzzy rules is empirical and based on qualitative assumptions to determine cause-effect relationships of operational problems of microbiological origin in AS systems (e.g. if SRT is high and DO is low, the risk of foaming is high). This is an empirical assumption included in the model by means of a fuzzy rule but the model uses deterministic values, for example, of SRT and DO, to infer a deterministic risk of foaming.

The estimation of the risk of filamentous bulking, foaming and/or rising sludge is performed continuously during the simulated time period, yielding to a new value at every time step, when a new set of simulation output data becomes available. It should be noted that whenever the output results of the risk model indicate that conditions for a specific problem (filamentous bulking, foaming or rising sludge) are satisfied for more than one cause (branch), the highest value of the risk will be selected for this problem.

Risk filtering

The appearance of one of these microbiology-related solids separation problems in an activated sludge system requires a high risk for a long and sustained period of time. Therefore for long simulation periods the results of the risk assessment model are smoothed by means of an exponential filter (**Equation 5.4**) that takes this issue into account. The exponential filter has a time constant related to the dynamics of each specific problem and to the SRT (2 hours for rising sludge and 3 days for filamentous bulking, foaming problems and SRT). In case more than one cause (branch) is satisfied for each individual risk, this filter is applied after the maximum value has been selected at each time step.

The filter can be written as:

$$y_{filtered}(t) = \alpha \cdot y_{filtered}(t-1) + (1-\alpha) \cdot y(t) \quad \textbf{(Eq. 5.4)}$$

where
$y_{filtered}$ represents the filtered data;
y is the raw data;
α is calculated according to,

$$\alpha = 1 - \frac{1}{T \cdot n_s} \quad \textbf{(Eq. 5.5)}$$

where
T represents the time constant in days;
n_s is the number of output samples per day in the simulation (here $n_s = 96$).

An exponential filter also facilitates the visualisation and interpretation of results. At the time of application of the risk model the user can choose his own time constant depending on his interests. For example, in **Section 6.3.1.1 Filter time constant variation** there is a study of the effect of the time constant variation on the effect of the filter (**Figure 6.17**).

The AS risk model has been implemented independently of the existing AS models. Although the MATLAB 6.5 Fuzzy Toolbox (Mathworks, Inc.) was initially used to develop the MFs and build the rule base, the proposed risk assessment procedure has been developed so as to be software independent.

5.1.3 Model outcome

The AS risk model provides new plant performance criteria relating to the risk of occurrence of operational problems of microbiological origin in AS systems. It provides six different vectors corresponding to time series signals for the risks of the following problems: filamentous bulking due to low DO, filamentous bulking due to nutrient deficiency, filamentous bulking due to low organic loading, foaming due to low F/M ratio, foaming due to HRBOM fraction and rising sludge.

The risk indices for filamentous bulking, foaming and rising sludge can be integrated into a single overall risk index. To achieve that, an integrated index for filamentous bulking must first be obtained as the maximum value, at each time step, among the smoothed time series signals of the three risk indices of filamentous bulking problems (caused by low DO concentrations, low F/M ratios or nutrient deficiencies). At the same time, the maximum value at each time step of the smoothed signals of the risks of foaming due to low F/M ratio on the one hand and due to HRBOM fraction on the other hand provides the integrated foaming index. The final aggregation simply consists of taking the maximum value at every time step from among the integrated risk for bulking, the integrated risk for foaming and the risk for rising sludge, in order to produce the overall risk index. For a specific AS system, these integrated values give an idea of the overall risk of occurrence of solids separation problems as well as indicating which problem to address first.

The results from the risk assessment are reported and quantified in four different ways for each of the operational problems of microbiological origin, for the integrated risks of bulking and foaming and for the overall risk index: (i) a time series plot (or data) showing the evolution of the risk occurrence for a specific settling problem (or for one of the integrated indices) during the evaluation period. In this plot 0 means no risk while 1 indicates the highest possible risk; (ii) the percentage of time in violation (%TIV) during which the plant is experiencing severe risk (an arbitrary but customisable ≥ 0.8 limit value of risk is used for defining a severe problem) of operational problems of microbiological origin; (iii) the most dangerous situation during the evaluation period, computed as the longest time interval during which the plant is exposed to an uninterrupted severe risk of experiencing a specific settling problem, and (iv) the average (AV) risk.

These new settling criteria complement traditional plant performance criteria such as operating costs, EQI and controller performance which are traditionally used for comparing the performance based on economical and environmental criteria, of different CSs in a simulation environment (see Copp, 2002).

5.1.4 Extension of the activated sludge risk model

Two extensions have been added to the existing AS risk model: (i) the deflocculation problem and (ii) the temperature effect. Deflocculation was considered for inclusion because it is one of the most common operational problems of microbiological origin. Temperature, as will be shown in **Section 5.1.4.2 Temperature influence**, has been widely reported to have an influence on operational problems of microbiological origin. Its effect has been included to some extent by taking into account the existing bibliography and the microbiological species already considered in the AS risk model.

5.1.4.1 Deflocculation

For the correct diagnosis of deflocculation problems it is usually necessary to examine the activity of microorganisms in the AS under the microscope. Since this cannot be done in the BSM, the main operational causes according to the existing literature have been taken into account in quantifying the risk. DO is one the most important variables involved in this diagnosis. The knowledge is summarised in **Figure 5.15**. Very low DO is insufficient and causes old sludge (Wilén and Balmér, 1999), and too much aeration can break the floc (Comas *et al.*, 2003). If the sludge age also influences, if it is too low, it can cause deflocculation (Barbusiński and Kościelniak, 1995; Wilén *et al.*, 2000).

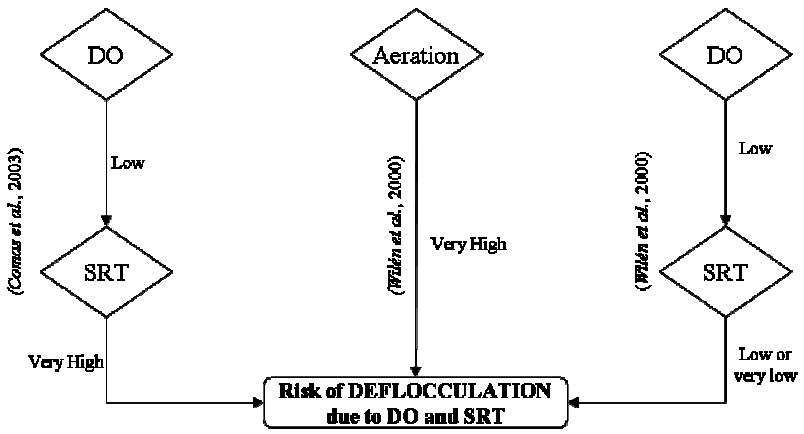

Figure 5.15. Flow diagram developed to evaluate the risk of deflocculation.

The flow diagram shown in **Figure 5.15** can be turned into the decision matrix presented in **Table 5.3**. The range of the input variables is the same as that presented in **Table 5.1**.

Table 5.8. Decision matrix for the risk of deflocculation.

		SRT (d)				
		Very low	**Low**	**Normal**	**High**	**Very high**
DO (mg $O_2 \cdot L^{-1}$)	**Very low**	High	Medium	Medium	Medium	High
	Low	High	Medium	Low	Medium	High
	Normal	Medium	Low	Low	Low	Medium
	High	High	Medium	Low	Medium	High
	Very high	High	High	High	High	High

The response surface from the decision matrix above is presented in **Figure 5.16**. The general principle is that at extreme values of DO and SRT the risk of deflocculation is high (red areas). While DO and SRT values are around normal, the risk of deflocculation is low (blue areas).

When the overall integrated risk is calculated in addition to the integrated risk of bulking, the integrated risk of foaming and the risk of rising, the risk of deflocculation will be added as well.

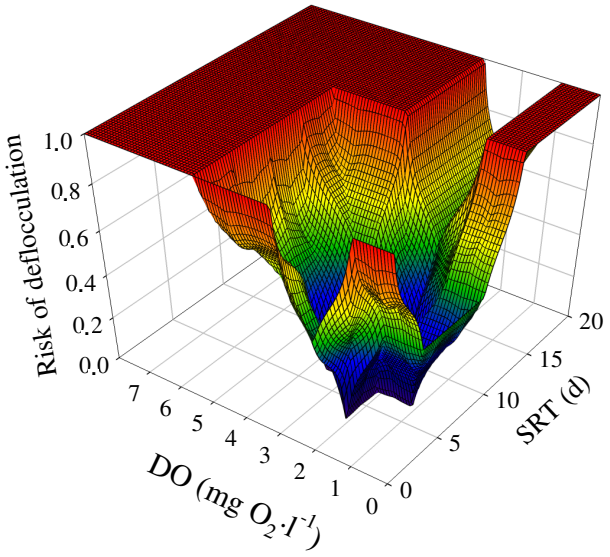

Figure 5.16. Risk of deflocculation.
(SRT -d- vs. DO –mg$O_2 \cdot l^{-1}$-)

5.1.4.2 Temperature influence

The temperature effect in the AS risk model is only considered in the case of rising sludge. For this specific operational problem of microbiological origin temperature affects the critical nitrate concentration for rising sludge to appear. The higher temperature is the lower critical concentration of nitrate. Apart from rising sludge temperature effect was not considered in the rest of operational problems of microbiological origin. For this reason, the AS risk model was extended to include temperature in other risks.

A review of the literature revealed that most of the studies regarding the effect of temperature on settling properties were linked to *Microthrix parvicella* which presents the best documented cases.

Eikelboom *et al.* (1998) state that bulking and foaming problems due to the abundance of *Microthrix parvicella* follow a typical seasonal pattern, with growth favoured during winter and early spring. According to Rossetti *et al.* (2005), *Microthrix parvicella* have different growth rates at different temperatures: Its optimum growth is at 25º C, there is some growth around 8ºC, very poor growth around 35º C and no growth above 35º C. They also report some examples of bulking caused by *Microthrix parvicella* (due to low F/M and high SRT) in WWTPs at temperatures between 12-15ºC as well as bulking in Danish WWTPs during the winter.

In order to include the temperature effect in the AS risk model, two of the individual risks, those related to *M. parvicella* (risk of foaming due to low F/M ratio, the left part of **Figure 5.2, Section 5.1.1.2 Foaming decision tree** and risk of bulking due to low organic loading, the right part of **Figure 5.1, Section 5.1.1.1 Filamentous bulking decision tree**), are multiplied by an empirical factor provided by **Equation 5.6** (see also **Figure 5.17**):

$$Factor\ Risk = 1.2 \cdot e^{\frac{-(T-5)^2}{625}} \quad \textbf{(Eq. 5.6)}$$

where
T is the temperature in ºC.

(in the case of risk of bulking due to low organic loading – a decision tree with two branches - the temperature effect is included after the maximum value of the two branches has been selected, for each time step, i.e. at each time step the maximum value of the risks calculated from the two branches of this decision tree is chosen and then the T factor risk is applied).

This Gaussian function decreases the risk above 15ºC considering that although *Microthrix Parvicella* has its optimum growth at 25ºC, other species present in the mixed liquor also increase their activity and thus, there is no population imbalance. On the other hand, for temperatures below 15ºC the risk increases and even though *Microthrix parvicella* shows less activity it is still appreciable (Rossetti *et al.*, 2005) in front of other species in the mixed liquor which also decrease or even stop their activity creating a population imbalance. Thus, in a general way, the idea behind this function is to represent the relative activity of *Microthrix parvicella* in front of the rest of the species. Note that this idea does not mean that for low temperature the risk is high and vice versa. It means that when operational conditions are favourable for foaming or bulking development, low temperatures will increase the risk while high temperatures will decrease it.

Once the T effect factor is applied, the risk obtained is limited to 1, i.e. all the values above 1.0 must be set to 1.0.

Example: Supposing a risk of 0.18 of low F/M foaming, a temperature of 20ºC and application of the empirical factor of **Equation 5.6**, the risk becomes:

$$\text{Factor Risk} = 1.2 \cdot e^{\frac{-(20-5)^2}{625}}$$

$$\text{Factor Risk} = 0.83$$

$$\text{Risk with T} = 0.83 * 0.18$$

$$\text{Final Risk} = 0.149\%$$

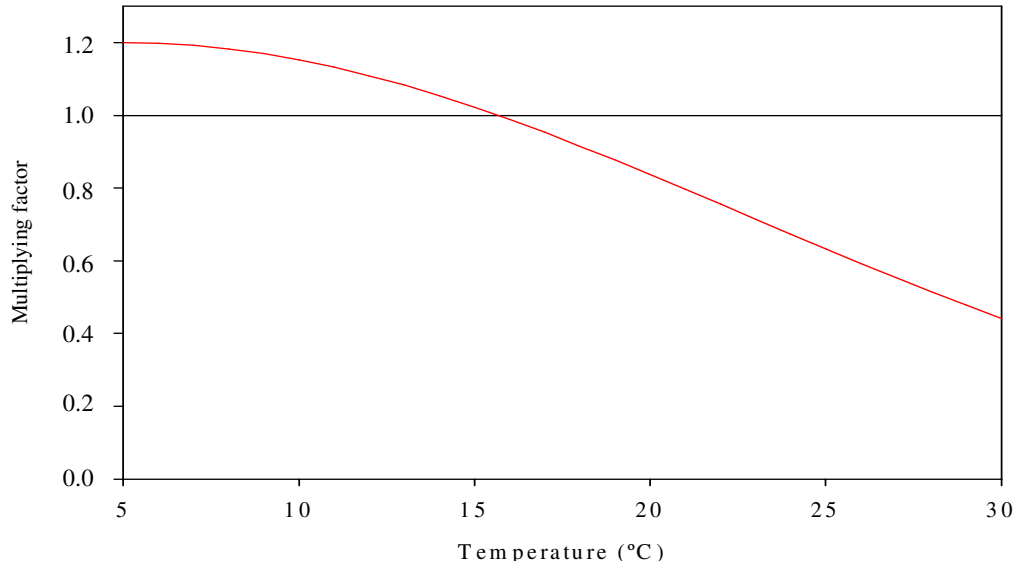

Figure 5.17. Variation of the factor risk with temperature (at T=15ºC -BSM1 conditions- Factor=1.0).

5.2 Anaerobic digestion risk model

The section is divided into three main parts: (i) development, divided between a black-box approach and a knowledge-based approach; (ii) implementation of the AD risk model developed, and finally (iii) model outcomes, showing the response of the AD risk model.

5.2.1 Development

The first step in the development of the AD risk model was a black box approach (**Section 5.2.1.1 Black box approach**). Given that real data from a pilot plant was available it was decided to use a wrapper approach (Kohavi and John, 1997). An ANN was used so that the most important variables related to biological foaming could be selected objectively. Afterwards, a search of the literature (**Section 5.2.1.2 Knowledge-based approach**) concerning biological FAD was performed. At the end of this section conclusions are drawn on these two approaches to the implementation of the AD risk model.

5.2.1.1 Black box approach

The methodology is a feature (i.e. variable) selection method based on a wrapper approach which employs the leave-one-out search method. This method, in each step, evaluates the accuracy of the learning algorithm at each step when one of the features is left out, and then removes the feature yielding the least reduction in accuracy - for

instance, an error value (Ng *et al.*, 2008). ANNs are used as learning algorithms to select a subset of features and the Root Mean Square Error (RMSE) are used as evaluation criteria. **Figure 5.18** depicts the flow chart of the methodology.

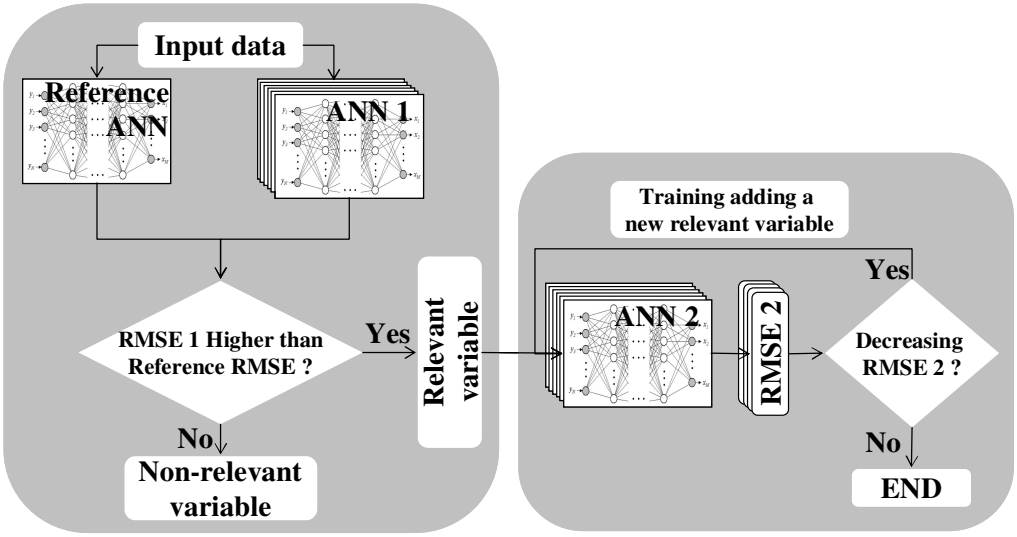

Figure 5.18. Flow chart of the methodology used to choose the most relevant variables.

The procedure starts with the training of the Reference ANN ten times with all the variables. The average RMSE is calculated and stored as the Reference Error.

Next, one input variable is removed and a new ANN (ANN 1 in **Figure 5.18**) is trained ten times without it. This step is repeated for each input variable, resulting in an ANN 1 for each input variable removed, with a related average RMSE1. Whenever a relevant variable is removed, the average RMSE 1 of the related ANN 1 will increase with respect to the average Reference Error. However, whenever a non-relevant variable is removed the RMSE 1 of the related ANN 1 will decrease. Therefore, the variables with an RMSE 1 higher than the Reference Error are selected as relevant variables.

Among the relevant variables, the one with the highest RMSE 1 is selected first and a new ANN (this time ANN 2) is again trained ten times, using it as the only input. If the related average RMSE (RMSE 2) is higher than the average Reference Error it means no improvement has been found, so the variable with the second highest average RMSE 1 is selected and a new ANN 2 is trained (once again ten times) using both variables. Again, its average RMSE 2 is compared with the Reference Error. This iterative process is repeated until an average RMSE 2 lower than the average Reference RMSE is obtained.

Acidogenic states

An example of this methodology was tested on a well-documented operational problem: acidogenic states (described in **Section 2.2.2.1 Acidogenic states**). Experimental data were obtained from a 1 m^3 pilot plant upflow fixed bed digester from INRA, France. This AD system is fully instrumented with on-line sensors in both the liquid phase (pH, flow rates, VFA, TOC and COD concentrations) and in the gas phase (i.e. CO_2, CH_4, H_2) and has been in operation for more than ten years. Since bicarbonate alkalinity was high and quite constant during these experiments, it was not considered in the following. For further details about the pilot plant's features and instrumentation, see Steyer *et al.* (2002). **Table 5.9** shows the input and output variables involved in this part of the study.

Outputs (i.e. occurrences of acidogenic states) were provided by a fuzzy modular expert system presented in Lardon *et al.* (2005). In this fuzzy system, several of the system states were diagnosed (i.e. normal, acidogenic, underload, organic overload, hydraulic overload and toxics) using the same input variables shown in **Table 5.9**.

Table 5.9. Input variables.

Inflow rate ($l \cdot h^{-1}$)	pH in the digester	Gas flow rate ($l \cdot h^{-1}$)	% of H_2 in the gas phase	% of CH_4 in the gas phase	VFA concentration in digester ($mg \cdot l^{-1}$)	COD in digester ($mg\ COD \cdot l^{-1}$)
qIn	phDig	qGas	h2Gas	ch4Gas	vfaDig	codtDig

Reference ANN and ANNs 1: **Table 5.10** shows the main features of the Reference ANN. When the standard deviation error of the residuals falls between the maximum and minimum values, which are set a priori, the ANN can be considered to be correctly trained. Values of the standard deviation error equal to the minimum boundary indicate over-fitting, i.e. higher than necessary precision has been obtained at the expense of good generalisation ability.

Table 5.10. Main Reference ANN features.

Hidden neurons	Maximum standard deviation error of the residuals	Minimum standard deviation error of the residuals	Standard deviation error of the residuals	Reference Error
1	0.15	0.01	0.0545	0.1294

However, when the standard deviation error of the residuals is equal to the maximum boundary, poor precision has been obtained.

The next step was to train the different ANNs 1. **Figure 5.19** shows the resulting average RMSE 1 for each training session, in which each label indicates the ANN trained without the variable shown.

The highest difference is for the ANN trained and validated without the codtDig variable. This indicates that this variable is the most important for ANN performance. In order of decreasing relevance the variables are: qIn, vfaDig and phDig.

ANNs 2: The input variable with the highest validation error was first used to train ANN2 (i.e. the ANN with the selected variables). To find out the input variable combination with the minimum RMSE 2, the variable which had the highest validation error among the remaining variables was added to the first ANN2 as an input (i.e. the first ANN with codtDig, the second with qIn, the third with vfaDig and the last with phDig). The results are provided in **Table 5.11**.

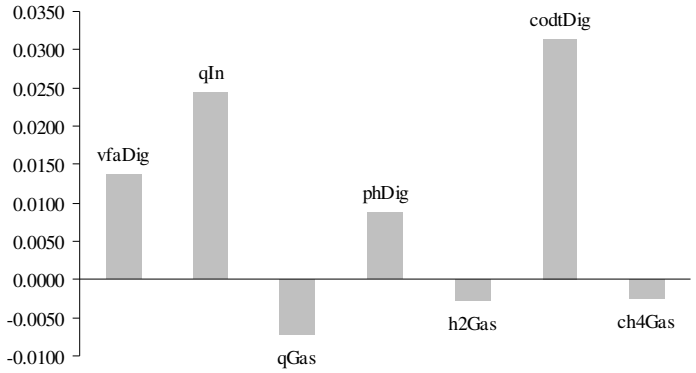

Figure 5.19. Average RMSE minus average Reference RMSE for each input variable removed.

Table 5.11. RMSE 2 for acidogenic states using the selected variables in relevance order.

ANN input variables	codtDig	codtDig; qIn	codtDig; qIn; vfaDig	codtDig; qIn; vfaDig; phDig
RMSE 2	0.1856	0.13106	0.13175	0.10952

Because codtDig is the most relevant, the training of ANNs 2 starts with this variable. However, it alone is not enough to diagnose acidogenic states with better precision than the Reference ANN (Reference Error 0.1294). Nor is it able to reproduce the precision of the Reference ANN together with qIn. When vfaDig is added, even though the RSME 2 increases compared to the previous combination, better precision is still not obtained. The best result is obtained when the four variables are used together (codtDig, qIn, vfaDig and phDig). These results, at least for phDig, vfaDig and codtDig, are widely recognised as key variables when diagnosing acidogenic states. But it is important to recognise that in addition to codtDig, vfaDig and phDig, other variables somehow not directly related to acidogenic states could be chosen, of which qIn is the most appropriate.

Foaming

Experimental data were obtained from the same pilot plant to detect foam forming. From among all the variables, a first selection was made based on the common variables which are available in real plants. Some others were not selected, for instance temperature since this is usually constant and it would be difficult to extract information from its profile. **Table 5.12** gives the input variables involved in this study.

Table 5.12. Input variables.

Inflow rate	VFA concentration in digester	TOC in digester	pH in the inflow rate	pH in the digester	CO_2 percentage in the gas phase	CH_4 percentage in the gas phase
qIn	vfaDig	tocsDig	phIn	phDig	co2Gas	ch4Gas

Foaming appearance in the digester was used as output, based on heuristic knowledge provided by the experts. It was noticed that when foaming appeared in the digester high variations in the gas flow rate and pressure appeared, due to the sudden release of gas bubbles trapped inside the foam. Hence, in order to get a suitable foaming index between 0 and 1, a fuzzy system was used. **Table 5.13** presents the decision matrix to determine the intensity of the gas flow rate and pressure variations.

Table 5.13. Decision matrix to estimate the real risk of foaming.

		Gas flow rate variation (%)		
		Low	**Medium**	**High**
Total Gas pressure variation (%)	**Low**	Low	Low	Normal
	Medium	Low	Normal	High
	High	Normal	High	High

The limits for the different membership functions (all chosen to be triangular except for the high membership function which is trapezoidal) were also set according to the experts' knowledge. They realised that for variations above 20% of both total gas pressure and gas flow rate the risk of foaming was high and variations around 10% should be treated as normal. According to this, the limits of the membership functions

were set as shown in **Table 5.15**. Variations were calculated taking the percentage of a given input in a time t with respect to the time t-1.

Table 5.15. Membership function limits for the Gas pressure and flow rate variation.

	Gas flow rate variation (%)		
	Low	**Medium**	**High**
Total Gas pressure variation (%)	[-1,0,5]	[0,10,30]	[15,25,100,101]
Gas flow rate variation (%)	[-1,0,5]	[0,10,30]	[15,25,100,101]

It is important to point that even though foaming can be estimated this way; this is an approach to study variables influence or relation.

Reference ANN and ANNs 1: The average RMSE for the Reference ANN and the seven ANNs 1 are presented in **Table 5.14**.

Table 5.14. Reference ANN and ANNs 1 average RMSE

Reference	**qIn**	**vfaDig**	**tocsDig**	**phIn**	**phDig**	**co2Gas**	**ch4Gas**
0.11700	0.11934	0.11377	0.12764	0.12654	0.11328	0.11796	0.12179

Figure 5.20 shows the differences between the RMSE of each variable and the Reference RMSE. As depicted, five variables have an RMSE higher than the Reference RMSE. The variables selected as relevant were qIn; tocsDig; phIn; co2Gas and ch4Gas.

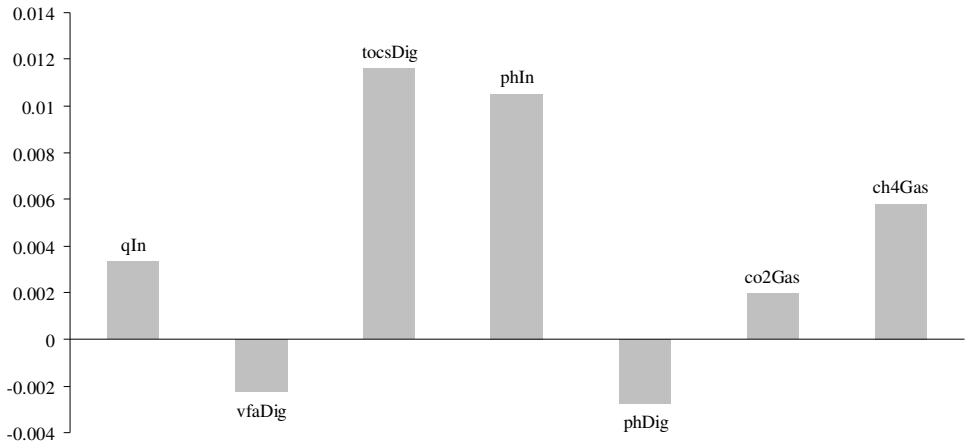

Figure 5.20. Average RMSE minus average Reference RMSE for each variable.

ANNs 2: To train ANNs 2 first tocsDig was selected first. Because its average RMSE 2 was higher than the average Reference RMSE the second most relevant variable was added and ANN 2 was trained again. **Table 5.16** summarises the average RMSE 2 for each ANN.

Table 5.16. Average RMSE 2 for the relevant variables.

	tocsDig	**tocsDig; phIn**	**tocsDig; phIn;ch4Gas**	**tocsDig;phIn; ch4Gas;qIn**	**tocsDig;phIn; ch4Gas;qIn; co2Gas**
RMSE 2	0.12666	0.12256	0.12141	0.12138	0.11944

In all cases the RMSE 2 was higher than the Reference Error. However, a t-test comparing the averages between each RMSE 2 and the RMSE of the Reference ANN revealed that in the last ANN 2 (last column in **Table 5.16**), the average RMSE 2 was not significantly different from the Reference RMSE. This means that even though the

average RMSE 2 is not lower than the Reference RMSE, by removing two variables from the whole input, similar results can be obtained.

The significance of gas-related variables (i.e. co2Gas and ch4Gas) is probably due to the approach taken to determine foaming (i.e. the fuzzy system used). However, the addition of co2Gas to the relevant variables reduces RMSE 2, and according to Zhao and Viraraghavan (2004) high CO_2 production is indicative of poor digestion but not linked to a specific problem. What it is more important to highlight is the other variables' relevance, especially that of tocsDig and qIn which are related to OLR.

5.2.1.2 Knowledge-based approach

Two main factors structure existing knowledge about biological foaming: (i) the microbiology of the process and (ii) the key operational characteristics of the digester.

As stated in **2. State-of-the-art**, it is important not to forget that from a microbiological point of view biological foaming is an operational problem of microbiological origin and mostly related to *M. parvicella* in particular. Therefore, the presence of filamentous microorganisms in WAS plays an important role when treating secondary sludge.

The relationship between foaming and OLR from an operational point of view has already been explained in **2. State-of-the-art**. Metcalf and Eddy (2003) provide more details and state that proper OLRs for anaerobic digesters are between 1.6 and 4.8 kg $VS \cdot m^{-3} \cdot d^{-1}$. Similarly, the operation manual of the Water Environment Federation (WEF, 1996) suggests an OLR of between 1.6 and 6.2 kg $VS \cdot m^{-3} d^{-1}$. However, when foaming occurs the range is much narrower. Ross and Ellis (1992) show in their study that increasing Organic Loading Rates (OLR) and retention times can cause foaming. In addition, Massart *et al.* (2006) say that inconsistent feeding in the digester is one of the causes of biological foaming. They state, for instance, that to prevent biological FAD, the OLR should be maintained between 1.6 and 2.4 kg $VS \cdot m^{-3} \cdot d^{-1}$ with a recommended daily variation of 5 to 10%. Murto *et al.* (2004) found that an OLR higher than 2.6 kg $VS \cdot m^{-3} \cdot d^{-1}$ can also produce excessive foaming.

5.2.1.3 Conclusions

In the black box approach a set of relevant variables relating to biological foaming in anaerobic digesters have been selected. Of the seven variables, two have shown themselves to be non-relevant in relation to foaming. This is an indication of the inherently complex interrelationships between all the variables in this operational problem of microbiological origin. As stated above, the relevance of the gas related variables is probably due to the approach taken to estimate the risk of foaming. From an operational point of view, the wrapper approach results indicate that foaming is related to $Q_{in,a}$ and the total organic carbon (TOC) present.

However, the review of the literature has revealed it is necessary to take into account the role of filamentous bacteria in AD biological foaming, and a consistent feeding rate. Given that the pilot plant was not treating secondary sludge, it was not possible to consider the effect of filamentous bacteria in the black box approach. The need to add the effect of the filamentous bacteria made it more feasible to use the results from the AS risk model. To obtain a compact risk assessment model, it is easier to integrate two knowledge-based models rather than a knowledge-based model and a black box one.

In addition, the knowledge-based approaches are less specific to a particular domain (the BSM2 in our case) since they rely more on general knowledge. In other words, a KBS overcomes the limitation of using a black box system trained with data from a given plant, which would have hampered implementation of the black box model in a BSM given that the ranges of the variables involved in the ANN training are not the same. For this reason it was decided in the end to implement the AD risk model in a fuzzy logic rule based system using the variables found with the wrapper approach and the knowledge from the literature.

5.2.2 Knowledge formalisation

To obtain the risk of presence of filamentous bacteria in the digester's feed, results from the AS risk model concerning risk of foaming due to a low F/M in the AS system were used. Specifically, the foaming in AS (FAS) risk, related to the growth of *M. parvicella* and nocardioforms was selected as one input for the AD risk model. This means that the AD risk model is applicable for anaerobic digesters fed with WAS or mixed sludge containing both WAS and primary sludge.

As pointed out in **Section 5.2.1.1 Black box approach**, the role of OLR is important in relation to biological foaming. Therefore, the OLR, the percentage of the daily average organic loading rate variation (OLRvar), and the presence of filamentous microorganisms in the feed were all considered relevant parameters in terms of AD biological foaming. The combination of FAS risk, OLR and OLRvar, according to expert knowledge, leads to three different decision matrices, which form the knowledge base of the AD risk model. Each decision is made up of the decision rules referring to a different degree of FAS risk (low, medium and high; right axis of **Figure 5.21**). The rules for each decision matrix are obtained by combining different degrees of OLR (left axis of **Figure 5.21**) and OLRvar (bottom axis of **Figure 5.21**) for each value of FAS risk. For a given FAS risk (i.e. low, medium or high) the figure shows that the FAD risk increases as OLR and OLRvar increase. For a given OLR and OLRvar the FAD risk rises as FAS risk increases.

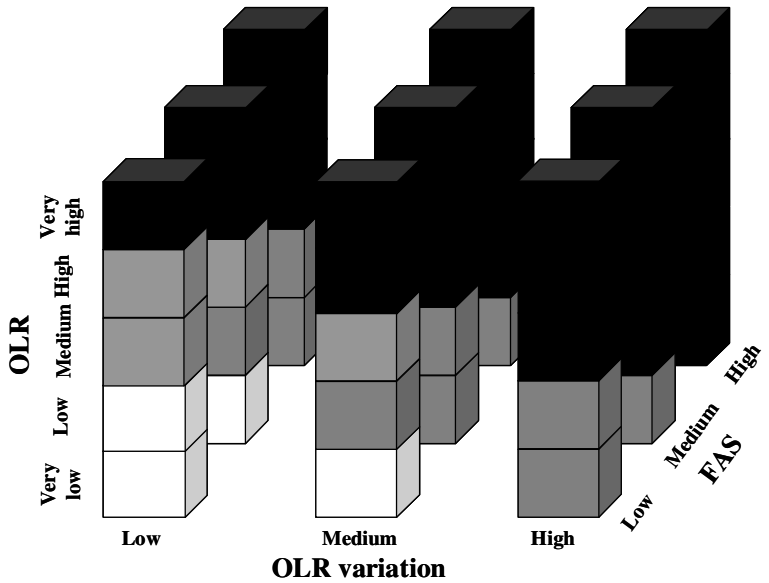

Figure 5.21. Decision matrices of the AD risk model. Degree of FAD risk indicated by colours: white boxes indicate low FAD risk, grey boxes are for medium FAD risk and black boxes represent high FAD risk.

Table 5.17. MF features of the AD risk model.

Variable		Very Low	Low	Medium	High	Very High
OLR	**Shape**	Trapezoidal	Triangular	Triangular	Triangular	Trapezoidal
(kg VS·m^{-3}·d^{-1})	**Range**	[-0.1,0,1,1.8]	[1.2,1.8,2.4]	[1.8,2.6,3.4]	[2.4,3.4,4.4]	[3.4,4.4,5,10]
OLRvar	**Shape**	-	Trapezoidal	Triangular	Trapezoidal	-
(%)	**Range**	-	[-0.1,0,10,15]	[10,15,20]	[15,20,30,100]	-
FAS risk	**Shape**	-	Trapezoidal	Triangular	Trapezoidal	-
(from 0 to 1)	**Range**	-	[-0.1,0,0.3,0.5]	[0.2,0.6,0.8]	[0.6,0.8,1]	-
FAD risk	**Shape**	-	Triangular	Triangular	Triangular	-
(from 0 to 1)	**Range**	-	[-0.2,0,0.2]	[0.2,0.5,0.8]	[0.8,1,1.2]	-

The AD risk model has been implemented by means of the MATLAB® fuzzy toolbox (MathWorks Inc.). The Mamdani method has been selected as the fuzzy inference method (Mamdani and Assilian, 1975). The shape of the MFs of different input and output variables (OLR, OLRvar, FAS risk and FAD risk) are trapezoidal or triangular and have different ranges (see **Table 5.17**).

5.2.3 Model outcome

The output of the model, FAD risk, indicates the potential for the development of foaming in the anaerobic digester. The FAD risk value provided by the model ranges from 0 (very unlikely) to 1 (most likely). The AD risk model outputs are (i) FAD risk profile vs. time; (ii) the %TIV at high (>0.8) FAD risk; (iii) the worst situation in the simulation period and, (iv) the average (AV) FAD risk. **Figure 5.22** shows the response surfaces for FAD risk depending on OLR and OLRvar for each FAS risk MF (i.e. **Figure 5.22a** for low, **Figure 5.22b** for medium and **Figure 5.22c** for high FAS risk). **Figure 5.22** also illustrates how the high FAD risk zone (in red) of the surfaces becomes wider as FAS risk increases from low to high. The inverse effect is shown for the low FAD risk zone (in blue).

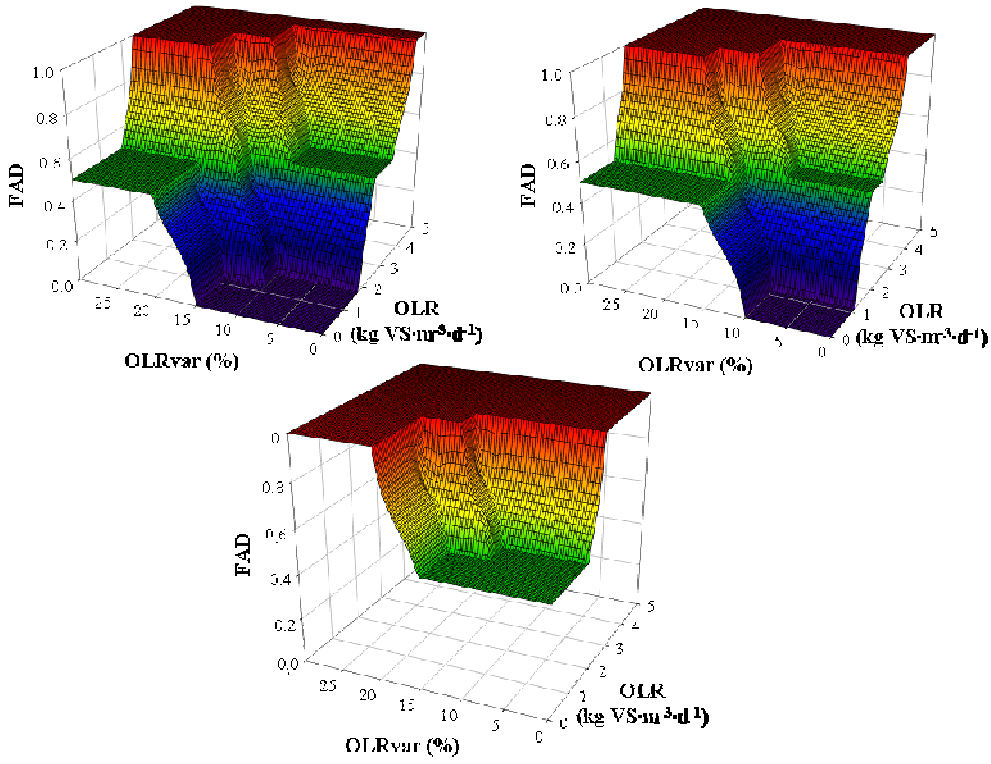

Figure 5.22. Response surfaces for FAD risk for each FAS risk MF value: (a) Low; (b) Medium and (c) High FAS risk.

To consider the low dynamics of foaming development, the outcome risk is filtered by means of the exponential filter presented in **Section 5.1.3 Model outcome** with a time constant of three days, although this can be customised by the user of the AD risk model. This filter also prevents sudden, unrealistic changes from very high to very low values for FAD risk in time steps that are too short.

5.3 Concluding remarks

In this chapter the AS and AD risk model development have been presented. The availability of data has driven the development. For the AS risk model decision trees have been developed containing heuristic knowledge from experts and literature. The decision trees have been afterwards implemented in a fuzzy logic rule-based system to infer a risk index for the main operational problems of microbiological origin (i.e. filamentous bulking, biological foaming and rising sludge). Response surfaces for each risk of operational problems of microbiological origin depending on its inputs have been shown. An extension of the risk model has been performed to include the risk of deflocculation and the temperature effect on risks related to *Microthrix parvicella*.

The final AD risk model is a mixture of two approaches. In one hand, a wrapper approach based on ANN is first tested on acidogenic states providing relevant variables proving to be a useful tool for feature selection. Afterwards has been applied to estimate the real risk from gas flow rate and pressure variations. The wrapper approach has allowed to identify the main variables related to foaming (mainly related to OLR). On the other hand, the literature research on AD foaming suggested including factors as the OLR variation and the presence of filamentous bacteria in the feed. Finally, variables from the data mining and from those suggested by the literature have been used as inputs for the final implementation of the AD risk model in a fuzzy-logic rule-based system to be integrated with the existing AS risk model.

CHAPTER 6

RISK MODEL IMPLEMENTATION AND APPLICATION IN BENCHMARK SIMULATION MODELS

Part of the work in this chapter has appeared in:

Dalmau J., Comas J., Rodríguez-Roda I., Pagilla K. and Steyer J.P. (2009b). Risk model development and simulation for foaming in anaerobic digestion. Bioresource Technology, ***101****(12), 4306-4314.*

Dalmau J., Comas J. and Rodríguez-Roda I. (2009c). Extension of a risk model to include deflocculation and temperature. Water Science and Technology (submitted).

6. Risk model implementation and application in benchmark simulation models

In this chapter, implementation into the BSM platforms is presented followed by the BSM1, BSM1_LT and BSM2 applications of the AS risk model and the AD risk model (only in the BSM2 case) evaluated using different scenarios. Evaluation first comprises an open-loop case, variation in operational parameters and two CSs for the BSM1. The performance of the AS risk model in the BSM1_LT is then evaluated using a filter with different time constants and including the effect of temperature. Finally, the AD risk model is evaluated within the BSM2.

6.1 Benchmark simulation model implementation

This section describes how the different input variables for each of the individual fuzzy risks are obtained or calculated from the simulation outputs for any BSM platform. This is important in order to implement the AS and AD risk models in any BSM platform (i.e. MATLAB™ & Simulink™, FORTRAN, WEST®, GPS-X™, SIMBA). In the Annex the reader will find the detailed code for the MATLAB implementation of both AS (BSM1 and BSM1_LT) and AD (BSM2) risk models. The current MATLAB implementation of the risk model is also available from the benchmark website (www.benchmarkwwtp.org).

6.1.1 Bulking due to nutrient deficiency

The risk of bulking due to nutrient deficiency is calculated using just one input. The BOD to nutrient (either N or P) ratio. Note that since the BSMs use ASM1 P is not considered. Hence, although the parameters for BOD/P are presented in **Table 5.1**, its calculation is not performed in the BSM implementation of the risk model. For nitrogen, calculations are as follows:

- BOD5toN: The BOD5/N ratio is evaluated for the influent wastewater ($BOD_{5,in}$ / $N_{tot,\ in}$; **Equation 6.1**).

$$BOD_5\ \text{to}\ N = \frac{BOD_{5,in}}{N_{tot,in}} \quad \textbf{(Eq. 6.1)}$$

where

$N_{tot,in} = S_{NO,in} + S_{NH,i} + S_{ND,i} + X_{ND,}i + i_{XB} \cdot (X_{B,H,i}+X_{B,A,i}) + i_{XP} \cdot (X_{P,i}+X_{I,i})$ **(Eq. 6.3)**

$BOD_{5,in} = 0.65 \cdot (S_S + S_{S,EC} + X_S + (1-f_p) \cdot (X_{B,H}+X_{B,A}))$ **(Eq. 6.2)**

where

$S_{S,EC}$: S_S from an EC source.

6.1.2 Bulking due to low dissolved oxygen

Input variables for the risk of bulking due to low DO are the DO itself and the F/M ratio as explained below.

- Dissolved oxygen (DO): The DO concentration is obtained from biological reactor 3 (1st aerobic, $S_{O,3}$).

- The F/M ratio is calculated in two different ways within the AS risk model even though the MFs are the same. While F/M 1 (F/M removed) is calculated on the basis of the daily mass flow rate of COD removed from the whole plant per unit of biomass, F/M 2 (F/M fed) aims to detect low organic loading (daily mass flow rate of supplied BOD per unit of biomass; **Eq. 6.11**).

  F/M 1 or process loading factor (F/M removed; **Equation 6.4**) (Grady *et al.*, 1999)

$$F/M\ 1 = \frac{(CODin - CODeff)}{Biomass} \quad \textbf{(Eq. 6.4)}$$

  where

$$COD_{in} = (S_S + S_I + S_{S,EC} + X_S + X_{B,H} + X_{B,A} + X_P + X_I) \cdot Q_{in} \quad \textbf{(Eq. 6.5)}$$

  $S_{S,EC}$: S_S from an EC source.

$$COD_{eff} = (S_S + S_I + X_S + X_{B,H} + X_{B,A} + X_P + X_I) \cdot Q_{eff} \quad \textbf{(Eq. 6.6)}$$

$$Biomass = 0.75 \cdot (\sum_{n=1}^{n=5} (X_{B,H,as,n} + X_{B,A,as,n}) \cdot V_{as,n}) \quad \textbf{(Eq. 6.7)}$$

6.1.3 Bulking due to low organic loading

The risk of bulking due to low organic loading is depending on the S_S and SRT calculated as follows:

- Readily biodegradable organic matter (S_S): The readily biodegradable organic matter (S_S) concentration is evaluated in reactor 1. If there is an EC from an additional Qcarb stream, S_S from this stream should be included, i.e. $S_{S,EC}$.

- SRT: The SRT is calculated as the total mass of TSS within the five reactors divided by the daily mass of TSS removed from the plant via the WAS and the effluent (Grady *et al.*, 1999; **Equation 6.8**).

$$SRT = \frac{\sum_{i=1}^{5} (TSS_{as,i} \cdot V_{as,i})}{TSS_w + TSS_{eff}} \quad \textbf{(Eq. 6.8)}$$

  where

  $TSS_{as,i}$ is the concentration in each biological reactor,

  $V_{as,i}$ is the volume of each biological reactor,

$$TSS_{eff} = (0.75 \cdot (X_{S,e} + X_{B,H,e} + X_{B,A,e} + X_{P,e} + X_{I,e})) \cdot Q_{eff} \quad \textbf{(Eq. 6.9)}$$

$$TSS_w = (0.75 \cdot (X_{S,w} + X_{B,H,w} + X_{B,A,w} + X_{P,w} + X_{I,w})) \cdot Q_w \quad \textbf{(Eq. 6.10)}$$

  As it has been commented in **Section 5.1.2.3 Defuzzyfication,** the SRT is filtered according to the already presented **Equations 5.4 and 5.5**:

$$SRT\ filtered = \alpha \cdot SRT(t-1) + (1-\alpha) \cdot SRT(t) \quad \textbf{(Eq. 5.4)}$$

where

$$\alpha = 1 - \frac{1}{\left(\tau \cdot \frac{1440}{15}\right)} \quad \textbf{(Eq. 5.2)}$$

τ = time constant in days (usually 3 days).

- F/M 2 (F/M fed; WEF, 1996; **Equation 6.11**):

$$F/M\ 2 = \frac{BOD_{5,in}vec}{Biomass} \quad \textbf{(Eq. 6.11)}$$

where

$$BOD_{5,in}vec = BOD_{5,in} \cdot Q_{in} \quad \textbf{(Eq. 6.12)}$$

As explained before if there is an EC from an additional Q_{carb} stream, BOD_5 (only S_S) from this stream should be included as $S_{S,EC}$.

6.1.4 Foaming due to low food to microorganisms ratio

The inputs for foaming due to low F/M ratio are F/M 2 and SRTvec, which have already been explained.

6.1.5 Foaming due to high readily biodegradable organic matter fraction

The input F/M 2 for foaming due to HRBOM has already been explained.

- S_S/X_S: The readily biodegradable organic matter (S_S) to slowly biodegradable organic matter (X_S) ratio is evaluated for the influent wastewater ($S_{S,in}/X_{S,in}$). If there is an additional Q_{carb} stream, S_S from this stream should be included as $S_{S,EC}$.

6.1.6 Rising sludge

Inputs for rising sludge are the nitrate concentration from reactor 5 and the NGPT calculated as follows:

- Nitrate concentration (S_{NO}): The nitrate concentration is obtained from reactor 5.
- NGPT (Henze *et al.*, 1993; **Equation 6.13**):

$$NGPT = \frac{S_{NO}HighLimit}{Rdn} + t_{delay} \quad \textbf{(Eq. 6.13)}$$

where
S_{NO}HighLimit is equal to 8 g $N \cdot m^{-3}$ at 15ºC (in the BSM1) and a function of temperature in the BSM1_LT and the BSM2:

$$S_{NO}(\text{High Limit}) = 11.003972 \cdot e^{-0.020295 \cdot T} \quad \textbf{(Eq. 6.14)}$$

$$Rdn = \left(\frac{1-Y_H}{2.86\cdot Y_H}\right)\cdot\left(\mu_H\cdot\frac{S_S Out\,Reac5}{K_S + S_S Out\,Reac5}\right)\cdot\left(\frac{S_{NO} Out\,Reac5}{K_{NO} + S_{NO} Out\,Reac5}\right)\cdot X_{BH} OutBottomClarifier \cdot \eta_g$$

(**Eq. 6.15**)

where

$$\mu_H = 4\cdot e^{((\log(4/3)/5)\cdot(T-15))} \quad (\textbf{Eq. 6.16})$$

$$t_{delay} = \frac{S_O}{\frac{2.86\cdot Rdn}{\text{nitrifiers fraction}}} \quad (\textbf{Eq. 6.17})$$

Nitrifiers fraction = 1

- Sludge Volume in Clarifier (see **Section 5.1.2 Knowledge formalisation**):

$$\text{Sludge Volume in Clarifier} = \frac{\sum_{i=1}^{i=10} TSS_i\cdot V_i}{TSS_{10}} \quad (\textbf{Eq. 6.18})$$

where
i= number of the secondary settler layer,
V=volume of the secondary settler layer (m^{-3}),
TSS= concentration of solids in the ith secondary settler layer ($kg\cdot m^{-3}$).

6.1.7 Deflocculation

The inputs for deflocculation are DO and SRTvec which have already been explained.

6.1.8 Anaerobic digestion biological foaming

The risk of foaming in the anaerobic digester is calculated as follows:

- Inputs for the AD risk model are calculated as follows (**Equation 6.19**). At the end, the FAD risk is filtered with a 3-day exponential filter.

$$OLR = \frac{VS}{HRT} \quad (\textbf{Eq. 6.19})$$

where
VS = 0.75 · (Xch+Xpr+Xli+Xi)
VS are calculated after the ASM1/ADM1 interface and before the anaerobic digester.
HRT is calculated as in **Equation 6.20**.

$$HRT = \frac{V_{liq}}{Q_{in,a}} \quad (\textbf{Eq. 6.20})$$

where
V_{liq} is the volume of the anaerobic digester liquid phase,
$Q_{in,a}$ is the anaerobic digester's inflow rate.

- OLR daily variation (**Equation 6.21**):

$$\text{OLR var} = \frac{\overline{\text{OLR}}(t) - \overline{\text{OLR}}(t-1)}{\overline{\text{OLR}}(t)} \cdot 100 \quad \textbf{(Eq. 6.21)}$$

where

$\overline{\text{OLR}}$ is the daily mean of OLR; (t) is the current day; (t-1) previous day.

- FAS risk is equal to the filtered *LowFtoMFoaming2* of the AS risk model.

6.2 Benchmark Simulation Model No1 application

In this section the results for each of the AS risk model operational problems of microbiological origin are shown for the open-loop scenario. Next, the risk model's performance is shown when three different operational parameters are modified: Q_r, Q_w and K_La. The last section evaluates the AS risk model's performance in different scenarios: open-loop and two CSs. In all cases, the AS risk model is applied to the results of the BSM1.

6.2.1 Open-loop

Open-loop in dry weather has been chosen as a reference scenario to show the AS risk model's performance. The specifications used for the BSM1 simulation are the showed in **Table 6.1**.

Table 6.1. Specifications used for the BSM1 dry weather open-loop simulation.

K_La3 (d^{-1})	K_La4 (d^{-1})	K_La5 (d^{-1})	Q_W ($m^3 \cdot d^{-1}$)	Q_{intr} ($m^3 \cdot d^{-1}$)	Q_r ($m^3 \cdot d^{-1}$)	Q_{carb} ($m^3 \cdot d^{-1}$)	Bypass
240	240	84	385	55338	18446	0	No

In **Figures 6.1 - 6.13** each risk of a different operational problems of microbiological origin is shown, together with its related inputs for a 7-day open-loop simulation. Nutrient deficiency risk is close to 0 for the whole evaluation period (**Figure 6.1**). Since this risk depends on the influent characteristics, in normal operational conditions, it will be low.

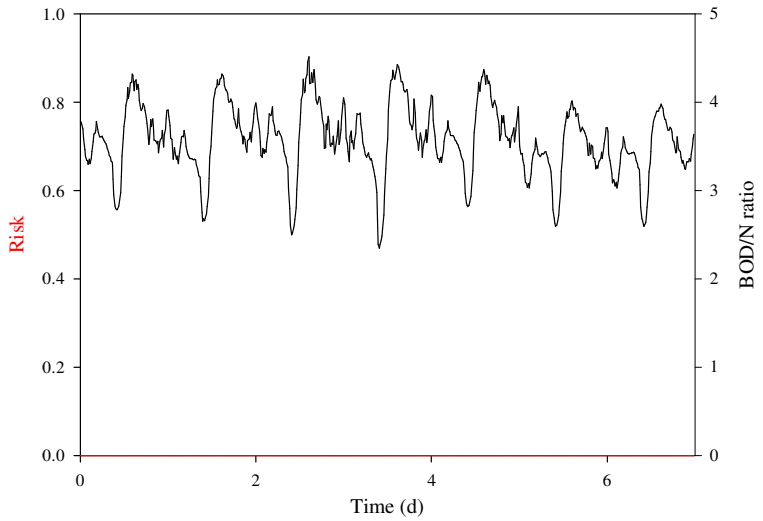

Figure 6.1. Risk of bulking due to nutrient deficiency.
Red line: risk; Black line: BOD/N ratio.

The risk of bulking due to low DO (**Figure 6.2**) follows the removed COD daily profile. Whenever F/M is high there is an increase in the COD removed, which is linked to DO consumption. Since DO is not controlled, as it becomes limited the risk of bulking increases. Whenever F/M is low, the opposite effect is seen. Low COD removal causes the DO to accumulate more easily (peaks in DO), which decreases the risk of bulking. Low loadings occur during the weekend, which decreases the risk of bulking even more.

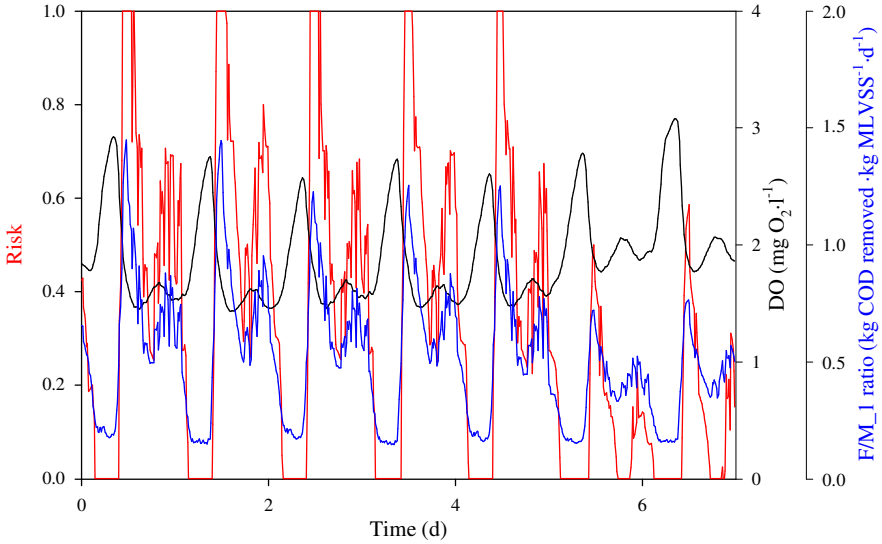

Figure 6.2. Risk of bulking due to low DO.
Red-line: risk; blue line: F/M1 ratio; black line: DO.

In **Figure 6.3**, since the SRT is almost constant, the risk of bulking due to low F/M is affected mainly by S_S. It is clearly noticeable that when the S_S concentration is high the risk of bulking decreases, whereas the opposite effect is seen when low S_S concentrations are found.

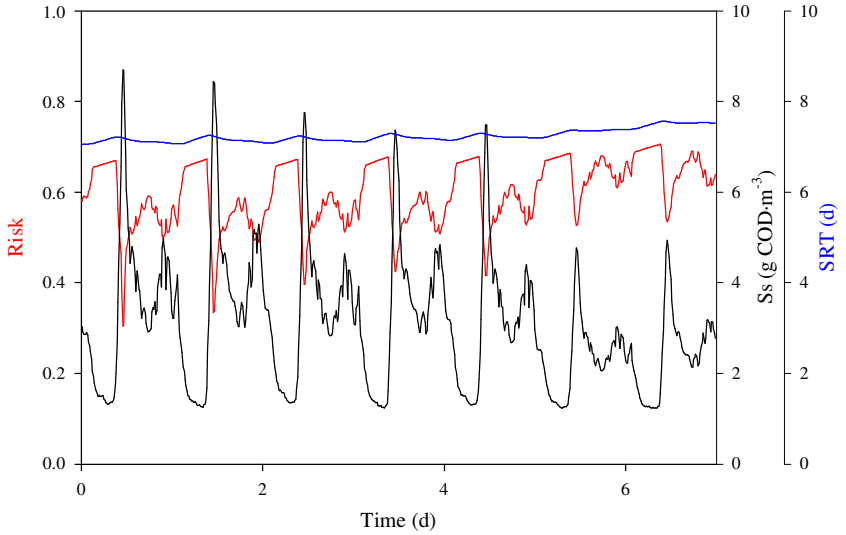

Figure 6.3. Risk of bulking due to low F/M.
Red line: risk; black line: soluble substrate; blue line: SRT.

As in **Figure 6.3**, the SRT remains fairly constant throughout the week in **Figure 6.4**, which means the risk profile is driven by the F/M 2 ratio. High F/M in relation to the

morning influent lowers the risk of bulking, while low nocturnal F/M increases it. Again, during the weekend loadings are lower so the risk of bulking increases. At this point it is important to highlight that despite the fact there are two different causes of bulking due to low organic loading (as explained in **Section 5.1.1.2 Foaming decision tree**), only the highest risk value between both branches will be used for evaluation purposes (see **Section 5.1.2.3 Defuzzyfication**).

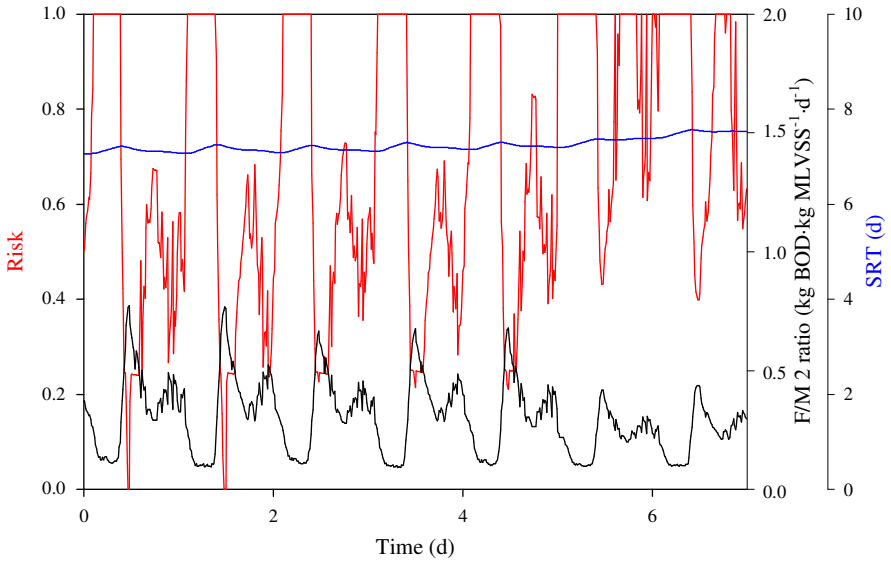

Figure 6.4. Risk of bulking due to low F/M 2.
Red line: risk; black line: F/M 2 ratio; blue line: SRT.

In **Figure 6.5** risk of foaming increases with low F/M 2 ratios and vice-versa. SRT is fairly constant for the seven days of evaluation. F/M 2 has a profile that has already been shown, decreasing at night and increasing in the morning and afternoon.

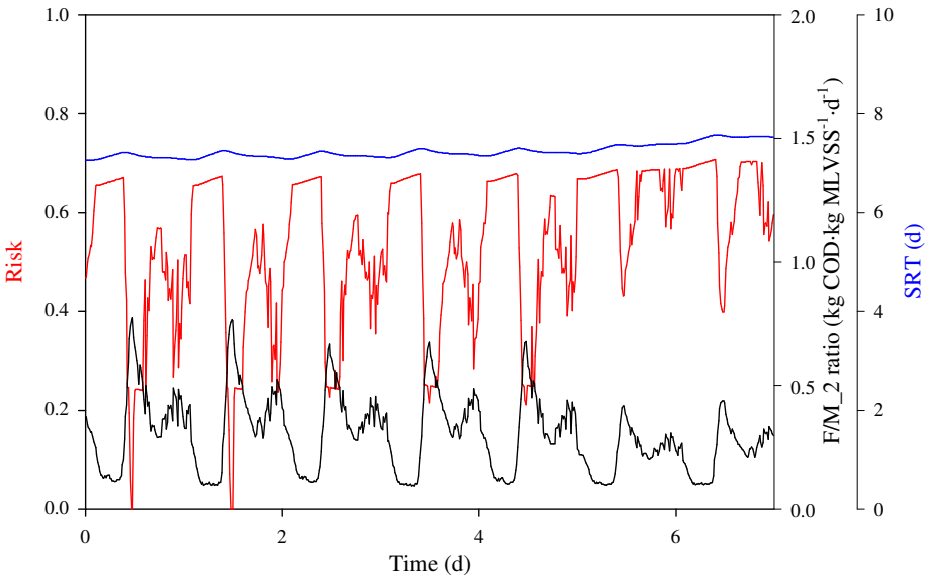

Figure 6.5. Risk of foaming due to low F/M.
Red line: risk; black line: F/M; blue line: SRT.

Figure 6.6 shows peaks of risk of foaming in the morning, when F/M 2 and S_S/X_S ratios are high. However, in no case do they reach 0.6. The rest of the day and at weekends the risk remains almost 0.

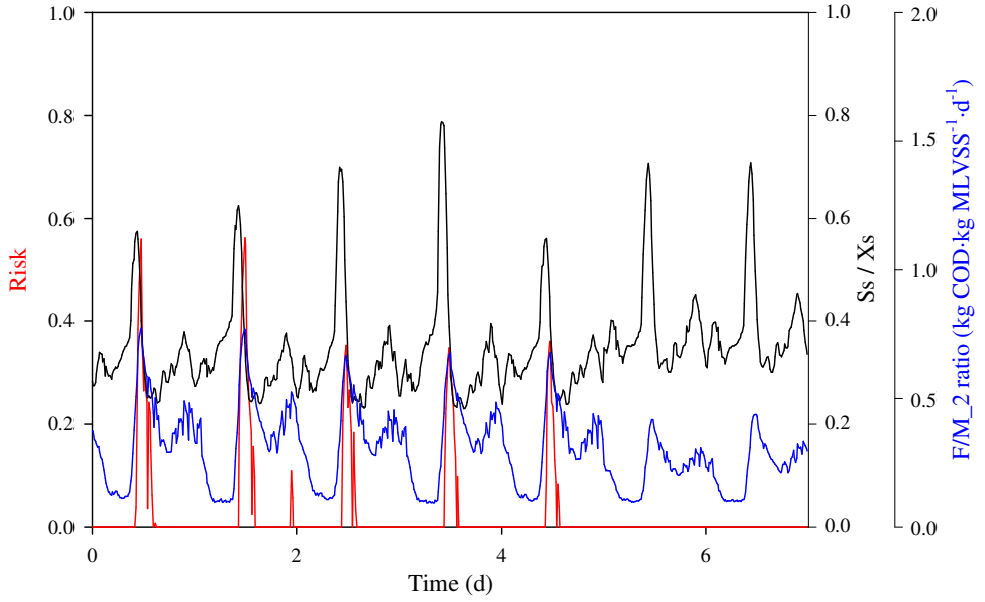

Figure 6.6. Risk of foaming due to HRBOM (1).
Red line: risk; black line: S_S/X_S ratio; blue line: F/M 2 ratio.

For the given SRT (**Figure 6.7**), the risk of foaming is almost 0 for the whole evaluation period despite the daily peaks in the S_S/X_S ratio. As was done for the risk of bulking due to low F/M (see **Figures 6.3 and 6.4**), the same integration of the two causes of the risk of foaming due to HRBOM is performed for evaluation purposes.

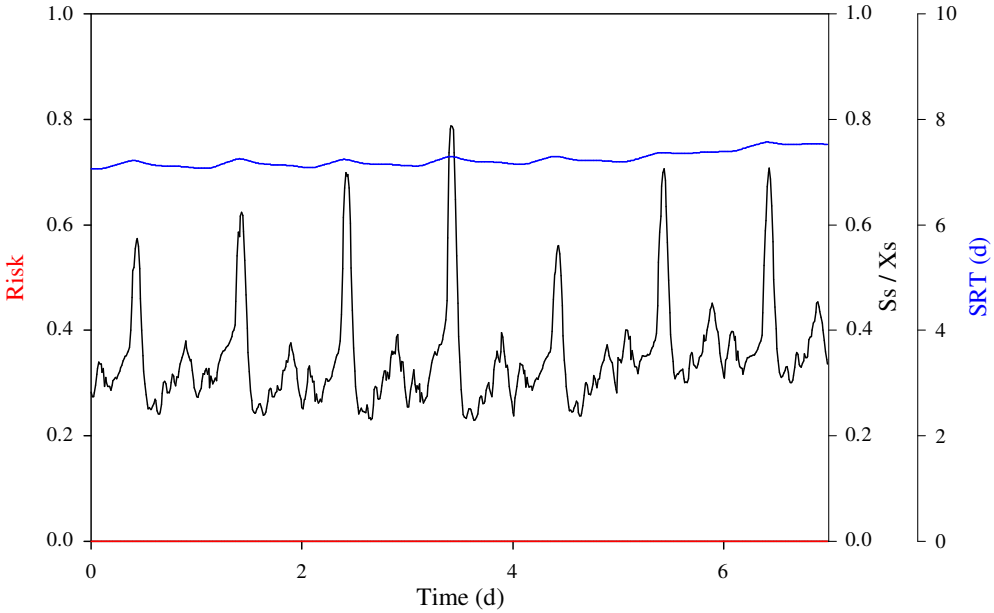

Figure 6.7. Risk of foaming due to HRBOM (2).
Red line: risk; black line: S_S/X_S ratio; blue line: SRT.

Figure 6.8 shows how the rising sludge risk increases during mornings and afternoons and decreases at night. This behaviour is due to the ammonium present in the influent,

which is higher in the morning and afternoon than at night. There is an increase in the S_{NO} during the weekend (days 6 and 7), which is due to the lower F/M hampering the denitrification process and resulting in an increased concentration and a prolonged risk of rising sludge.

In **Figure 6.9** the risk of deflocculation is in general quite low since both SRT and DO values are within a normal range. The risk changes accordingly when DO reaches its highest or lowest values. As F/M is lower during the weekend, the lowest values of DO are slightly higher than during the week; this is the cause of the low risk of deflocculation during the weekend.

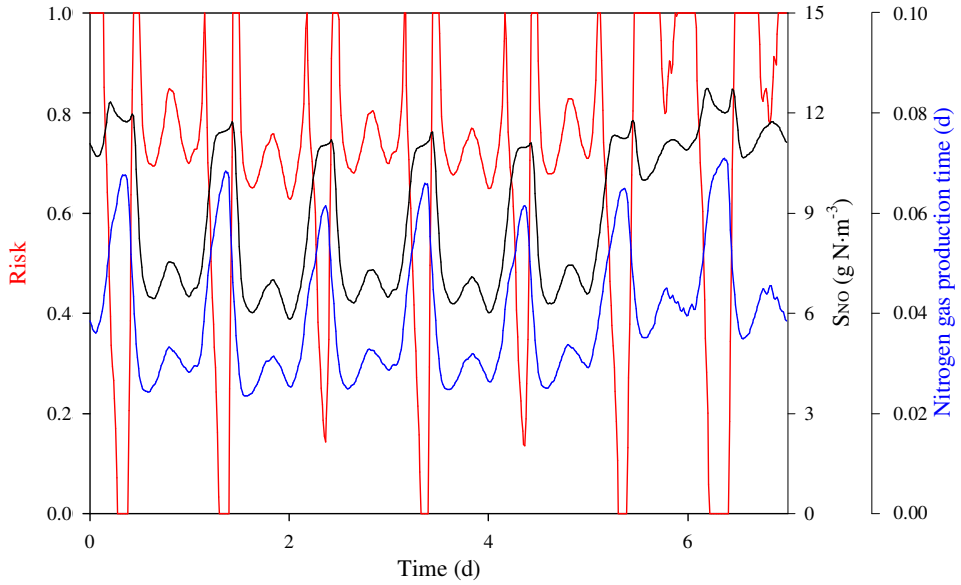

Figure 6.8. Risk of rising sludge.
Red Line: risk; black line: nitrate concentration in the effluent of the 5th biological reactor; blue line: NGPT.

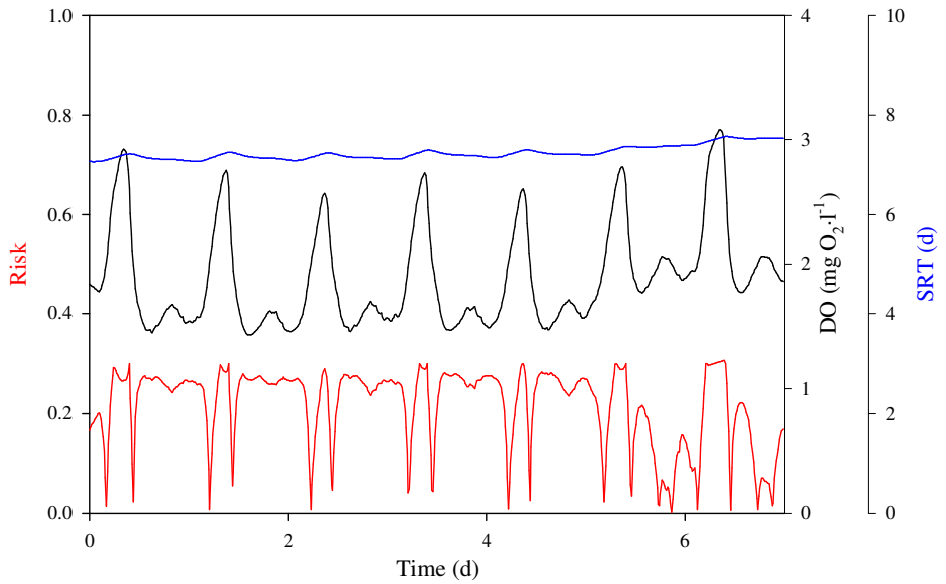

Figure 6.9. Risk of deflocculation.
Red line: risk; black line: DO; blue line: SRT.

Figure 6.10 clearly shows that nutrient deficiency has no effect on the global bulking risk. Low F/M bulking has a greater effect than low DO bulking throughout the week.

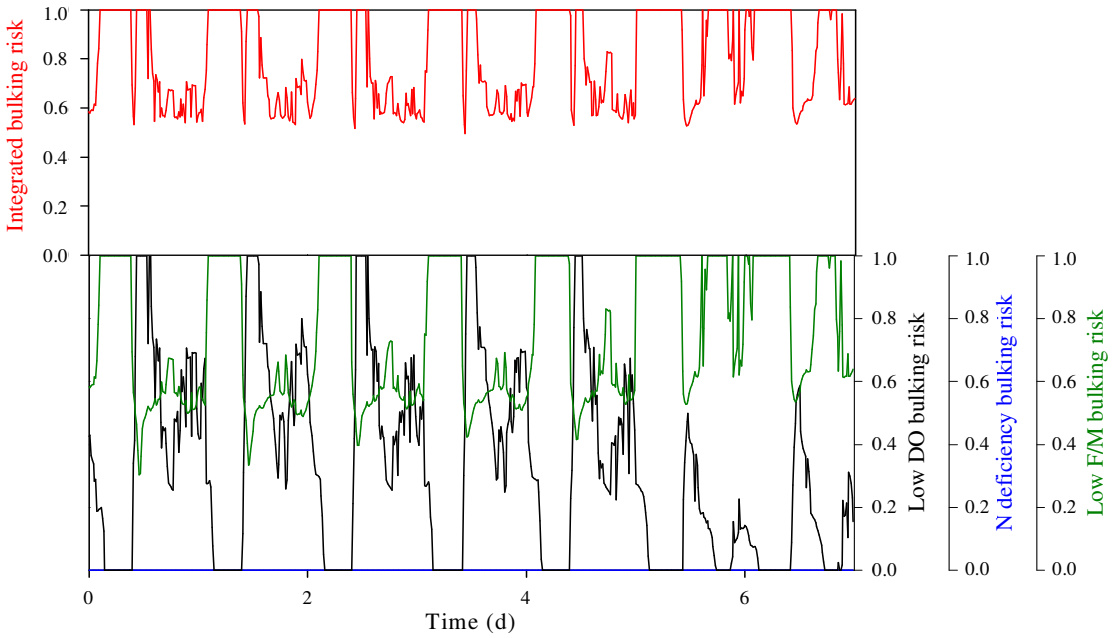

Figure 6.10. Integrated bulking risk.
Top plot in red: integrated risk of bulking; bottom plot: risk of bulking due to nutrient deficiency (blue), low DO (black) and low F/M (green).

In **Figure 6.11** the same risk integration is performed for the risk of foaming. In this case, the risk of foaming due to low F/M is clearly drives the integrated risk of foaming.

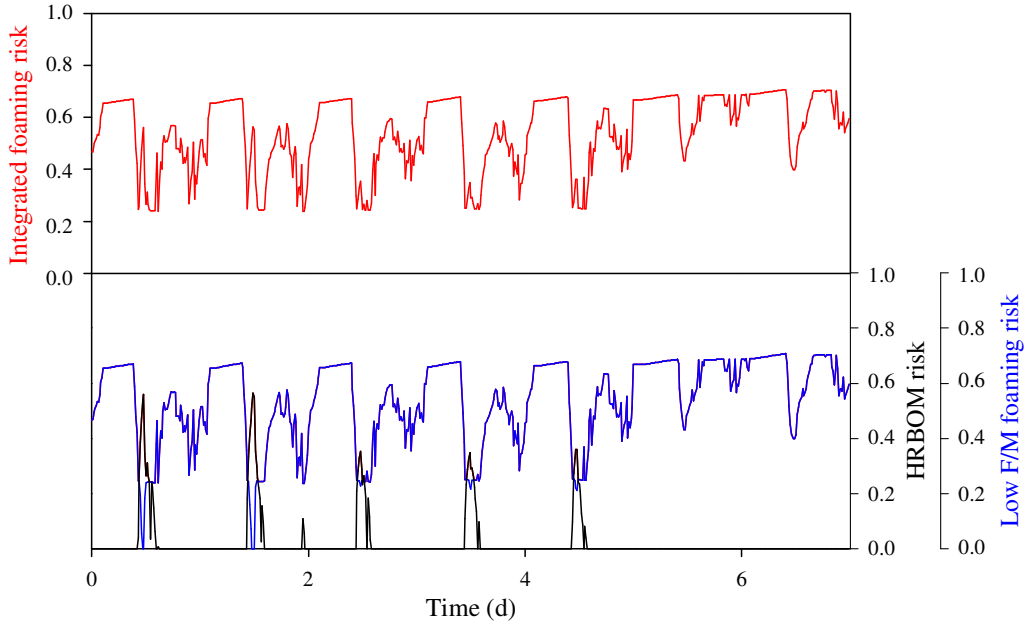

Figure 6.11. Integrated foaming risk.
Top plot in red: integrated risk of foaming; bottom plot: risk of foaming due to HRBOM (black) and low F/M (blue).

Last is the overall integrated risk which takes the maximum value of each integrated risk. **Figure 6.12** shows a one-day zoom (from days 1 to 2) of the evaluation week for the easier identification of each risk. In **Figure 6.13** overall risk is shown for the whole week. It can be seen that in the open-loop dry weather case the bulking risk is the main contributor to high values of overall risk. However, risk of rising sludge is also shows a contribution, although at lower values of overall risk.

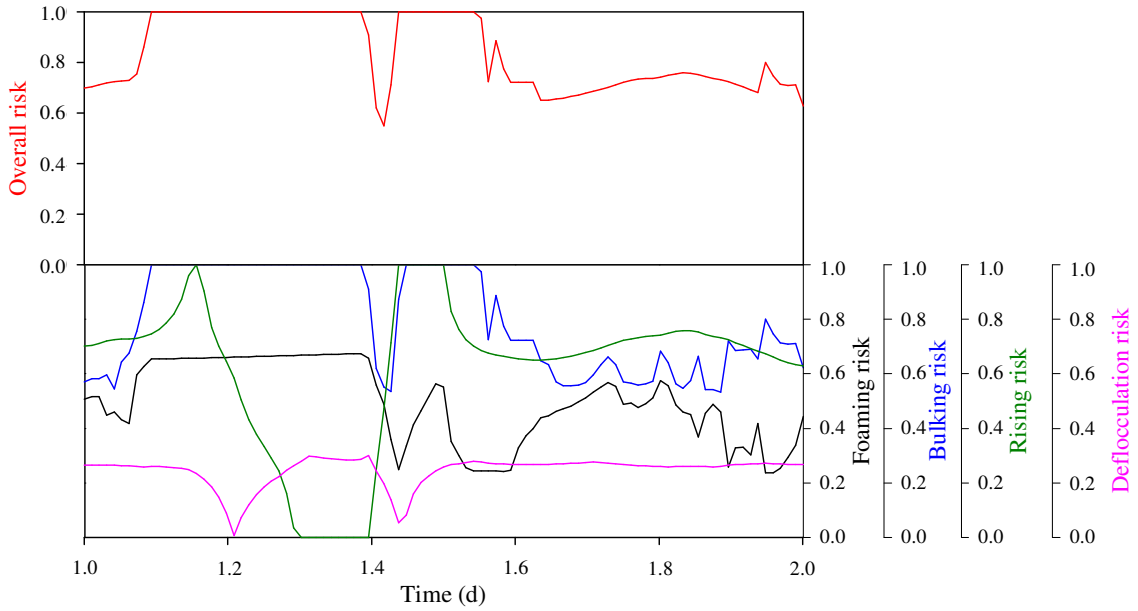

Figure 6.12. Integrated overall risk index for day 2 of evaluation.
Top plot in red: integrated overall risk; bottom plot: integrated risks of foaming (black), bulking (blue), rising (green) and deflocculation (pink).

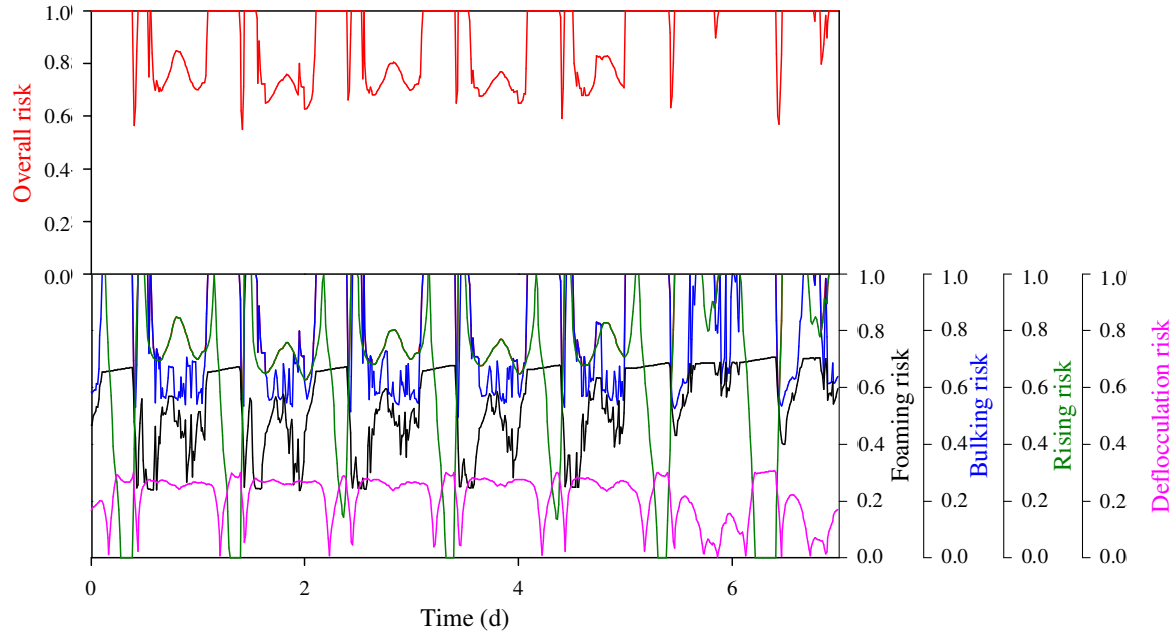

Figure 6.13. Integrated overall risk for the seven-day evaluation period.
Top plot in red: integrated overall risk; bottom plot: integrated risks of foaming (black), bulking (blue), rising (green) and deflocculation (pink).

The variation of the risk profiles highlights the need for a filter given that the daily variations will be reflected in long-term simulations (see **Section 6.3 Long-term Benchmark Simulation Model No1**).

6.2.2 Operational parameters influence

The objective of this section is not finding the best operational conditions (i.e. conditions with the lowest risks) but to evaluate the performance of the risk model. To achieve this, the effect of the main operational parameters on the different risks in the open-loop dry weather scenario has been used. The specifications for the simulations are the same as those in **Section 6.2.1 Open-loop.** In total, seven simulations have been performed. For Q_r, 18446 $m^3 \cdot d^{-1}$ x0.5 and x1.5 are considered. For Q_w the simulations are 385 $m^3 \cdot d^{-1}$ x0.5 and x1.5 (the Q_w used in **Section 6.2.1 Open-loop**). Finally, 240 d^{-1} x0.5, x1 (open-loop case) and x1.5 for biological reactors 3 and 4 and 84 d^{-1} x0.5, x1 and x1.5 for biological reactor 5 (the same $K_L$as used in **Section 6.2.1 Open-loop**) are considered for DO (K_La). **Table 6.2** summarises the simulations which have been performed using the standard protocol for BSM1 (150 days steady-state simulation with constant influent followed by 28 days with dynamic dry weather influent).

Table 6.2. Specifications used for the BSM1 dry weather open-loop simulations with operational parameters changes.

Simulation	K_La3 (d^{-1})	K_La4 (d^{-1})	K_La5 (d^{-1})	Q_r ($m^3 \cdot d^{-1}$)	Q_w ($m^3 \cdot d^{-1}$)
K_La x0.5	120	120	42	18446	385
K_La x1 (Open-loop)	240	240	84	18446	385
K_La x1.5	360	360	168	18446	385
Q_r x1.5	240	240	84	28416	385
Q_r x0.5	240	240	84	9472	385
Q_w x0.5	240	240	84	18446	192
Q_w x1.5	240	240	84	18446	573

The results (AV risk and %TIV) of the AS risk model for each simulation are presented in **Table 6.3.** The highest AV and %TIV for each operational problem of microbiological origin have been shadowed. It can be seen that risk of bulking due to nutrient deficiency and risk of foaming due to HRBOM is almost 0 for all the simulations. Risk of bulking due to low DO is high for the K_La x0.5 simulation. With regard to risk of bulking due to low F/M, this reaches relatively high values which are, in some cases, at high risk close to 50% of %TIV and AVs above 0.7 or 0.8. However, the highest values in terms of %TIV and AV are for Q_w x0.5 since the high MLVSS concentration lowers the F/M ratio and increases the risk of bulking for low F/M accordingly. Likewise, this explains the high %TIV and AV risk of foaming due to low F/M in the Q_w x0.5 simulation. For these conditions, F/M is low, which causes an increased risk. For Q_r x1.5 the risks of bulking and foaming due to low F/M are relatively high for the same reason; the increased Q_r causes an increase in the MLVSS in the biological reactors which lowers the F/M ratio, thereby increasing the risk. The risk of foaming due to HRBOM is very low for all the simulations. Regarding the risk of rising sludge, Q_w x0.5, Q_r x0.5 and K_La x1.5 have a high AV and %TIV. In the Q_w case, the low flow rate accumulates biomass in the whole AS system. The less Q_w there is, the more heterotrophic biomass accumulates in the secondary settler increasing its residence time and consequently, the risk of rising sludge. This reduces the NGPT, which increases the risk of rising sludge. In the case of K_La, DO is directly related to the nitrification process, so the higher the DO the more nitrate will be present in the effluent of the 5th biological reactor, thereby increasing the risk of rising sludge. Finally, the high rising sludge risk for the Q_r x0.5 simulation is directly related to the retention time at the bottom of the secondary settler. The risk of deflocculation is high in the Q_w x0.5

simulation due to the high SRT. Integrated risks are useful for showing clearly which operational problems of microbiological origin are the most relevant for each simulation. The K_La x0.5 simulation has the highest %TIV for integrated bulking followed by the Q_w x0.5 simulation. The highest risk of integrated foaming in terms of risk AV and %TIV is for the Q_w x0.5 simulation. The worst scenarios for rising sludge are Q_w x0.5, Q_r x0.5 and K_La x1.5 simulations. AVs for overall risk are slightly higher for K_La x1.5 than for K_La x0.5 and Q_w x0.5 simulations. %TIV for the overall risk are high in all cases but especially so in the K_La x0.5, x1.5 and Q_w x0.5 simulations.

Table 6.3. Evaluation criteria for different simulation conditions.

Operational parameter		Qr			Q_w			K_La		
Risk related criteria		**x0.5**	**x1 (OL)**	**x1.5**	**x0.5**	**x1 (OL)**	**x1.5**	**x0.5**	**x1 (OL)**	**x1.5**
Nutrient deficiency Bulking	**TIV(%)**	0.00	0.00	0.00	0.00	0.00	0.00	0.00	0.00	0.00
	AV	≈ 0.00	≈ 0.00	≈ 0.00	≈ 0.00	≈ 0.00	≈ 0.00	≈ 0.00	≈ 0.00	≈ 0.00
Low DO Bulking	**TIV(%)**	9.82	8.18	7.29	11.31	8.18	10.86	58.18	8.18	0.00
	AV	0.30	0.32	0.34	0.36	0.32	0.31	0.64	0.32	0.06
Low F/M Bulking	**TIV(%)**	0.00	42.41	49.26	65.03	42.41	0.00	36.46	42.41	42.86
	AV	0.48	0.75	0.82	0.87	0.75	0.48	0.63	0.75	0.75
Low F/M Foaming	**TIV(%)**	0.00	0.00	44.94	58.93	0.00	0.00	0.00	0.00	0.00
	AV	0.24	0.54	0.67	0.80	0.54	0.24	0.50	0.54	0.54
HRBOM Foaming	**TIV(%)**	0.00	0.00	0.00	0.00	0.00	0.00	0.00	0.00	0.00
	AV	0.18	0.03	0.02	0.01	0.03	0.18	0.04	0.03	0.02
Rising sludge	**TIV(%)**	52.08	34.08	4.31	55.80	34.08	10.71	0.00	34.08	60.27
	AV	0.81	0.68	0.41	0.86	0.68	0.52	≈0.00	0.68	0.71
Deflocculation	**TIV(%)**	0.00	0.00	0.00	60.12	0.00	0.00	0.00	0.00	0.00
	AV	0.21	0.22	0.29	0.82	0.22	0.19	0.41	0.22	0.32
Integrated Bulking	**TIV(%)**	9.82	50.59	56.55	76.34	50.59	10.86	94.64	50.59	42.86
	AV	0.61	0.81	0.86	0.91	0.81	0.61	0.94	0.81	0.76
Integrated Foaming	**TIV(%)**	0.00	0.00	44.94	58.93	0.00	0.00	0.00	0.00	0.00
	AV	0.31	0.55	0.68	0.80	0.55	0.31	0.52	0.55	0.55
Overall Risk	**TIV (%)**	61.31	65.33	56.99	89.14	65.33	20.09	94.64	65.33	94.64
	AV	0.85	0.89	0.87	0.94	0.89	0.70	0.94	0.89	0.98
Plant performance criteria										
OCI		17040	16148	15782	14880	16148	17210	14475	16148	17852
EQI (kg pollutants·d^{-1})		8467	6690	6294	6145	6690	7858	21828	6690	6170

When comparing each simulation it is noticeable that Q_w x0.5 simulation has, in many cases, the highest values of AVs and %TIV except for risk of bulking due to low DO and risk of rising sludge. On the other hand, Q_r x0.5 and Q_w x1.5 simulations have the lowest %TIV and AVs (except for rising sludge in the first case). Hence, it could be concluded that, in general, low MLVSS and normal DO in the biological reactors provide proper conditions for controlling the risk of operational problems of microbiological origin. However, when the relevant criteria of the BSM1 are taken into account, it can be seen that these simulations are not the best option from an environmental and/or economic perspective. Low DO (K_La x0.5) has the worst EQI due to low efficiency. In terms of economic criteria the worst value corresponds to the K_La x1.5 simulation due to high aeration costs. Note that the best options correspond to those conditions in which the risk of operational problems is relatively high: K_La x0.5 simulation (from an economical perspective) and Q_w x0.5, due to low aeration costs and low SP, respectively.

6.2.3 Closed-loop

Two CSs are compared together with the open-loop for different weather influents using the BSM1. CS1 consists of two control loops which control the DO level (2 mg $O_2 \cdot L^{-1}$) in the last aerated reactor and the nitrate concentration (1 mg $N \cdot L^{-1}$) in the second anoxic reactor by manipulating the K_La of the last aerated biological reactor and the Q_{intr}, respectively. CS2 is equivalent to strategy-1 except that the Q_r is not constant (18446

$m^3 \cdot d^{-1}$) but proportional to the Q_{in} with a gain of 2. **Figure 6.14** illustrates the time series plots obtained for risk of bulking due to low DO and low F/M, risk of foaming due to low F/M ratio, and rising sludge for both CSs using the rain influent scenario of the BSM1.

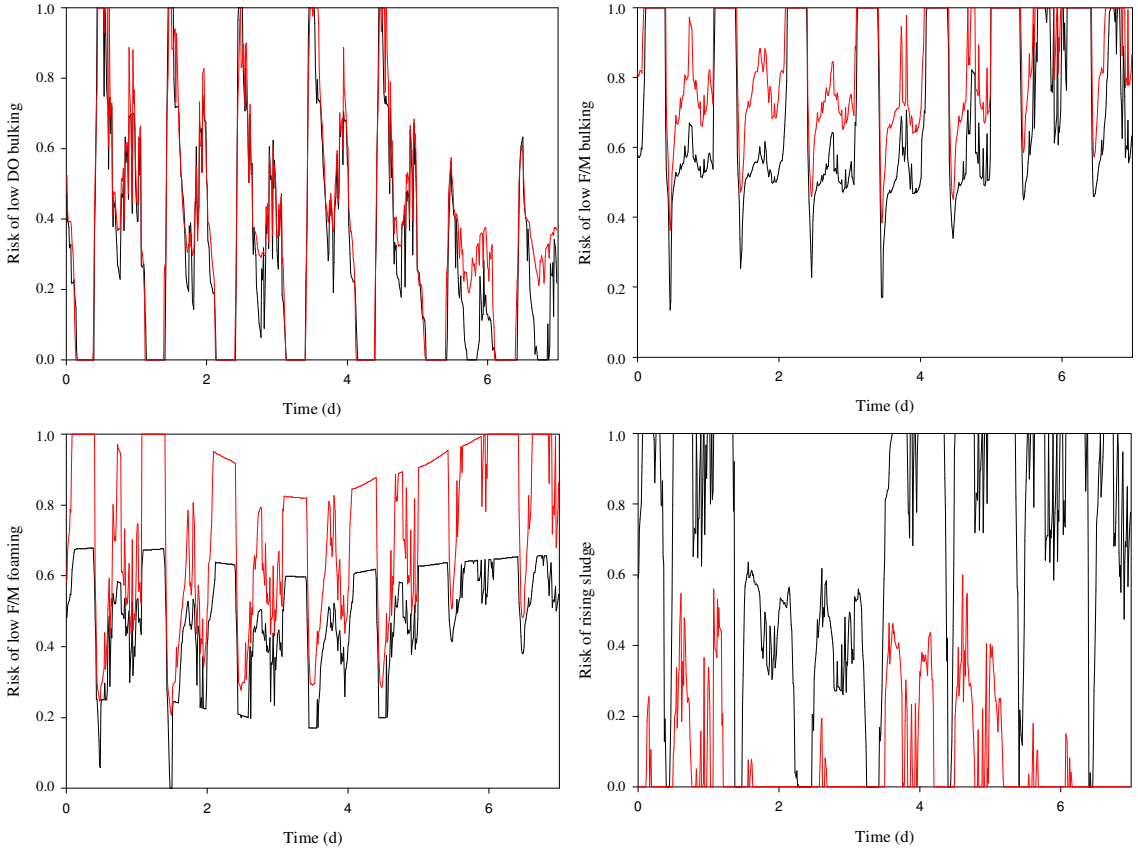

Figure 6.14. Risk of operational problems of microbiological origin during rain influent conditions: risk of bulking due to low DO (top left), risk of bulking due to low F/M (top right), risk of foaming due to low F/M ratio (bottom left) and rising sludge (bottom right). In each, the black line indicates CS1 while the red line represents CS2.

Figure 6.14 shows that different CSs yield different estimates of the risk of the system experiencing operational problems of microbiological origin. The figure illustrates that there is not much difference between the two CSs with regard to the risk of aerobic bulking (**Figure 6.14** - top left), just a slight difference during the weekend. The risk of this problem occurring is low for almost all of the time since the existing DO controller maintains an adequate set point based on the F/M ratio experienced by the plant. In contrast, operational conditions imposed by CS2 lead to higher risks for low F/M bulking and even more for foaming (*M. parvicella* and Nocardioforms) during rainy influent conditions (**Figure 6.14** - top right and bottom left, respectively). For both problems, the higher Q_r of CS2 causes higher biomass concentrations in the biological reactors, and thus contributes to very low substrate concentrations. On the other hand, this CS drastically reduces the risk of experiencing rising sludge problems because the sludge retention time in the clarifier decreases (**Figure 6.14** - bottom right). Filamentous bulking caused by nutrient deficiency is not plotted as the risk of occurrence of this type of problem is never high because the nitrogen load is high throughout the simulation. Note that phosphorus is not considered in the ASM1 model.

Similarly, foaming caused by a HRBOM fraction is never experienced because conditions favouring this type of foaming do not occur.

Table 6.4 shows the values of the settling quality criteria together with the plant performance evaluation criteria in relation to EQI and OCI for both CSs, and an open-loop CS with constant actuator settings exposed to all three influent scenarios (i.e. dry, rain and storm).

Table 6.4. Plant performance obtained using three CSs for different influent scenarios.

RISK RELATED CRITERIA		Dry influent			Rain influent			Storm influent		
Bulking due to nutrient deficiency	**TIV(%)**	0.00	0.00	0.00	0.00	0.00	0.00	0.00	0.00	0.00
	AV	≈ 0.00	≈ 0.00	≈ 0.00	≈ 0.00	≈ 0.00	≈ 0.00	≈ 0.00	≈ 0.00	≈ 0.00
Bulking due to low DO	**TIV(%)**	8.18	7.29	11.61	10.56	6.99	10.42	12.05	10.42	13.39
	AV	0.32	0.33	0.38	0.30	0.30	0.35	0.32	0.33	0.37
Bulking due to low F/M ratio	**TIV(%)**	42.41	41.81	63.24	40.18	40.77	58.93	42.26	42.71	64.14
	AV	0.75	0.74	0.86	0.68	0.72	0.85	0.73	0.74	0.86
Foaming due to low F/M ratio	**TIV(%)**	0.00	0.00	55.21	0.00	0.00	50.59	0.00	0.00	55.06
	AV	0.54	0.54	0.78	0.42	0.50	0.74	0.50	0.53	0.77
Foaming due to HRBOM fraction	**TIV(%)**	0.00	0.00	0.00	0.00	0.00	0.00	0.00	0.00	0.00
	AV	0.03	0.02	0.01	0.05	0.03	0.01	0.03	0.02	0.01
Rising sludge	**TIV(%)**	34.08	77.23	0.00	23.81	52.23	0.00	28.42	70.54	1.49
	AV	0.68	0.86	0.13	0.60	0.70	0.07	0.64	0.82	0.16
Deflocculation	**TIV(%)**	0.00	0.00	0.00	0.00	0.00	0.00	0.00	0.00	0.00
	AV	0.22	0.24	0.45	0.13	0.19	0.37	0.19	0.22	0.41
Integrated bulking	**TIV(%)**	50.59	49.11	74.85	50.74	47.77	69.34	54.31	53.12	77.38
	AV	0.81	0.81	0.91	0.79	0.79	0.89	0.82	0.82	0.91
Integrated foaming	**TIV(%)**	0.00	0.00	55.21	0.00	0.00	50.59	0.00	0.00	55.06
	AV	0.55	0.55	0.78	0.45	0.51	0.74	0.52	0.53	0.78
Overall risk	**TIV(%)**	65.33	86.90	74.85	63.69	70.68	69.34	66.52	87.94	77.97
	AV	0.89	0.95	0.91	0.85	0.88	0.89	0.88	0.95	0.91
PERFOMANCE CRITERIA										
OCI		16148[a]	16424[b]	15607[c]	15732[a]	15764[b]	14927[c]	16966[a]	17171[b]	16344[c]
EQI ($kg \cdot d^{-1}$)		6690	6038	5574	8935	7816	7326	8022	7042	6547

[a] Open-loop (constant actuator settings; $K_La3=K_La4=240$, $K_La5=84$; $Q_r=Q_{in\ avg.}$; $Q_{intr.}=3 \cdot Q_{in\ avg.}$)
[b] CS1
[c] CS2

From the results in **Table 6.4** it can be concluded that both closed-loop CSs improve plant performance compared to the open-loop strategy, when only traditional plant performance evaluation criteria regarding EQI for the three weather influent scenarios (dry, rain and storm) are considered. In terms of economic criteria, CS1 is a worse option than open-loop, while CS2 presents a more economic alternative.

With regard to the settling quality criteria, the %TIV and the AV risk of bulking due to nutrient deficiency values are almost 0 in all cases. In terms of risk of bulking due to low DO, the same behaviour is observed in both CSs. CS1 has a lower risk than open-loop due to the DO controller. However, CS2 has a slightly higher risk than CS1 due to the increased Q_r. The higher the Q_r, the higher the MLVSS concentration is in the biological reactor, and hence, some low DO conditions can occur in CS2 despite the DO control. This last fact explains the behaviour of the risks of bulking and foaming due to low DO. For open-loop and CS1 only small differences appear. For CS2 the increased MLVSS concentration in the biological reactors can cause more low F/M conditions.

In terms of risk of rising sludge, CS2 has the lowest values of %TIV and AV risk given that it has the lowest S_{NO} and the highest NGPT due to the nitrate control. With regard to CS1 and open-loop, although CS1 %TIV is higher than that of open-loop, its AV value is quite high as well. The basic difference between CS1 and open-loop is that despite the S_{NO} controller, the fact that Q_r is proportional to the Q_{in} means that when the Q_{in} is low, Q_r is low as well, thereby increasing the retention time at the bottom of the secondary settler which in turn increases the risk of rising sludge. For the open-loop,

since Q_r is constant the retention time at the bottom of the secondary settler is constant as well, thereby reducing the possibility of causing rising sludge.

For CS2, the risk of deflocculation is higher than for CS1 and open-loop due to the higher MLVSS concentration caused by the increased Q_r. Nevertheless, the risk of deflocculation is not severe in any of the cases.

The integrated risk of bulking and foaming follows the same behaviour as that of the individual risks. However, the overall risk is influenced by the risk of rising sludge (i.e. CS1 has the highest risk, and CS2 the lowest).

6.3 Long-term Benchmark Simulation Model No1 application

The first part of this section is devoted to the filtering of the results of an open-loop simulation obtained after applying the AS risk model. There is also a discussion of the effect of different time constants of the filter. In the second part, the temperature effect on *Microthrix parvicella* is shown. Finally, an example of the AS risk model performance for a 3 DO CS is discussed.

6.3.1 Open-loop

In this section the filter effect on the results of a BSM1_LT open-loop case are evaluated. The specifications for the simulation are shown in **Table 6.5** (based on Vrecko *et al.*, 2006). The simulation is based on the influent files by Gernaey *et al.* (2006) for BSM1_LT (BSM2 influent files after the primary clarifier). It should be pointed that the evaluation periods for all the simulations in BSM1_LT start on July 1st. Hence, the initial period corresponds to summer. The middle of the evaluation period is in winter and the end is the beginning of summer.

Table 6.5. Specifications used for the BSM1_LT simulation.

K_La3 (d^{-1})	K_La4 (d^{-1})	K_La5 (d^{-1})	Q_w ($m^3 \cdot d^{-1}$)	Q_{intr} ($m^3 \cdot d^{-1}$)	Q_r ($m^3 \cdot d^{-1}$)	Q_{carb} ($m^3 \cdot d^{-1}$)	Bypass
240	240	240	300	55338	18446	0	No

The filter has already been described in **Section 5.1.2 Knowledge formalisation.** This exponential filter should be applied for long simulation runs i.e. for simulation runs longer than 1 month. Therefore, for the case of BSM1_LT and BSM2, this filter has been applied to the following individual risks: bulking due to low DO values, bulking due to low organic loading, bulking due to nutrient deficiency, foaming due to low F/M ratio, foaming due to HRBOM fraction, rising sludge and deflocculation. For BSM1 the filter is not used.

In the BSM1_LT, the filter is applied with a time constant of 3 days for foaming, bulking and deflocculation risk and 2 hours for rising sludge. **Figure 6.15** depicts the effect of the filter on the risk of bulking due to low DO. It is difficult to interpret the risk without the filter because the daily dynamics appear too close (in black). However, when the 3-day filter is applied the seasonal effect on the risk of filamentous bulking (in red) becomes noticeable. There is a first period (summer, days 0-100 approx.) with a relatively high risk of bulking due to low DO followed by a period (winter, days 150-270) with a lower risk. These seasonal changes are due to the change in the F/M ratio, which during the summer is low. The opposite effect occurs during the winter.

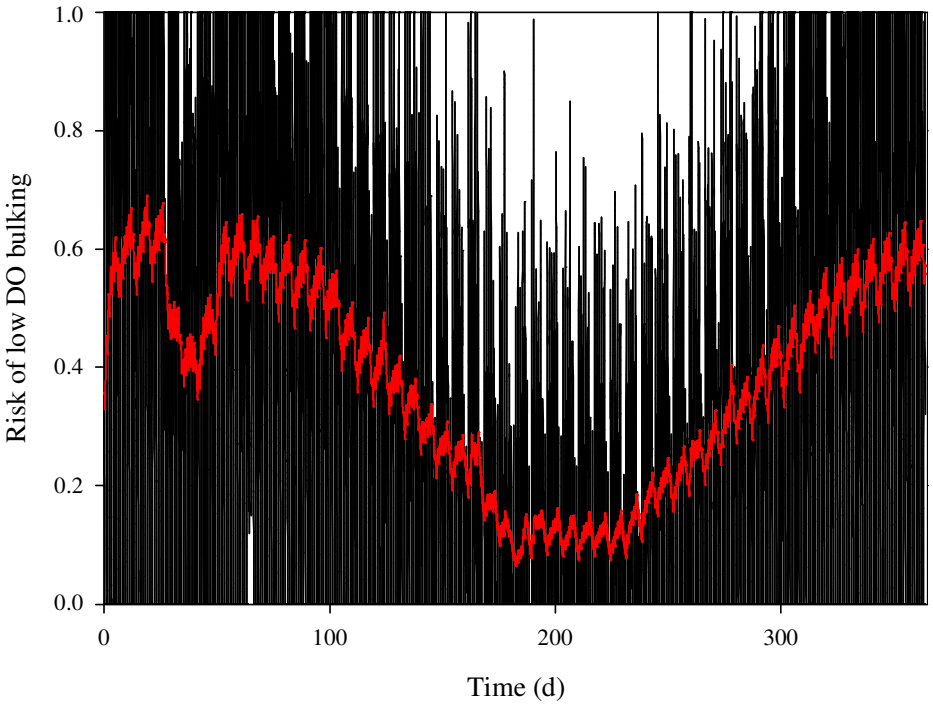

Figure 6.15. Filter effect on risk of bulking due to low DO.
Black line: without filter; Red line: with filter.

Figure 6.16 depicts a zoom from **Figure 6.15** of days 98 to 105. Higher risks are present during the weekdays due to higher F/M than during the weekend (lower F/M). For the filtered risk there is similar behaviour, increasing during the day with the higher F/M and dropping during the night due to low F/M. At the weekend the risk decreases as well.

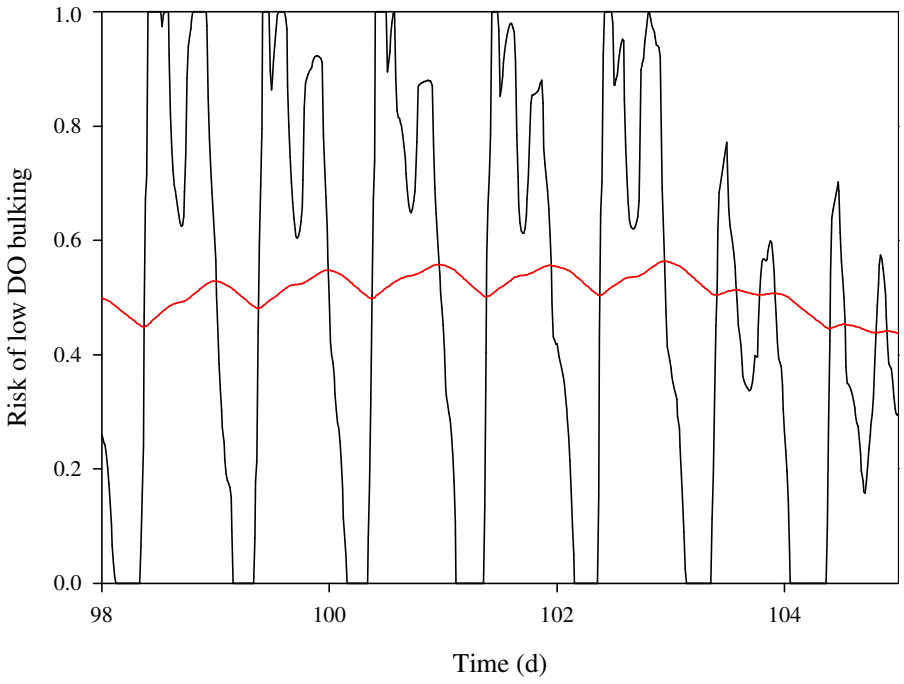

Figure 6.16. One-week (days 98 to 105) zoom from Figure 6.15.
Black line: without filter; red line: with filter.

6.3.1.1 Filter time constant variation

Figure 6.17 represents the effect of changing the time constant in the filter. The risk shown is that related to bulking due to low DO. There is a significant change from the 1-day to the 3-days time constant. The 1-day time constant is not yet smooth enough. On the other hand, the change from a 3-day to a 7-day time constant is not as significant. Thus, the 3-day time constant was selected. It allows to represent the slow dynamics behaviour making the interpretation of the results more feasible. As in **Figure 6.16,** the weekly behaviour is represented by the small peaks in the 3-day filtered risk. The behaviour of the risk and its causes are the same as those explained in relation to **Figure 6.16**.

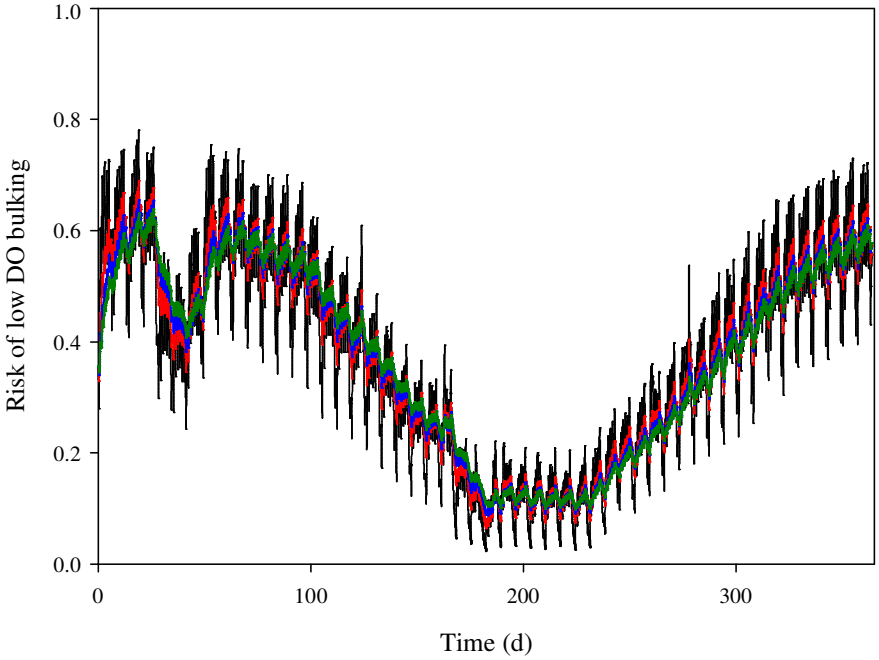

Figure 6.17. Risk of bulking due to low DO.
Black line: 1-day; red line: 3-day; blue line: 5-day; green line: 7-day.

6.3.2 Temperature influence

The open-loop case with a filter time-constant of 3 days has been used to evaluate the effect of temperature on one of the operational problems of microbiological origin, namely the risk of foaming due to low F/M which is caused by *M. parvicella* (see **Section 5.1.4.2 Temperature influence**).

Figure 6.18 depicts the temperature effect on the risk of foaming due to low F/M (black line: with temperature effect; Red line: without temperature effect). If we look at the seasonal effect, the risk decreases during summer. On the other hand, without the temperature effect only a few peaks go above 0.8 during the winter. The temperature effect raises the risk above 0.8 for longer time periods during the winter, thereby increasing the %TIV of foaming. The AV risk of foaming due to low F/M remains the same (0.61) but the %TIV of foaming due to low F/M increases from 10% without the temperature effect to 28% with the temperature effect. Apart from the rise in the %TIV, the high risks of foaming due to low F/M are now centred on the winter period which is indeed more realistic.

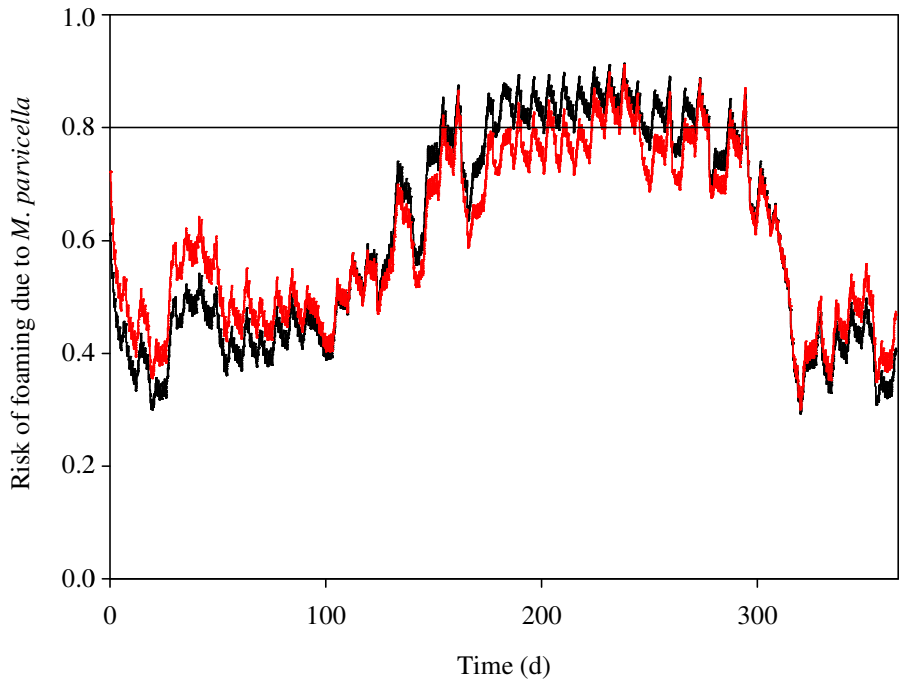

Figure 6.18. Risk of foaming due to low F/M caused by *M.Parvicella.* Black line: risk with T effect; red line: risk without temperature effect.

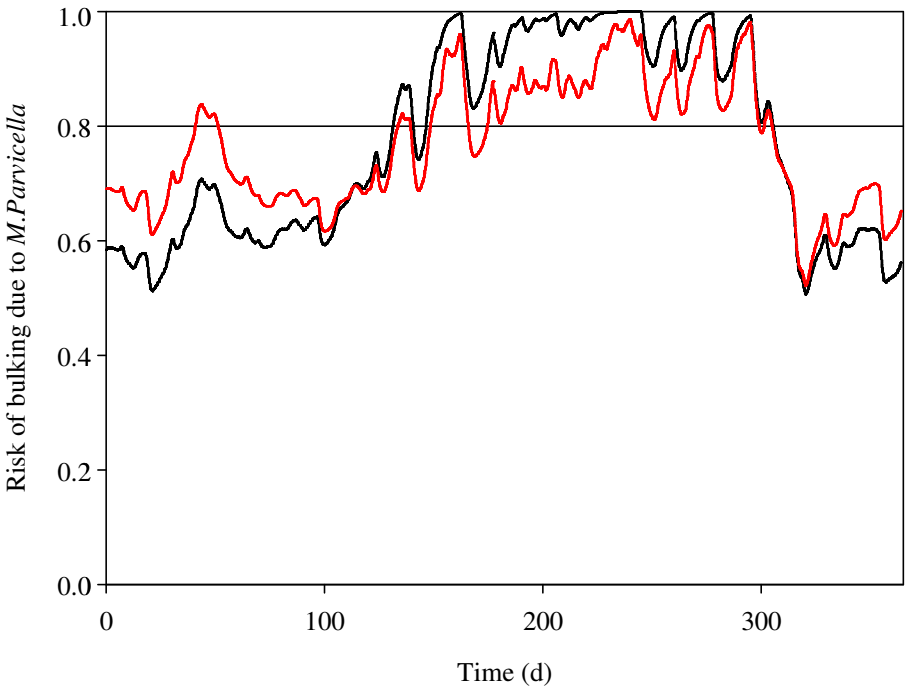

Figure 6.19. Risk of bulking due to low F/M caused by *M.Parvicella.* Black line: risk with T effect; red line: risk without temperature effect.

The risk of bulking due to low F/M affected by the temperature correction is shown in **Figure 6.19** (black line: with temperature effect; red line: without temperature effect). During the summer period the temperature effect decreases the risk of bulking due to low F/M. On the other hand, the risk of bulking due to low F/M during winter is even more increased. Globally, the AV risk with and without the T effect is 0.77 while

the %TIV in high risk is 44% without the T effect and 46% with it. With regard to the risk of bulking due to low F/M, note that the risk model investigates two different risks and then the maximum between them is selected at each time step. This can have a smoothing effect on the profiles when comparing **Figures 6.18** and **6.19**.

6.3.3 Closed-loop

The CS tested is based on identical DO control loops in the three aerobic reactors of the BSM1 plant, where DO is controlled at a constant set point (2 $mgO_2 \cdot L^{-1}$) by manipulating K_La (3DO CS). The rest of specifications are as stated for the open-loop case.

Several conclusions can be drawn from **Table 6.6**. One is that aerobic filamentous bulking, foaming due to HRBOM fraction, bulking due to nutrient deficiency and deflocculation are not really a problem at any time of the year for this CS. The low %TIV and AV risk values for these problems are due to the continuous high DO level in the aerobic biological reactors (set point values of 2 $mgO_2 \cdot L^{-1}$), the predominance of low values for the S_S/X_S ratio and the absence of shortage of nitrogen. On the other hand, the risk of experiencing rising sludge is severe for almost the entire evaluation period (315 days, 86% of the time). Indeed, due to the high nitrification capacity as a result of applying the selected DO CS and the low biodegradable substrate concentration in the influent, the plant experiences incomplete denitrification.

Table 6.6 provides the results for the risk criteria for the 3DO CS and the open-loop case. For the specific case of risk of bulking due to low DO, the risk is lower for the CS since DO is controlled. On the other hand, problems related to rising sludge are higher, given that the DO controller allows more nitrification. This nitrate is the cause of the higher risk of rising sludge. The integrated values for filamentous bulking, foaming and rising sludge are given. The higher %TIV of rising sludge compared to the risks of bulking and foaming (89.67% *versus* 47.29% and 27.33%, respectively) shows the former problem to be the riskier one for the 3DO CS, and thus the one to be tackled first. **Table 6.6** also shows the overall risk value of experiencing operational problems of microbiological origin for this CS.

Table 6.6. Settling quality criteria for the 3DO CS applied to the BSM1_LT.

RISK RELATED CRITERIA	CS		Open-loop	
	TIV (%)	AV	TIV (%)	AV
Bulking due to nutrient deficiency	0.00	≈ 0.00	0.00	≈ 0.00
Bulking due to low DO	0.00	0.24	18.05	0.38
Bulking due to low F/M	47.28	0.77	47.46	0.79
Foaming due to low F/M ratio	27.33	0.61	27.60	0.61
Foaming due to HRBOM fraction	0.00	0.03	0.00	≈ 0.00
Rising sludge	89.67	0.94	86.44	0.92
Deflocculation	0.00	≈ 0.00	0.00	≈ 0.00
Integrated bulking	47.29	0.79	47.46	0.79
Integrated foaming	27.33	0.61	27.60	0.61
Overall risk	95.67	0.97	89.59	0.95
PERFORMANCE CRITERIA				
OCI	14590		16660	
EQI	9315		9244	

Finally, EQI and OCI show similar results. OCI is lower for CS than for open-loop due to the DO controller since aeration is more optimized. However, EQI is slightly higher for CS than for open-loop due to the fact that the DO controller might not provide enough DO for nitrification. On the other hand, in the open-loop case the aerobic

reactors are over-aerated (as high OCI indicates) so more nitrification can be possible so less ammonia is lost through the effluent.

6.4 Benchmark Simulation Model No2 application

This section is devoted to the application in BSM2. Since the principal addition is the anaerobic digester the results are centred on the AD risk model. The section is composed of four parts: open-loop which will show the general results of the AD risk model; influence of operational parameters (Q_w and Q_r) on the evaluation results; closed-loop, which includes the evaluation of two different CSs; and finally an evaluation from a plant-wide perspective including the results of the AS and AD risk model is presented.

6.4.1 Open-loop

An open-loop case study with constant values for the main plant-wide WWTP operational parameters has been simulated to illustrate the performance of the AD risk model. **Table 6.7** shows the specifications of the open-loop BSM2 simulation. Influent files used are the ones presented in Gernaey *et al.* (2006) for BSM2.

Table 6.7. Specifications used for the open-loop BSM2 simulation.

K_La3 (d^{-1})	K_La4 (d^{-1})	K_La5 (d^{-1})	Q_w ($m^3 \cdot d^{-1}$)	Q_{intr} ($m^3 \cdot d^{-1}$)	Q_r ($m^3 \cdot d^{-1}$)	Q_{carb} ($m^3 \cdot d^{-1}$)	Bypass
120	120	60	300	61944	20648	2	No

In terms of operational parameters related to the FAD risk, Q_w was fixed at 300 $m^3 \cdot d^{-1}$ and Q_r was equal to $Q_{in,0}$. **Figure 6.20** presents the FAD risk profile as a function of time together with OLR, OLRvar, and FAS risk profiles.

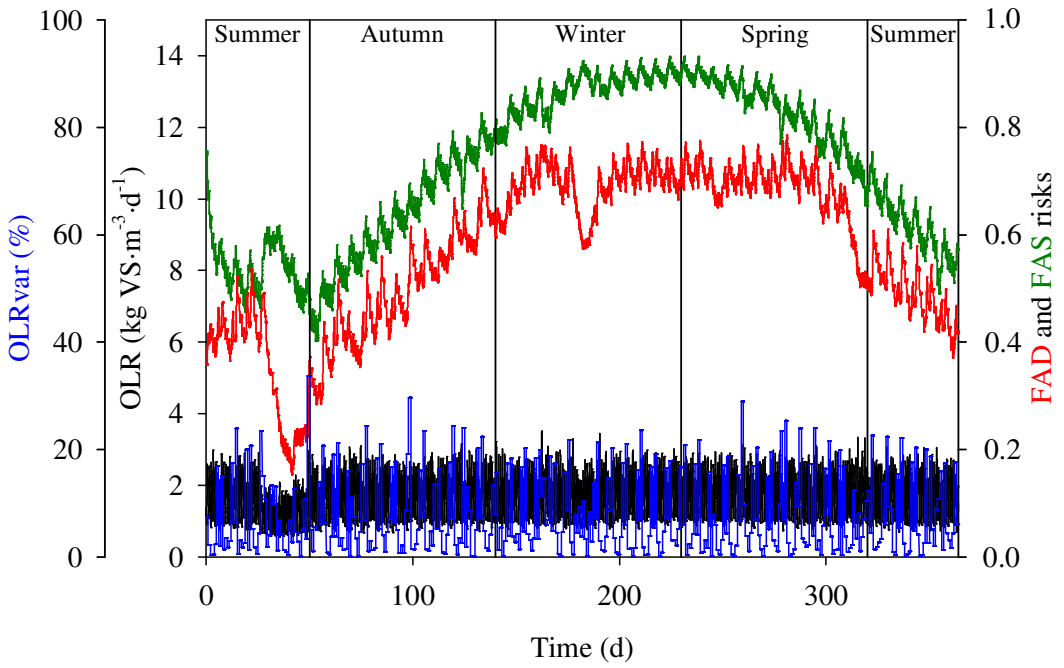

Figure 6.20. Simulated results of the AD risk model for the open-loop case for one-year simulation (from July 1st). OLR (black line); OLRvar (blue line); FAS risk (green line); FAD risk (red line).

In general terms, the FAD risk trend is similar to that of the FAS risk. However, at the end of the summer (days 30-50, approximately), there is a divergence in the FAD risk

with respect to the FAS risk due to a higher decrease in both OLR and OLRvar, which compensates for the increase in FAS risk over the same days. From approximately day 170 until the onset of summer (day 310), FAD risk stabilises well at around 0.7. In this period the FAD risk reaches the highest values possible with low OLR (1.2-2.4 $kgVS \cdot m^{-3} \cdot d^{-1}$) and between low and medium OLRvar (5-20%). In other words, FAD risk no longer increases (unlike FAS risk) because it has reached the maximum value possible with the current values of OLR and OLRvar. FAD risk would only increase, at these levels of FAS risk, due to higher OLR and/or OLRvar. FAD risk drops considerably for a few days (around day 185) in line with OLRvar values, although the FAS risk is relatively high during these days. The drop is consequence of quite constant VS concentration in the inflow for a few days. From day 270, FAD risk shows a decreasing trend that follows the FAS risk, and a sharper drop around day 320 due to another sharp decrease in OLRvar values around the same day.

6.4.2 Operational parameters influence

Among the main control handles in a WWTP (DO, Q_r and Q_w), two main operational parameters may influence the FAD risk: Q_w and Q_r. Q_w influences the amount of solids going to the anaerobic digester, changing OLR accordingly. Even though it is also possible to control the primary sludge flow rate to the anaerobic digester the purpose here is to test the effect of the main control handles on the FAD risk. Q_r has a direct effect on the amount of solids in the biological reactors, which is directly related to the F/M ratio on which the FAS risk depends, i.e. low Q_r maintains a low solids concentration in the aerated biological reactors so F/M is increased and the FAS risk lowered, and vice versa.

For both Q_r and Q_w simulations the previously presented open-loop case is used. For each Q_r simulation Q_w has been kept at 300 $m^3 \cdot d^{-1}$. Also, for each Q_w simulation Q_r has been kept at Q_{in} x1. Q_w has been varied from 100 to 700 $m^3 \cdot d^{-1}$ in 100 $m^3 \cdot d^{-1}$ steps, while Q_r has been tested from x0.25 to x1.5 Q_{in} in 0.25 steps.

6.4.2.1 Return activated sludge flow rate

Table 6.8 summarises the AV FAD risk, FAS risk, OLR and OLRvar for each Q_r.

Table 6.8. AV FAD risk, FAS risk, OLR and OLRvar for each Q_r.

Q_r ($m^3 \cdot d^{-1}$)	Q_{in} x0.25	Q_{in} x0.5	Q_{in} x0.75	Q_{in} x1	Q_{in} x1.25	Q_{in} x1.5
AV FAD risk	0.412	0.545	0.565	0.571	0.574	0.574
AV FAS risk	0.438	0.655	0.701	0.725	0.739	0.748
AV OLR ($kgVS \cdot m^{-3} \cdot d^{-1}$)	1.85	1.76	1.72	1.69	1.67	1.66
AV OLRvar (%)	7.14	7.40	7.49	7.53	7.55	7.58

Table 6.8 shows how AV FAD risk increases from 0.412 for Q_{in} x0.25 to 0.571 for Q_{in} x1. From this point on, AV FAD risk remains constant at 0.574. As noted above, at low Q_r, FAS risk is low as well as FAD risk. At higher Q_r, the inverse effect is seen, with increased AV FAS and FAD risk. AV OLRvar increases at the same time as the AV OLR decreases as Q_r increases. This trend is explained by the higher relative variation of OLR whereby lower values of OLR and similar values of OLR increments will give a higher percentage of OLRvar. **Figure 6.21** shows the profile of FAD risk for Q_r equivalent to Q_{in} x0.25, x1 and x1.5.

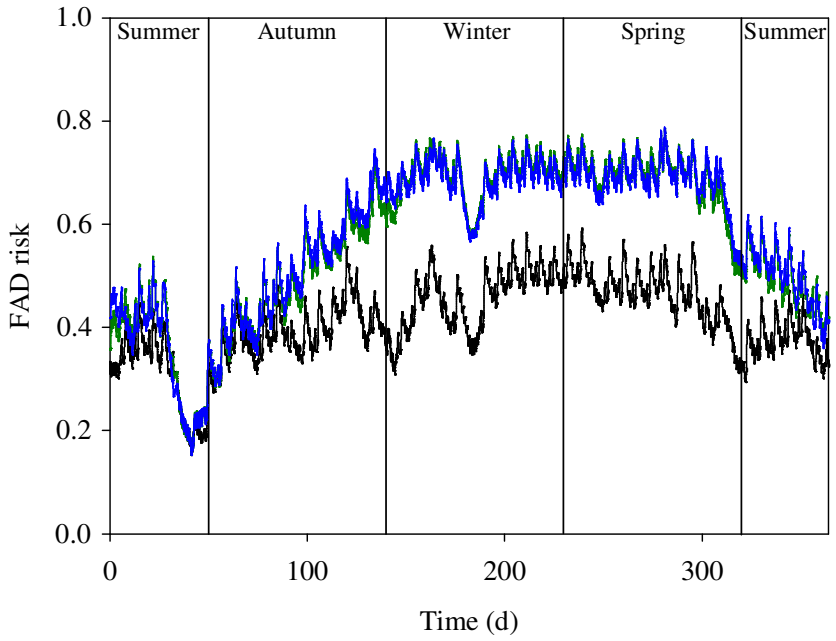

Figure 6.21. Profiles of FAD risk for Q_r equivalent to Q_{in} x0.25 (black line), Q_{in} x1 (green line) and Q_{in} x1.5 (blue line).

From the profile it can be seen that the differences in the AVs appear in the winter and spring periods, when the FAD risk is significantly lower for Q_r equal to the Q_{in} x0.25 case. During the winter FAD risk is higher for Q_r equal to Q_{in} x1 and x1.5 cases, given that FAS risk tends to increase in this period. On the other hand, this effect does not appear for the lowest Q_r (Q_{in} x0.25) because of the low FAS risk associated with low Q_r (0.438 on AV). In late summer (days 0-50) there are only slight differences between the different FAD risks due to the fact that the FAS risk is low. FAD risks are relatively low (around 0.4 for days 0-30) and later, when OLR decreases (effect shown in **Figure 6.20**), the FAD risks drops to its minimum (around 0.2) as a consequence.

6.4.2.2 Waste activated sludge flow rate

Table 6.9 shows the AV FAD risk, FAS risk, OLR and OLRvar for each Q_w. When Q_w increases, AV FAD also increases slightly at first from 0.548 to 0.572, but then descends to 0.432. The increase in AV OLR explains the rise in AV FAD risk for Q_w from 100 to 200 $m^3 \cdot d^{-1}$. It then descends to 0.432 (for Q_w equal to 700 $m^3 \cdot d^{-1}$), given that FAS risk decreases drastically from 0.766 to 0.475 with the increase in Q_w (from 200 to 700 $m^3 \cdot d^{-1}$). From Q_w equal to 200 $m^3 \cdot d^{-1}$, OLR does not increase enough to become relevant compared to the FAS risk. AV OLRvar decreases with the increasing AV OLR as in the previous case (i.e. Q_r study), although this time the effect is increased for the Q_w of 100 $m^3 \cdot d^{-1}$ given the low AV OLR. Thus, for a given daily OLR oscillation it is important not to have too low OLR since OLRvar could increase the FAD risk.

Table 6.9. AV FAD risk, FAS risk, OLR and OLRvar for each Q_w.

Qw ($m^3 \cdot d^{-1}$)	**100**	**200**	**300**	**400**	**500**	**600**	**700**
AV FAD risk	0.548	0.572	0.571	0.559	0.534	0.496	0.432
AV FAS risk	0.779	0.766	0.725	0.679	0.633	0.581	0.475
AV OLR ($kgVS \cdot m^{-3} \cdot d^{-1}$)	1.39	1.61	1.69	1.74	1.79	1.82	1.85
AV OLRvar	9.01	7.76	7.53	7.52	7.55	7.53	7.51

Figure 6.22 depicts the profiles of the FAD risk for three different Q_w: 100, 300 and 700 $m^3 \cdot d^{-1}$. During the summer period not many differences are appreciable between each Q_w. The low FAD risks during this period are due to the low FAS risks, characteristic for summer periods. During the winter period FAD risk increases, and the increase is more significant for low Q_w values (100 to 300 $m^3 \cdot d^{-1}$) than for values equal to 700 $m^3 \cdot d^{-1}$. This is due to the fact that for high Q_w the increase in OLR is not as significant as the decrease in FAS risk, as the FAD risk profile shows.

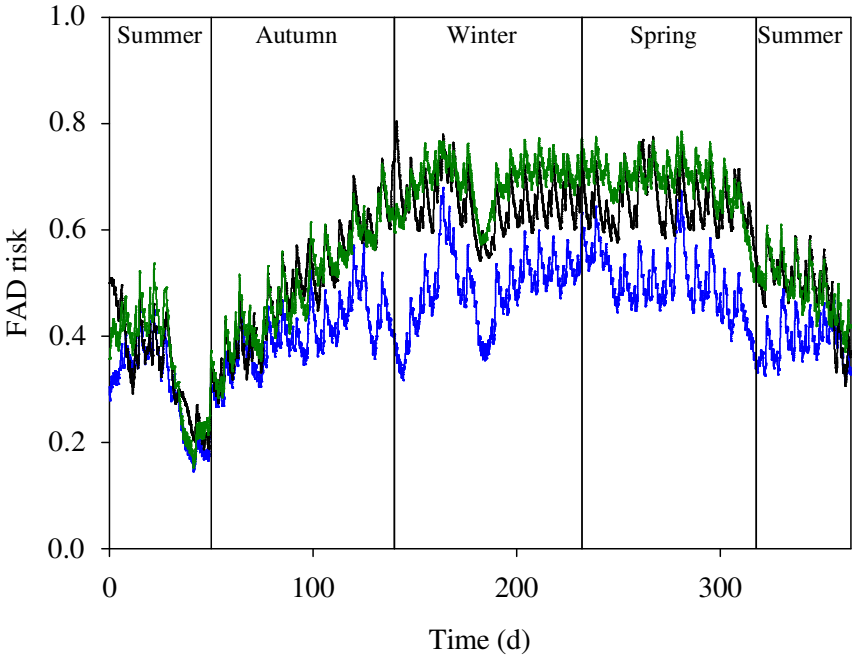

Figure 6.22. Profiles of FAD risk for 100 (black line), 300 (green line) and 700 (blue line) $m^3 \cdot d^{-1}$ Q_w.

6.4.3 Closed-loop

In order to test its performance, two closed-loop cases with automatic controllers involving manipulation of variables related to the AD risk model inputs were used to test its performance.

The first CS (CS1) involves the BSM2 default DO controller (Nopens *et al.*, 2008) which consists of a PI DO controller with a set point of 2 g $O_2 \cdot m^{-3}$ in tank reactor 4 by manipulating the K_La. For tanks reactors 3 and 5 the same K_La is applied with a gain of 1 and 0.5, respectively. CS1 also includes a TSS controller in the last aerated tank with a setpoint of 4400 $gTSS \cdot m^{-3}$ (3400 $gTSS \cdot m^{-3}$ if T<15ºC) which manipulates Q_w (for further details of this controller see Vrecko *et al.*, 2006). This CS shows the effect of controlling the solids inventory in the AS system. The variability of Q_w is also reflected in the OLRvar value.

The second CS (CS2) involves the same DO controller plus an ideal proportional-integral OLR controller which manipulates Q_w with an OLR setpoint of 1.75 $kgVS \cdot m^{-3} \cdot d^{-1}$.

6.4.3.1 Dissolved oxygen and mixed liquor suspended solids

Figure 6.23 shows the simulated results for CS1. The OLR range is for almost the entire simulation time in the same range as in the open-loop case. During the winter

period the general FAD risk trend is similar to the open-loop case, although this time the manipulation of Q_w causes more peaks in OLRvar, which is also reflected in peaks appearing in the FAD risk profile. Likewise, noticeable changes in the OLR profile are reflected in FAD risk as well. For instance, during the summer period the same effect as was presented in **Figure 6.20** is present here (i.e. the decrease in FAD risk linked to the decrease in OLR and OLRvar). As a result, keeping the solids inventory constant in the biological reactors can causes more instability in the anaerobic digester in relation to FAD risk.

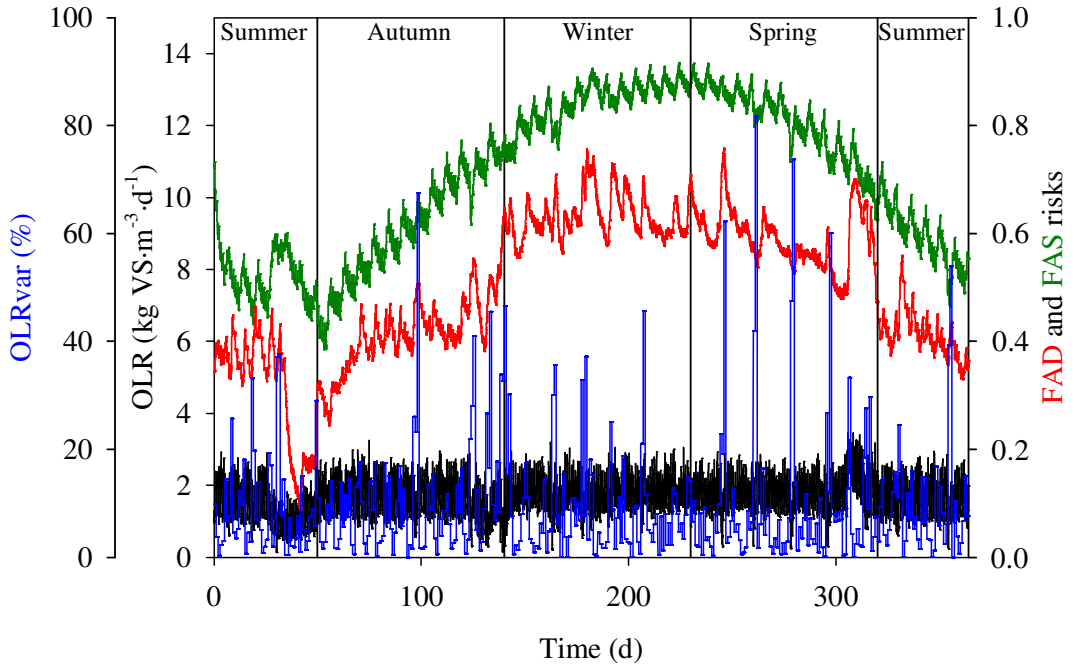

Figure 6.23. AD risk model CS1 results for one-year simulation (from July 1st). OLR (black line); OLRvar (blue line); FAS risk (green line); FAD risk (red line).

6.4.3.2 Dissolved oxygen and organic loading rate

Figure 6.24 shows the profile of the AD risk model input variables for CS2 together with the FAD risk. It can be clearly seen how the OLR controller drastically reduces OLRvar, the effect of which can also be appreciated in the OLR since oscillations have almost disappeared. This low OLRvar causes the FAD risk to stabilise around 0.45 even though FAS risk is high, especially during the winter and early spring periods. The only exception to this almost constant FAD risk is during the summer period, a result of the low solids concentration associated with this season, which is also the reason for low FAS risk.

Table 6.10 shows the benchmark evaluation criteria (EQI and OCI) together with %TIV of FAD and AV FAD risk for the three cases presented (open-loop, CS1 and CS2).

Table 6.10. AV FAD risk, %TIV at high FAD risk and benchmark evaluation criteria for open-loop, CS1 and CS2.

	Open-loop	CS1	CS2
AV FAD risk	0.57	0.54	0.45
TIV (%)	0.00	0.34	0.00
EQI (kg pollutant units·d^{-1})	5657	6499	6677
OCI	9208	6812	6735

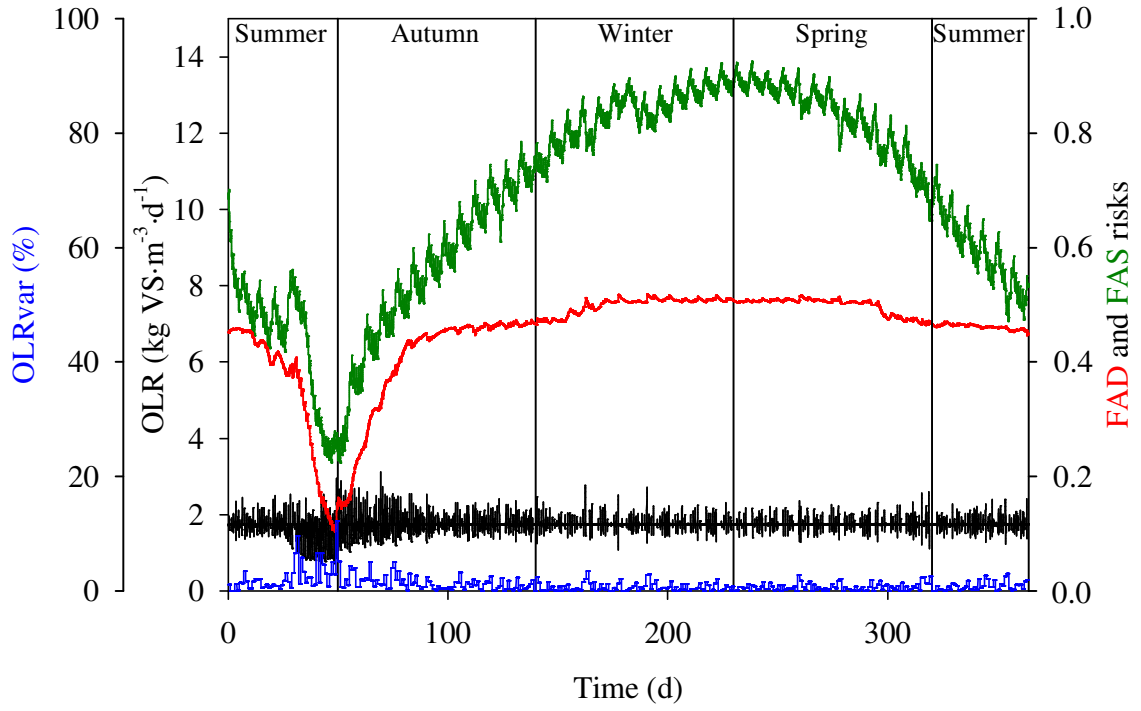

Figure 6.24. AD risk model CS2 results for one-year simulation (from July the 1st). OLR (black line); OLRvar (blue line); FAS risk (green line); FAD risk (red line).

The highest FAD risk corresponds to the open-loop case and the lowest FAD risk corresponds to the CS2 case, since the OLR controller regulates the OLR to a safe setpoint (1.75 kg $VS \cdot m^{-3} \cdot d^{-1}$). The %TIV of FAD is higher for CS1 due to the control of the TSS concentration in the AS. For example, whenever TSS is high the automatic controller increases the Q_w, which increases the OLR in the anaerobic digester. EQI is worse for CS2 than for open-loop and CS1, given the fact that the OLR control is performed regardless of the TSS in the AS. Thus TSS concentration in the AS biological reactors could be lower than the concentration required to achieve optimal removal efficiency. The operational cost is lower for CS2 due to the low OLRvar linked to low Q_w variations, as can be seen from the OLRvar profiles in **Figures 6.23 and 6.24**. Moreover, OLR is slightly higher in CS2 than CS1, leading to higher methane production (MP) and, therefore, a decrease in costs. As is evident, there is a trade-off between the optimal performance in the AS and the anaerobic digester regarding EQI and OCI. The results of the risk model emphasise the need for plant-wide supervisory CSs to minimise poor trade-off effects, while at the same time aiming for sustainable sludge and wastewater treatment.

6.4.4 Plant-wide application

In this part four CSs and the open-loop case are compared within the BSM2, using all the new evaluation criteria together with the standard ones. **Table 6.11** presents the control loops and indicates which is used in each CS simulated.

After simulation, the one-year simulation results were evaluated (**Table 6.12**) using standard evaluation criteria and the new criteria generated by the risk model. The highest values among CSs are in red and the lowest in green. Taking into account environmental criteria (EQI) the best CS is the No4, closely followed by CS2. The worst strategy in relation to EQI is CS1 due to its total N %TIV, given that nitrogen is

highly weighted in EQI calculation. Although CS4 would be the best option environmentally, it does not have the lowest values in effluent AV total N, COD, BOD or TSS but neither does it have the highest. On the other hand, CSs that have the lowest values in some of the effluent AVs (CS1, CS2 and CS3), they have the highest values in others.

Table 6.11. AS and AD CSs implemented.

FEATURES	3 DO	Q_{intr}	Q_{carb}	TSS	OLR
Measured variables	S_O in biological reactors 3, 4 and 5	S_{NO} in biological reactor 2	S_{NO} in biological reactor 2	TSS in biological reactor 5	TSS in AD inflow
Controlled variables	S_O in biological reactors 3, 4 and 5	S_{NO} in biological reactor 2	S_{NO} in biological reactor 2	TSS in biological reactor 5	OLR
Setpoint	2 mg $O_2 \cdot l^{-1}$ in biological reactors 3 and 4 and 1 mg O_2 in biological reactor 5.	1 g $N \cdot m^{-3}$	1 g $N \cdot m^{-3}$	4400 g $TSS \cdot m^{-3}$ (T<15ºC) 3400 g $TSS \cdot m^{-3}$ (T>15ºC)	1.75 kg $VS \cdot m^3 \cdot d^{-1}$
Manipulated variable	K_La	Q_{intr}	Q_{carb}	Q_w	Q_w
Control algorithm	PI	PI	PI	Cascaded PI	Cascaded PI
Applied to	CS1, CS2, CS3 and CS4	CS1	CS2, CS3 and CS4	CS3	CS4

In contrast to the situation with EQI, the best option regarding OCI would be CS1 given the absence of an external carbon source (EC=0). CS2, CS3 and CS4 have the highest OCI compared to CS1 and OL given that CS2, CS3 and CS4 have high SP for disposal caused by the EC addition. Despite this, the highest MP for CS3 compensates its higher PE and SP costs compared to CS2 and CS4. This shows that while strategies with an EC are generally the most expensive ones they are environmentally favourable.

With regard to AV AE is the highest for CS2 since the EC increases the TSS. Despite the DO control, O_2 requirements can sometimes be difficult to meet unless there is a TSS controller (CS3). OL has the lowest AV AE since the DO provided is constant, which is also the cause of the high AV Kjeldahl nitrogen concentration in its effluent. The digester's MP is the highest in CS3 since this strategy wastes more sludge than CS4 to maintain the TSS concentration in the biological reactors, a fact reflected in the PE and the higher SP for disposal for CS3. However, the higher MP compensated the higher SP and results in a lower OCI for CS3 than for CS4. The low total Kjeldahl nitrogen of CS1, together with the highest effluent total nitrogen AV concentration, indicate that, despite the internal recycle, there is not enough organic matter (no EC is added in this CS) to denitrify. This is the reason for the greatest %TIV of total N for CS1. %TIV of COD is very low for all the CSs as well as for TSS and BOD5.

With regard to the new criteria most of the highest risks are present in CS2 while CS3 has the lowest. The highest risk of bulking due to low DO is for OL in which the DO is not controlled. Since CS2 incorporates an EC, which has the effect of increasing MLVSS, the risks related to low F/M are high. The risk of rising sludge for CS2 is the highest given that the EC increases the MLSS, as commented. This increase means that more biomass is present in the system and the solids retention time in the secondary settler is probably higher.

Hence, uncontrolled denitrification is more likely to take place. In contrast, for CS3 the AV risk of rising sludge is lower thanks to the TSS controller. The risk of deflocculation is only relevant in the OL case. The uncontrolled TSS causes high SRTs, which are the main reason for the high risk. As a consequence, the integrated risks

reflect what is explained above with CS3 having low integrated risks and CS2 the highest. With regard to the anaerobic digester, the lowest risk is for CS4, which includes the OLR controller. However, the AV FAD risk is low for CS3 as well. The highest AV FAD risk is for CS2, which includes an EC that causes higher OLR. At the same time, CS2 has the highest risk of foaming due to low F/M, which also negatively influences the FAD risk in the anaerobic digester.

Table 6.12. Evaluation criteria for the open-loop and the four simulated CSs.

STANDARD CRITERIA	Units	OL	CS1	CS2	CS3	CS4
EQI	kg poll.units·d^{-1}	5657.5	6523.3	5184.3	5402.2	5147.5
OCI	-	9208.2	6927.7	12403	12377	12449
Effluent total Kjeldahl N AV conc.	g N·m^{-3}	3.7294	2.2419	2.5209	3.0576	2.5411
Effluent total N AV conc.	g N·m^{-3}	11.204	18.638	11.048	11.992	11.078
Effluent COD AV conc.	g COD·m^{-3}	50.056	49.193	51.000	47.189	49.994
Effluent BOD5 AV conc.	g BOD·m^{-3}	2.6742	2.4802	2.8407	2.8639	2.8652
Effluent TSS AV conc.	g·m^{-3}	15.897	15.365	16.663	13.733	15.895
SP AV	kg SS·d^{-1}	8940.9	8602.8	9270.6	9764.4	9392.7
AE AV	kWh·d^{-1}	4000.0	4478.9	4857.5	4420.6	4761.6
PE AV	kWh·d^{-1}	441.54	236.17	441.68	458.87	446.41
EC addition AV	kg COD·d^{-1}	2400.0	0.0000	4578.3	5013.3	4705.2
ME AV	kWh·d^{-1}	768.00	780.23	768.56	769.11	769.74
HE AV	kWh·d^{-1}	0.00000	0.00000	0.00000	0.00000	0.00000
MP AV	kg CH_4·d^{-1}	6357.0	6219.0	6480.1	7198.2	6641.4
Total N %TIV	%	0.10874	62.760	0.21463	3.3682	0.20318
COD %TIV	%	0.06010	0.06582	0.16312	0.05151	0.13450
Ammonia %TIV	%	8.2704	0.16598	0.22035	4.9823	0.31479
TSS %TIV	%	0.39492	0.27759	0.88713	0.25183	0.64675
BOD5 %TIV	%	0.12019	0.11447	0.23466	0.14309	0.21177
NEW CRITERIA						
Nutrient deficiency AV	-	0.0001178	0.0001176	0.0001521	0.0001773	0.0001936
Nutrient deficiency %TIV	%	0.00000	0.00000	0.00000	0.00000	0.00000
Bulking due to low DO AV	-	0.59284	0.34227	0.28257	0.44744	0.31948
Bulking due to low DO %TIV	%	0.00000	0.00000	0.00000	0.00000	0.00000
Bulking due to low F/M AV	-	0.73643	0.79179	0.77267	0.62252	0.74944
Bulking due to low F/M %TIV	%	42.462	51.874	46.162	16.638	43.129
Foaming due to low F/M AV	-	0.63752	0.63821	0.63903	0.47900	0.60925
Foaming due to low F/M %TIV	%	14.372	12.031	18.029	0.00000	13.047
HRBOM foaming AV	-	0.05011	0.03460	0.04067	0.13444	0.05970
HRBOM foaming %TIV	%	0.00000	0.00000	0.00000	0.00000	0.00000
Rising sludge AV	-	0.35977	0.26669	0.65952	0.15169	0.54887
Rising sludge %TIV	%	0.0000	9.4408	51.242	2.3781	36.372
Deflocculation AV	-	0.92690	0.53440	0.53390	0.27310	0.5196
Deflocculation %TIV	%	81.880	0.00000	0.00000	0.00000	0.00000
Integrated bulking AV	-	0.78160	0.79187	0.77274	0.68013	0.75754
Integrated bulking %TIV	%	42.462	51.874	46.162	16.638	43.129
Integrated foaming AV	-	0.63752	0.63821	0.63903	0.48015	0.60958
Integrated foaming %TIV	%	14.372	12.031	18.029	0.0000	13.047
Overall risk AV	-	0.78160	0.80822	0.86078	0.68745	0.81634
Overall risk %TIV	%	42.462	57.489	71.803	19.013	59.884
FAD AV	-	0.57132	0.59163	0.61364	0.51486	0.51142
FAD %TIV	%	0.00000	0.00000	0.00000	0.00000	0.00000

To sum up, **Table 6.12** shows that there is a trade-off between environmental and economic criteria. CSs that reach low EQI are more expensive and vice versa. Nevertheless, there are some CSs which do not have the lowest OCI and neither the lowest EQI that can also be considered as good control options.

6.5 Comparison of results for different platform implementations

A ring test to compare the results of the BSM implementations in different platforms has been performed by the *benchmarkers*. The simulation results have been put together (in Excel files) to compare the performance of each BSM platform with the others. At the benchmark website (IWA Task Group on Benchmarking of Control Strategies for WWTPs, 2009) the results of the ring test are available. Likewise, a ring test has been initiated in the final step in the risk model's implementation.

An example is given in this section of the table for the BSM1 ring test showing the standard evaluation criteria. The results presented here include dry weather influent open-loop with the specifications detailed in **Section 6.2.1 Open-loop**. Although, only one scenario is presented, the ring test includes many of these specifications (i.e. steady-state; open-loop dry, rain and storm weather, and two closed-loop scenarios with dry, rain and storm weather, with and without ideal sensors and actuators).

Table 6.13 presents the ring testing effluent AV results for the BSM1 related to all the evaluation criteria. These are the current results, up-to-date and despite the fact that in a few cases relative errors reach 1%, in absolute terms the differences are really small. For the AV loads **Table 6.13** shows the values for the same simulation platforms. A few differences can be found in the AV loads, but again, the variations are quite small. The quality indexes have higher differences in absolute terms but they are low in relative terms. The same is true for the energy related variables and OCIs, they have high values so the relative errors are low. With regard to the effluent violations, GPS-X still has a significant error related to the ammonia violation.

The results of the AS risk model implementation in FORTRAN are presented and compared with the MATLAB implementation in **Table 6.13.** As it can be seen from **Table 6.13**, results for the risks are very close. The highest difference (relative error: 3.8%) is for AV low F/M foaming risk, but the absolute error (0.02045) is quite low. This error is then spread to the integrated foaming risk, but nevertheless the absolute error is still low (0.02005).

Table 6.13. Ring testing of results for open-loop dry weather influent.

EFFLUENT AV	WEST	FORTRAN	MATLAB	SIMBA 5.0	GPS-X
Flow rate ($m^3 \cdot d^{-1}$)	18061.89318	18055.20000	18061.3325	18061.37998	18061.33185
S_I conc. (g COD·m^{-3})	30	30	30	30	30
S_S conc. (g COD·m^{-3})	0.972399074	0.97260	0.97352	0.971510068	0.967547301
X_I conc. (g COD·m^{-3})	4.581212966	4.58000	4.5794	4.579374757	4.583419008
X_S conc. (g COD·m^{-3})	0.221970527	0.22320	0.22285	0.222179916	0.223590033
X_{BH} conc. (g COD·m^{-3})	10.21139358	10.22000	10.2208	10.2196214	10.20701106
X_{BA} conc. (g COD·m^{-3})	0.542090406	0.54200	0.54217	0.543215499	0.540758698
X_P conc. (g COD·m^{-3})	1.7561667	1.75700	1.7572	1.758148745	1.757690504
S_O conc. (g -COD·m^{-3})	0.746397075	0.74530	0.74639	0.745912774	0.806677254
S_{NO} conc. (g N·m^{-3})	8.839813428	8.79700	8.8238	8.841852803	8.859889068
S_{NH} conc. (g N·m^{-3})	4.738039059	4.79800	4.7589	4.706617978	4.820471892
S_{ND} conc. (g N·m^{-3})	0.728480117	0.73090	0.72901	0.728040444	0.724824368
X_{ND} conc. (g N·m^{-3})	0.01563669	0.01571	0.015691	0.015649163	0.015741476

S_{ALK} conc. (mol HCO_3^-·m^{-3})	4.453274063	4.46100	4.4562	4.451157017	4.475732412
TSS conc. (g·m^{-3})	12.98462563	12.99000	12.9917	12.99190524	12.96854347
Kjeldahl N conc. (g N·m^{-3})	6.722677364	6.78600	6.7448	6.691585946	6.801325888
EFFLUENT AV	**WEST**	**FORTRAN**	**MATLAB**	**SIMBA 5.0**	**GPS-X**
Total N conc. (g N·m^{-3})	15.56249079	15.58000	15.5686	15.53343875	15.66121496
Total COD conc. (gCOD·m^{-3})	48.28523325	48.30000	48.2958	48.29405038	48.2800166
BOD_5 conc. (g·m^{-3})	2.771893717	2.77500	2.7746	2.773874982	2.769771378
EFFLUENT AV LOAD	**WEST**	**FORTRAN**	**MATLAB**	**SIMBA 5.0**	**GPS-X**
S_I (kg COD·d^{-1})	541.8567953	541.65600	541.84	541.8413993	541.8399554
S_S (kg COD·d^{-1})	17.5633682	17.56049	17.583	17.54681249	17.47519288
X_I (kg COD·d^{-1})	82.74537921	82.69282	82.7093	82.70982754	82.78265169
X_S (kg COD·d^{-1})	4.009207954	4.02992	4.025	4.012875894	4.03833379
X_{BH} (kg COD·d^{-1})	184.4371	184.52414	184.6007	184.5804653	184.3522139
X_{BA} (kg COD·d^{-1})	9.791179002	9.78592	9.7924	9.811221543	9.766822301
X_P (kg COD·d^{-1})	31.71969534	31.72299	31.7369	31.75459254	31.74623147
S_O (kg COD·d^{-1})	13.48134424	13.45654	13.4807	13.47221404	14.56966558
S_{NO} (kg N·d^{-1})	159.6637658	158.83159	159.3704	159.6960632	160.0213966
S_{NH} (kg N·d^{-1})	85.57795534	86.62885	85.9513	85.0080157	87.0641425
S_{ND} (kg N·d^{-1})	13.15773005	13.19655	13.1668	13.1494151	13.09129345
X_{ND} (kg N·d^{-1})	0.282428222	0.28365	0.28341	0.282645475	0.284312027
S_{ALK} (kmol HCO_3^-·d^{-1})	80.43456041	80.54425	80.4845	80.39403823	80.83768835
TSS (kg·d^{-1})	234.5269211	234.53705	234.6482	234.6517371	234.2291672
Kjeldahl N (kg N·d^{-1})	121.4242804	122.52259	121.8197	120.8592764	122.8410039
Total N (kg N·d^{-1})	281.0880462	281.30002	281.1902	280.5553396	282.8624004
Total COD (kg COD·d^{-1})	872.1227249	872.06616	872.2873	872.2571945	872.0014014
BOD_5 (kg·d^{-1})	50.0656482	50.10318	50.1124	50.10001006	50.02575999
QUALITY INDEXES	**WEST**	**FORTRAN**	**MATLAB**	**SIMBA 5.0**	**GPS-X**
IQI (kg poll.units·d^{-1})	52079.74047	52100	52100	52081.35708	52081.39492
EQI (kg poll.units·d^{-1})	6680.673934	6700	6690.1049	6664.499613	6725.955334
Daily AV SP (kg SS·d^{-1})	2675.297029	2669	2670.3382	2671.732382	2672.554704
ENERGY RELATED VARIABLES	**WEST**	**FORTRAN**	**MATLAB**	**SIMBA 5.0**	**GPS-X**
AV AE (kWh·d^{-1})	3341.386667	3341	3341.3867	3341.386667	3341.386667
AV PE (kWh·d^{-1})	388.17	388.2	388.17	388.17	388.17
AV carbon source dosage (kgCOD·d^{-1})	0	0	0	0	0
AV ME (kWh·d^{-1})	240	240	240	240	240
OPERATIONAL COST INDEXES	**WEST**	**FORTRAN**	**MATLAB**	**SIMBA 5.0**	**GPS-X**
SP cost	12203.85054	12180	12178.4499	12185.40322	12191.62768
AE cost	3341.386667	3341	3341.3867	3341.386667	3341.386667
PE cost	388.17	388.2	388.17	388.17	388.17
Carbon source dosage cost	0	0	0	0	0
ME cost	240	240	240	240	240
OCI	16173.40721	16150	16148.0067	16154.95989	16161.18435
EFFLUENT VIOLATIONS (TIV)	**WEST**	**FORTRAN**	**MATLAB**	**SIMBA 5.0**	**GPS-X**
Total N (%)	8.029365819	8.23	8.1845	7.589285714	0.892857143
Total COD (%)	0	0	0	0	0
Ammonia (%)	62.44441035	62.9	62.5	62.05357143	57.58928571
TSS (%)	0	0	0	0	0
BOD5 (%)	0	0	0	0	0
INDIVIDUAL AS RISKS	**WEST**	**FORTRAN**	**MATLAB**	**SIMBA 5.0**	**GPS-X**
Nutrient deficiency bulking (AV)	-	0	0.00011765	-	-
Nutrient deficiency bulking (TIV - % -)	-	0	0	-	-
Low DO bulking (AV)	-	0.324	0.32341	-	-
Low DO bulking (TIV - % -)	-	8.06	8.1845	-	-
Low F/M bulking (AV)	-	0.728	0.74557	-	-
Low F/M bulking (TIV - % -)	-	42.5	42.4107	-	-
Low F/M foaming (AV)	-	0.559	0.53855	-	-
Low F/M foaming (TIV - % -)	-	0	0	-	-
HRBOM foaming (AV)	-	0.026	0.025602	-	-
HRBOM foaming (TIV - % -)	-	0	0	-	-
Rising sludge (AV)	-	0.682	0.68191	-	-
Rising sludge (TIV - % -)	-	33.9	34.0774	-	-
INTEGRATED RISKS	-			-	-
Bulking (AV)	-	0.803	0.81015	-	-
Bulking (TIV - % -)	-	50.6	50.5952	-	-
Foaming (AV)	-	0.567	0.54695	-	-
Foaming (TIV - % -)	-	0	0	-	-
Rising (average)	-	0.682	0.68191	-	-
Rising (TIV - % -)	-	33.9	34.0774	-	-

6.6 Concluding remarks

In this chapter the detailed implementation of the risk model in BSMs has been presented showing how the inputs for the risk model are calculated from the simulation results. This is relevant for the implementation of the risk model in BSM regardless the simulation platform used (i.e. MATLAB™ & SIMULINK™, WEST®, GPS-X™, etc.).

BSM1 has provided an example of how the AS risk model responds to changes in operational parameters and a first example of control strategies comparison in different weather influent scenarios. In terms of BSM1_LT the AS risk model filter and temperature effect have been evaluated. The analysis of four different time constants has shown that the 3-day provided a more feasible interpretation of the risk model results. The profiles of the risks show that the filter is valuable when taking into account the slow dynamics related to some of the operational problems of microbiological origin. The inclusion of temperature to represent the seasonal dynamics in BSM1_LT has allowed to test the extension of the AS risk model with temperature applied to *Microthrix parvicella* related risks. The results have shown that the AS risks related to *Microthrix parvicella* were increased during winter periods and decreased during summer showing a behaviour according to what is stated in the literature. BSM2 has allowed to test the whole risk model focusing in the AD part. Firstly, general results have been presented in an open-loop case study showing the profile for the risk of foaming in AD. Secondly, variation of the main operational parameters has shown the influence of both external recycle and waste sludge flow rates in the FAD risk. Next, two control strategies affecting the AD organic loading rates have been tested. The results have shown that a control strategy with a control of the TSS in the biological reactors causes a higher variation in the AD loading rates increasing the risk of foaming in the AD. Following, the results in a plant-wide basis have been presented comparing the open-loop case with four different control strategies showing the influence of the external carbon sources on the risk of foaming in the AD.

It is also important to highlight that BSM in its different layouts have shown to be a really useful and versatile tool in which to implement to test and evaluate each part and the whole risk model.

CHAPTER 7

GENERAL DISCUSSION AND FUTURE WORK

Part of the work shown here has been presented in:

Dalmau J., Comas J., Rodriguez-Roda I., Latrille E. and Steyer J.P. (2009d). Validation of a knowledge-based risk model for biological foaming in anaerobic digestion simulation. Environmental Engineering and Management Journal, ***9****(2), 223-229.*

7. General discussion and future work

The intention of this chapter is to point out some aspects on the general results (not the specific results of each simulation which have already been discussed previously), validation, adaptation and possibilities related to the risk model as well as the current and future work.

7.1 Mechanistic approaches

The main factor that limits the development of general mechanistic models of filamentous bacteria is that they require detailed information on kinetics, morphology, specific substrates or processes related to some of the populations causing operational problems of microbiological origin. There are still species to identify or others the role of which it is not clear and is to be determined. There is also a lack of information on certain influent and process characteristics that can affect the populations balance. Current mechanistic models can represent specific species or they can consider only certain substrates or characteristics, but they fail when applied to other conditions or plants since model parameters cannot be determined or validated. In fact, mechanistically modelling provides indeed valuable knowledge for future development of a general deterministic model of the filamentous bacteria related to operational problems of microbiological origin. Hence, a mechanistic model of the filamentous bacteria would really valuable from the perspective of understanding the complex mechanisms of filamentous bacteria development. However, a general or validated model is not yet available. Within this framework, the risk model presented in this thesis represents a general approach to estimate the risk of operational problems of microbiological origin, which do not have a mechanistic model yet.

7.2 Validation

One of the limitations of the mechanistic models for operational problems of microbiological origin is the lack of a validated model. This is still an open question since validation is still difficult even in the case of the risk model. A validation of the risk model based on real data from a pilot plant or a full-scale WWTP is very difficult due to the fact that the risk model is giving the risk of a particular operational problem of microbiological origin but this risk is often not registered in real plants. Most of times episodes of operational problems of microbiological origin are not registered or microbiological observations are not performed when the problem appears. It is also important to highlight that the aim of the risk model is not to diagnose operational problems of microbiological origin with absolute certainty but to quantify whether the simulated conditions bring about a severe risk for leading the system towards a favourable situation with operational problem of microbiological origin. Moreover, the risk model was not developed to be applied in full-scale facilities but to complement dynamic simulations when comparing operational procedures and CSs (and thus, for example, the model uses variables not available in typical full-scale databases, such as S_S and X_S). The availability and reliability of data sets is the limiting factor. Even in the case of available real data to validate the risk model, it will only be validated on its boundaries (0 and 1 risks). Validating the intermediate values of the risk model is almost impossible, since they indicate that favourable conditions to develop operational problems of microbiological origin are met.

The knowledge embodied in the AS risk model is obtained from an extensive bibliography research and heuristic knowledge. The experiences of operational problems of microbiological origin are very well documented and discussed. This is the reason of the wide agreement and consensus on causes related to AS operational problems of microbiological origin present in the bibliography and in the day-to-day WWTP operation. From my point of view AS risk model provides a reliable tool for risk assessment during the evaluation of simulation results. In terms of the risk of foaming in AD still lacks of a consensus on the key factors that favour its development. Many publications point to different causes ending up in a more diffuse knowledge difficult to gather, causing the selection of the key variables more difficult.

Preliminary AD risk model validation

A preliminary validation of the AD risk model is presented here. It is difficult to adapt the real data to the data used by the model. Also several approximations and assumptions had to be made to calculate AD risk model input variables from real data. Below the approximations made to adapt the data are shown. Firstly, OLR for the AD risk model is calculated as shown in **Equation 6.19** and taking HRT from **Equation 6.20**.

Since AD risk model OLR calculation is based on VS but calculated as TSS from simulation results, it was necessary to transform the measured TOC (tocsDig) into VS (TSS in fact). According to Metcalf and Eddy (2003), for untreated wastewater, the BOD to TOC ratio (BOD/TOC) is between 1.2 and 2.0 (1.6 was taken as the average). There is also a relation between BOD and COD ranging from 0.3 to 0.8 (0.55 was taken as the average). Therefore, putting together both ratios, COD can be expressed as a function of TOC (**Equation 7.2**).

$$COD = 2.9 * tocsDig \quad (\textbf{Eq. 7.2})$$

where,

tocsDig: TOC in the digester ($mg \cdot L^{-1}$)

COD in mg COD $\cdot$ L^{-1}.

In Copp (2002) it is pointed out that there is a relation between TSS and particulate compounds (**Equation 7.3**).

$$TSS = 0.75 \cdot COD_p \quad (\textbf{Eq. 7.3})$$

where,

COD_p in mg COD $\cdot$ L^{-1}.

Since the pilot plant had influent wastewater from a winery and not from an AS system the FAS risk was set to 0 to represent the absence of *Microthrix parvicella* in the influent.

A last assumption is made in order to simplify the conversion supposing that all the TSS can be accounted as VS. This way, we consider that all the COD measured in the pilot

plant can be degraded as it was VS. Thus, from **Equations 7.2** and **7.3** we get **Equation 7.4**.

$$VS = \frac{2.175 \cdot tocsDig}{1000} \quad \textbf{(Eq. 7.4)}$$

where

VS in $kg \cdot L^{-1}$.

To obtain the real risk of biological foaming in the AD, the same approach as used in **Section 5.2.1.1 Black box approach (within *foaming* part)** was used here.

Data gathered during approximately three months was used to validate the AD risk model. **Figure 7.1** shows the profiles for the simulated biological foaming risk (SFR) from the AD risk model and the foaming index estimated from real data (FR).

From **Figure 7.1** some aspects can be pointed out. First of all, reasonable good fitting is achieved (RMSE=0.06). Secondly, it becomes clear that there are two differentiated periods, approximately the first month and the last two months. The first period is characterized by the stability of the system with a good coincidence between SFR and FR (both showing low foaming risk), whereas the second shows much more oscillations and peaks revealing a probably more unstable period. In this last period, at some specific points (i.e. around days 33, 43 and 58) there are some divergences where the model shows a relatively high foaming risk when the real data show high risk of foaming. It is important to note that the inherent uncertainty of the mechanisms of foaming, that hinders the development of mechanistic models, cannot be included in the AD risk model. This can be the main reason behind the main differences in the validation results. Although the results can be evaluated in absolute terms, the general trends of the instability are indeed detected by the AD risk model allowing it to assess operational conditions of the anaerobic digester that can favour biological foaming.

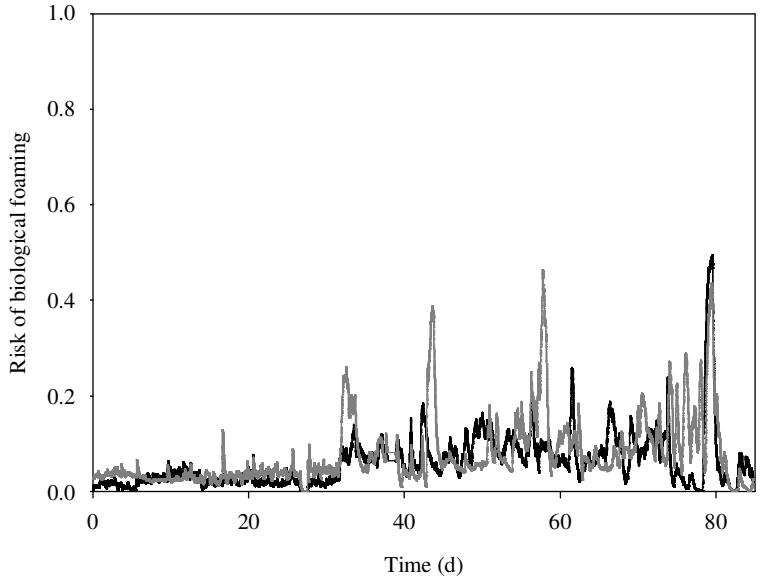

Figure 7.1. Evaluation of the validation.
Simulated FAD risk in black. Real FAD risk in grey.

As commented above, the most important limitation to be able to validate the risk model is to measure or to estimate the key variables when the foaming episodes are not registered. Hence, the approximations made to calculate the AD risk model inputs are indeed another cause of the divergences in the validation process. Even though it is difficult to take into account the effect of filamentous bacteria in the AD influent, further validation with real data from an anaerobic digester treating sludge from an AS system would be of interest. Another reason for the deviations in the validation can be the fact that we are comparing here the potential FAD risk (from the AD risk model) with the estimation of a real risk. In other words, foaming might be present in a real plant, however, when evaluating the operational conditions with the AD risk model its results could indicate that there is a low risk and vice versa.

7.3 Adaptation

By adaptation we mean the implementation of mainly the AS risk model to other configurations (SBR, oxidation ditch, etc.). Changes are certainly required, e.g. the calculation of SRT and F/M ratio must be adequately re-defined and the sampling point for estimating the readily biodegradable substrate or DO level properly located, although the underlying mechanisms for evaluating the risk of occurrence of operational problems of microbiological origin are the same. In the case of the AD risk model its application to other configurations (UASB, EGSB, etc.) is more straightforward and the modifications are more linked to changes of the ranges of the OLR and HRT rather than the sampling point. It is worth to highlight that each risk model can be used independently. In the case of the AD risk model, if it is applied to an anaerobic digester which is not treating secondary sludge, the FAS risk used as input should be set to 0.

Finally, a comment related to the customization of the risk model. As a compromise, the limits of the fuzzy MFs of the AD risk model were initially chosen from among the normal values, as described in **Sections 5.1.2** and **5.2.2 Knowledge formalisation**. However, it is worth remembering that the user can change these limits according to their own configuration. Likewise, the customization can include changes in the threshold to determine the severe risk index.

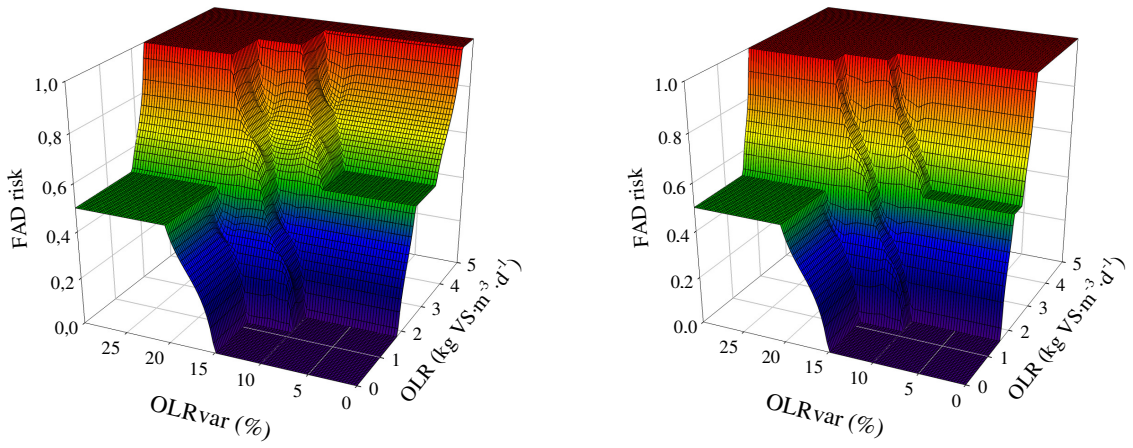

Figure 7.2. (a)Response surface for FAD risk for low FAS risk MF. (b) Adapted surface

Figure 7.2 illustrates an example showing how the response surface for low FAS risk would change, according to Massart *et al.* (2006), using the OLR normal values (between 1.6 and 2.4 kg $VS \cdot m^{-3} \cdot d^{-1}$). It becomes clear that the narrower range of the OLR causes an increase in the red zone of high FAD risk for values of OLR at 2.5 kg $VS \cdot m^{-3} \cdot d^{-1}$ or higher.

7.4 Further possibilities and future work

The usefulness of the approach has been demonstrated for objective comparison of CSs. However, this risk model can also be helpful when using WWTP modelling and simulation for other purposes, such as design optimisation, scenario testing, trouble shooting, learning tool or operational improvement.

For example, the risk model offers the possibility to improve models of the sludge settling characteristics by using the risk index to change the settleability parameters, as presented in the work of Flores-Alsina *et al.* (2009b). In this work, in order to simulate the effects of filamentous bulking sludge, the settling parameters of the Takács secondary clarifier model (Takács *et al.*, 1991) are changed during the simulation. The effects of bulking are reflected on the performance causing poor sludge compaction and consequently low RAS and WAS concentrations. It is shown that including the effects of bulking sludge leads to a more realistic process performance prediction. This approach allowed the authors study the effects of filamentous bulking sludge for different CSs in the work by Flores-Alsina *et al.* (2009c). Some strategies that showed good performance would be dismissed when the effects of filamentous bulking are represented in the secondary settler. This will also allow investigating the use of a high and sustained risk signal in a feedback loop to adapt the set points of simulated CSs. By including the risk assessment in the control loop, the identification of unsafe operational conditions would allow avoiding the system being led towards a serious destabilization and restoring it back to normal operation.

Another example of the application of the risk model is the case presented by Sin *et al.* (2006). In their work a model-assisted optimization of the operation of an SBR is performed. The best strategy found when confronted with reality became unstable and bulking appeared. They probably would not have chosen the strategy if they could have applied the risk model which would have shown at least higher risks for that strategy.

Another possibility of the risk model could be its further expansion to other WWTP processes (SHARON, anammox, microbial fuel cells, biofouling of membrane bio-reactors, etc.), to viscous bulking or modifications to consider non-microbiological problems such as surfactants in the feed (either wastewater or sludge), surface active polymers added during thickening, physicochemical conditions in the digesters leading to surface active conditions, etc.

A sensitivity analysis of the risk assessment model will be of high interest as future work not only to understand and analyse the knowledge embodied in the decision trees, but also to highlight the relevance and linearity of the variables (both for operation – e.g. SRT – and design – e.g. volume) and the accuracy of the measurements. Also, parameters related to the fuzzy approach (number/shape of the MFs, overlapping, etc.) should be analysed. The sensitivity analysis can also enhance the customization of the risk model offering the possibility to identify the most sensible variables. Afterwards, a

calibration process based on those variables could provide a more reliable risk model for adaptation to a specific model.

In spite of the difficulties to validate the risk model, the risk model will be confronted with full-scale reliable data. Although the risk of a problem is not registered in full scale plants, we will look for possible correlations between the simulated risk and some operational parameters related to bulking or foaming such as e.g. SVI.

CHAPTER 8

CONCLUSIONS

8. Conclusions

The conclusions of this thesis have been divided into two parts. The first one is devoted to the risk model and the second one to its implementation and application to the BSM.

8.1 Risk model

This thesis explains the development a knowledge-based risk model that integrates numerical modelling and qualitative aspects to simulate plant-wide operational problems of microbiological origin. The risk model includes the most common operational problems of microbiological origin in the WWTPs: Filamentous bulking, activated sludge biological foaming, rising sludge, deflocculation and anaerobic digestion biological foaming. The development of the activated sludge risk model and the anaerobic digestion risk model has been linked to the availability of real data.

- The activated sludge risk model has been developed from heuristic knowledge from experts and literature, identifying the key knowledge related to each operational problem of microbiological origin. This knowledge has been formalized in several decision matrices and implemented in fuzzy logic, defining the membership functions and rules for all the decision matrices.

- The anaerobic digestion risk model has been developed using available real data from a pilot plant. A wrapper approach with a hill-climbing elimination strategy implemented in artificial neural networks as induction algorithm has been used to select the most relevant variables related to anaerobic digestion biological foaming and later integrated with knowledge from literature.

Both risk models have been finally implemented using fuzzy logic by defining each of the membership functions for all the inputs and outputs as well as the rules for the decision matrices.

Regarding the outcomes of the risk model, two risk indices (percentage of time in violation and average) have been defined to allow their use as evaluation criteria for simulation results. As a result, plant performance evaluation criteria based on plant operational cost and effluent quality indexes, typically calculated when comparing control strategies by simulation, can now be complemented with a risk assessment for the occurrence of operational problems of microbiological origin. Hence the risk model provides an overall approach for plant-wide evaluation of operational problems of microbiological origin, allowing model users to have a complete set of criteria and thereby avoid biased evaluations of the simulation results. Adding an additional criterion to classical evaluation criteria is important when benchmarking control strategies and can lead to different conclusions with respect to a specific control scheme. Thus control approaches with an increased risk for suffering from endemic operational problems of microbiological origin can be avoided. This way, some simulated control strategies which can have a positive impact in terms of environmental and/or economical criteria may prove to be not suitable when anaerobic digester performance is evaluated, meaning that new conclusions can be drawn from the simulation evaluation process when risk of microbiology-related problems are considered.

8.2 Benchmark Simulation Model implementation and application

The risk model has been implemented and applied to the BSM by adapting it to the BSM1, BSM1_LT and BSM2. In each BSM configuration the risk model has been adapted bearing in mind the characteristics of each specific configuration.

- For the BSM1 only the activated sludge risk model has been applied, that is to say, the filamentous bulking, biological foaming, rising sludge and deflocculation.
- For the BSM1_LT the temperature effect has been added to the operational problems of microbiological origin related to *M. parvicella* (i.e. Bulking due to low F/M and foaming due to low F/M).
- For the BSM2 apart from the temperature effect, the anaerobic digestion risk model for biological foaming has been applied.

Simulations with all the BSMs have been performed to evaluate the results of the activated sludge and anaerobic digestion risk models. In each BSM configuration at least the open-loop and a closed-loop case have been simulated to study the effects of the variation of different parameters on the risk model performance.

- BSM1 open-loop results in general revealed a daily behaviour related to the incoming loadings. The operational parameters variation have shown that low values of WAS and extreme values of DO cause a major effect on the activated sludge risk model results.
- In the BSM1_LT the temperature effect has been evaluated. It has been shown how the risks of bulking and foaming due to *M. parvicella* have decreased during summer and increased during winter. Besides, the effect of the exponential filter has been evaluated using a time constant between 1 and 7 days. A large decrease of the noise was achieved and it facilitates taking into account the slow dynamics of the development of operational problems of microbiological origin. Finally, a control strategy based on the DO in the three aerated biological reactors has decreased drastically the risk of filamentous bulking.
- The anaerobic digestion risk model for biological foaming has been incorporated in the BSM2. The performance of the anaerobic digestion risk model has been evaluated based on an open-loop scenario to show the influence of the input variables on the risk of biological foaming. There exists a relevant influence of the foaming in activated sludge risk although this effect is diminished by changes in the organic loading rate and its daily variation. The effect of the operational parameters related to the foaming in anaerobic digestion risk has been studied. Results have shown that increments of the values of return activated sludge and waste activated sludge flow rates have a higher effect on the results of the anaerobic digestion risk model than lower values. Finally, two control strategies have been used to evaluate the anaerobic digestion risk model. They have shown how a control strategy based on the organic loading rate is able to maintain relatively low levels of foaming in anaerobic digestion risk whereas a control strategy based on total suspended solids control can destabilize the anaerobic digester by increasing the organic loading rate variation.

- BSMs apart from being a suitable tool to test and compare control strategies have proved to be really useful tools to test the risk model enhancing the evaluation of the results and allowing to show them in a understandable way.

Regarding the plant-wide comparison of control strategies, the results have shown that there is a trade-off between economically and environmentally save options. However, some intermediate control strategies can also be good control options. The risk model has shown that some of the intermediate options can become interesting when the risk of operational problems of microbiological origin is considered. Otherwise, without the risk model's third dimension these options would have been discarded.

CHAPTER 9

REFERENCES

9. References

Andreasen K. and Nielsen P.H. (2000). Growth of *Microthrix parvicella* in nutrient removal activated sludge plants: Studies of *in situ* physiology. *Water Research,* **34**(5), 1559-1569.

Barber W.P. (2005). Anaerobic digester foaming: causes and solutions. *Water 21,* February, 45-49.

Barbusiński K. and Kościelniak H. (1995). Influence of substrate leading intensity on floc size in activated sludge process. *Water Research*, **29**(7), 1703-1710.

Barjenbruch M. and Kopplow O. (2003). Enzymatic, mechanical and thermal pre-treatment of surplus sludge. *Advances in Environmental Research,* **7**, 715-720.

Batstone D.J., Keller J. and Steyer J.P. (2005). A review of ADM1 extensions, applications and analysis 2002-2005. *Proceedings of the First International Workshop on the IWA anaerobic digestion model No. 1 (ADM1)*. Lyngby, Denmark, 2-4 Sept , 1-9.

Batstone, D.J., Keller, J., Angelidaki, I., Kalyuzhnyi, S., Pavlostathis, S., Rozzi, A., Sanders, W., Siegrist, H. and Vavilin, V. (2002) The IWA Anaerobic Digestion Model No1. *Water Science and Technology*, **45**(10), 63-73.

Belanche L., Valdés J.J., Comas J., Rodríguez-Roda I. and Poch M. (2000). Prediction of the bulking phenomenon in wastewater treatment plants. *Artificial Intelligence in Engineering,* **14**(4), 307-317.

Bellman R. and Zadeh L.A. (1970). Decision-making in a fuzzy environment. *Management Science,* **17**, 141-164.

Bernard O., Hadj-Sadok Z., Dochain D., Genovesi A. and Steyer J.P. (2001). Dynamical model development and parameter identification for an anaerobic wastewater treatment process. *Biotechnology and Bioengineering,* **74**(4), 424-438.

Bishop C.M. (1994). Neural Networks and their applications. *Review of Scientific Instruments,* **65**(6), 1803-1832.

Blackall L.L., Harbers A.E., Greenfield P.F. and Hayward A.C. (1991) Activated sludge foams: effects of environmental variables on organisms growth and foam formation. *Environmental Technology,* **12**, 241-248.

Blumensaat F. and Keller J. (2005). Modelling of two-stage anaerobic digestion using the IWA Anaerobic Digestion Model No.1 (ADM1). *Water Research,* **39**(1), 171-183.

Brdjanovic D., Van Loosdrecht M.C.M., Hooijmans C.M., Alaerts G.J. and Heijnen J.J. (2000). Modeling COD, N and P removal in a full-scale WWTP Haarlem Waarderpolder. *Water Research,* **34**(3), 846-858.

Carrasco E.F., Rodríguez J., Puñal A., Roca E. and Lema J.M. (2004). Diagnosis of acidification states in an anaerobic wastewater treatment plant using a fuzzy-based expert system. *Control Engineering Practice,* **12**(1), 59-64.

Casey T.G., Ekama, G.A., Wentzel, M.C. and Marais, Gv.R. (1995). Filamentous organisms bulking in nutrient removal activated sludge systems. Paper 1: a historical overview of causes and control. *Water SA,* **21**(3), 231-238.

Cenens C., Smets I.Y., Ryckaert V.G. and van Impe J.F. (2000a). Modelling the competition between floc-forming and filamentous bacteria in activated sludge waste water treatment systems – I. Evaluation of mathematical models based on kinetic selection theory. *Water Research,* **34**(9), 2525-2534.

Cenens C., Smets I.Y. and van Impe J.F. (2000b). Modelling the competition between floc-forming and filamentous bacteria in activated sludge waste water treatment systems – II. A prototype mathematical model based on kinetic selection and filamentous backbone theory. *Water Research,* **34**(9), 2535-2541.

Cirne D.G., Paloumet X., Björnsson L., Alves M. M. and Mattiasson B. (2007). Anaerobic digestion of lipid-rich waste – Effects of lipid concentration. *Renewable Energy,* **32**(6), 965-975.

Comas J., Rodríguez-Roda I., Gernaey K.V., Rosen C., Jeppsson U. and Poch M. (2008). Risk assessment modelling of microbiology-related solids separation problems in activated sludge systems. *Environmental Modelling and Software,* **23**(10-11), 1250-1261.

Comas J., Rodríguez-Roda I., Poch M., Gernaey K.V., Rosen C. and Jeppsson U. (2006). Extension of the IWA/COST simulation benchmark to include expert reasoning for system performance evaluation. *Water Science and Technology*, **53**(4-5), 331-339.

Comas J., Rodríguez-Roda I., Sánchez-Marrè M., Cortés U., Freixó A., Arráez J. and Poch M. (2003). A knowledge-based approach to the deflocculation problem: integrating on-line, off-line, and heuristic information. *Water Research*, **37**, 2377-2387.

Copp, J., Jeppsson, U. and Rosen, C. (2003). Towards an ASM1-ADM1 state variable interface for plant-wide wastewater treatment modelling. *Proceedings of the 76th Annual WEF Conference and Exposition*. Los Angeles, USA, 11–15 Oct.

Copp J.B. (2002). The COST Simulation Benchmark – Description and Simulator Manual. *Office for Official Publications of the European Communities*, Luxembourg, ISBN 92-894-1658-0.

Copp J.B. (1999). Development of standardised influent files for the evaluation of activated sludge control strategies. *IAWQ Scientific and Technical Report Task Group: Respirometry in control of the Activated Sludge Process – internal report.*

Dalmau J., Comas J., Rodríguez-Roda I., Latrille E. and Steyer J.P. (2009a). Selecting the most relevant variables for anaerobic digestion imbalances: two case studies. *Water Environment Research* (accepted).

Dalmau J., Comas J., Rodríguez-Roda I., Pagilla K. and Steyer J.P. (2009b). Risk model development and simulation for foaming in anaerobic digestion. *Bioresource Technology,* **101**(12), 4306-4314.

Dalmau J., Comas J. and Rodríguez-Roda I. (2009c). Extension of a risk model to include deflocculation and temperature. *Water Science and Technology* (submitted).

Dalmau J., Comas J., Rodriguez-Roda I., Latrille E. and Steyer J.P. (2009d). Validation of a knowledge-based risk model for biological foaming in anaerobic digestion simulation. *Environmental Engineering and Management Journal,* **9**(2), 223-229.

Dalmau J., Comas J., Rodriguez-Roda I., Latrille E. and Steyer J.P. (2008). A neural network approach for selecting the most relevant variables for foaming in anaerobic digestion. *Proceedings of the International Congress on Environmental Modelling and Software. 4th Biennial Meeting (iEMSs 2008)*, Barcelona, Spain, 7-10 March.

Dalmau J., Comas J., Rodríguez-Roda I., Latrille E. and Steyer J.P. (2007). Using artificial neural networks for selecting relevant information in anaerobic digestion. *Proceedings of the 11th IWA Specialist Conference on Anaerobic Digestion.* Brisbane, Australia, 23-27 September.

De La Rubia M.A., Perez M., Romero L.I. and Sales D. (2006). Effect of solids retention time (SRT) on pilot scale anaerobic thermophilic sludge digestion. *Process Biochemistry*, **41**, 79-86.

Dupla M., Conte T., Bouvier J.C., Bernet N. and Steyer J.P. (2004). Dynamic evaluation of a fixed bed anaerobic digestion process in response to toxic shocks, *Water Science and Technology*, **49**(1), 61–68.

Eikelboom D.H., Andreadakis A. and Andreasen K. (1998). Survey of filamentous populations in nutrient removal plants in four European countries. *Water Science and Technology,* **37**(4-5), 281-289.

Eikelboom D.H. (1994). The *Microthrix parvicella* puzzle. *Water Science and Technology,* **29**(7), 271-279.

Eikelboom D.H. and van Buijsen H.J.J. (1983). Microscopic sludge investigation manual, 2nd ed, TNO Research Institute for Environmental Hygiene, Delft, The Netherlands.

Ersahin M.E., Insel G., Dereli R.K., Ozturk I. and Kinaci C. (2007). Model based evaluation for the anaerobic treatment of corn processing wastewaters. *Clean – Soil, Air, Water,* **35**(6), 576-581.

Fiter M., Güell D., Comas J., Colprim J., Poch M. and Rodríguez-Roda I. (2005). Energy saving in a wastewater treatment process: an application of fuzzy logic control. *Environmental Technology,* **26**(11), 1263–1270.

Flores-Alsina X., Rodríguez-Roda I., Sin G. and Gernaey K.V. (2009a). Uncertainty and sensitivity analysis of control strategies using the benchmark simulation model No1 (BSM1). *Water Science and Technology,* **59**(3), 491-499.

Flores-Alsina X., Comas J., Rodríguez-Roda I., Gernaey K.V. and Rosen C. (2009b). Including the effects of filamentous bulking sludge during the simulation of wastewater treatment plants using a risk assessment model. *Water Research* (accepted).

Flores-Alsina X., Comas J., Rodríguez-Roda I., Poch M., Gernaey K.V. and Jeppsson U. (2009c). Evaluation of plant-wide WWTP control strategies including the effects of filamentous bulking sludge. *Proceeding of the 10th IWA Conference on Instrumentation Control and Automation.* Cairns, Australia, 14-17 June.

Gerardi M.H. (2002). Settleability problems and loss of solids in the activated sludge process. *John Wiley & Sons,* Hoboken, New Jersey, USA.

Gernaey K.V., Rosen C. and Jeppsson U. (2006). WWTP dynamic disturbance modelling – an essential module for long-term benchmarking development. *Water Science and Technology,* **53**(4-5), 225-234.

Gernaey K.V., van Loosdrecht M.C.M., Henze M., Lind M. and Jorgensen S.B. (2004). Activated sludge wastewater treatment plant modelling and simulation: state of the art. *Environmental Modelling and Software,* **19**, 763-783.

Grady C.P.L., Daigger G.T. and Lim H.C. (1999). Biological wastewater treatment. *Marcel Dekker*, 2nd ed., New York, USA.

Grau P., Copp J., Vanrolleghem P.A., Takács I. and Ayesa E. (2009). A comparative analysis of different approaches for integrated WWTP modelling. *Water Science and Technology,* **59**(1), 141-147.

Grau P. (2007). Nueva metodologia de modelado matemático integral de las EDAR. PhD Thesis. Escuela Superior de Ingenieros, University of Navarra, Spain.

Grau P. (1991). Criteria for nutrient-balanced operation of activated sludge process. *Water Science and Technology,* **24**(3-4), 251-258.

Guiot S.R. (1991). Modeling of the upflow anaerobic sludge bed-filter system: A case with hysteresis. *Water Research*, **25**(3), 251-262.

Hansen K.H., Angelidaki I. and Ahring B.K. (1998). Anaerobic digestion of swine manure: Inhibition by ammonia. *Water Research*, **32**(1), 5-12.

Henze M., Gujer W., Mino T. and van Loosdrecht M.C.M. (2000). Activated Sludge Models ASM1, ASM2, ASM2d and ASM3. *IWA STR No 9*. IWA Publishing, London, UK.

Henze M., Dupont R., Grau P. and De la Sota A. (1993). Rising sludge in secondary settlers due to denitrification. *Water Research,* **27**(2), 231–236.

Henze M., Grady C.P.L. Jr, Gujer W., Marais G.v.R. and Matsuo T. (1987). Activated sludge model no. 1. *IWA STR No 1,* IWA Publishing, London, UK.

Hickey R.F., Vanderwielen J. and Switzenbaum M.S. (1987). The effects of organic toxicants on methane production and hydrogen gas levels during the anaerobic digestion of waste activated sludge. *Water Research,* **21**(11), 1417-1427.

Hug T., Gujer W. and Siegrist H. (2006). Modelling seasonal dynamics of "*Microthrix parvicella*". *Water Science and Technology*, **54**(1), 189-198.

IWA Task Group on Benchmarking of Control Strategies for WWTPs. (Last checked: 06/08/2009). www.benchmarkwwtp.com

Jenkins D., Richard M. G. and Daigger G.T. (2003). Manual on the Causes and Control of Activated Sludge Bulking, Foaming and other Solids Separation Problems. 3rd ed. *IWA Publishing,* London, UK, ISBN 1-56670-647-5.

Jeppsson U., Pons M.N., Nopens I., Alex J., Copp J.B., Gernaey K.V., Rosen C., Steyer J.P. and Vanrolleghem P.A. (2007). Benchmark simulation protocol no 2: general protocol and exploratory case studies. *Water Science and Technology,* **56**(8), 67-78.

Jeppsson U., Rosen C., Alex J., Copp J., Gernaey K.V., Pons M.N. and Vanrolleghem P.A. (2006). Towards a benchmark simulation model for plant-wide control strategy performance evaluation of WWTPs. *Water Science and Technology,* **53**(1), 287-295.

Kappeler J. and Gujer W. (1994a). Development of a mathematical model for "aerobic bulking". *Water Research,* **28**(2), 303-310.

Kappeler J. and Gujer W. (1994b). Verification and applications of a mathematical model for "aerobic bulking". *Water Research,* **28**(2), 311-322.

Knobel A.N. and Lewis A.E. (2002). A mathematical model of a high sulphate wastewater anaerobic treatment system. *Water Research,* **36**(1), 257-265.

Knoop S. and Kunst S. (1998). Influence of temperature and sludge loading on activated sludge settling, especially on *Microthrix parvicella. Water Science and Technology*, **37**(4-5), 27-35.

Kohavi R. and John G.H. (1997). Wrappers for feature subset selection. *Artificial Intelligence,* **97**, 273-324.

Lalman J.A. and Bagley D.M. (2001). Anaerobic degradation and methanogenic inhibitory effects of oleic and stearic acids. *Water Research¸* **35**(12), 2975-2983.

Lardon L., Puñal A., Martínez J.A. and Steyer J.P. (2005). Modular expert system for the diagnosis of operating conditions of industrial anaerobic digestion plants. *Water Science and Technology*, **52**(1-2), 427-433.

Lardon L. (2004). Représentation et gestion des incertitudes pour le diagnostic par la théorie de Dempster-Shafer: application aux procédés biologiques. *PhD Thesis*, University of Montpellier, France

Lau O.A., Strom P.F. and Jenkins D. (1984). Growth kinetics of Sphaerotilus natans and a floc former in pure and continuous culture. *Journal of Water Pollution Control Federation,* **56**, 41-51.

Lemmer H. and Baumann M. (1988). Scum actinomycetes in sewage treatment plants – part 2. *Water Research,* **22**(6), 761-763.

Lin C.Y. (1992). Effect of heavy metals on volatile fatty acid degradation in anaerobic digestion. *Water Research,* **26**(10), 177-183.

Ma Y., Peng Y. and Wang S. (2006). New automatic control strategies for sludge recycling and wastage for the optimum operation of predenitrification processes. *Journal of Chemical Technology and Biotechnology*, **81**(1), 41-47.

Magrí A., Corominas Ll., López H., Campos E., Balaguer M.D., Colprim J. and Flotats X. (2005). A model for the simulation of the SHARON process: pH as a key factor. *Environmental Technology*, **28**(3), 255-265.

Makinia J., Rosenwinkel K.-H. and Phan L.-C. (2006). Modification of ASM3 for the determination of biomass adsorption/storage capacity in bulking sludge control. *Water Science and Technology,* **53**(3), 91-99.

Mamdani E.H. and Assilan S. (1975). An experiment in linguistic synthesis with a fuzzy logic controller. *International Journal of Man-Machine Studies,* **7**, 1–13.

Marchaim U. and Krause C. (1993). Propionic to acetic acid ratios in overloaded anaerobic digestion. *Bioresource Technology,* **43**, 195-203.

Martínez M. (2006). A dynamic knowledge-based decision support system to handle solids separation problems in activated sludge systems: Development and validation. PhD Thesis. Universitat de Girona, Spain.

Martínez M., Mérida-Campos C., Sánchez-Marré, Comas J. and Rodríguez-Roda I. (2006). Improving the efficiency of case-based reasoning to deal with activated sludge solids separation problems. *Environmental Technology*, **27**(6), 585-596.

Martins A.M.P., Pagilla K., Heijnen J.J. and van Loosdrecht M.C.M. (2004). Filamentous bulking sludge – a critical review. *Water Research*, **38**, 793-817.

Massart N., Bates R., Corning B. and Neun G. (2006). Design and operational considerations to avoid excessive anaerobic digester foaming. *79th Water Environment Federation Technical Exhibition and Conference*, Dallas, USA, 21-25 October.

Meijer S.C.F. (2004). Theoretical and practical aspects of modelling activated sludge processes. PhD Thesis. Delft University of Technology, The Netherlands.

Merkel W., Manz W., Szewzyk U. and Krauth K. (1999). Population dynamics in anaerobic wastewater reactors: Modelling and in situ characterization. *Water Research,* **33**(10), 2392-2402.

Metcalf and Eddy Inc. (2003). Wastewater engineering: Treatment and reuse. 3rd ed., *McGraw-Hill*, New York, USA, ISBN 978-0-07-041878-3.

Moral H., Aksoy A. and Gokcay C.F. (2008). Modelling of the activated sludge process by using artificial neural networks with automated architecture screening. *Computers and Chemical Engineering,* **32**(10), 2471-2478.

Müller A., Marsili-Libelli S., Aivasidis A., Lloyd T., Kroner S. and Wandrey C. (1997). Fuzzy control of disturbances in a wastewater treatment process. *Water Research,* **31**(12), 3157-3167.

Murto M., Björnsson L. and Mattiasson B. (2004). Impact of food industrial waste on anaerobic co-digestion of sewage sludge and pig manure. *Journal of Environmental Management*, **70**, 101-107.

Musvoto E.V., Lakay M.T., Casey T.G., Wentzel M.C. and Ekama G.A. (1999). Filamentous organisms bulking in nutrient removal activated sludge systems. Paper 8: The effect of nitrate and nitrite. *Water SA*, **25**(4), 397-407.

Ng W.W.Y., Yeung D.S., Firth M., Tsang E.C.C. and Wang X.Z. (2008). Feature selection using localized generalization error for supervised classification problems using RBFNN. *Pattern Recognition*, **41**, 3706-3719.

Nguyen D. and Widrow B. (1990). Improving the learning speed of 2-layer neural networks by choosing initial values of the adaptive weights. *Proceedings of Int. Joint Conf. Neural Networks.* Washington DC, USA, January 15-19, 21-26.

Nopens I., Batstone D.J., Copp J.B., Jeppsson U., Volcke E., Alex J. and Vanrolleghem P.A. (2009). An ASM/ADM model interface for dynamic plant-wide simulation. *Water Research,* **43**(7), 1913-1923.

Nopens I., Benedetti L., Jeppsson U., Pons M.N., Alex J., Copp J.B., Gernaey K.V., Rosen C., Steyer J.P. and Vanrolleghem P.A. (2008). Benchmark Simulation Model No2 – Finalisation of plant layout and default control strategy. *Proceedings of the IWA World Water Congress and Exhibition,* Vienna, Austria, 7-12 September.

Otterpohl R. and Freund M. (1992). Dynamic models for clarifiers of activated sludge plants with dry and wet weather flows. *Water Science and Technology,* **26**(5-6), 1391-1400.

Otterpohl R., Raak M. and Rolfs T. (1994). A mathematical model for the efficiency of the primary clarification. *IAWQ 17th Biennial International Conference*. Budapest, Hungary, 24-29 July.

Pagilla K.R., Craney K.C. and Kido W.H. (1997). Causes and effects of foaming in anaerobic sludge digesters. *Water Science and Technology,* **36**(6-7), 463-470.

Palm J.C., Jenkins D. and Parker D.S. (1980). Relationship between organic loading, dissolved oxygen concentration and sludge settleability in the completely-mixed activated sludge process. *Journal of Water Pollution Control Federation,* **52***,* 2484-2506.

Pedrycz W. (1995). Fuzzy control engineering: reality and challenges. *IEEE International Conference on Fuzzy Systems 2.* Yokohama, Japan, 20-24 March, (2), 437-446.

Poch M., Comas J., Rodríguez-Roda I., Sànchez-Marrè M. and Cortés U. (2004). Designing and building real environmental decision support systems. *Environmental Modelling and Software,* **19**(9), 857–873.

Puñal A., Palazzotto L., Bouvier J.C., Conte T. and Steyer J.P. (2003). Automatic control of volatile fatty acids in anaerobic digestion using a fuzzy logic based approach. *Water Science and Technology,* **48**(6), 103-110.

Ráduly B., Gernaey K.V., Capodaglio A.G., Mikkelsen P.S. and Henze M. (2007). Artificial neural networks for rapid WWTP performance evaluation: methodology and case study. *Environmental Modelling and Software*, **22**(8), 1208-1216.

Ramírez I. and Steyer J.P. (2008). Modelling microbial diversity in anaerobic digestion. *Water Science and Technology,* **57**(2), 265-270.

Richard M.G. (1989). Activated Sludge Microbiology. *Water Pollution Control Federation*, Alexandria, USA.

Rodriguez-Roda I., Comas J., Colprim J., Poch M., Sànchez-Marrè M., Cortés U., Baeza J. and Lafuente J., (2002). A hybrid supervisory system to support wastewater treatment plant operation: implementation and validation. *Water Science and Technology,* **45**(4–5), 289–297.

Rosen C., Vrecko D., Gernaey K.V., Pons M.N. and Jeppsson U. (2006). Implementing ADM1 for plant-wide benchmark simulations in Matlab/Simulink. *Water Science and Technology,* **54**(4), 11-19.

Rosen C., Jeppsson U. and Vanrolleghem P.A. (2004). Towards a common benchmark for long-term process control and monitoring performance evaluation. *Water Science and Technology,* **50**(11), 41-49.

Ross D.R. and Ellis L.-A.M. (1992). Laboratory-scale investigation of foaming in anaerobic digesters. *Water Environment Research,* **64**(2), 154-162.

Rossetti S., Tomei M.C., Nielsen P.H. and Tandoi V. (2005). "*Microthrix parvicella*", a filamentous bacterium causing bulking and foaming in activated sludge systems: a review of current knowledge. *FEMS Microbiology Reviews,* **29**, 49-64.

Scruggs C.E. and Randall C.W. (1998). Evaluation of filamentous microorganism growth factors in an industrial wastewater activated sludge system. *Water Science and Technology,* **37**(4-5), 263-270.

Serralta J., Ferrer J., Borrás L. and Seco A. (2004). An extension of ASM2d including pH calculation. *Water Research,* **38**(19), 4029-4038.

Sin G., Villez K. and Vanrolleghem P.A. (2006). Application of a model-based optimization methodology for nutrient removing SBRs leads to falsification of the model. *Water Science and Technology*, **53**(4-5), 95-103.

Smets I.Y., Banadda E.N., Deurink J., Renders N., Jenné R. and van Impe J.F. (2006). Dynamic modeling of filamentous bulking in lab-scale activated sludge processes. *Journal of Process Control,* **16**, 313-319.

Spering V., Makinia J. and Rosenwinkel K.-H. (2009). Analyzing and improving a mechanistic model for the *Microthrix parvicella* in activated sludge systems.

Proceedings of the 1st IWA/WEF Wastewater Treatment Modelling Seminar (WWTmod2008). 1-3 June, Mont Sainte-Anne, Quebéc, Canada.

Stafford D.A., Wheatley B.I. and Hughes D.E. (1980). Anaerobic digestion. *Applied Science Publishers Ltd,* London, UK, ISBN 0-85334-904-5.

Starkey J.E. and Karr J.E. (1984). Effect of low dissolved oxygen concentration on effluent turbidity. *Journal of Water Pollution Control Federation,* **56**(7), 837-843.

Steyer J.P., Bouvier J.C., Conte T., Gras P. and Sousbie P. (2002). Evaluation of a four year experience with a fully instrumented anaerobic digestion process. *Water Science and Technology*, **45**(4-5), 495-502.

Takács I. and Fleit E. (1995). Modelling of the micromorphology of the activated sludge floc: Low DO, Low F/M bulking. *Water Science and Technology*, **31**(2), 235-243.

Takács I., Patry G.G. and Nolasco D. (1991). A dynamic model of the clarification thickening process. *Water Research,* **25**(10), 1263-1271.

Van Veldhuizen H.M., van Loosdrecht M.C.M. and Heijnen J.J. (1999). Modelling biological phosphorous and nitrogen removal in a full scale activated sludge process. *Water Research,* **33**(16), 3459-3468.

Vanhooren H. and Nguyen K. (1996). Development of a simulation protocol for evaluation of respirometry-based control strategies. *Technical Report*, University of Gent and University of Ottawa, Gent, Belgium.

Vanrolleghem P.A., Jeppsson U., Carstensen J., Carlsson B. and Olsson G. (1996). Integration of WWT plant design and operation – A systematic approach using cost functions. *Water Science and Technology,* **34**(3-4), 159-171.

Vavilin V.A., Rytow S.V. and Lokshina Y.L. (1995). Modelling hydrogen partial pressure change as a result of competition between the butyric and propionic groups of acidogenic bacteria. *Bioresource Technology*, **54**(2), 171-177.

Vrecko D., Gernaey K.V., Rosen C., Jeppsson U. (2006). Benchmark Simulation Model No 2 in Matlab-Simulink: Towards plant-wide WWTP control strategy evaluation. *Water Science and Technology* **54**(8), 65-72.

Wanner J. (1994). Activated Sludge Bulking and Foaming Control. *Technomic Publishing Co.* Lancaster, PA, USA, ISBN 1-56676-121-2.

Water Environment Federation. (1996). Operation of municipal wastewater treatment plants. Manual of practice. *Water Environment Federation*, 2nd volume, 5th edition, Alexandria, USA.

Westlund A.D., Hagland E. and Rothman M. (1998). Foaming in anaerobic digesters caused by *Microthrix parvicella. Water Science and Technology,* **37**(4-5), 51-55.

Whitmore T.N., Lazzari M. and Lloyd D. (1985). Comparative studies of methanogenesis in thermophilic and mesophilic anaerobic digesters using membrane inlet mass spectrometry. *Biotechnology Letters,* **7**(4), 283-288.

Wilén B.M., Keiding K. and Nielsen P.H. (2000). Anaerobic deflocculation and aerobic reflocculation of activated sludge. *Water Research,* **34**(16), 3933-3942.

Wilén B.M. and Balmér P. (1999). The effect of dissolved oxygen concentration on the structure, size and size distribution of activated sludge flocs. *Water Research,* **33**(2), 391-400.

Yong M., Yong-Zhen P., Xiao-Lian W. and Shu-Ying W. (2006). Intelligent control of aeration and external carbon addition for improving nitrogen removal. *Environmental Modelling and Software,* **21**(6), 821–828.

Zhao H.W. and Viraraghavan T. (2004). Analysis of the performance of an anaerobic digestion system at the Regina wastewater treatment plant. *Bioresource Technology*, **95**, 301-307.

ANNEXES

ACTIVATED SLUDGE RISK MODEL SCRIPT FOR BENCHMARK SIMULATION MODELS IN MATLAB/SIMULINK

Note that this script is for the BSM1, code within a box is different, as noted, for either BSM1_LT or BSM2.

```
% RISK MODEL
% Implementation of Expert rules to detect suitable conditions for settling problems with biological origin

% Some limit values according to literature
% SRT limit
SRTReasonableLimit=20;

% Settler SNO limit (rising sludge)
SNOHighLimit=8;

% Influent organic matter and nitrogen loading
BOD5invec1 = BOD5in.*inpart(:,15);
CODinvec1 = CODin.*inpart(:,15);
S_sinvec1 = inpart(:,2).*inpart(:,15);
TNin1 = (SNKjin+SNOin);
TNinvec1 =inpart(:,15).*TNin1;

% Influent organic matter(from the chemical addition)
BOD5invec2= CARBONSOURCECONC.*Qcarbonvec;
CODinvec2 = CARBONSOURCECONC.*Qcarbonvec;
S_sinvec2 = CARBONSOURCECONC.*Qcarbonvec;

%total Influent organic matter and nitrogen loading (sewer+ chemical addition)
BOD5invec3=BOD5invec1 + BOD5invec2; %total influent BOD5 (AS + external carbon)
CODinvec3= CODinvec1 + CODinvec2; %total influent COD (AS + external carbon)
S_sinvec3 = S_sinvec1 + S_sinvec2; % total influent Ss (AS+ external carbon)

BOD5in3 = BOD5invec3./(inpart(:,15)+ Qcarbonvec);
CODin3 = CODinvec3./(inpart(:,15)+ Qcarbonvec);
S_sin3 = S_sinvec3./(inpart(:,15)+ Qcarbonvec);
```

```
% Effluent organic matter and nitrogen loading
CODevec=settlerpart(:,31).*CODe;

For BSM2:

% Effluent organic matter and nitrogen loading
CODevec=settlerpart(:,37).*CODe;
```

```
% determining Biomass in activated sludge biological reactors
Biomassvec=0.75*(reac1part(:,5)*VOL1+reac1part(:,6)*VOL1+reac2part(:,5)*VOL2+reac2part(:,6)*VOL2+reac3part(:,5)*VOL3+reac3part(:,6)*VOL3+reac4part(:,5)*VOL4+reac4part(:,6)*VOL4+reac5part(:,5)*VOL5+reac5part(:,6)*VOL5); %XBH + XBA in aerated biological reactors only, in TSS units
TSSvecreactor=reac1part(:,14)*VOL1+reac2part(:,14)*VOL2+reac3part(:,14)*VOL3+reac4part(:,14)*VOL4+reac5part(:,14)*VOL5; %TSS in aerated tanks

% determining FtoM_1 (kg COD removed/kg MLVSS·d) Only biomass in activated sludge biological reactors considered
FtoM_1vec = (CODinvec3 - CODevec)./Biomassvec;
```

```
% determining FtoM_2 (kg BOD5/kg MLVSS·d)
FtoM_2vec = BOD5invec3./Biomassvec;
```

```
% determining SRT
%Waste sludge production
Qwasteflow = settlerpart(:,16);
TSSwasteconc = settlerpart(:,41);
TSSuvec2 =TSSwasteconc.*Qwasteflow;
TSSevec2=settlerpart(:,30).*settlerpart(:,31); %TSS in the effluent, in g/d

For BSM2:

% determining SRT
TSSwasteconc = settlerpart(:,53); % solids concentration at the lower layer of the settler
TSSuvec2 = TSSwasteconc.*Qwflow; % solids flow in the waste
TSSuvec3 = settlerpart(:,36).*settlerpart(:,37); % solids flow in the effluent
```

```
% SRT for sludge in aeration biological reactors, settler not considered
SRTvec =TSSvecreactor./(TSSuvec2+TSSevec2); % TSS in reactor / TSS removed from the system
SRTvec = smoothing_data(SRTvec,3)'; % SRTvec filtering using 3 days data
 for i=1:length(SRTvec) %To replace SRTvec values >SRTReasonableLimit for SRTReasonableLimit
   if SRTvec(i)>SRTReasonableLimit
     SRTvec(i)=SRTReasonableLimit;
    else
     SRTvec(i)=SRTvec(i);
   end
end

% Determining possible bulking conditions due to nutrient deficiency
% Check for nitrogen deficiency Bulking (check for BOD5/N ratio)
BOD5toN = BOD5in3./TNin1;
NDefBulking1=zeros(1,length(BOD5toN));
Nfis=readfis('Deficiency'); %to load the N Deficiency fuzzy inference system developed with the Matlab
fuzzy toolbox
NDefBulking1=evalfis([BOD5toN], Nfis); %To evaluate the output of the Nfis fuzzy system for a given
input
NDefBulking1 = NDefBulking1;
NDefBulking1_smoothed = smoothing_data(NDefBulking1,3)';
NofNDefBulking1 = find (NDefBulking1> 0.8); %To find the values higher than 0.8
NofDif0NDefBulking1 = find (NDefBulking1 > 0.0001); %To find the values higher than 0.0001
      % to find the worst situation: the most dangerous situation during the evaluation period, computed as
the largest
      % time interval that the plant is in uninterrupted severe risk of NDef bulking problem.
LengthNDefBulking=zeros(1,length(NofNDefBulking1)); % all indexes with NDefBulking > 0.8
for i=1:length(NofNDefBulking1)
  j=i;
  k=1;
  if j~=length(NofNDefBulking1)
    while isequal(NofNDefBulking1(j)+1,NofNDefBulking1(j+1))
      k=k+1;
      j=j+1;
      if j==length(NofNDefBulking1) break
      end
    end
    LengthNDefBulking(i)=k;
  end
  LengthNDefBulking(length(NofNDefBulking1))=1;
end
MaxLengthNDefBulking=max(LengthNDefBulking);
```

```
MaxLengthNDefBulkingIndex=find(LengthNDefBulking==MaxLengthNDefBulking);

%Display N deficiency Bulking problems
disp('Qualitative criteria for settling problems')
disp('----------------------------------------')
 if not(isempty(NofNDefBulking1))
   disp('The plant has experienced high (>0.8) risk for the development of filamentous bulking due to N
deficiency')
   disp(['during ',num2str(min(totalt,length(NofNDefBulking1)*sampletime)),' days, i.e. ',
num2str(min(100,length(NofNDefBulking1)*sampletime/totalt*100)),'% of the operating time.'])
   disp(['AV  risk ',num2str(sum(NDefBulking1*sampletime)/totalt),''])
   disp(['The most dangerous situation was between days ',
num2str(min(totalt,NofNDefBulking1(MaxLengthNDefBulkingIndex(1))*sampletime)+starttime),' and ',
num2str(min(totalt,(NofNDefBulking1(MaxLengthNDefBulkingIndex(1))+MaxLengthNDefBulking)*sa
mpletime)+starttime),])
   disp(' ')
else
   disp('The plant has experienced high (>0.8) risk for the development of filamentous bulking due to N
deficiency')
   disp(['during ',num2str(min(totalt,length(NofNDefBulking1)*sampletime)),' days, i.e. ',
num2str(min(100,length(NofNDefBulking1)*sampletime/totalt*100)),'% of the operating time.'])
   disp(['AV  risk ',num2str(sum(NDefBulking1*sampletime)/totalt),''])
   disp(' ')
end

% Determining possible aerobic bulking conditions
bulkingfis=readfis('LowDOBulking'); %to load the Low DO Bulking fuzzy inference system developed
with the Matlab fuzzy toolbox
LowDOBulking1=evalfis([FtoM_1vec  reac3part(:,8)],  bulkingfis);  %To  evaluate  the  output  of  the
bulkingfis fuzzy system for a given input
LowDOBulking1 = LowDOBulking1;
LowDOBulking1_smoothed = smoothing_data(LowDOBulking1,3)';
NofLowDOBulking1 = find (LowDOBulking1 > 0.8); %To find the values higher than 0.8
NofDif0LowDOBulking1 = find (LowDOBulking1 > 0.0001); %To find the values higher than 0.0001

% to find the worst situation: the most dangerous situation during the evaluation period, computed as the
largest time interval that the plant is in uninterrupted severe risk of Low DO bulking problem.
LengthLowDOBulking=zeros(1,length(NofLowDOBulking1));
for i=1:length(NofLowDOBulking1)
  j=i;
  k=1;
  if j~=length(NofLowDOBulking1)
    while isequal(NofLowDOBulking1(j)+1,NofLowDOBulking1(j+1))
      k=k+1;
      j=j+1;
      if j==length(NofLowDOBulking1) break
      end
    end
    LengthLowDOBulking(i)=k;
  end
  LengthLowDOBulking(length(NofLowDOBulking1))=1;
end
MaxLengthLowDOBulking=max(LengthLowDOBulking);
MaxLengthLowDOBulkingIndex=find(LengthLowDOBulking==MaxLengthLowDOBulking);

%Display Low DO Bulking problems
if not(isempty(NofLowDOBulking1))
  disp('The plant has experienced high (>0.8) risk for the development of aerobic (low DO) filamentous
bulking')
```

```
   disp(['during ',num2str(min(totalt,length(NofLowDOBulking1)*sampletime)),' days, i.e.
',num2str(min(100,length(NofLowDOBulking1)*sampletime/totalt*100)),'% of the operating time.'])
   disp(['AV  risk ',num2str(sum(LowDOBulking1*sampletime)/totalt),''])
   disp(['The most dangerous situation was between days ',
num2str(min(totalt,(NofLowDOBulking1(MaxLengthLowDOBulkingIndex(1)))*sampletime)+starttime),
' and ',
num2str(min(totalt,(NofLowDOBulking1(MaxLengthLowDOBulkingIndex(1))+MaxLengthLowDOBulk
ing)*sampletime)+starttime),])
   disp(' ')
else
   disp('The plant has experienced high (>0.8) risk for the development of aerobic (low DO) filamentous
bulking')
   disp(['during ',num2str(min(totalt,length(NofLowDOBulking1)*sampletime)),' days, i.e.
',num2str(min(100,length(NofLowDOBulking1)*sampletime/totalt*100)),'% of the operating time.'])
      disp(['AV  risk ',num2str(sum(LowDOBulking1*sampletime)/totalt),''])
   disp(' ')
end

%Determining conditions for Low F/M bulking
bulkingfis=readfis('FtoMBulking_1');%to load the Low F/M Bulking fuzzy inference system developed
with the Matlab fuzzy toolbox
%To evaluate the output of the bulkingfis fuzzy system (low F/M bulking) for a given input; inpart
(:,2)=influent SS
LowFtoMBulking1=evalfis([reac1part(:,2) SRTvec], bulkingfis); %react(:,2)=reactor SS

bulkingfis=readfis('FtoMBulking_2');%to load the Low F/M Bulking_2 fuzzy inference system developed
with the Matlab fuzzy toolbox
%To evaluate the output of the bulkingfis fuzzy system (low F/M bulking) for a given input; inpart
(:,2)=influent SS
LowFtoMBulking2=evalfis([FtoM_2vec SRTvec], bulkingfis);%F/M_2 food to microorganisms ratio

[Fil,Col]=size(LowFtoMBulking1);
if Fil==1
LowFtoMBulking1 = LowFtoMBulking1';
end

[Fil,Col]=size(LowFtoMBulking2);
if Fil==1
LowFtoMBulking2 = LowFtoMBulking2';
end

LowFtoMBulking=max(LowFtoMBulking1,LowFtoMBulking2);

% Temperature factor correction of risk due to Microthrix parvicella (Only for BSM2)

Factor=1.2*exp(-((reac5part(:,16)-5).^2/625));
LowFtoMBulking=LowFtoMBulking.*Factor;

for i=1:length(LowFtoMBulking);
if LowFtoMBulking(i)>1;
   LowFtoMBulking(i)=1;
else
   LowFtoMBulking(i)=LowFtoMBulking(i);
end
end

LowFtoMBulking_smoothed = smoothing_data(LowFtoMBulking,3)';
NofLowFtoMBulking=find (LowFtoMBulking> 0.8);
NofDif0LowFtoMBulking = find (LowFtoMBulking > 0.0001);% to find the worst situation: the most
dangerous situation during the evaluation period, computed as the largest
```

```
      % time interval that the plant is in uninterrupted severe risk of
      % Low F/M bulking problem
if not(isempty(NofLowFtoMBulking))
    LengthLowFtoMBulking=zeros(1,length(NofLowFtoMBulking));
    for i=1:length(NofLowFtoMBulking)
      j=i;
      k=1;
      if j~=length(NofLowFtoMBulking)
        while isequal(NofLowFtoMBulking(j)+1,NofLowFtoMBulking(j+1))
          k=k+1;
          j=j+1;
          if j==length(NofLowFtoMBulking) break
          end
        end
        LengthLowFtoMBulking(i)=k;
      end
      LengthLowFtoMBulking(length(NofLowFtoMBulking))=1;
    end
    MaxLengthLowFtoMBulking=max(LengthLowFtoMBulking);
    MaxLengthLowFtoMBulkingIndex=find(LengthLowFtoMBulking==MaxLengthLowFtoMBulking);

%Display Low F/M Bulking problems
    disp('The plant has experienced severe (>0.8) risk for the development of low F/M filamentous
bulking')
    disp(['during ',num2str(min(totalt,length(NofLowFtoMBulking)*sampletime)),' days, i.e.
',num2str(min(100,length(NofLowFtoMBulking)*sampletime/totalt*100)),'% of the operating time.'])
    disp(['AV  risk ',num2str(sum(LowFtoMBulking*sampletime)/totalt),''])
    disp(['The most dangerous situation was between days ',
num2str(min(totalt,NofLowFtoMBulking(MaxLengthLowFtoMBulkingIndex(1))*sampletime)+starttime
),' and ',
num2str(min(totalt,(NofLowFtoMBulking(MaxLengthLowFtoMBulkingIndex(1))+MaxLengthLowFtoM
Bulking)*sampletime)+starttime),])
    disp(' ')
 else % LowFtoMBulking is empty
   disp('The plant has experienced severe (>0.8) risk for the development of low F/M filamentous bulking')
   disp(['during ',num2str(min(totalt,length(NofLowFtoMBulking)*sampletime)),' days, i.e.
',num2str(min(100,length(NofLowFtoMBulking)*sampletime/totalt*100)),'% of the operating time.'])
   disp(['AV  risk ',num2str(sum(LowFtoMBulking*sampletime)/totalt),''])
   disp(' ')
end

% Determining possible foaming conditions due to limited substrate (lowFtoM Foaming)
foamingfis=readfis('FoamingNocMic'); %to load the Low F/M Foaming fuzzy inference system
developed with the Matlab fuzzy toolbox
%To evaluate the output of the foamingfis fuzzy system (low F/M foaming) for a given input
LowFtoMFoaming2=evalfis([FtoM_2vec SRTvec], foamingfis);
```

```
% Temperature factor correction of risk due to Microthrix parvicella (Only BSM2)

Factor=1.2*exp(-((reac5part(:,16)-5).^2/625));
LowFtoMFoaming2=LowFtoMFoaming2.*Factor;

for i=1:length(LowFtoMFoaming2);
if LowFtoMFoaming2(i)>1;
   LowFtoMFoaming2(i)=1;
else
   LowFtoMFoaming2(i)=LowFtoMFoaming2(i);
end
end
```

```
LowFtoMFoaming2_smoothed = smoothing_data(LowFtoMFoaming2,3)';
NofLowFtoMFoaming2 = find (LowFtoMFoaming2 > 0.8);
NofDif0LowFtoMFoaming2 = find (LowFtoMFoaming2 > 0.0001); %To find the values higher than
0.0001

% to find the worst situation: the most dangerous situation during the evaluation period, computed as the
largest
      % time interval that the plant is in uninterrupted severe risk of
      % Low F/M Foaming problem.
if not(isempty(NofLowFtoMFoaming2))
    LengthLowFtoMFoaming=zeros(1,length(NofLowFtoMFoaming2));
    for i=1:length(NofLowFtoMFoaming2)
      j=i;
      k=1;
      if j~=length(NofLowFtoMFoaming2)
        while isequal(NofLowFtoMFoaming2(j)+1,NofLowFtoMFoaming2(j+1))
          k=k+1;
          j=j+1;
          if j==length(NofLowFtoMFoaming2) break
          end
        end
        LengthLowFtoMFoaming(i)=k;
      end
      LengthLowFtoMFoaming(length(NofLowFtoMFoaming2))=1;
    end
    MaxLengthLowFtoMFoaming=max(LengthLowFtoMFoaming);

MaxLengthLowFtoMFoamingIndex=find(LengthLowFtoMFoaming==MaxLengthLowFtoMFoaming);

%Display Low F/M Foaming problems
    disp('The plant has experienced high (>0.8) risk for the development of low F/M foaming')
    disp(['during ',num2str(min(totalt,length(NofLowFtoMFoaming2)*sampletime)),' days, i.e.
',num2str(min(100,length(NofLowFtoMFoaming2)*sampletime/totalt*100)),'% of the operating time.'])
    disp(['AV  risk ',num2str(sum(LowFtoMFoaming2*sampletime)/totalt),''])
    disp(['The most dangerous situation was between days ',
num2str(min(totalt,NofLowFtoMFoaming2(MaxLengthLowFtoMFoamingIndex(1))*sampletime)+startti
me),' and ',
num2str(min(totalt,(NofLowFtoMFoaming2(MaxLengthLowFtoMFoamingIndex(1))+MaxLengthLowFt
oMFoaming)*sampletime)+starttime),])
    disp(' ')
else
    disp('The plant has experienced high (>0.8) risk for the development of low F/M foaming')
    disp(['during ',num2str(min(totalt,length(NofLowFtoMFoaming2)*sampletime)),' days, i.e.
',num2str(min(100,length(NofLowFtoMFoaming2)*sampletime/totalt*100)),'% of the operating time.'])
    disp(['...and risk for the development of low F/M foaming ',
num2str(min(100,length(NofDif0LowFtoMFoaming2)*sampletime/totalt*100)),'% of the operating
time.'])
    disp(['AV  risk ',num2str(sum(LowFtoMFoaming2*sampletime)/totalt),''])
    disp(' ')
end

% Determining possible foaming conditions due to high readily biodegradable organic matter fraction
foamingfis=readfis('Foaming1863_1');%to load the HRBOM fraction foaming fuzzy inference system
developed with the Matlab fuzzy toolbox
HighRBOMfractionFoaming1=evalfis([FtoM_2vec (S_sin3./inpart(:,4))], foamingfis);

HighRBOMfractionFoaming2 = [];
```

```
foamingfis=readfis('Foaming1863_2');%to load the HRBOM fraction foaming_2 fuzzy inference system developed with the Matlab fuzzy toolbox
%To evaluate the output of the foamingfis fuzzy system (due to high readily biodegradable organic matter fraction) for a given input, in another way
HighRBOMfractionFoaming2=evalfis([SRTvec (S_sin3./inpart(:,4))], foamingfis);% SS/XS ratio

[Fil,Col]=size(HighRBOMfractionFoaming1);
if Fil==1
  HighRBOMfractionFoaming1=HighRBOMfractionFoaming1';
end
[Fil,Col]=size(HighRBOMfractionFoaming2);
if Fil==1
  HighRBOMfractionFoaming2=HighRBOMfractionFoaming2';
end

HighRBOMfractionFoaming=max(HighRBOMfractionFoaming1,HighRBOMfractionFoaming2);
HighRBOMfractionFoaming= HighRBOMfractionFoaming;

HighRBOMfractionFoaming_smoothed=smoothing_data(HighRBOMfractionFoaming,3)';
NofHighRBOMfractionFoaming=find(HighRBOMfractionFoaming> 0.8);
NofDif0HighRBOMfractionFoaming = find(HighRBOMfractionFoaming > 0.0001); %To find the values higher than 0.0001

 if not(isempty(NofHighRBOMfractionFoaming))
     LengthHighRBOMfractionFoaming=zeros(1,length(NofHighRBOMfractionFoaming));
     for i=1:length(NofHighRBOMfractionFoaming)
       j=i;
       k=1;
       if j~=length(NofHighRBOMfractionFoaming)
          while isequal(NofHighRBOMfractionFoaming(j)+1,NofHighRBOMfractionFoaming(j+1))
            k=k+1;
            j=j+1;
            if j==length(NofHighRBOMfractionFoaming) break
            end
          end
          LengthHighRBOMfractionFoaming(i)=k;
       end
       LengthHighRBOMfractionFoaming(length(NofHighRBOMfractionFoaming))=1;
     end
MaxLengthHighRBOMfractionFoaming=max(LengthHighRBOMfractionFoaming);
MaxLengthHighRBOMfractionFoamingIndex=find(LengthHighRBOMfractionFoaming==MaxLengthHighRBOMfractionFoaming);

%Display Low SsXs foaming problems
disp('The plant has experienced high (>0.8) risk for the development of foaming due to high Ss/Xs fraction')
disp(['during ',num2str(min(totalt,length(NofHighRBOMfractionFoaming)*sampletime)),' days, i.e. ',num2str(min(100,length(NofHighRBOMfractionFoaming)*sampletime/totalt*100)),'% of the operating time.'])
disp(['AV  risk ',num2str(sum(HighRBOMfractionFoaming*sampletime)/totalt),''])
disp(['The most dangerous situation was between days ',
num2str(min(totalt,NofHighRBOMfractionFoaming(MaxLengthHighRBOMfractionFoamingIndex(1))*sampletime)+starttime),' and ',
num2str(min(totalt,(NofHighRBOMfractionFoaming(MaxLengthHighRBOMfractionFoamingIndex(1))+MaxLengthHighRBOMfractionFoaming)*sampletime)+starttime),])
disp(' ')
else % HighRBOMfractionFoaming is empty
disp('The plant has experienced high (>0.8) risk for the development of foaming due to high Ss/Xs fraction')
```

```
disp(['during ',num2str(min(totalt,length(NofHighRBOMfractionFoaming)*sampletime)),' days, i.e.
',num2str(min(100,length(NofHighRBOMfractionFoaming)*sampletime/totalt*100)),'% of the operating
time.'])
disp(['AV  risk ',num2str(sum(HighRBOMfractionFoaming*sampletime)/totalt),''])
disp(' ')
end

%Determining possible suitable conditions for Rising sludge
i=0;
SsOutReac5=reac5part(:,2);
SNOOutReac5=reac5part(:,9);
SoOutReac5=reac5part(:,8);
Rising1=zeros(1,length(SNOOutReac5));
XBHOutReac5= reac5part(:,5);
XBHOutBottomClarifier= settlerpart(:,5);

SludgeVolumeInClarifier=(settlerpart(:,32).*600+settlerpart(:,33).*600+settlerpart(:,34).*600+settlerpart(
:,35).*600+settlerpart(:,36).*600+settlerpart(:,37).*600+settlerpart(:,38).*600+settlerpart(:,39).*600+settl
erpart(:,40).*600+settlerpart(:,41).*600)./settlerpart(:,41);%%changed in BSM2*

nitrifiers_fraction=1;

Rdn2=((1-
Y_H)./(2.86.*Y_H)).*(mu_H*(SsOutReac5./(K_S+SsOutReac5))).*(SNOOutReac5./(K_NO+SNOOutR
eac5)).*XBHOutBottomClarifier.*ny_g;
t_delay=(SoOutReac5./(2.86*Rdn2/nitrifiers_fraction));

For BSM2:

SNOHighLimit= 11.003972.*(exp(-0.020295*reac5part(:,16)));
mu_H= 4*exp((log(4/3)/5)*(reac5part(:,16)- 15));
Rdn2=((1-
Y_H)./(2.86.*Y_H)).*(mu_H.*(SsOutReac5./(K_S+SsOutReac5))).*(SNOOutReac5./(K_NO+SNOOutR
eac5)).*XBHOutBottomClarifier.*ny_g; %considering DO=0 mgO2/L
t_delay=(SoOutReac5./(2.86*Rdn2/nitrifiers_fraction));


Limit1=SludgeVolumeInClarifier./(Qrflow+1);
Limit2=(SludgeVolumeInClarifier./(Qrflow+1))+0.01;
Limit3=(SludgeVolumeInClarifier./(Qrflow+1))+0.02;

for i=1:length(SNOOutReac5)
Risingfis = newfis('Rising');
%%%definition of the inputs
Risingfis = addvar(Risingfis,'input','Sno',[0 40]);
Risingfis = addmf(Risingfis,'input',1,'L','trapmf',[-1.429 -1.429 2 5]);
Risingfis = addmf(Risingfis,'input',1,'N','trimf',[2 5 8]);
Risingfis = addmf(Risingfis,'input',1,'H','trapmf',[5 8 40.27 41.87]);
Risingfis = addvar(Risingfis,'input','ratiodn',[0 2.2]);
Risingfis = addmf(Risingfis,'input',2,'H','trapmf',[Limit2(i) Limit3(i) 2.205 2.272]);
Risingfis = addmf(Risingfis,'input',2,'L','trapmf',[-0.135 -0.0437 Limit1(i) Limit2(i)]);
Risingfis = addmf(Risingfis,'input',2,'N','trimf',[Limit1(i) Limit2(i) Limit3(i)]);
%%%definition of the outputs
Risingfis = addvar(Risingfis, 'output','Rising',[-0.2 1.2]);
Risingfis = addmf(Risingfis,'output',1,'Low','trimf',[-0.2 0 0.2]);
Risingfis = addmf(Risingfis,'output',1,'Medium','trimf',[0.2 0.5 0.8]);
Risingfis = addmf(Risingfis,'output',1,'High','trimf',[0.8 1 1.2]);
%%%definition of the rules
rulelist =[
```

```
3 1 1 1 1
2 1 1 1 1
2 3 1 1 1
2 2 2 1 1
1 1 1 1 1
1 2 1 1 1
1 3 1 1 1
3 3 2 1 1
3 2 3 1 1
];
Risingfis = addrule(Risingfis, rulelist);
%writefis(Risingfis,'Risingfis');
Rising1(i)=evalfis([SNOOutReac5(i) ((SNOHighLimit./Rdn2(i))+t_delay(i))], Risingfis);
AAA(i)=((SNOHighLimit./Rdn2(i))+t_delay(i));
end

Rising1=Rising1;
NofRising1 = find (Rising1 > 0.8);%To find the values higher than 0.8
NofDif0Rising1 = find (Rising1 > 0.0001); %To find the values higher than 0.0001
Rising1_smoothed=smoothing_data(Rising1,0.0833)'; % risk filtering with 2 hours time constant; in
BSM1 only to be used for plotting purposes
% to find the worst situation and display results: the most dangerous situation during the evaluation
period,
% computed as the largest time interval that the plant is in uninterrupted severe risk of Rising problem.
LengthNofRising=zeros(1,length(NofRising1));
for i=1:length(NofRising1)
j=i;
k=1;
if j~=length(NofRising1)
while isequal(NofRising1(j)+1,NofRising1(j+1))
k=k+1;
j=j+1;
if j==length(NofRising1) break
end
end
LengthNofRising(i)=k;
end
LengthNofRising(length(NofRising1))=1;
end
MaxLengthRising=max(LengthNofRising);
MaxLengthRisingIndex=find(LengthNofRising==MaxLengthRising);

if not(isempty(NofRising1))
disp('The plant has experienced high (>0.8) risk for the development of rising sludge')
disp(['during ',num2str(min(totalt,length(NofRising1)*sampletime)),' days, i.e.
',num2str(min(100,length(NofRising1)*sampletime/totalt*100)),'% of the operating time.'])
disp(['AV  risk ',num2str(sum(Rising1*sampletime)/totalt),''])
disp(['The most dangerous situation was between days ',
num2str(min(totalt,NofRising1(MaxLengthRisingIndex(1))*sampletime)+starttime),' and ',
num2str(min(totalt,(NofRising1(MaxLengthRisingIndex(1))+MaxLengthRising)*sampletime)+starttime),
])
disp(' ')
else
disp('The plant has experienced high (>0.8) risk for the development of rising sludge')
disp(['during ',num2str(min(totalt,length(NofRising1)*sampletime)),' days, i.e.
',num2str(min(100,length(NofRising1)*sampletime/totalt*100)),'% of the operating time.'])
disp(['AV  risk ',num2str(sum(Rising1*sampletime)/totalt),''])
end

%Determining possible suitable conditions for Deflocculation
```

```
 deflocculationfis=readfis('HighSRTDeflocculationConditions'); %to load the Low DO Bulking fuzzy inference system developed with the Matlab fuzzy toolbox

Deflocculation_risk=evalfis([SRTvec reac3part(:,8)], deflocculationfis); %To evaluate the output of the bulkingfis fuzzy system for a given input

Deflocculation_smoothed=smoothing_data(Deflocculation_risk,3)';

NofDeflocculation_risk = find (Deflocculation_risk > 0.8);%To find the values higher than 0.8
LengthDeflocculation_risk=zeros(1,length(NofDeflocculation_risk));

for i=1:length(NofDeflocculation_risk)
   j=i;
   k=1;
if j~=length(NofDeflocculation_risk)
      while isequal(NofDeflocculation_risk(j)+1,NofDeflocculation_risk(j+1))
         k=k+1;
         j=j+1;
         if j==length(NofDeflocculation_risk) break
         end
         end
      LengthDeflocculation(i)=k;
   end
   LengthDeflocculation_risk(length(NofDeflocculation_risk))=1;
end

MaxLengthDeflocculation_risk=max(LengthDeflocculation_risk);
MaxLengthDeflocculation_riskIndex=find(LengthDeflocculation_risk==MaxLengthDeflocculation_risk);

if not(isempty(NofDeflocculation_risk))
   disp(' ')
   disp('The plant has experienced high (>0.8) risk for the development of deflocculation')
   disp(['during ',num2str(min(totalt,length(NofDeflocculation_risk)*sampletime)),' days, i.e.
',num2str(min(100,length(NofDeflocculation_risk)*sampletime/totalt*100)),'% of the operating time.'])
   disp(['The most dangerous situation was between days ',
num2str(min(totalt,NofDeflocculation_risk(MaxLengthDeflocculation_riskIndex(1))*sampletime)+7),'
and ',
num2str(min(totalt,(NofDeflocculation_risk(MaxLengthDeflocculation_riskIndex(1))+MaxLengthDefloc
culation_risk)*sampletime)+7),])
   disp(['AV  risk ',num2str(sum(Deflocculation_risk*sampletime)/totalt),''])
end

if isempty(NofDeflocculation_risk)
    disp(' ')
    disp('The plant has not experienced high (>0.8) risk for the development of deflocculation')
end

% Calculating the overall risk (taking the max at every time step)
disp('Overall risk')
disp('------------')
[Fil,Col]=size(NDefBulking1);
if Fil==1
NDefBulking1 = NDefBulking1';
end

[Fil,Col]=size(LowDOBulking1);
if Fil==1
LowDOBulking1 = LowDOBulking1';
end
```

```
[Fil,Col]=size(LowFtoMBulking);
if Fil==1
LowFtoMBulking = LowFtoMBulking1';
end

%selects the maximum bulking period between NDef Bulking and LowDO bulking
Bulking1=max(NDefBulking1, LowDOBulking1);
%selects the maximum bulking period between the previous Bulking and LowFM bulking
Bulking=max(Bulking1, LowFtoMBulking);

NofBulking = find (Bulking > 0.8);%To find the values higher than 0.8
NofDif0Bulking = find (Bulking > 0.0001); %To find the values higher than 0.0001
  disp('The plant has experienced severe (>0.8) risk for (integrated) BULKING')
  disp(['during ',num2str(min(totalt,length(NofBulking)*sampletime)),' days, i.e.
',num2str(min(100,length(NofBulking)*sampletime/totalt*100)),'% of the operating time.'])
  disp(['AV  risk ',num2str(sum(Bulking*sampletime)/totalt),''])
% time interval that the plant is in uninterrupted severe risk of (integrated) Bulking problem.
LengthBulking=zeros(1,length(NofBulking));
for i=1:length(NofBulking)
  j=i;
  k=1;
  if j~=length(NofBulking)
    while isequal(NofBulking(j)+1,NofBulking(j+1))
      k=k+1;
      j=j+1;
      if j==length(NofBulking) break
      end
    end
    LengthBulking(i)=k;
  end
  LengthBulking(length(NofBulking))=1;
end
MaxLengthBulking=max(LengthBulking);
MaxLengthBulkingIndex=find(LengthBulking==MaxLengthBulking);
if not(isempty(NofBulking))
   disp(['The most dangerous situation was between days ',
num2str(min(totalt,NofBulking(MaxLengthBulkingIndex(1))*sampletime)+starttime),' and ',
num2str(min(totalt,(NofBulking(MaxLengthBulkingIndex(1))+MaxLengthBulking)*sampletime)+startti
me),])
end
disp(' ')

[Fil,Col]=size(LowFtoMFoaming2);
if Fil==1
LowFtoMFoaming2 = LowFtoMFoaming2';
end

[Fil,Col]=size(HighRBOMfractionFoaming);
if Fil==1
HighRBOMfractionFoaming = HighRBOMfractionFoaming';
end

%selects the maximum foaming period between SsXs and Low FM foaming
Foaming=max(LowFtoMFoaming2,HighRBOMfractionFoaming);

NofFoaming=find (Foaming > 0.8);%To find the values higher than 0.8
NofDif0Foaming = find (Foaming > 0.0001); %To find the values higher than 0.0001
  disp('The plant has experienced severe (>0.8) risk for (integrated) FOAMING')
```

```
  disp(['during ',num2str(min(totalt,length(NofFoaming)*sampletime)),' days, i.e.
',num2str(min(100,length(NofFoaming)*sampletime/totalt*100)),'% of the operating time.'])
  disp(['AV  risk ',num2str(sum(Foaming*sampletime)/totalt),''])
  disp(' ')

% time interval that the plant is in uninterrupted severe risk of (integrated) Foaming problem.
LengthFoaming=zeros(1,length(NofFoaming));
for i=1:length(NofFoaming)
  j=i;
  k=1;
  if j~=length(NofFoaming)
    while isequal(NofFoaming(j)+1,NofFoaming(j+1))
      k=k+1;
      j=j+1;
      if j==length(NofFoaming) break
      end
    end
    LengthFoaming(i)=k;
  end
  LengthFoaming(length(NofFoaming))=1;
end
MaxLengthFoaming=max(LengthFoaming);
MaxLengthFoamingIndex=find(LengthFoaming==MaxLengthFoaming);
if not(isempty(NofFoaming))
  disp(['The most dangerous situation was between days ',
num2str(min(totalt,NofFoaming(MaxLengthFoamingIndex(1))*sampletime)+starttime),' and ',
num2str(min(totalt,(NofFoaming(MaxLengthFoamingIndex(1))+MaxLengthFoaming)*sampletime)+start
time),])
end

[Fil,Col]=size(Rising1);
if Fil==1
Rising1 = Rising1';
end

%%%% Deflocculation
[Fil,Col]=size(Deflocculation_risk);
if Fil==1
Deflocculation_risk = Deflocculation_risk';
end

%%%%selects the maximum period between bulking and foaming
OR1 = max(Bulking,Foaming);
%%%%selects the maximum period between bulking,foaming and rising
OR2 = max(OR1,Rising1);
%%%%selects the maximum period between bulking,foaming, rising and deflocculation
OR = max(OR2,Deflocculation_risk);

NofOR = find (OR > 0.8);%To find the values higher than 0.8
NofDif0OR = find (OR > 0.0001); %To find the values higher than 0.0001
  disp('The plant has experienced OVERALL severe (>0.8) risk for OVERALL SETTLING
PROBLEMS')
  disp(['during ',num2str(min(totalt,length(NofOR)*sampletime)),' days, i.e.
',num2str(min(100,length(NofOR)*sampletime/totalt*100)),'% of the operating time.'])
  disp(['AV  risk ',num2str(sum(OR*sampletime)/totalt),''])
% time interval that the plant is in uninterrupted OVERALL severe risk of SETTLING PROBLEMS.
LengthOR=zeros(1,length(NofOR));
for i=1:length(NofOR)
  j=i;
  k=1;
```

```
  if j~=length(NofOR)
    while isequal(NofOR(j)+1,NofOR(j+1))
      k=k+1;
      j=j+1;
      if j==length(NofOR) break
      end
    end
    LengthOR(i)=k;
  end
  LengthOR(length(NofOR))=1;
end
MaxLengthOR=max(LengthOR);
MaxLengthORindex=find(LengthOR==MaxLengthOR);
disp(['The most dangerous situation was between days ',
num2str(min(totalt,NofOR(MaxLengthOR(1))*sampletime)+starttime),' and ',
num2str(min(totalt,(NofOR(MaxLengthORindex(1))+MaxLengthOR)*sampletime)+starttime),])
disp(' ')
```

ANAEROBIC DIGESTION RISK MODEL SCRIPT FOR BSM IN MATLAB/SIMULINK

```
%% Variable calculation

% Inflow VS calculation, as Xch+Xpr+Xli+Xi

VS=0.75*(digesterinpart(:,14)+digesterinpart(:,15)+digesterinpart(:,16)+digesterinpart(:,24));

% HRT as volume of the liquid phase/inflow rate

HRT=V_liq./digesterinpart(:,27);

% OLR

OLR=VS./HRT;

% %% OLR daily AV variation.

% OLR daily average.

k=96;
for b=1:364;
   OLRmean(b)=mean(OLR(k*b-95:k*b));
end

% Variation of the daily average OLR

for b=2:364;
   OLRmeanvar(b)=(abs(OLRmean(b)-OLRmean(b-1))/OLRmean(b-1))*100;
   OLRmeanvar(1)=mean(OLRmeanvar);
end

% To set the same variation for a whole day

for b=1:364;
    OLRvar(k*b-95:k*b)=OLRmeanvar(b);
end

%% Launch the fuzzy toolbox

LowFtoMFoaming2_smoothed =smoothing_data(LowFtoMFoaming2,3);
FADfis=readfis('prova');
FAD_risk=evalfis([OLR OLRvar' LowFtoMFoaming2_smoothed '],FADfis);
FAD_risk_smoothed=smoothing_data(FAD_risk,3);
av=mean(FAD_risk_smoothed)

%% Display the results

NofFAD_risk = find (FAD_risk_smoothed> 0.8);
LengthFAD_risk=zeros(1,length(NofFAD_risk));

for i=1:length(NofFAD_risk)
j=i;
  k=1;
  if j~=length(NofFAD_risk)
     while isequal(NofFAD_risk(j)+1,NofFAD_risk(j+1))
       k=k+1;
       j=j+1;
```

```
if j==length(NofFAD_risk) break
            end
        end
        LengthFAD_risk(i)=k;
    end
LengthFAD_risk(length(NofFAD_risk))=1;
end
MaxLengthFAD_risk=max(LengthFAD_risk);
MaxLengthFAD_riskIndex=find(LengthFAD_risk==MaxLengthFAD_risk);

disp(' ')
disp('Results of the AD Risk Model')
disp('-----------------------------------------------')

if not(isempty(NofFAD_risk))
   disp(' ')
   disp('The anaerobic digester has experienced high (>0.8) risk for the development of foaming')
   disp(['during ',num2str(min(totalt,length(NofFAD_risk)*sampletime)),' days, i.e.
',num2str(min(100,length(NofFAD_risk)*sampletime/totalt*100)),'% of the operating time.'])
   disp(['AV  risk 'av''])
   disp(['The most dangerous situation was between days ',
num2str(min(totalt,(NofFAD_risk(MaxLengthFAD_riskIndex(1)))*sampletime)+7),' and ',
num2str(min(totalt,(NofFAD_risk(MaxLengthFAD_riskIndex(1))+MaxLengthFAD_risk)*sampletime)+
7),])
end

if isempty(NofFAD_risk)
   disp(' ')
   disp('The anaerobic digester has NOT experienced high (>0.8) risk for the development of foaming')
   disp(['AV  risk 'av''])
end
```

EXPONENTIAL FILTER SCRIPT FOR MATLAB/SIMULINK

```
function [smoothed_data]=smoothing_data(dataset,timeconstant)

T=timeconstant; %time constant, days

samplingtime=15;

alpha=1-1/(T*(1440/samplingtime));

smoothed_data(1)=dataset(1);

for i=2:length(dataset)

smoothed_data(i)=alpha*smoothed_data(i-1)+(1-alpha)*dataset(i);

end
```

ACRONYMS

AD	anaerobic digestion
ADM1	anaerobic digestion model no.1
AE	aeration energy
AI	artificial intelligence
ANN	artificial neural network
AS	activated sludge
ASM1	activated sludge model no1
ASM2	activated sludge model no2
ASM2d	activated sludge model no2d
ASM3	activated sludge model no3
AV	average
BOD	biochemical oxygen demand
BSM1	benchmark simulation model no1
BSM1_LT	benchmark simulation model no1 long term
BSM2	benchmark simulation model no2
C	carbon
COD	chemical oxygen demand
COST	Cooperation in Science and Technology
CS	control strategy
DO	dissolved oxygen
EC	external carbon source
EQI	effluent quality index
FAD	foaming in anaerobic digestion
FAS	foaming in activated sludge
F/M	food to microorganisms ratio
H	hydrogen
HE	heating energy
HRBOM	high readily biodegradable organic matter
HRT	hydraulic retention time
IQI	influent quality index
IWA	International Water Association
KBS	knowledge-based system
K_La	oxygen transfer coefficient
K_S	half-velocity constant
LCFA	long chain fatty acids
ME	mixing energy
MF	membership function
MLSS	mixed liquor suspended solids
MLVSS	mixed liquor volatile suspended solids
N	nitrogen
NGPT	nitrogen gas production time
O	oxygen
OCI	operational cost index
OL	Open-loop
OLR	organic loading rate
OLRvar	percentage of the daily average organic loading rate variation
P	phosphorous

PAO	phosphate accumulating organism
PE	pumping energy
PI	proportional integral controller
$\mathbf{Q_{carb}}$	external carbon flow rate
$\mathbf{Q_{eff}}$	effluent flow rate
$\mathbf{Q_{in}}$	influent flow rate
$\mathbf{Q_{in,a}}$	anaerobic digester's inflow rate
$\mathbf{Q_{intr}}$	internal recycle flow rate
$\mathbf{Q_r}$	external recycle flow rate
$\mathbf{Q_W}$	waste sludge flow rate
RAS	return activated sludge
RMSE	root mean square error
S	sulphur
SBR	sequencing batch reactor
SP	sludge production
SRT	solids retention time
SVI	sludge volume index
TIV	time in violation
TOC	total organic carbon
TSS	total suspended solids
V	volume
VFA	volatile fatty acids
VS	volatile solids
WAS	waste activated sludge
WEF	Water Environment Federation
WWTP	wastewater treatment plant